

N 68-85987

(ACCESSION NUMBER)

(THRU)

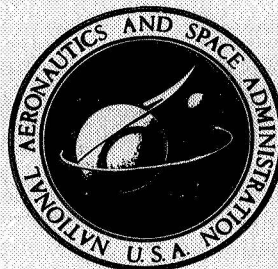
238
(PAGES)

(CODE)

(NASA CR OR TMX OR AD NUMBER)

(CATEGORY)

NASA CONTRACTOR REPORT



NASA CR-66678-8

NASA CR-66678-8

GPO PRICE \$ _____

CFSTI PRICE(S) \$ _____

Hard copy (HC) ____

Microfiche (MF) ____

ff 653 July 65

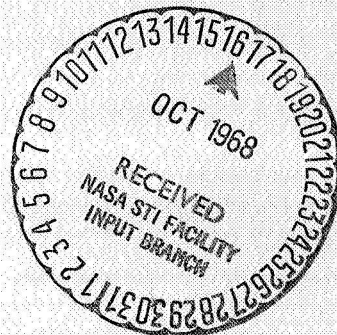
MARS HARD LANDER CAPSULE STUDY

Volume IV Capsule Point Designs and Supporting Analysis

Prepared by

GENERAL ELECTRIC
RE-ENTRY SYSTEMS

for Langley Research Center



31 JULY 1968

NATIONAL AERONAUTICS AND SPACE ADMINISTRATION-WASHINGTON, D. C.

MARS HARD LANDER CAPSULE STUDY

Volume IV
(Book #4)

CAPSULE POINT DESIGNS AND SUPPORTING ANALYSIS

Distribution of this report is provided in the interest of information exchange. Responsibility for the contents resides in the author or organization that prepared it.

Issued by Originator as General Electric Document No. 68SD952-8 (Vol. IV, Book 4)

PREPARED UNDER CONTRACT NO. NAS 1-8098 BY

GENERAL  ELECTRIC

RE-ENTRY SYSTEMS
3198 Chestnut Street, Philadelphia, Pa. 19101

FOR
LANGLEY RESEARCH CENTER

NATIONAL AERONAUTICS & SPACE ADMINISTRATION

FOREWORD

The Mars "Hard Lander" Study Final Report is divided into four volumes and bound in eight books. The titles of the volumes and a brief description of the contents of each book are presented below.

VOLUME I - SUMMARY (CR-66678-1)

Volume I contains a summary of the study activity, the conclusions reached, and a description of a possible design implementation suggested by the study results.

This study indicates that meaningful scientific payloads of approximately 1500 pounds can be placed on the Mars surface, survive for several months, and transmit more than a hundred million bits of data to Earth.

In addition, the study provided data which shows that a smaller Capsule of 700 to 900 pounds has the ability to transmit approximately 10 million bits of imagery and additional scientific surface data.

VOLUME II - MISSION AND SCIENCE DEFINITION (CR-66678-2)

Volume II contains a description of the 'reference' mission plans, both direct entry and out-of-entry, the mission analyses conducted to define the reference plans, the assumed Mars models considered, and the science definition tasks accomplished to select entry and surface science packages/measurement sequences specifically designed to satisfy LRC's scientific goals.

VOLUME III - CAPSULE PARAMETRIC STUDY (CR-66678-3, -4)

A discussion of the analysis and results derived in determining the Capsule subsystems' design characteristics parametrically is provided for the range of assumed Mars Models and the reference mission plans. The synthesis of these subsystems into complete Capsule systems is presented in terms of Capsule performance, total imagery data obtainable, and surface lifetime.

CR-66678-3 presents the Capsule System Parametric Synthesis and Entry and Retardation Subsystem Studies. CR-66678-4 presents both studies of the Lander and Re-entry Subsystems and Appendices associated with the Parametric Study.

VOLUME IV- CAPSULE POINT DESIGNS AND SUPPORTING ANALYSES (CR-66678-5, -6, -7, -8)

Volume IV contains a presentation of the detailed Capsule 'Point Designs', and their supporting analyses, derived to identify specific hardware approaches, weights, and system configurations; and confirm the correctness of the parametric results. In addition to the Capsule's engineering and design details, the results include development status, probability of success, and constraints imposed on the Orbiter by the Capsule mission.

CR-66678-5 contains a definition of the Capsule Point Design Requirements and descriptions of Point Designs 1 and 2. CR-66678-6 contains descriptions of Point Designs 3 and 4 and CR-66678-7 of Point Designs 5 and 6. CR-66678-8 provides additional information on Impact Attenuation, Surface Environment Definition, Effects on Point Designs due to Variations in Assumed Design Parameters as well as the Effects of a Lander on the Mariner Orbiter.

TABLE OF CONTENTS

APPENDICES

| Section | | Page |
|---------|--|------|
| A | IMPACT ATTENUATION AND STRUCTURE | A-1 |
| A.1 | Attenuation Requirements and Criteria | A-1 |
| A.1.1 | Gross Vehicle Response | A-1 |
| A.1.2 | Response of Individual Components | A-1 |
| A.2 | Discussion of Dynamic Analysis of Components | A-2 |
| A.2.1 | Discussion of Results | A-5 |
| A.3 | Deflections Due to Dynamic Response | A-8 |
| A.3.1 | Discussion of Results | A-9 |
| B | SURFACE ENVIRONMENTAL DEFINITION AND INTERPRETATION.. | B-1 |
| B.1 | Definition | B-1 |
| B.1.1 | Surface Strength | B-1 |
| B.1.2 | Depth of Penetration | B-1 |
| B.1.3 | Effect of Impact Velocity on Penetration | B-3 |
| B.1.4 | Surface Rocks and Roughness | B-5 |
| B.1.5 | Surface Friction | B-6 |
| B.1.6 | Slopes | B-6 |
| B.1.7 | Wind Effects | B-7 |
| B.1.8 | Secondary Impact of the Lander Vehicle | B-11 |
| B.2 | Interpretation of Environmental Specifications | B-14 |
| B.2.1 | Large Amplitudes of Sway Angle | B-17 |
| B.2.2 | Slopes | B-17 |
| B.2.3 | Wind Speed | B-19 |
| C | EFFECTS ON POINT DESIGNS DUE TO VARIATIONS IN ASSUMED DESIGN PARAMETERS | C-1 |
| C.1 | Martian Surface Definitions and Touchdown Conditions | C-1 |
| C.2 | Material Performance Variations | C-3 |
| D | CONSTRAINTS IMPOSED ON ORBITER | D-1 |
| D.1 | Mission and System Summary | D-1 |
| D.1.1 | Introduction | D-1 |
| D.1.2 | Mission Guidelines | D-1 |
| D.1.3 | Mariner Mars '71 Summary | D-1 |
| D.1.4 | Mariner Mars '73 Summary | D-7 |
| D.2 | System Description | D-12 |
| D.2.1 | Orbiter Requirements | D-12 |
| D.2.2 | Configuration Selection | D-12 |
| D.2.3 | Orbiter Description | D-28 |
| D.2.4 | Flight Capsule Interfaces | D-39 |
| D.2.5 | MM '71 and MM '73 Command Structures | D-51 |
| D.2.6 | Flight Sequence | D-51 |
| D.2.7 | Space Vehicle | D-51 |

TABLE OF CONTENTS (Cont'd)

| Section | | Page |
|---------|--|-------|
| D.3 | Propulsion Subsystem | D-72 |
| | D.3.1 Functional Description | D-72 |
| | D.3.2 Subsystem Operation | D-74 |
| | D.3.3 Comparison to Mariner '71 Design | D-74 |
| | D.3.4 Subsystem Characteristics | D-76 |
| D.4 | Engineering Mechanics | D-79 |
| | D.4.1 Structure | D-79 |
| | D.4.2 Temperature Control Subsystem | D-105 |
| D.5 | Telecommunications | D-112 |
| | D.5.1 Radio Frequency Subsystem | D-112 |
| | D.5.2 Command Subsystem | D-119 |
| | D.5.3 Flight Telemetry Subsystem | D-124 |
| | D.5.4 Data Storage Subsystem | D-128 |
| | D.5.5 Data Automation Subsystem | D-135 |
| | D.5.6 Relay Subsystem | D-136 |
| D.6 | Guidance, Control, and Power | D-144 |
| | D.6.1 Power Subsystem | D-144 |
| | D.6.2 Central Computer and Sequencer | D-150 |
| | D.6.3 Altitude Control Subsystem | D-160 |
| | D.6.4 Scan Control Subsystem | D-167 |
| D.7 | Science | D-170 |
| D.8 | References | D-171 |

LIST OF ILLUSTRATIONS

| <u>Section</u> | | <u>Page</u> |
|----------------|--|-------------|
| A-1 | Dynamic Analysis Model | A-3 |
| A-2 | Dynamic Analysis Model with Damping | A-3 |
| A-3 | Shock Pulse for Lander Capsule | A-6 |
| A-4 | Peak Component Acceleration Response as a Function of Mount Stiffness | A-7 |
| A-5 | Analytical Model | A-9 |
| A-6 | Component Mounting Peak Deflection as a Function of Mount Stiffness | A-10 |
| A-7 | Component Mounting Peak Deflection vs Peak Acceleration | A-11 |
| A-8 | Structural Dynamics Model | A-12 |
| A-9 | Touchdown Situations Producing Angular Accelerations | A-13 |
| B-1 | Penetrations - Effects on Average Deceleration | B-4 |
| B-2 | Omnidirectional Lander Touchdown Upon a Slope | B-7 |
| B-3 | Multidirectional Lander Touchdown Upon a Slope | B-7 |
| B-4 | Gross Cross Sectional Area vs Stroke for Omnidirectional Lander | B-8 |
| B-5 | Gross Cross Sectional Area vs Stroke for a Typical Multi- directional Shape | B-9 |
| B-6 | Interaction of Environmental Definitions to Define Lander Touchdown Conditions (Omnidirectional Lander) | B-10 |
| B-7 | Interaction of Environmental Definitions to Define Lander Touchdown Conditions (Multidirectional Lander) | B-10 |
| B-8 | Omnidirectional Lander with Sway, Wind, and Slope Touchdown Conditions | B-12 |
| B-9 | Multidirectional Lander with Sway, Wind, and Slope Touchdown Conditions | B-12 |
| B-10 | Lander Impact Configurations | B-15 |
| B-11 | Cumulative Distribution Function for Pendulum Angle Using Sinusoidal Approximation | B-18 |
| B-12 | Cumulative Distribution Function for Pendulum Angle Based on Elliptic Integral Formulation of the Problem | B-18 |
| B-13 | Cumulative Distribution Function for Slope Angle | B-19 |
| B-14 | Cumulative Distribution Function for Wind Speed Variation Based on NASA/LRC Preliminary Specification | B-21 |
| B-15 | Cumulative Distribution Function for Secondary Impact Velocity for a Wind Speed of 110 fps | B-24 |
| B-16 | Histogram for Secondary Impact Velocity Based on a Wind Speed of 110 fps | B-25 |
| B-17 | Cumulative Distribution Function for Secondary Impact Velocity Based on a Wind Speed of 220 fps | B-27 |
| B-18 | Histogram for Secondary Impact Velocity for a Wind Speed of 220 fps | B-29 |

LIST OF ILLUSTRATIONS (Cont'd)

| <u>Section</u> | | <u>Page</u> |
|----------------|--|-------------|
| D-1 | Mariner Mars '69 Flyby Spacecraft | D-2 |
| D-2 | Mariner Mars '71 Orbiter | D-5 |
| D-3 | Mariner Mars '73 Spacecraft (Out-of-Orbit Entry Capsule) | D-8 |
| D-4 | Spacecraft Configuration, Direct Entry Capsule | D-14 |
| D-5 | MM '73 Spacecraft Evolution, Out-of-Orbit Entry Capsule | D-15 |
| D-6 | Screening of Candidate Out-of-Orbit Entry Configurations | D-16 |
| D-7 | Configuration 1 | D-19 |
| D-8 | Configuration 1 with Multiple Engines | D-20 |
| D-9 | Configuration 2 | D-21 |
| D-10 | Configuration 2 with Alternate Tanks | D-22 |
| D-11 | Configuration 8 | D-23 |
| D-12 | Spacecraft Configuration, Out-of-Orbit Capsule | D-29 |
| D-13 | Mariner Mars '73 Functional Block Diagram | D-31 |
| D-14 | Spacecraft Configuration - Minimum Science Direct Entry Capsule | D-40 |
| D-15 | Spacecraft Configuration - Maximum Science Direct Entry Capsule | D-41 |
| D-16 | Spacecraft Configuration - Minimum Science Out-of-Orbit Entry Capsule | D-42 |
| D-17 | Spacecraft General Arrangement | D-43 |
| D-18 | Spacecraft Fields of View | D-45 |
| D-19 | '73 Mars Mission Profiles | D-65 |
| D-20 | Conceptual Launch Configurations and Integration Details | D-67 |
| D-21 | Maximum Allowable Payload Weight and C.G. Height Based on Centaur Strength Capability | D-70 |
| D-22 | Propulsion Subsystem Schematic | D-73 |
| D-23 | Propulsion Subsystem Weights as a Function of Payload Weights .. | D-78 |
| D-24 | Acoustic Fields Within Standard 10-Foot Diameter Titan Fairing .. | D-81 |
| D-25 | Predicted Acoustic Fields Within Proposed Bulbous (16-Foot Diameter) Titan Fairing | D-82 |
| D-26 | Schematic of Orbiter Modular Arrangement (Applicable to All Missions/Configurations) | D-84 |
| D-27 | Propulsion Module Structural Elements | D-87 |
| D-28 | Structural Elements of Capsule Adapter | D-91 |
| D-29 | Brief Schematic Diagram of Proposed Redesign of IRS Detector Positioning | D-110 |
| D-30 | Mariner Mars '73 Radio Subsystem Block Diagram | D-113 |
| D-31 | Margin vs Range for Low Gain Antennas | D-116 |
| D-32 | Out-of-Plane Loss due to Single Axis Steering of 63 Inch High Gain Antenna | D-118 |
| D-33 | Margin vs Range for High Gain Antenna | D-120 |
| D-34 | Command Margin vs Range | D-121 |
| D-35 | Ranging Channel Range vs Antenna Gain | D-122 |
| D-36 | Command Subsystem | D-123 |

LIST OF ILLUSTRATIONS (Cont'd)

| <u>Section</u> | | <u>Page</u> |
|----------------|---|-------------|
| D-37 | Flight Telemetry Subsystem | D-125 |
| D-38 | Worst Case Data Rate Capability (210 ft DSNA) | D-129 |
| D-39 | Worst Case Data Rate Capability (85 ft DSNA) | D-130 |
| D-40 | Mariner Mars '73 Orbiter Data Storage Subsystem | D-132 |
| D-41 | Tape Recorder Collection Profile During Periapsis Passage | D-133 |
| D-42 | Tape Recorder Readout Profile | D-134 |
| D-43 | Data Automation Subsystem | D-137 |
| D-44 | Relay Subsystem | D-139 |
| D-45 | 160 kbps and 1340 kbps Synchronization Loops | D-140 |
| D-46 | Relay Antenna (Turnstile Over-Ground) | D-141 |
| D-47 | Relay Antenna Pattern | D-142 |
| D-48 | Power Subsystem Functional Block Diagram | D-145 |
| D-49 | Coded Command Word Formats | D-153 |
| D-50 | CC&S Functional Block Diagram, MM '73 | D-154 |
| D-51 | Approach Guidance Subsystem Block Diagram | D-166 |
| D-52 | Scan Control Subsystem | D-168 |

LIST OF TABLES

| Table | | Page |
|-------|---|-------|
| B-1 | Penetrations Calculated from Fig. 3.1 of Ref. B-1 (Kornhauser) . . . | B-3 |
| B-2 | Penetrations Calculated by Young's Equation, Ref. B-2 | B-4 |
| B-3 | Statistical Distribution of Slope Angle | B-20 |
| B-4 | Compound Versus Simple Probabilities | B-20 |
| B-5 | Probability of Slope Intervals | B-21 |
| B-6 | Probability of Pendulum Intervals | B-22 |
| B-7 | Secondary Impact Velocity Probability for 110 fps | B-23 |
| B-8 | Secondary Impact Velocity Cumulative Probability for 110 fps | B-24 |
| B-9 | Secondary Impact Velocity Probability for 220 fps | B-26 |
| B-10 | Secondary Impact Velocity Cumulative Probability for 220 fps | B-27 |
| D-1 | Mars Mission Comparison | D-3 |
| D-2 | Major Subsystem Changes | D-11 |
| D-3 | Design and Test Assumptions | D-25 |
| D-4 | Mission and Project Comparison | D-27 |
| D-5 | Flight Capsule Command List | D-48 |
| D-6 | Flight Capsule Power Requirements | D-50 |
| D-7 | MM '71 and '73 Command Correlation | D-52 |
| D-8 | Command Summary | D-63 |
| D-9 | Propulsion Requirements | D-72 |
| D-10 | Comparison of MM '71 and MM '73 Propulsion Systems | D-75 |
| D-11 | Propulsion Subsystem Weight Breakdown - Direct Entry | D-76 |
| D-12 | Propulsion Subsystem Principal Dimensions - Direct Entry | D-77 |
| D-13 | Propulsion Subsystem Performance | D-77 |
| D-14 | Titan III/Centaur Flight Limit Environments and Criteria | D-80 |
| D-15 | Environmental Changes Dictated by Proposed (16-foot Diameter) Bulbous Fairing | D-81 |
| D-16 | Major Orbiter Structural Elements | D-85 |
| D-17 | Structural Elements of Mariner Mars '71 Propulsion Module | D-94 |
| D-18 | Structural Elements of Capsule Adapter (Typical Lightweight Direct Entry Capsule) | D-97 |
| D-19 | Structural Elements of Spacecraft Adapter (Typical Lightweight Direct Entry Capsule) | D-98 |
| D-20 | Structural Elements of Capsule Adapter (Typical Heavyweight Direct Entry Capsule) | D-99 |
| D-21 | Structural Elements of Spacecraft Adapter (Typical Heavyweight Direct Entry Capsule) | D-100 |
| D-22 | Structural Elements of Propulsion Module (Out-of-Orbit Capsule) . . . | D-101 |
| D-23 | Structural Elements of Capsule Adapter (Out-of Orbit Entry Capsule) . | D-104 |
| D-24 | Structural Elements of Spacecraft Adapter (Out-of-Orbit Entry Capsule) | D-105 |
| D-25 | Thermal Coatings | D-108 |
| D-26 | Radio Modes | D-107 |

LIST OF TABLES (Cont'd)

| Table | | Page |
|-------|---|-------|
| D-27 | Summary of R-F Link Performance | D-119 |
| D-28 | Data Rates Versus Mission Phase | D-126 |
| D-29 | Relay Data Collection | D-128 |
| D-30 | Time Between Samples (sec) | D-128 |
| D-31 | Recorder Characteristics | D-135 |
| D-32 | Spacecraft Subsystem Power Allocation (Out-of-Orbit Entry) | D-146 |
| D-33 | Spacecraft Subsystem Power Allocation (Direct Entry) | D-147 |
| D-34 | Abbreviations | D-149 |
| D-35 | Nominal Flight Phases and Gross Power Requirements for Out-of-Orbit Entry Case | D-151 |
| D-36 | Nominal Flight Phases and Gross Power Requirements for Direct Entry Case | D-151 |
| D-37 | Command List Memory Capacity Usage | D-155 |
| D-38 | Mariner Mars '69 Science Payload | D-170 |

APPENDIX A.
IMPACT ATTENUATION AND STRUCTURE

APPENDIX A. IMPACT ATTENUATION AND STRUCTURE

A.1 ATTENUATION REQUIREMENTS AND CRITERIA

A.1.1 GROSS VEHICLE RESPONSE

Impact attenuation and structural criteria affect the Capsule point design in two respects as they apply to the gross vehicle dynamic response and from the standpoint of individual scientific component isolation and response. From the standpoint of the gross Lander body, the impact criteria are principally concerned with the adequate sizing of the crushup attenuator system. In essence, the design must provide sufficient stopping distance to decelerate the Lander within the allowable deceleration g-limit while simultaneously dissipating the impact kinetic energy. At the same time, the deceleration pulse must be of a certain character to insure Lander survival upon impact. Implied in this requirement are a sufficient rise time and a broad flat deceleration pulse. When a crushup honeycomb design is made using the proper materials, this last criteria is inherently satisfied because of known material performance characteristics.

A.1.2 RESPONSE OF INDIVIDUAL COMPONENTS

Once the gross Lander impact attenuation system has been designed, more detailed study of component isolation and response characteristics for impact loadings must be undertaken. Initial studies have been performed to determine the feasibility of further attenuating the impact acceleration levels experienced by particularly sensitive components carried by the Lander. At the outset, a simplified dynamic model of the vehicle describing the load path from the ground to a typical component is required. As the vehicle dimensions and configuration become firm, a more precise model can be postulated and a refined analysis performed.

The average deceleration (G) experienced by the overall Lander, $V^2/2Y$, (Y is stroke) may be decreased for any particular component on a shock mount with stroke distance, δ , to a new value, $G_o = V^2/2(Y + \delta)$:

$$G/G_o = Y/(Y + \delta) \quad (A1)$$

Since most components will not have enough mounting space to permit a mount deflection of more than a few inches, and $Y \cong 8$ in. or more, it appears that the average rigid-body decelerations cannot be reduced much more than 20 percent or so on the individual components.

The main functions of shock mounting applied to the Mars Hard Lander components will be to prevent excessive dynamic responses of individual components to the acceleration-time inputs. If, for example, the higher frequency oscillations in the input pulse should tend to coincide with a lower mode of a component, the response could be amplified to a very high value, since this would be a case of forced vibrations. In this case, the shock mount can be designed to perform two functions:

1. Move the component-plus-mount frequency away from a resonance with the forcing function.
2. Provide damping to further reduce responses to high-frequency inputs.

The requirements for individual shock mounts will be developed in a full detail design by preparing a dynamic computer model of the Lander and its components and subjecting this model to the deceleration-time inputs expected on impact.

A.2 DISCUSSION OF DYNAMIC ANALYSIS OF COMPONENTS

An analysis was performed on a typical Hard Lander to quantitatively assess the conclusions just stated. This analysis is discussed below.

Three major structural spring-damper elements exist between ground and a typical component in the Lander vehicle. These are the container structure, the prime component mounting shelf and the local mounting structure to a particular component. A vibration analysis that considers each of these prime structural elements could use fig. A-1 as a model.

If a spring-damper structure exists that can attenuate the g-load from the ground to the component, this element will be attainable from a variety of combinations of primary shelf and local mount designs. Since the design of both of these structural elements is incomplete, no useful purpose is served by considering them separately. Thus, the model used in this shock response analysis is as shown in fig. A-2.

Thus, the solution of this two degree-of-freedom system can be used to determine the acceleration response of the component. The equations of motion of this system are:

$$M_1 \ddot{X}_3 + C_1 \dot{X}_3 + K_2 X_3 - C_2 \dot{X}_4 - K_2 X_4 = -M_1 \ddot{X}_g$$

$$M_2 (\ddot{X}_4 + \ddot{X}_3) + C_2 \dot{X}_4 + K_2 X_4 = -M_2 \ddot{X}_g$$

where

$$X_3 = X_1 - X_g$$

$$X_4 = X_2 - X_1$$

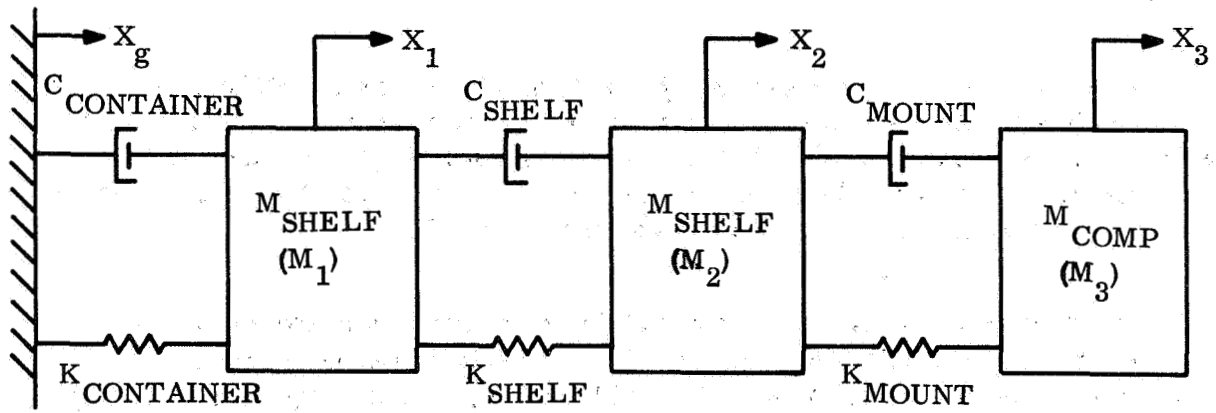


Figure A-1. Dynamic Analysis Model

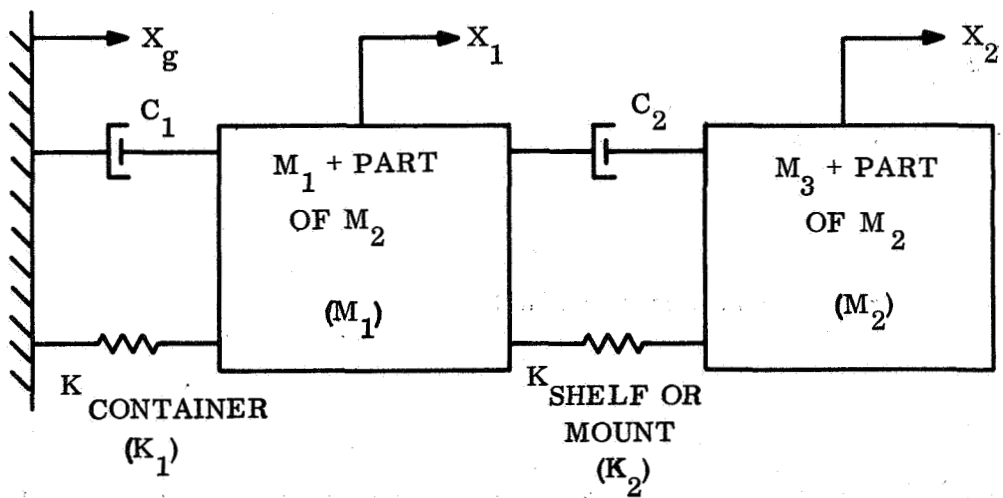


Figure A-2. Dynamic Analysis Model With Damping

The most general approach to the solution of the equations of motion is to find a general solution to the set of equations, and then parametrically vary each of the constants of the model to determine that combination that best reduces the acceleration response of the component. This is quite possible but would involve a great deal of labor. The number of parameters worthy of detailed study can be reduced by consideration of the nature of the solution and the allowable design variations open.

First, we may assume the masses to be fixed and the container stiffness K_1 to be fixed since these will, in general, be determined by factors other than the component response. Similarly, the damping in the container structure will probably be determined by factors beyond our control, so that C_1 may be established as a constant. Thus, the only parameters to be investigated are C_2 and K_2 .

For an initial trial, it is recognized that damping will play a relatively small role in containing the amplitude of component acceleration response, since the excitation is transient and not steady state. Therefore, we may neglect the existing damping in both the shelf and in the container, for this preliminary analysis. Thus, the constants of interest would be:

$$M_1^* = 220/386 = 0.5699 \frac{\text{lb-sec}^2}{\text{inch}}$$

$$M_2^* = 380/386 = 0.9845 \frac{\text{lb-sec}^2}{\text{inch}}$$

$$C_1 = 0$$

$$C_2 = 0$$

$$K_1 = 0.2209 \times 10^6 \text{ lb/inch}$$

with

$$K_2 = \text{the parameter to be studied.}$$

* Specific numerical values might be chosen as representative of current Lander configuration.

The only other information needed to complete the problem are the initial conditions and the forcing function. To determine the initial conditions, we assume that the Lander is dropping at constant velocity just prior to impact. This implies that there are no acceleration forces on the vehicle, which is obviously not correct. However, the forces and acceleration forces due to impact are much, much larger than those prior to impact, so that little accuracy will be lost by ignoring the "prior-to-impact" loads. Now if we consider the vehicle to be moving at constant velocity toward a non-moving planet, we can just as easily picture a planet moving toward a stationary vehicle. For this condition, the initial conditions of our dynamic model at impact are:

$$\dot{X}_1 = \dot{\dot{X}}_1 = \dot{X}_2 = \dot{\dot{X}}_2 = 0$$

The actual profile of impact and the simplification of that complex shape used in the present analysis are shown in fig. A-3.

From this point onward, the solution is an exercise in basic dynamics. Discussion or illustration of the procedure is omitted from this synopsis. The final result is two equations for the acceleration response of the mass M_2 as a function of time and of the spring K_2 . One of these equations is valid during the period when the forcing function is being applied, while the second describes the motion after the forcing function is removed. Two additional equations are also developed that define those times when the response hits a peak (the response is, of course, periodic and so has periodically repeating peaks). These last two equations are also functions of K_2 .

Using these equations for various values of K_2 , a curve of peak acceleration response of the components, as a function of K_2 may be calculated. The curve is shown in fig. A-4. The calculations can be carried out on the digital computer using, for example, the GE MSD PANACEA program.

A.2.1 DISCUSSION OF RESULTS

An indicative peak response, as a function of component mount stiffness, is shown in fig. A-4. The results indicate a definite spring rate exists for which the component acceleration response will be a minimum. For the present set of numbers, that stiffness is 2000 lbs/inch, but it must be recognized that the figure will vary as the other system parameters (K_1 , M_1 , M_2 , etc.) are varied. Further, at 2000 lbs/inch, the acceleration attenuation is about 8 to 1. However, that ratio will be highly dependent upon the actual pulse shape and upon the linearity (or lack of linearity) of the spring K_2 .

Lastly, we must recognize that an extremely simplified structural model was used whose response characteristics only roughly simulate the actual response.

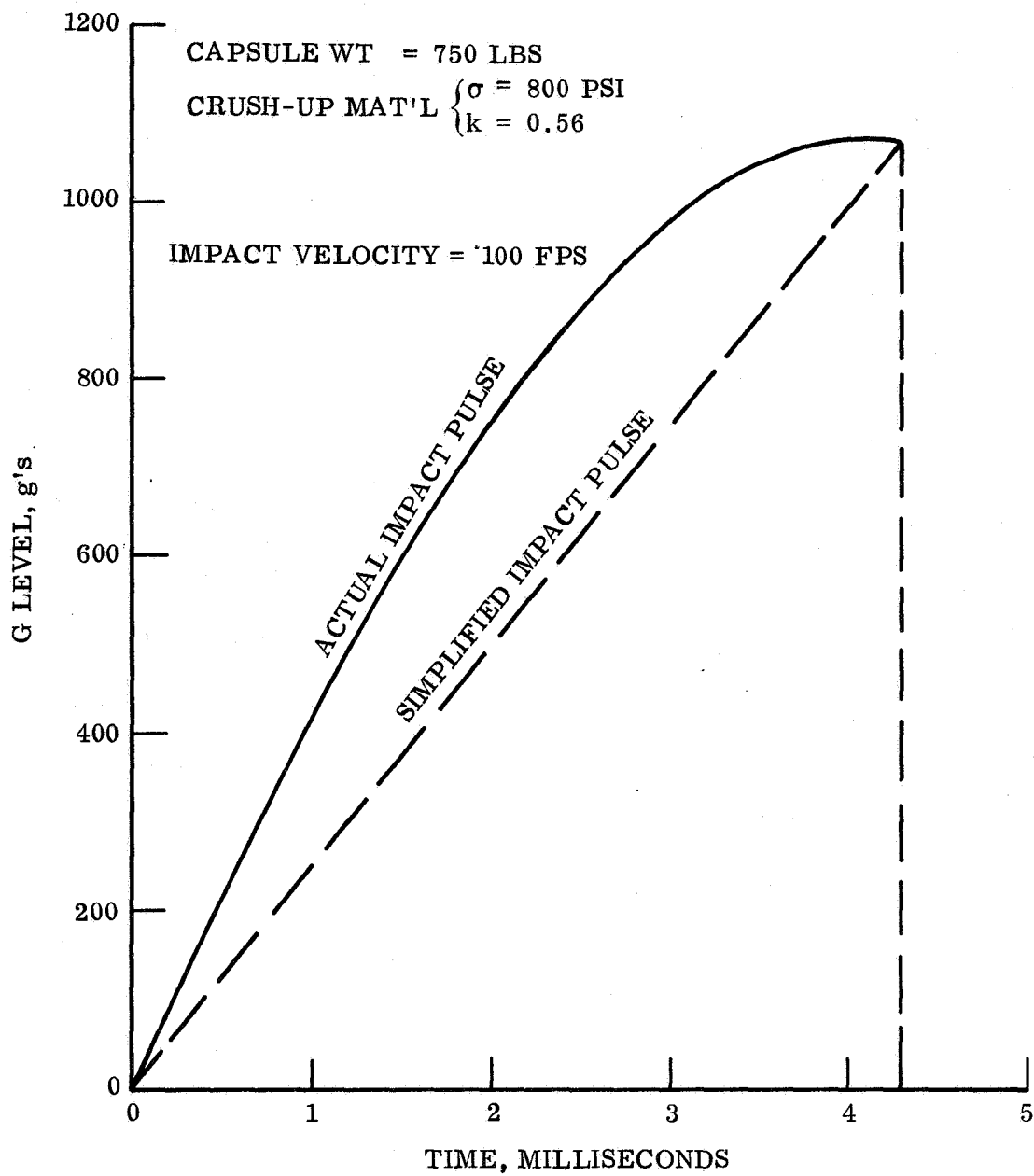


Figure A-3. Shock Pulse for Lander Capsule

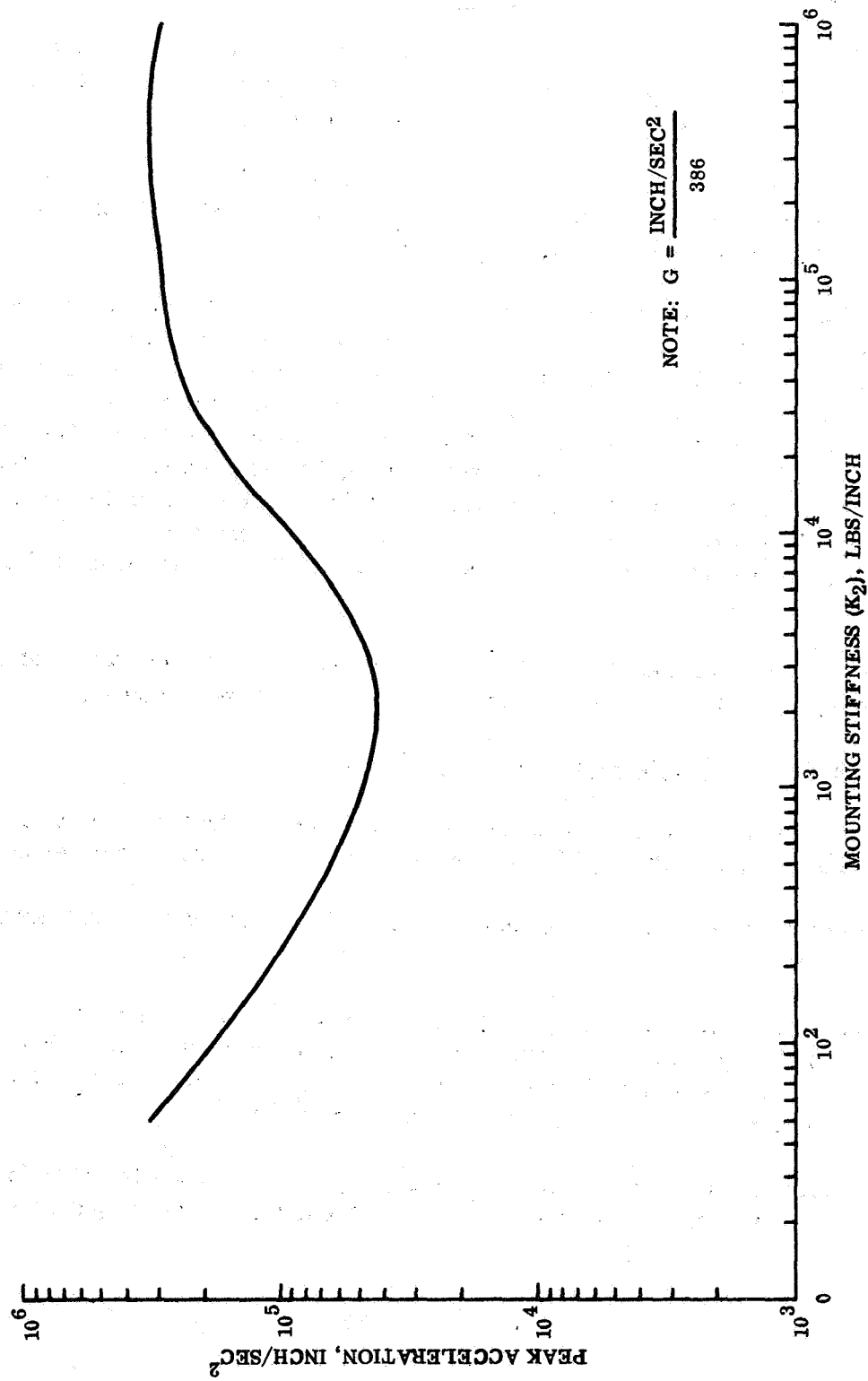


Figure A-4. Peak Component Acceleration Response as a Function of Mount Stiffness

The point to be emphasized is that the optimum spring rate of the present study may not be very close to the real optimum spring rate, and the acceleration attenuation achieved in the present model may not necessarily be achievable in practice.

What the analysis does indicate are the trends of the component acceleration response at impact and so indicates realistic design objectives for the component support structure and the component acceleration capability.

Thus attenuation of the impact g-level can be designed into the structure. A very conservative estimate of the attenuation achievable is 2:1, although with a very careful support design, 3:1 attenuation appears feasible.

To achieve this acceleration attenuation, a relatively soft component mounting is necessary, somewhere between 200 and 20,000 lbs/inch which infers a large deflection. While this seems like a wide tolerance, it must be recognized that the penalty for exceeding these bounds increases rapidly. Further, if the designer should design to the low end of this stiffness range, rubber supports would probably be needed. The stiffness properties of rubber are highly non-linear. If the rubber was to "bottom-out" during impact, the component might yet experience the full impact g-level or perhaps even more. On the other side, a metallic support of 20,000 lbs/inch might require relatively thin structure that would be very weak in all but the optimum impact direction.

Unfortunately, significant reduction on a g-response requires large deflections. The following analysis is for deflections of the dynamic Lander model.

A.3 DEFLECTIONS DUE TO DYNAMIC RESPONSE

Using the same dynamic model just described, one could compute the peak component displacement associated with a range of reasonable mounting stiffnesses.

The Hard Lander vehicle (and components) and its simplified representation are exactly the same as before.

The basic analytical model (fig. A-5) is where the deflection to be studied is X_4 and the forcing function is X_g , the equations of motion, assumptions, and model properties are those discussed above. Coordinate X_4 shows the deformation between the components and the primary container structure.

The triangular acceleration pulse shown in fig. A-5 is used here as in the previous work. Response may be calculated, both during and after application of the pulse.

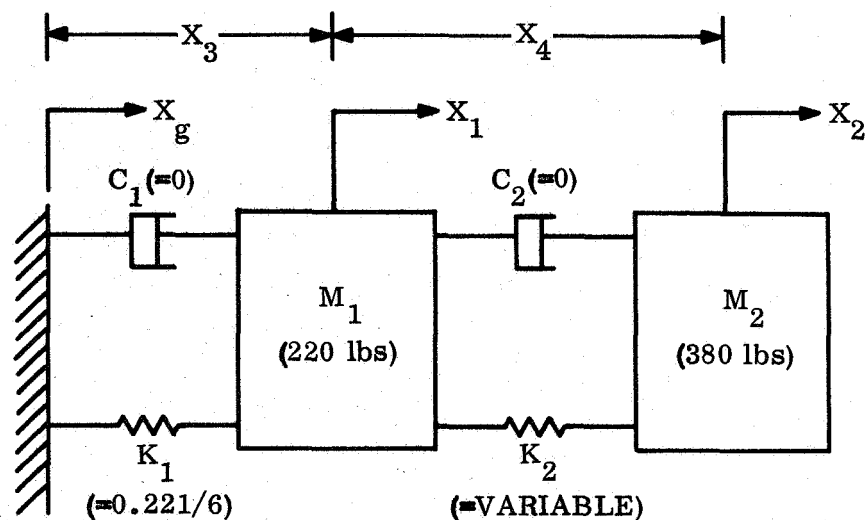


Figure A-5. Analytical Model

The peak values of response X_4 are then plotted against mounting stiffness (in the form of spring rate, lbs/in) in fig. A-6.

A.3.1 DISCUSSION OF RESULTS

The peak response of the component with respect to its support is shown in fig. A-6. As expected, the deflection is least for very stiff mounts. In addition, the curve shows no peaks or valleys (i.e., change in sign of the slope) which might allow large attenuation even with soft mounts. The necessity for as stiff a mount as possible to achieve minimum deflection will have to be weighted against the mid-range of stiffness necessary for acceleration attenuation as previously developed. A representative trade-off is shown graphically in fig. A-7.

Again it is emphasized that one must recognize that a simple structural model was used whose primary utility is to indicate trends which was the original objective of the analysis. Quantitatively, the calculations only roughly simulate the actual response. Thus, the trade-off available at this stage of analysis may be overconservative.

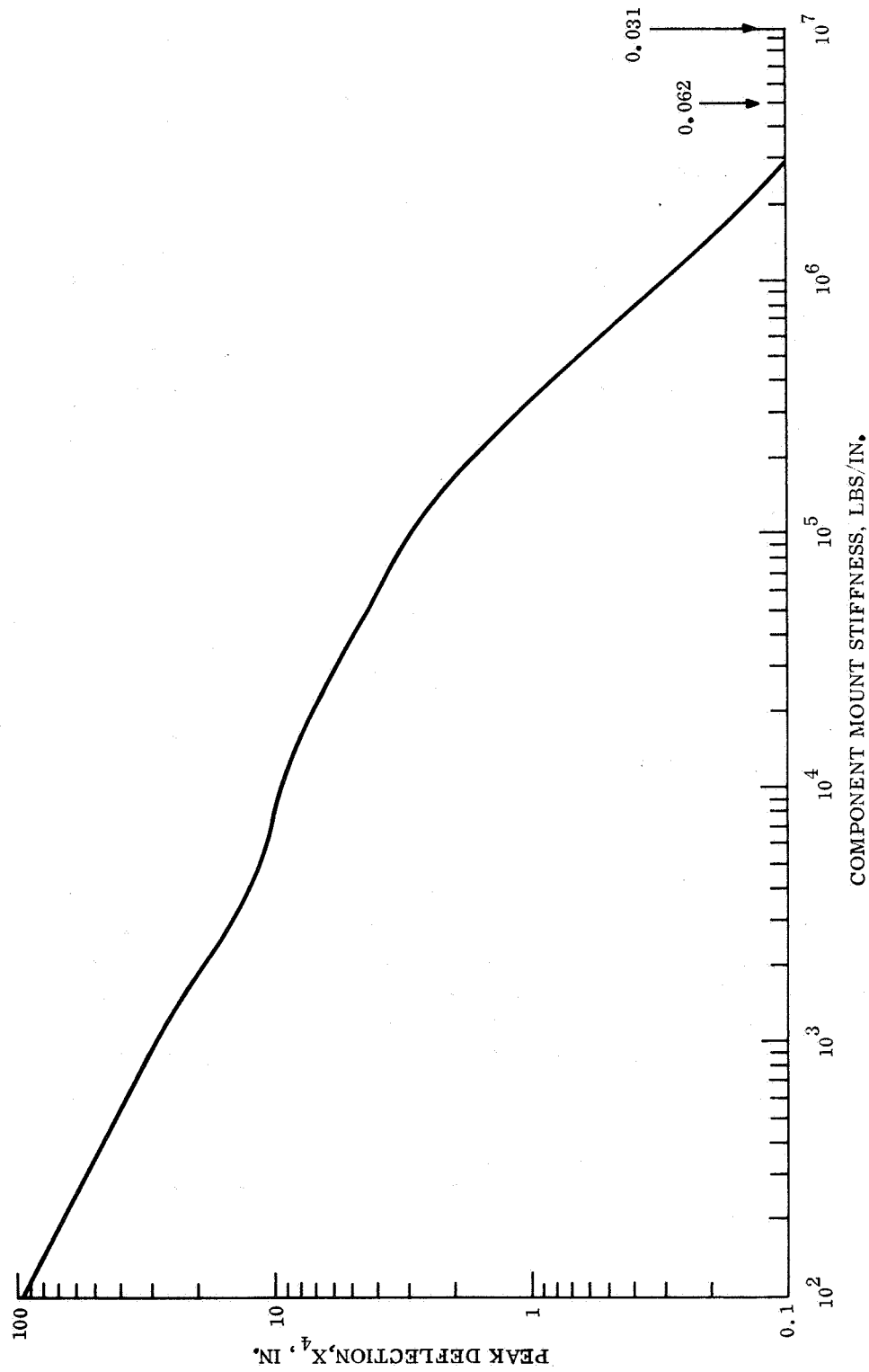


Figure A-6. Component Mounting Peak Deflection as a Function of Mount Stiffness

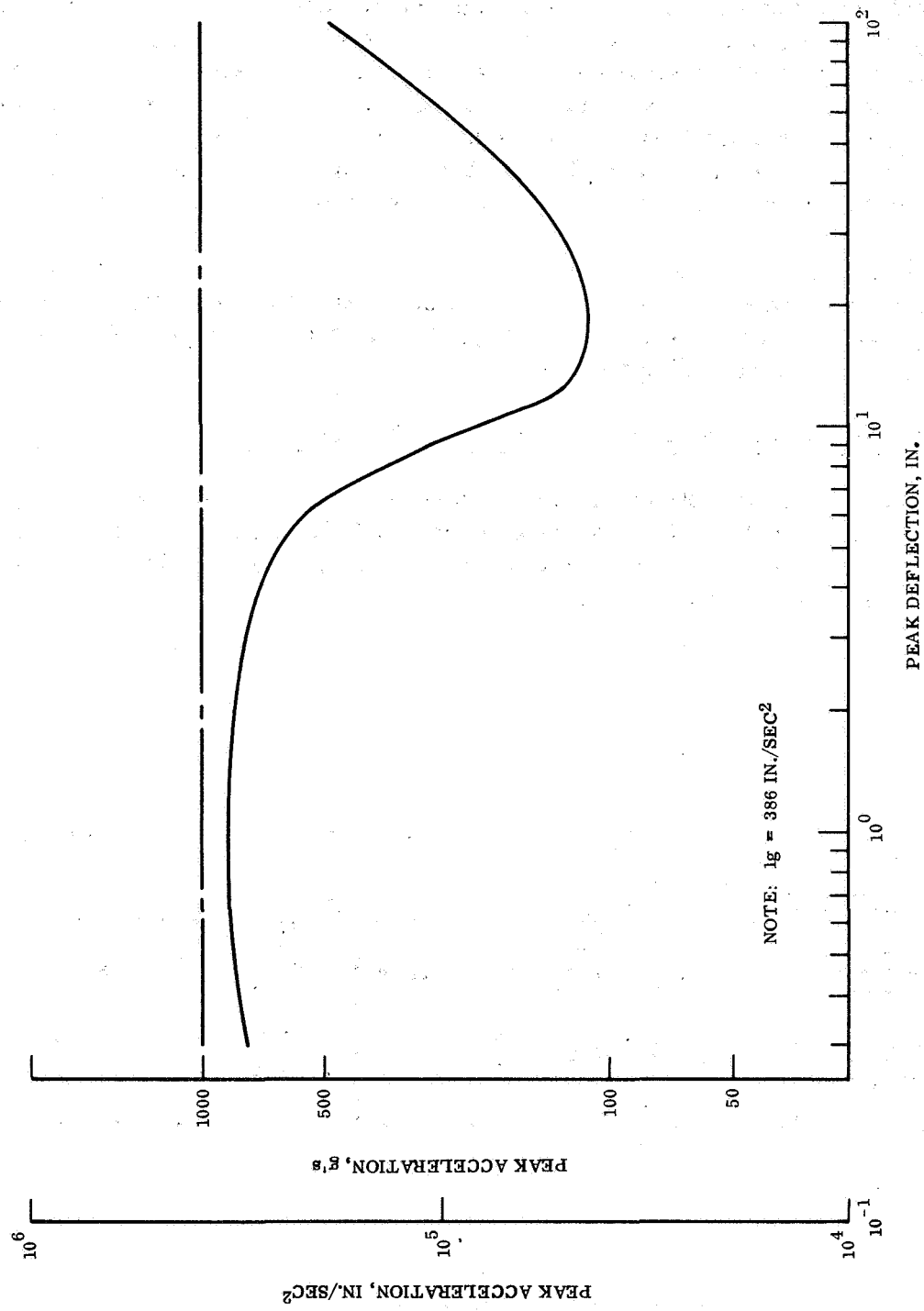


Figure A-7. Component Mounting Peak Deflection vs Peak Acceleration

More quantitative results could be obtained from a 3-DOF model. Three major structural spring-damper elements exist between ground and a typical component in the Lander vehicle—the container structure, the prime component mounting shelf, and the local mounting structure to a particular component. A vibration analysis that considers each of these prime structural elements could use fig. A-8 as a model. Looking at the three-mass system dynamically, the total spring rate from M_1 to M_3 is attainable from a variety of combinations of K_{shelf} and K_{mount} . However, the mass distribution between the models of figs. A-8 and A-5 is quite different. Since M_3 of fig. A-8 would be much less than M_2 of fig. A-5, much more control over the motion of the component can be exercised in the 3-DOF model.

As shown in fig. A-7, large reduction in g-response requires large deflections. In brief, it does not appear feasible to obtain significant reductions with shock mounts or by component mounting stiffness tailoring. These last devices are of primary use in minimizing g-level amplification effects.

A.3.1.1 Angular Accelerations: Their Effect On Components

When the Lander impacts on one edge, there is the possibility that high angular accelerations may produce high loading on components located at the outer extremity of the container. Two types of impacts can occur, namely, high angle impact and low angle impact as shown in fig. A-9.

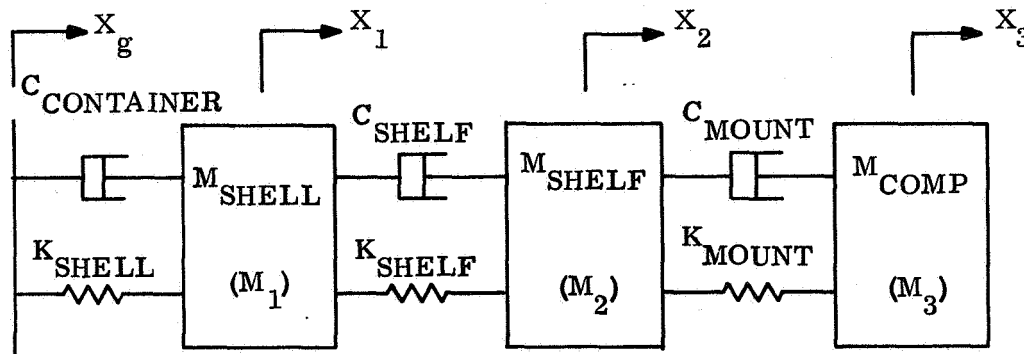


Figure A-8. Structural Dynamics Model

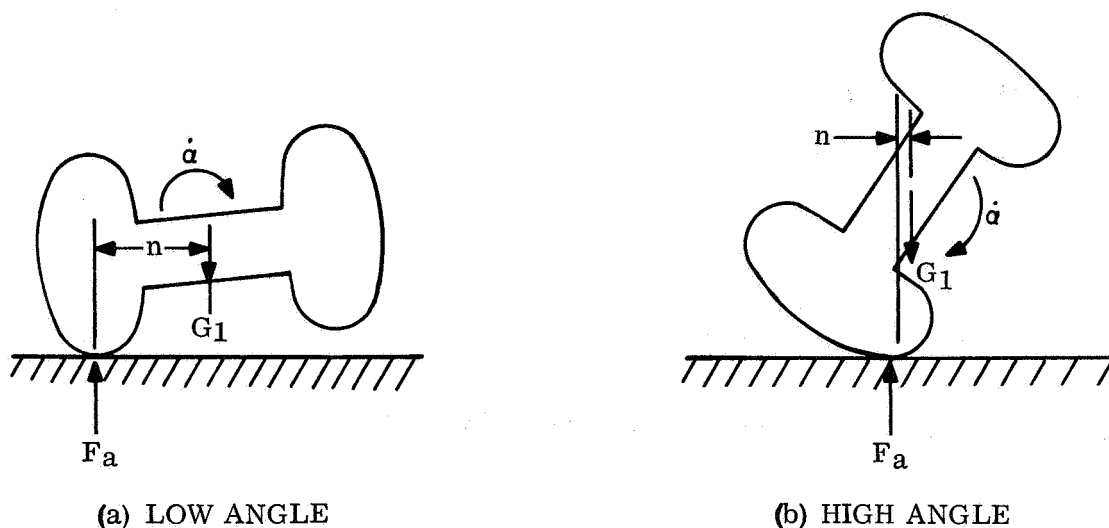


Figure A-9. Touchdown Situations Producing Angular Accelerations

A.3.1.1.1 Case a. High Angle Impact

The overall force, F_a , over the area of impact may be expected to be less than for normal impact, F_n , because area of crushup material is being loaded. Roughly, the force will be proportional to the area of contact. Thus $F_a < F_n$ and the deceleration of the c.g. will be less than the value $G_o = F_n/M$ for normal impact.

In fig. A-9(a) it is apparent that impact on one edge introduces a second major change in the form of an angular acceleration of the entire body.

Components near the point of contact will experience the highest accelerations, as follows:

$$G = G_1 + r_1 \ddot{\alpha}$$

$$G = F_a/M + r_1 \ddot{\alpha} \quad (A2)$$

Angular acceleration:

$$I \alpha = F_a r_1 \quad (A3)$$

Combining eq. A2 and eq. A3

$$\begin{aligned} G &= F_a/M + F_a r_1^2/I \\ &= (F_a/F_n) G_o (1 \pm Mr_1^2/I) \\ G/G_o &= (F_a/F_n) (1 + Mr_1^2/I) \end{aligned} \quad (A4)$$

Taking $r_1 = 2 \text{ ft}$, $M = 930 \text{ lbs}$, and $I = 2,020 \text{ lbs-ft}^2$

$$Mr_1^2/I = 1.84$$

$$G/G_o = 2.84 F_a/F_n$$

One would expect the area of contact to be considerably less than half that for normal impact, probably in the 1/10 to 1/3 range. It thus appears, roughly, that impact at a low angle will produce about the same decelerations as on normal impact, or probably lower.

A.3.1.1.2 Case b. Low Angle Impact

For this situation of impact angle, the same equations apply. In this case, however, analysis has shown that the force is about the same as the normal or flat impact

$$F_a \cong F_n$$

The moment arm, r , is much less than in case (a) because of shaping of the attenuator geometry, leading to the same conclusion (on the basis of preliminary analysis), that high angular acceleration g's will not result in higher total accelerations than a low angle impact.

**APPENDIX B. SURFACE ENVIRONMENTAL
DEFINITION AND INTERPRETATION**

APPENDIX B.

SURFACE ENVIRONMENTAL DEFINITION AND INTERPRETATION

B.1 DEFINITION

Martian surface conditions as well as impact velocity and kinematical requirements interact to determine the impact attenuation for the point designs. The surface conditions include the following elements: surface bearing strength, effective surface friction, slopes, rocks and protrusions, and winds.

B.1.1 SURFACE STRENGTH

Surface bearing strength is of especial importance in the design of crush-up impact attenuation systems. If an infinitely rigid surface is assumed, then maximum use will be made of the crush-up honeycomb, that is, the full theoretical stroke would be crushed. As elasticity and deformability are introduced into the surface model then less of the honeycomb will be crushed and the balance of the stopping distance required for proper deceleration will be furnished by penetration and crushing of the ground surface. For design purposes it is conservative to size the impact attenuation system based on an infinitely rigid ground surface. This approach allows one to safely descend upon extensive rock outcroppings as well as the less rigid (and more likely) situation of an elastic soil mass.

B.1.2 DEPTH OF PENETRATION

For impact upon elastic soil surfaces the approximate depth of penetration can be estimated as follows from existing empirical data.

Although it is possible to make calculations of dynamic penetration into soils by making assumptions on bearing strength, intergranular friction, and other sources of energy absorption as penetration proceeds, it is probably more accurate to make use of empirical data available on penetration of low-speed projectiles into soils. With the latter approach, the main source of uncertainty lies in the process of extrapolating results from known terrestrial soils to the less dense (assumed) Mars soil, rather than the errors inherent in making assumptions on the entire dynamic penetration process.

Data given on page 39 of ref. B-1 contain the results of many experimental measurements of the penetration of steel balls and other high density projectiles into sand, soft rock, and hard rock. Correlation is made via a ballistic density term, γ , as follows:

$$\gamma = \frac{W}{\frac{\pi}{6} \rho_s D^3} \quad (B1)$$

where W is the weight of the impacting body and $\frac{\pi}{6} \rho_s D^3$ is the weight of a steel sphere of diameter D . An approximate formula for penetration, Y , into dry sand at 210 fps may be obtained from fig. 3.1 of ref. B-1 as follows:

$$Y = 3.1 \gamma D \quad (B2)$$

For a typical Mars Lander vehicle with $D \cong 75$ in. and $W = 930$ lbs :

$$\gamma = \frac{930}{\frac{\pi}{6} (.283) (75)^3} = 0.0149$$

$$Y = 3.1 (.0149) (75) = 3.46 \text{ in.}$$

It is difficult to assess the difference between penetration of a toroidal shape like the Mars Lander design and the spheres used in the above calculation, but the correlation could be based on the relative submerged areas. For the sphere, the bearing area would be $\pi (DY - Y^2) = 776$ sq. in. while the toroid submerged 3.46 in. would have a bearing area over 2,000 sq. in. On this basis, the toroid would penetrate even less than 3.46 in.

Ref. B-2 presents the following empirical formula, based on more recent data on soil penetrations:

$$Y = 6.4 SN \sqrt{W/A} \ln (1 + 2 \nu^2 \times 10^{-5}) \quad (B3)$$

where S is a soil constant, N is a nose shape constant, and A is the frontal area of the projectile in sq. in. Taking $S = 5$ for a loose dry sand, $N = 0.6$, and $A \cong 2,500$ sq. in. :

$$Y = 6.4 (5) (0.6) \sqrt{930/2500} \ln 1.88 = 7.4 \text{ in.}$$

A possible cause of the factor-of-two difference between the estimates made previously may lie in the fact that ref. B-1 used data on small diameter steel balls (0.356 in. to 4.3 in.) while ref. B-2 used projectiles in the 3 in. to 18 in. range. Applied to the large size Mars Lander, one would therefore tend to lean toward the 7.4 in. prediction. In either case, however, it is perhaps sufficient to note that these penetrations into the least resistant soil (of the dry variety, that is) are quite small - mud penetrations are quite deep, and may be expected to be less for impact on harder media.

Note that the Mars soil is anticipated to have a density of $1 \pm 0.6 \text{ gm/cm}^3$, while the empirical results above were obtained with sand densities about 1.6 gm/cm^3 . The method of ref. B-1 would scale penetration inversely with target density, which would increase the 3.4 in. prediction to 5.54 in. for the least dense Mars soil. Ref. B-2 uses penetration inversely proportional to the square root of density, and the 7.4 in.

prediction is increased to 9.4 in. for the least dense Mars soil. To summarize, it appears that the highest empirical estimate is 9.4 in., and the expected value would be somewhat lower.

In regard to the g-loadings experienced by the lander, it must be noted that the total stopping distance is the significant parameter. For a constant deceleration process:

$$\text{Average } g = \frac{(210)^2 (12)}{64.4 Y} = \frac{8,220}{Y} \text{ g's} \quad (\text{B4})$$

In this case Y is the penetration plus the crushup stroke of the honeycomb, or about 12 in. plus soil penetration. Therefore, on impact with an unyielding surface, the average deceleration would be 685 g while the highest penetration estimate made previously will produce an average deceleration of 384 g. The greatest influence on g-loading is therefore found to be the crushup stroke rather than penetration, and the exact calculation of penetration is not of utmost practical importance.

B.1.3 EFFECT OF IMPACT VELOCITY ON PENETRATION

On normal impact of the Mars Hard Lander, with yielding and energy absorption provided primarily by the crushup material of the Lander and by the penetration process into the Mars surface (and only to a minor extent by local flexibilities within the component package), the assumption will be made that all components experience approximately the same deceleration-time history. In the discussion average decelerations will be used as a reference. Some additional factor should be applied later in final detailed design to account for departure of the pulse shape from a square wave.

Previously estimates of penetration into the Mars surface were made, using empirical data provided by ref. B-1 and ref. B-2 at an impact velocity of 210 fps. Since the impact velocity is expected to vary, further calculations are made for velocities from 100 fps to 300 fps. Average decelerations, $G = V^2/2Y$, are also included and plotted in fig. B-1 as follows:

TABLE B-1. PENETRATIONS CALCULATED FROM
FIG. 3.1 OF REF. B-1 (KORNHAUSER)

| V (fps) | 100 | 150 | 200 | 250 | 300 |
|------------|-------|-------|-------|-------|-------|
| P (dia.) | 1.1 | 2.0 | 3.0 | 4.0 | 6.0 |
| Y (inches) | 1.23 | 2.24 | 3.36 | 4.43 | 6.72 |
| Avg. G | 1,520 | 3,380 | 2,220 | 2,600 | 2,490 |

TABLE B-2. PENETRATIONS CALCULATED BY
YOUNG'S EQUATION, REF . B-2

| V (fps) | 100 | 150 | 200 | 250 | 300 |
|------------|------|-------|-------|-------|-------|
| Y (inches) | 2.14 | 4.34 | 6.87 | 9.49 | 12.05 |
| Avg G | 875 | 1,740 | 1,080 | 1,230 | 1,390 |

Note that the slopes of the curves are similar, despite the two-to-one difference in numerical values (discussed previously). 2,000g is selected as an order of magnitude approximation, constant in the 100 to 300 fps velocity range. Selection of a constant deceleration independent of velocity implies a constant-force penetration process, and in this case the force would be $(930)(2,000)$ = about 2,000,000 lbs. as the Lander penetrates the Mars surface.

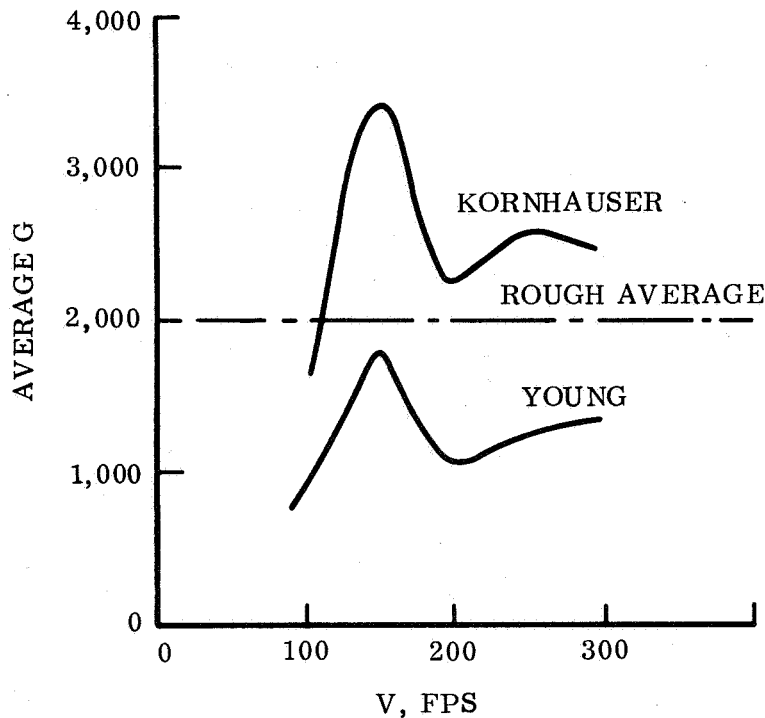


Figure B-1. Penetrations - Effect on Average Deceleration

Crushup of the honeycomb material is also a more-or-less constant force process. Assuming an 8 in. deflection at an impact velocity of 200 fps, the average deceleration on impact with a rigid surface would be $(200)^2/(2) (.667) (32.2) = 933g$. This is about half the surface-penetration resistance, which implies that most of the deflection will be obtained from the crushup rather than from surface penetration.

If the Mars surface resistance is constant and yields exactly at 2,000g and the honeycomb yields at 1,000g and does not increase in resistance as it crushes, the entire stopping process would resemble impact on a rigid surface, since the Mars surface would not be penetrated at all. However, one might expect the honeycomb resistance curve to have peaks above the Mars surface resistance curve, and the actual decelerations will be somewhat below 1,000g. For conservative estimates, however, 1,000g seems appropriate on normal impact and no adverse effects are expected at velocities within the range of interest for the Mars mission.

B.1.4 SURFACE ROCKS AND ROUGHNESS

Rocks and surface protrusions are specified by use of a characteristic dimension. For point design purposes the rocks are assumed of such proportions that they have a five inch damage potential or penetration capability. In sizing the attenuator for point designs the surface condition of rocks is treated by evaluating two expressions for honeycomb thickness and selecting the larger t-value for the thickness in a particular

$$t = \text{stroke} + \text{rock height} \quad (B5)$$

$$t = \frac{\text{stroke}}{\text{efficiency factor}} \times \text{factor of safety} \quad (B6)$$

direction around the Lander. The reasoning underlying eq. B5 is that after the full stroke is used, an additional depth of honeycomb equal to the height of a rock is available to protect the payload container against a penetration. This same material is considered as providing a factor of safety on stroke and provision for material crush-up efficiency. Eq. B6 is based on the following considerations. The theoretical stopping distance (stroke) is computed and increased by an amount to allow for a factor of safety and a stroke efficiency factor. The extra material is then counted as also active in providing the necessary rock protection capability to the crush-up system. This basis for this approach is the randomness of the factors contributing to the attenuation thickness. That is, the probability of encountering rocks of full penetrating capability (in this case, 5 in.) or more and the stroke efficiency being at its lowest value and the touchdown velocity conditions being more severe than as programmed in the mission are believed negligible and of such small consequence that the mission probability of success could not be significantly affected by assuming that these events do not occur concurrently.

B.1.5 SURFACE FRICTION

The Martian surface condition has been interpreted to include a roughness which produces surface friction. The friction is assumed to be sufficient to eliminate the component of the impact velocity vector parallel to the ground surface by sliding. This general assumption is all that is required since reasonable surfaces will gradually slow the lateral motion of the Lander unless or until an obstacle or protrusion is encountered in which case the crush-up material will actively protect the Lander payload from damage due to sidewise impact.

The result of this assumption is that the kinetic energy of impact is allocated to two distinct absorption processes. The normal velocity and, therefore, the associated kinetic energy are absorbed by the attenuator and (where applicable) ground penetration. The velocity parallel to the ground surface and its corresponding kinetic energy are absorbed by sliding friction.

B.1.6 SLOPES

The slopes which may be impacted by the Lander are important in sizing the impact attenuation system for two reasons. First, the vector resultant of descent and horizontal wind velocities will be more or less effective depending upon the slope impacted. This is true since the normal velocity component is used to compute the stroke. Second, the slopes encountered when considered along with the Lander-body orientation (for non-omnidirectional Landers) will influence the amount of material needed to wrap the Lander configuration as seen in elevation. This can be seen with the aid of figs. B-2 and B-3. For a fixed ϕ -angle it is apparent that an increasing θ implies that added material is required on the sides of the Lander.

For the purpose of detailed design, as the θ -angle increases the Lander must be investigated for crush-up along more directions. In this way the adequacy of crushed cross sectional area for various plane orientations is examined. This can best be explained by reference to figs. B-4 and B-5. Plotted in fig. B-4 is gross cross-sectional area against stroke for crush-up normal to various planes. For both omnidirectional (fig. B-2) and multidirectional (fig. B-3) Lander geometries it is seen that the magnitudes of the areas are different for different direction. This effect which is produced by Lander geometry and material behavior requires several θ -angles from the greatest slope to a flat surface to be examined. This point is further discussed in connection with each point design.

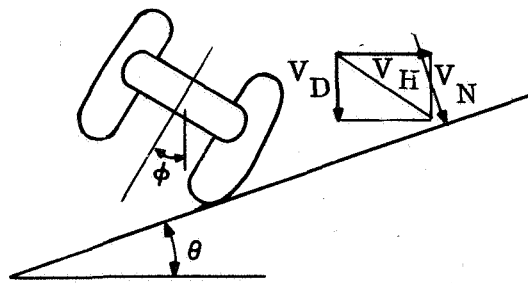


Figure B-2. Omnidirectional Lander
Touchdown Upon a Slope

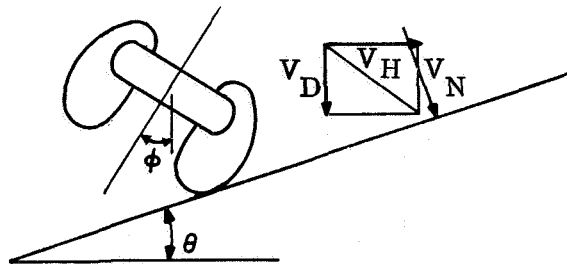


Figure B-3. Multidirectional Lander
Touchdown Upon a Slope

B.1.7 WIND EFFECTS

The wind specification has been interpreted as a steady state horizontal velocity component superimposed on the programmed descent velocity. The wind is treated as acting in the plane determined by the descent velocity vector V_D and the normal to the surface slope encountered. For point design purposes the wind magnitude was taken as 220 fps. The significance of the wind on the Lander design is elaborated upon later in this Appendix.

One other environmental constraint must be mentioned - parachute sway angle. For the various Hard Lander descent conditions this angle, as measured from the local vertical can be as large as 40° . The importance of this is that the orientation of the Lander can vary within a solid angle of 80° at the instant it impacts a sloping surface (refer to figs. B-6 and B-7). The net effect is that the normal velocity component perpendicular to the impacted slope is used to compute the stroke in the various principal directions. With this data the desired body contour can then be constructed. The details are presented with each specific point design.

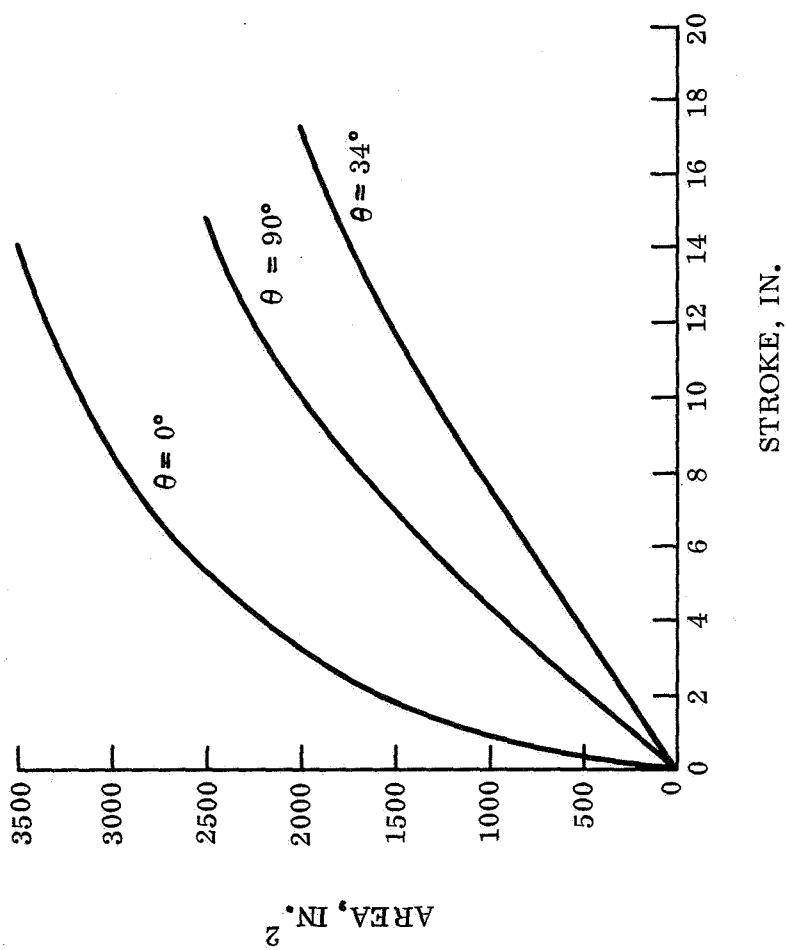


Figure B-4. Gross Cross Sectional Area vs Stroke for Omnidirectional Lander

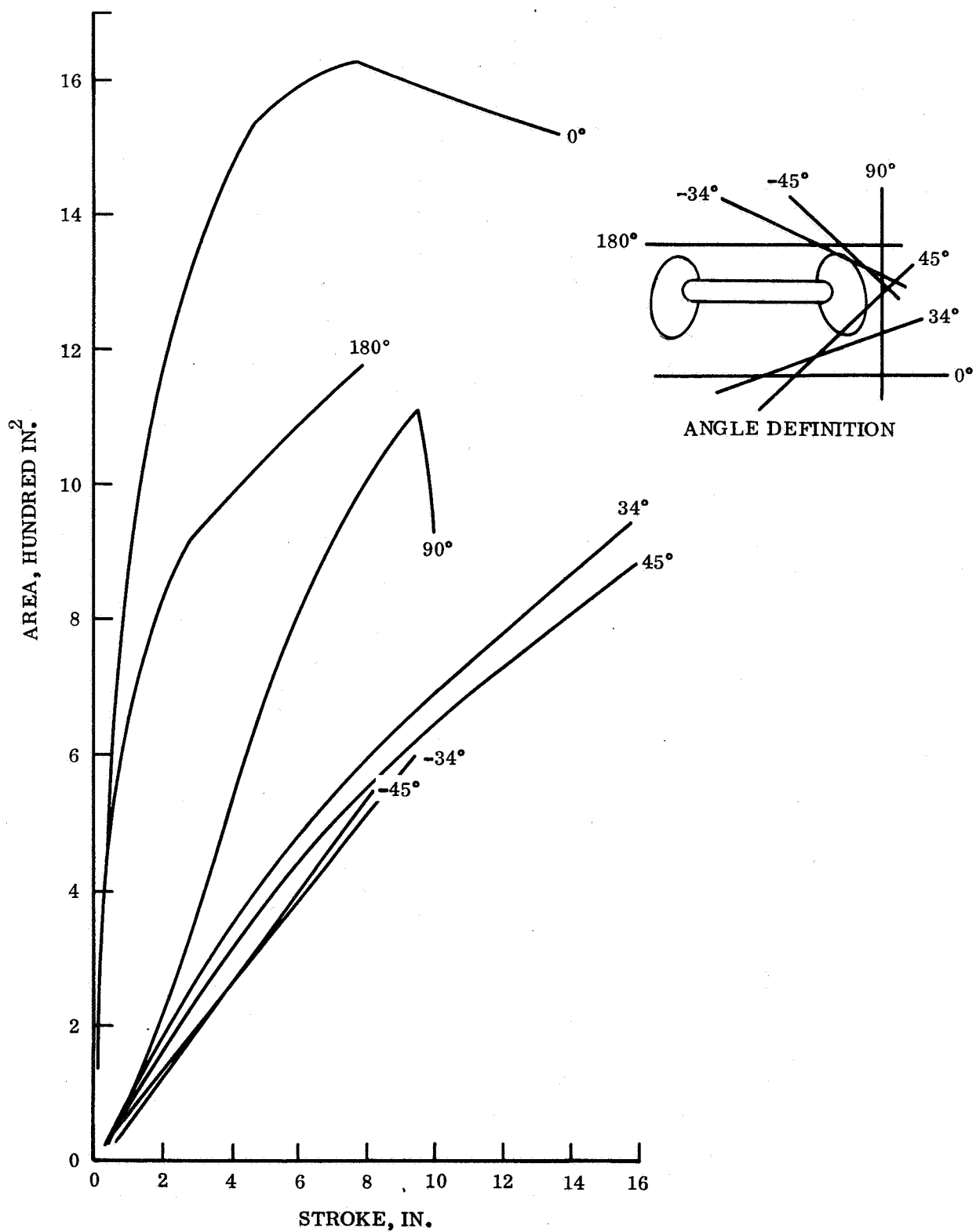


Figure B-5.. Gross Cross Sectional Area vs Stroke for a Typical Multidirectional Shape

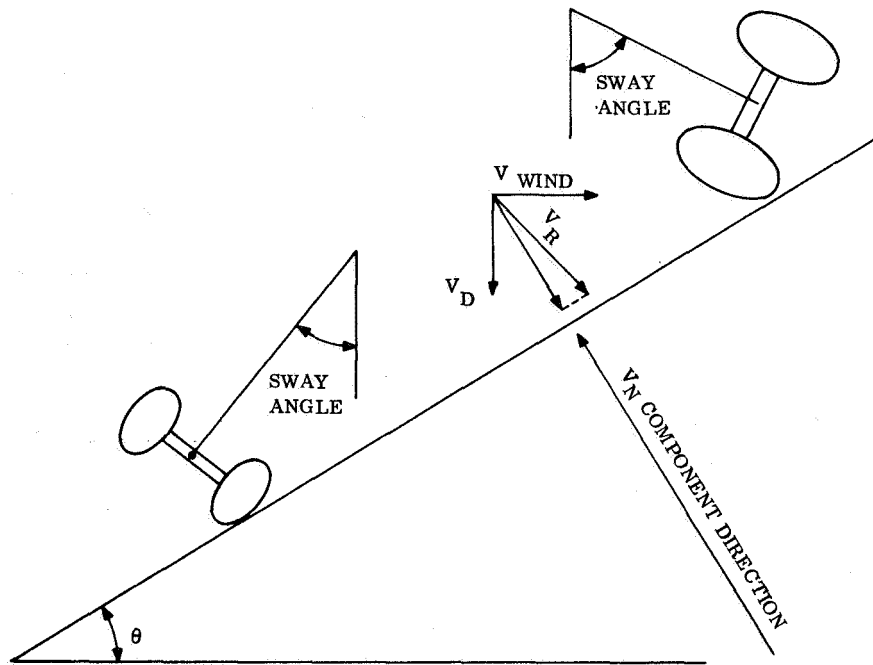


Figure B-6. Interaction of Environmental Definitions to Define Lander Touchdown Conditions (Omnidirectional Lander)

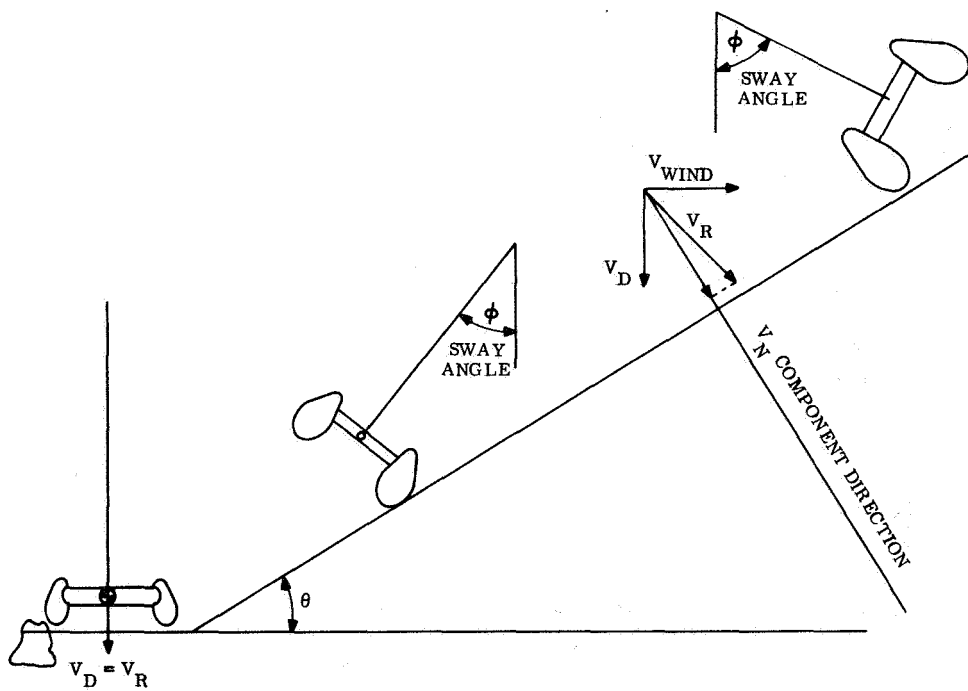


Figure B-7. Interaction of Environmental Definitions to Define Lander Touchdown Conditions (Multidirectional Lander)

B.1.8 SECONDARY IMPACT OF THE LANDER VEHICLE

The combined environmental conditions of wind, parachute sway, and varying surface slopes indicated that an investigation of secondary impacts of the Lander vehicle was warranted in order to determine post impact vehicle behavior.

This secondary impact condition can exist with certain combinations of parachute swing angles, surface wind velocities, and surface slopes. However, the probability of obtaining such unfavorable combinations is quite low. The purpose of this analysis is to determine the probabilities of obtaining secondary impacts (on the top side of the Mars Lander) at various velocities, and to ascertain what value of secondary impact velocity is appropriate for design purposes from a probabilistic point of view.

A complete dynamic analysis of the impact problem is quite difficult and tedious, and probably unwarranted in view of the unknowns in the physical quantities required to perform the complete analysis. For example, assumptions would be necessary on the characteristics of honeycomb material in the Lander configurational contours being crushed at an angle. Further, it would be necessary to make assumptions of the relative resistance of the Mars surface material in tangential deformation (friction, as it were) versus normal penetration. Fortunately, however, if the Lander is studied in a rigid-body mode with impulsive normal and tangential inputs, it is found that some of these unknowns are not required in order to obtain solutions of the motion after the first impact. In order to obtain an appropriate value of secondary impact velocity, therefore, the impulsive momentum approach is employed in the following analysis.

B.1.8.1 Equations of Motion

In this analysis, it is necessary to assume that the first impact is impulsive, and that the Lander has not rotated appreciably during the impact. Examination of this assumption shows that it does introduce some error, since typical impact durations will result in rotations of the order of 20 to 40° while the impact is in process. In the equations that follow, this geometry change effect could be taken into account as a second iteration. However, for purposes of this first approximate analysis, it will be assumed that the Lander does not rotate during the first impact.

Another major assumption necessary to obtain simple solutions is that there is negligible rebound or bounce, such that the point of impact is brought to rest both tangentially and normally during the impact. In this way, the impact point becomes an instant center of rotation, and the c.g. of the Lander must move with velocity V_2 normal to the instant center c.g. line after impact, as shown in figs. B-8 and B-9.

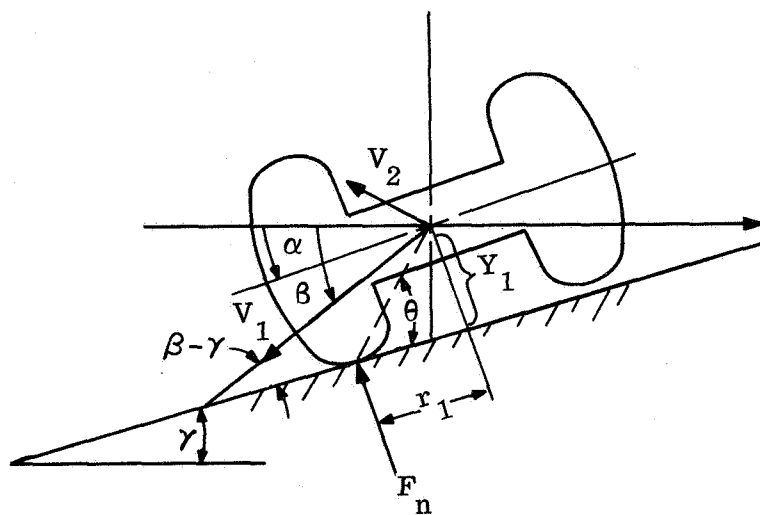


Figure B-8. Omnidirectional Lander with Sway, Wind, and Slope Touchdown Conditions

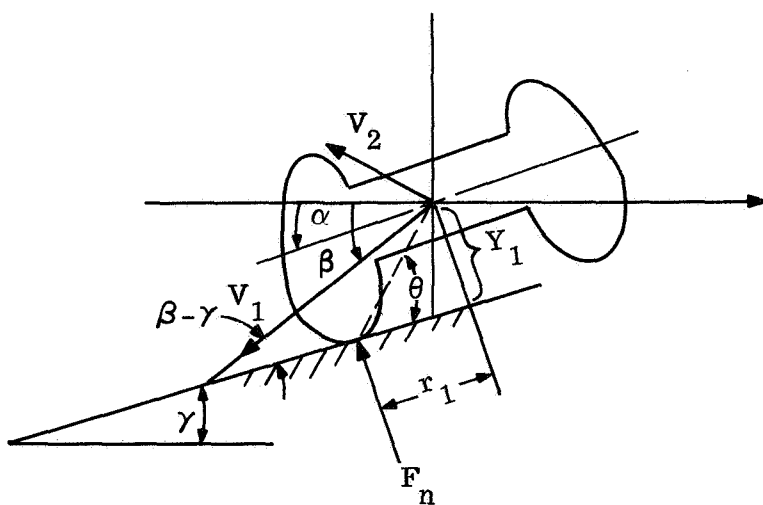


Figure B-9. Multidirectional Lander with Sway, Wind, and Slope Touchdown Conditions

Observe that the Lander will flip over only if $\theta > \beta - \gamma$, as shown in figs. B-8 and B-9. The angle θ is a function of the parachute swing angle, α , the surface angle γ , and the contours of the Lander.

$$\tan \theta = Y_1 / r_1 \quad (B7)$$

If motion stops at the point of contact:

$$V_2 = \dot{\alpha} \sqrt{r_1^2 + Y_1^2} = \frac{2r_1}{\cos \theta} \quad (B8)$$

Writing an impulse-momentum equation for motion normal to the Mars surface:

$$\int F_n dt = M [V_1 \sin (\beta - \gamma) + V_2 \cos \theta] \quad (B9)$$

Tangent to the Mars surface:

$$\int F_r dt = M [V_1 \cos (\beta - \gamma) - V_2 \sin \theta] \quad (B10)$$

Angular impulse-momentum:

$$Y_1 \int F_r dt - r_1 \int F_n dt = I \dot{\alpha} \quad (B11)$$

Combining eqs. B8, B9, B10 and B11:

$$\frac{V_2}{V_1} = \frac{\frac{Y_1}{r_1} \cos (\beta - \gamma) - \sin (\beta - \gamma)}{\left(\frac{I}{r_1^2 M} + 1 \right) \cos \theta + \frac{Y_1}{r_1} \sin \theta} \quad (B12)$$

The maximum velocity of a point on the Lander after it flips over will be the sum of the c.g. velocity and the rotational velocity:

$$\Sigma V = V_2 + r_2 \dot{\alpha}$$

$$\frac{\Sigma V}{V_2} = 1 + \frac{r_2}{r_1} \cos \theta \quad (B13)$$

B.1.8.2 Calculation of Secondary Impact Velocity

In order to facilitate a rapid hand calculation of ΣV , fig. B-10 was prepared with scaled figures of the Lander; from which Y_1 and r_1 were obtained by direct scaling. The angle θ was calculated from eq. B7 and $I/r_1^2 M$ calculated for $I = 2,020 \text{ lb-ft}^2$ and $M = 930 \text{ lbs}$. With these quantities and with r_2 taken as 2 ft as a reasonable estimate of the location of the point of secondary impact, eq. B12 and eq. B13 were employed to find ΣV . Fig. B-10 contains the results of the computations.

B.2 INTERPRETATION OF ENVIRONMENTAL SPECIFICATIONS

Application of the dynamic analysis of Appendix A yielded the results shown in fig. B-10 for the secondary impact velocity. Before these results may be used, however, some attention must be paid to the probabilistic character of the driving physical parameters especially

Surface slope angle - θ

Parachute sway angle - ϕ

Surface wind velocity - v

In the following section the general random character of these parameters is detailed based on the Preliminary Draft, Mars Engineering Model Parameters for Mission and Design Studies, Langley Research Center, May 1968. It is noted that an exhaustive rigorous statistical analysis was deferred for future final design activity pending more elaborate surface definition. The present first-order analysis is an indicator of significant trends and parameter sensitivity.

In general both the omnidirectional and multidirectional Landers will not dissipate their entire kinetic energy upon initial impact although they have the design capability to do so. As a result some provision might be made for repeated impacts on the same part of the Lander as was first contacted. Subsequent impacts on the identical surface are, however, assumed to be of such low probability that they may be neglected. Subsequent impacts on a portion of the Lander not crushed previously can be tolerated if such secondary hits are not more severe than the original velocity assumed in the Lander design. The adequacy of the velocities used in the omnidirectional and multidirectional vehicle designs are investigated later in this Appendix.

Secondary impact is significantly affected by both parachute sway and the slope angle encountered. Parachute sway is analytically treated as follows. The simplest approximation is that of a pendulum. For a given maximum sway angle and neglecting

wind effects, the statistical distribution of the sway angle is sinusoidal regardless of the Martian 'g' or the length of the parachute lines. If the sophistication of an atmosphere is introduced into the analysis, the distribution of the sway angle, φ , is still sinusoidal. The atmosphere will produce an amplitude decay and a reduced frequency, but it does not affect the basic distribution of φ . This cumulative distribution for the sway angle φ is given in fig. B-11.

B.2.1 LARGE AMPLITUDES OF SWAY ANGLE

Experience shows that the motion of a pendulum bob is periodic, and we have seen that it is approximately harmonic and therefore sinusoidal as a first approximation. The Martian gravity constant, 'g', and shroud length, r, do not affect this time duration vs. φ distribution or, consequently, the (probability) distribution of the pendulum angle, φ .

The presence of the Martian atmosphere means that each amplitude is slightly less than the one before due to damping. However, this effect is sufficiently small so that it may be neglected. We have studied small amplitudes of φ , where $\varphi \approx \sin \varphi$ is a good approximation. This is not true for $\varphi = 40^\circ$ ($0.69813 \neq 0.64279$). By conservation of energy (and with immersion in the fluid of the atmosphere neglected), a result for the probability of φ in terms of elliptic integrals is obtained.

Once again, a cumulative distribution function for φ may be derived and this is plotted as in fig. B-12.

Over-laying the plotted cumulative distribution function upon the sinusoidal approximation, the difference is scarcely visible to the eye.

However, the corresponding variations of frequency with amplitude (circular error) could be significant in the sense of horology.

B.2.2 SLOPES

Probabilistic considerations also surround surface slope definition as provided in the following table which is based on latest NASA/LRC specifications.

The information was derived from fig. III-C-4 of ref. B-3 (For consistency the abscissa was corrected to 38° and the residual statistically interpolated from 48° to 90° . (Normal probability paper was used, so that statistical interpolation, not linear, was employed). The cumulative distribution function for slope angle was developed and plotted as fig. B-13 and reduced to the convenient tabular form of table B-3.

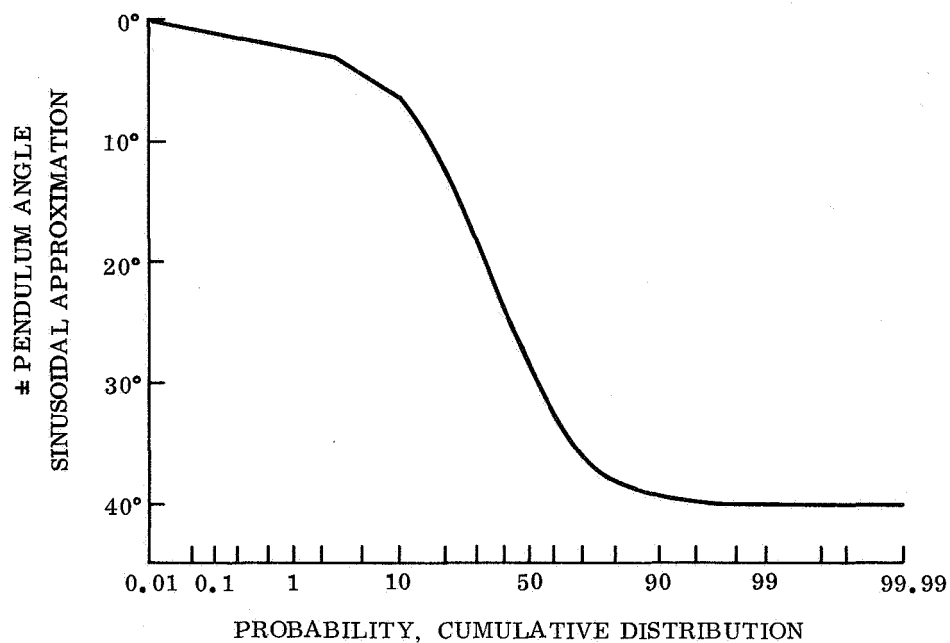


Figure B-11. Cumulative Distribution Function for Pendulum Angle Using Sinusoidal Approximation

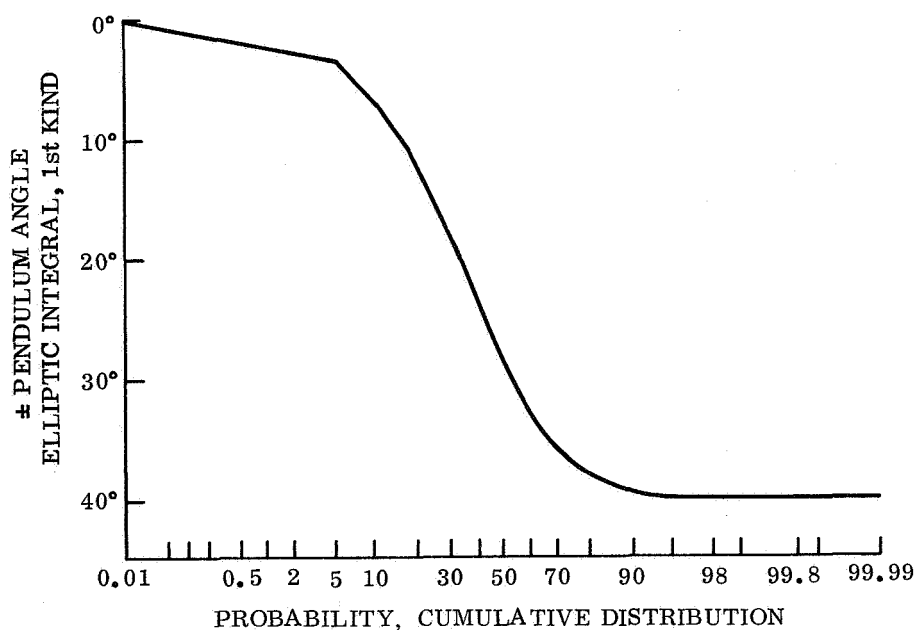


Figure B-12. Cumulative Distribution Function for pendulum Angle Based on Elliptic Integral Formulation of the Problem

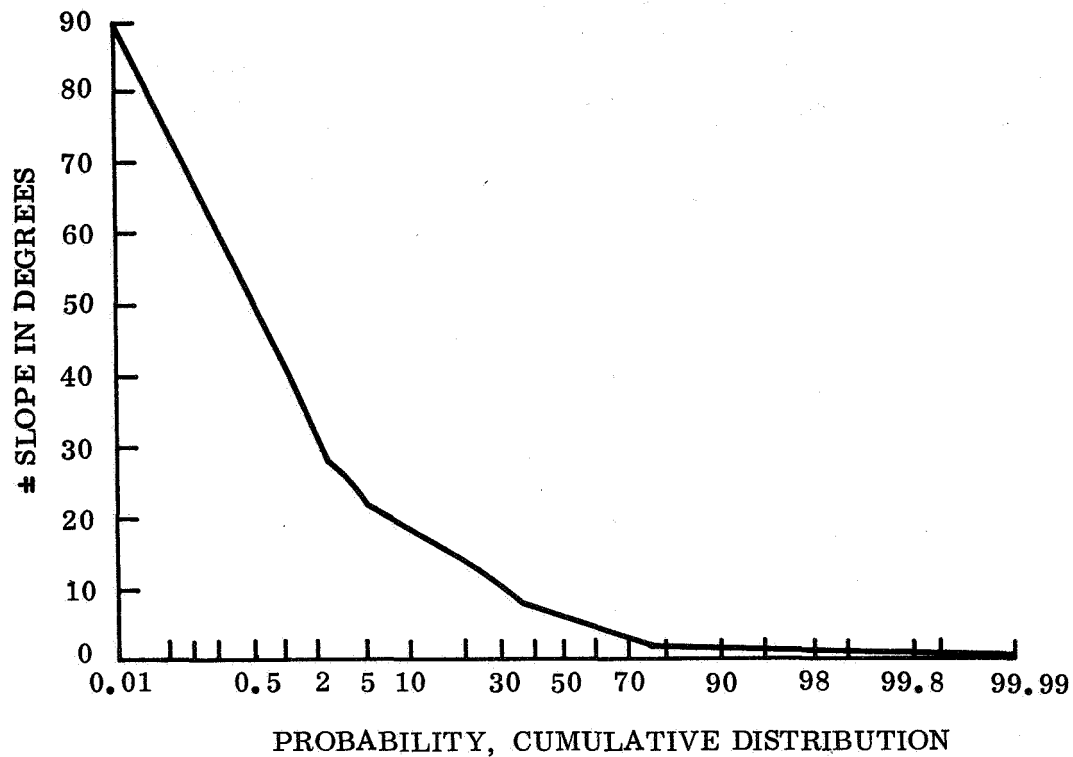


Figure B-13. Cumulative Distribution Function for Slope Angle

B.2.3 WIND SPEED

Probabilistic analyses were also extended to include surface wind speed. From ref. B-3, the median speed is 55m/sec, the maximum is 67 m/sec and the minimum is 37 m/sec. There are actually no maximum or minimums in statistics nor is there any physical reason for saying that wind speeds of 67.1 or 36.9 m/sec on Mars are impossible. Rather, we make the usual assumption that these are the $\pm 3\sigma$ equivalents, i. e., $P(s > 67) = P(s < 37) = 0.0013$. In this problem, this assumption is conservative i. e., the statement "S can exceed 67 only 0.13 percent of the time" is more conservative than "S cannot exceed 67." The associated cumulative distribution curve is drawn as fig. B-14.

B.2.3.1 Compound Probabilities

Previously we have developed cumulative distribution groups for pendulum angle ϕ , wind speed v and surface slope θ . If $f(\theta, v, \phi)$ is a monotonic function (changes in one direction only as its variables each change in one direction) then the α percent levels of f corresponding to the β percent levels of θ, v and ϕ are as presented in table B-4.

TABLE B-3. STATISTICAL DISTRIBUTION OF SLOPE ANGLE

| Angle (deg) | Distribution Probability (%) | Cumulative Probability (%) |
|----------------|---------------------------------|-------------------------------|
| 2 | 22 | 22 |
| 4 | 14 | 36 |
| 6 | 14 | 50 |
| 8 | 14 | 64 |
| 10 | 5 | 69 |
| 12 | 5 | 74 |
| 14 | 6 | 80 |
| 16 | 5 | 85 |
| 18 | 4 | 89 |
| 20 | 3 | 92 |
| 22 | 3 | 95 |
| 24 | 0.5 | 95.5 |
| 26 | 0.9 | 96.4 |
| 28 | 1.1 | 97.5 |
| 30 | 0.3 | 97.8 |
| 32 | 0.3 | 98.1 |
| 34 | 0.2 | 98.3 |
| 36 | 0.2 | 98.5 |
| 90 | 1.5 | 100 |

TABLE B-4. COMPOUND VS SIMPLE PROBABILITIES

| α (simple) (%) | $\beta = \sqrt[3]{\alpha}$ (compound) (%) |
|-----------------------|--|
| 0 | 0 |
| 5 | 36.8 |
| 10 | 46.4 |
| 20 | 58.5 |
| 30 | 66.9 |
| 40 | 73.7 |
| 50 | 79.4 |
| 60 | 84.3 |
| 70 | 88.8 |
| 80 | 92.8 |
| 90 | 96.6 |
| 95 | 98.3 |
| 100 | 100 |

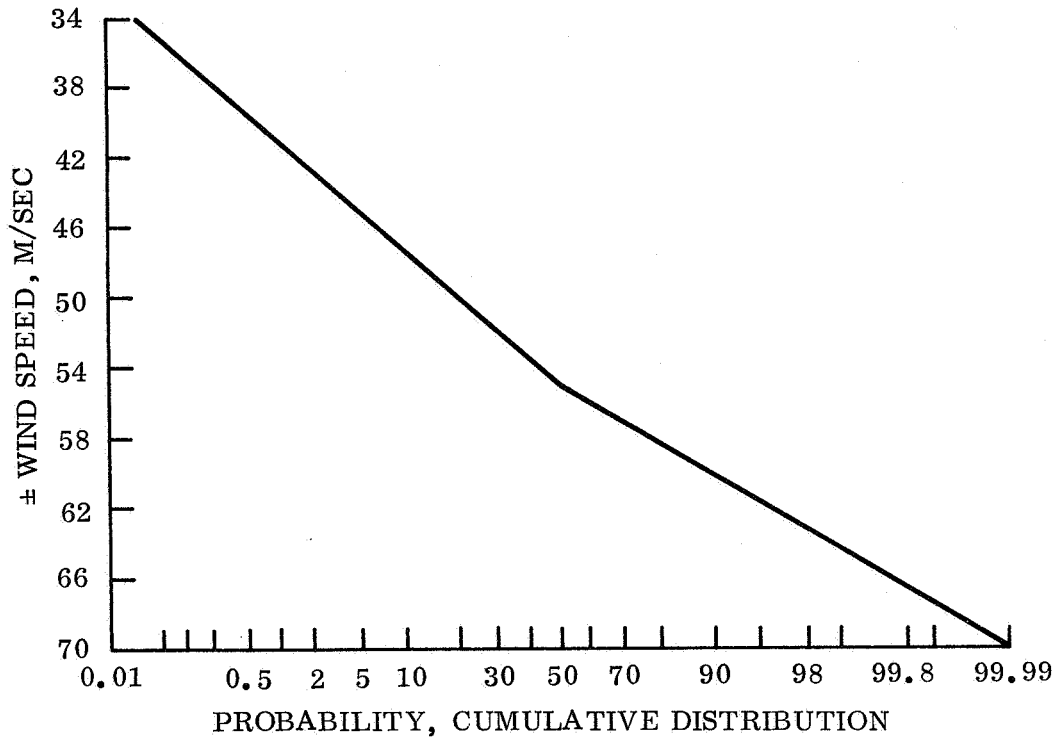


Figure B-14. Cumulative Distribution Function for Wind Speed Variation Based on NASA/LRC Preliminary Specification

This consideration enables one to report statistically on the function, the secondary velocity, f , by evaluating it 13 times. It is these compound probabilities which must be included in an extensive analysis of the secondary impact problem.

For convenience in computations, the matrix was calculated with uniformly spaced pendulum angles $\phi = -40^\circ, -20^\circ, 0^\circ, 20^\circ, 40^\circ$ and ground slopes $\theta = -30^\circ, -15^\circ, 0^\circ, 15^\circ$, and 30° .

For computing averages and other statistical measures, each result for ΣV must be weighted by its likelihood or probability. The slope values are considered to represent the slope intervals with the associated probability of column 3 in table B-5.

TABLE B-5. PROBABILITY OF SLOPE INTERVALS

| θ (deg) | Interval (deg) | Probability |
|----------------|----------------|-------------|
| -30 | -90, -22.5 | 0.0225 |
| -15 | -22.5, -7.5 | 0.1775 |
| 0 | -7.5, 7.5 | 0.6000 |
| 15 | 7.5, 22.5 | 0.1775 |
| 30 | 22.5, 90 | 0.0225 |

The probabilities were obtained from the cumulation distribution group for positive slope. Symmetry implies that the graph for negative shape is identical.

Similarly, the ϕ -angle values must represent the angular intervals with the associated probability given in table B-6.

TABLE B-6. PROBABILITY OF PENDULUM INTERVALS

| ϕ (deg) | Interval (deg) | Probability |
|--------------|----------------|-------------|
| -40 | -90, -40 | 0.025 |
| -20 | -40, -10 | 0.395 |
| 0 | -10, 10 | 0.160 |
| 20 | 10, 30 | 0.395 |
| 40 | 40, 90 | 0.025 |

A probabilistic weighting matrix can therefore be constructed

| θ -angle ↓ ↘ ϕ -angle | 0.025 | 0.395 | 0.160 | 0.395 | 0.025 | ck. sums |
|--|---------|---------|---------|---------|---------|----------|
| 0.0225 | 0.00056 | 0.00889 | 0.00360 | 0.00889 | 0.00056 | 0.02250 |
| 0.1775 | 0.00444 | 0.07011 | 0.02840 | 0.07011 | 0.00444 | 0.17750 |
| 0.6000 | 0.01500 | 0.23700 | 0.09600 | 0.23700 | 0.01500 | 0.60000 |
| 0.1775 | 0.00444 | 0.07011 | 0.02840 | 0.07011 | 0.00444 | 0.17750 |
| 0.0225 | 0.00056 | 0.00889 | 0.00360 | 0.00889 | 0.00056 | 0.02250 |
| | | | | | | 1.00000 |

Arranging the values of ΣV monotonically (as calculated for a wind velocity of 110 fps), results in table B-7.

This information is plotted as a cumulative distribution curve (fig. B-15) for the secondary velocity ΣV . It is noted that a wind of 110 fps was assumed for this computation.

Interpolating from the cumulative probability graph of fig. B-16 results in data for the histogram graph for

$$V_{\text{WIND}} = 110 \text{ fps}$$

TABLE B-7. SECONDARY IMPACT VELOCITY PROBABILITY FOR 110 FPS

| Value, X_i | Probability, p_i | Cumulative Probability (%) |
|---|--------------------|----------------------------|
| Cases of | 0 | 0.00360 |
| no flip of | 0 | 0.00389 |
| Lander | 0 | 0.02340 |
| | 0 | 0.02840 |
| | 0 | 0.00839 |
| | 0 | 0.00360 |
| | 19 | 0.09600 |
| | 48 | 0.23700 |
| | 52 | 0.07011 |
| | 53 | 0.23700 |
| | 72 | 0.07011 |
| | 97 | 0.01500 |
| | 108 | 0.00444 |
| | 115 | 0.00444 |
| | 119 | 0.00056 |
| | 125 | 0.07011 |
| | 127 | 0.07011 |
| | 128 | 0.00056 |
| | 151 | 0.01500 |
| | 156 | 0.00444 |
| | 159.5 | 0.00444 |
| | 179 | 0.00889 |
| | 180 | 0.00889 |
| | 189 | 0.00056 |
| | 226 | 0.00056 |
| | | 100 |
| median value = 52.1 | | |
| $x = \text{average value} = 61.8 = \sum p_i X_i$ | | |
| standard deviation = 40.8 = $\sqrt{\sum p_i (X_i - \bar{X})^2}$ | | |

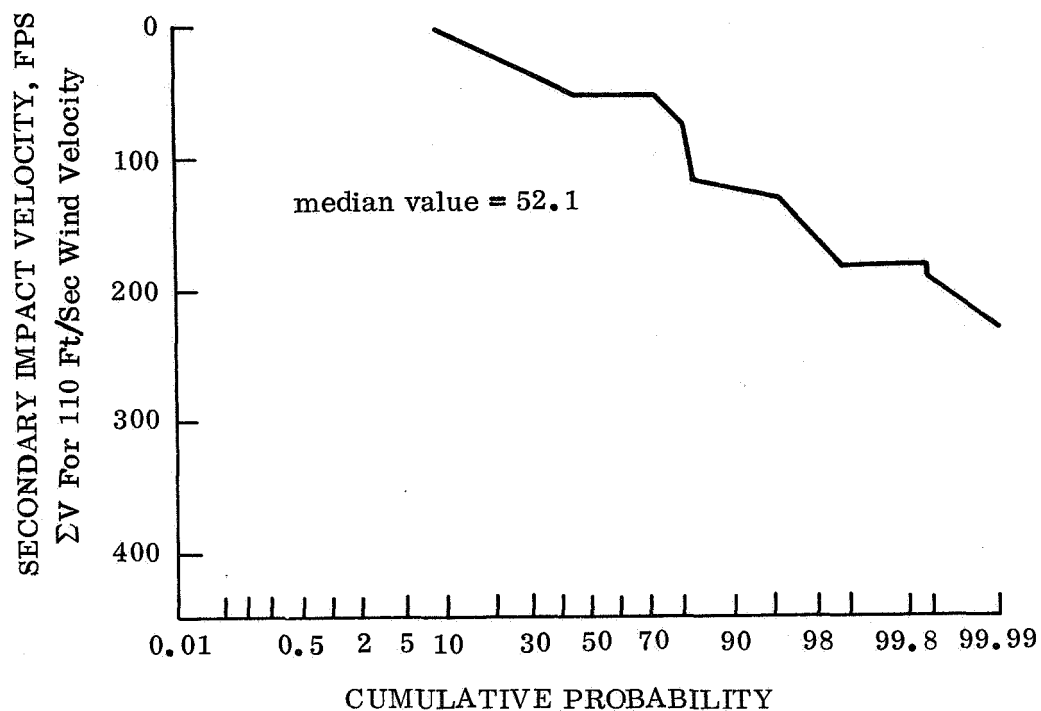


Figure B-15. Cumulative Distribution Function for Secondary Impact Velocity for a Wind Speed of 110 fps

TABLE B-8. SECONDARY IMPACT VELOCITY
CUMULATIVE PROBABILITY FOR 110 FPS

| ΣV Value | Cumulative Probability (%) | Probability Density (%) |
|----------|----------------------------|-------------------------|
| 0 | 8.2 | |
| 25 | 18 | 15 |
| 50 | 43 | 25 |
| 75 | 79 | 36 |
| 100 | 81 | 2 |
| 125 | 88.5 | 7.5 |
| 150 | 97.3 | 8.5 |
| 175 | 98.5 | 1.2 |
| 200 | 99.94 | 1.44 |
| 225 | 99.99 | 0.05 |
| 250 | 100 | 0.01 |

If the values of ΣV are arranged monotonically, but this time for a wind velocity of 220 fps, table B-9 can be constructed.

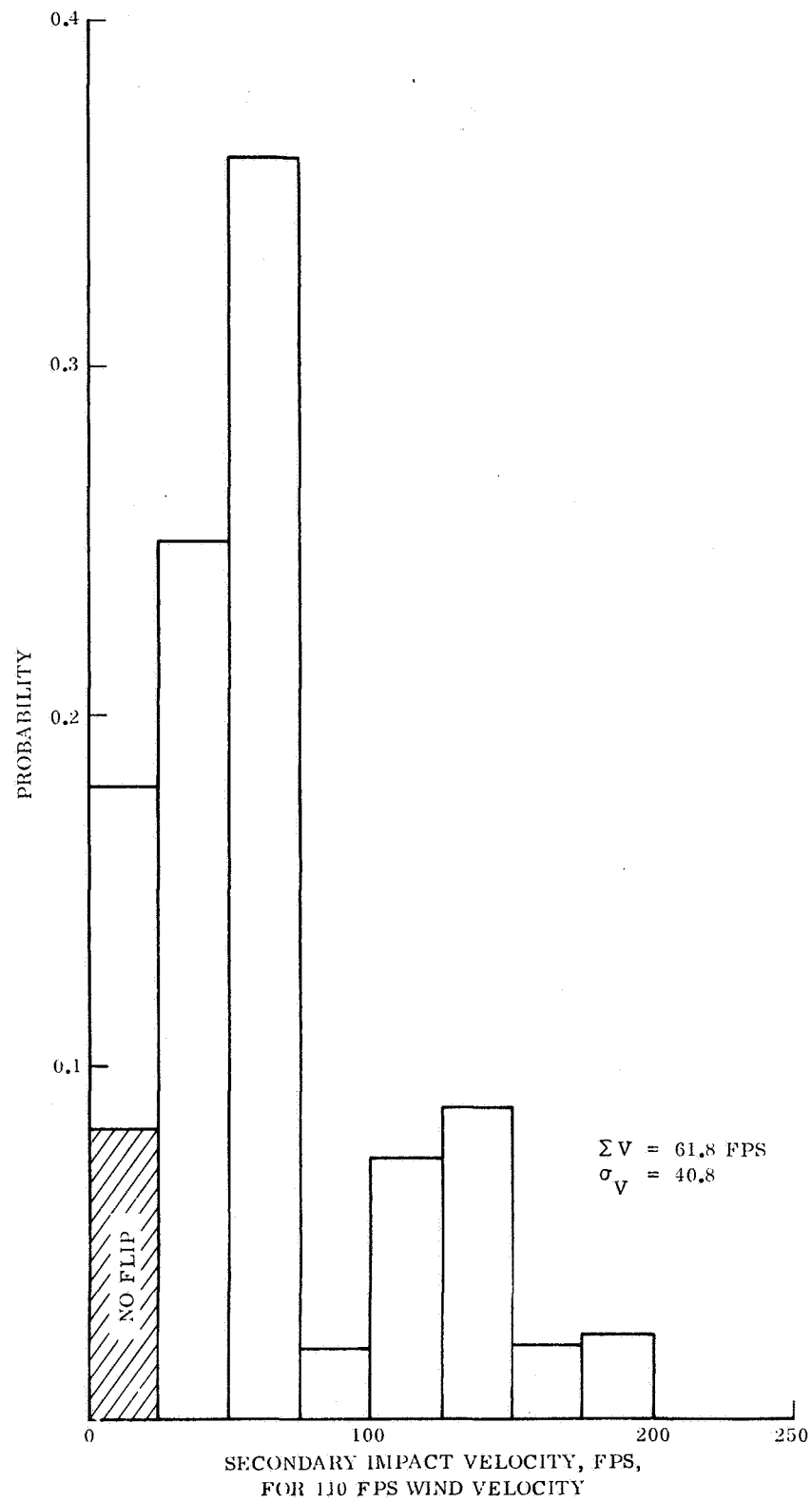


Figure B-16. Histogram For Secondary Impact Velocity Based on a Wind Speed of 110 fps

TABLE B-9. SECONDARY IMPACT VELOCITY PROBABILITY FOR 220 FPS

| Value X_i | Probability P_i | Cumulative Probability (%) |
|-------------------------|-------------------|----------------------------|
| 0 | 0.00889 | |
| 0 | 0.00889 | 1.8 |
| 129 | 0.09600 | 11.4 |
| 171 | 0.23700 | 35.1 |
| 177 | 0.23700 | 58.8 |
| 186 | 0.07011 | 65.8 |
| 205 | 0.07011 | 72.8 |
| 209 | 0.02840 | 75.6 |
| 230 | 0.02840 | 78.5 |
| 236 | 0.01500 | 80.0 |
| 252 | 0.00444 | 80.4 |
| 257 | 0.00444 | 80.9 |
| 264 | 0.00056 | 80.9 |
| 270 | 0.07011 | 87.9 |
| 273 | 0.07011 | 94.9 |
| 276 | 0.00056 | 95.0 |
| 297 | 0.00360 | 95.4 |
| 302 | 0.00444 | 95.8 |
| 308 | 0.00444 | 96.25 |
| 308 | 0.00360 | 96.6 |
| 320 | 0.00889 | 97.5 |
| 322 | 0.00889 | 98.4 |
| 331 | 0.00056 | 98.4 |
| 375 | 0.01500 | 99.9 |
| 378 | 0.00056 | 100 |
| Median Value 176.3 fps | | |
| Average Value 195.5 fps | | |
| Standard Deviation 56.9 | | |

The cumulative distribution function for secondary velocity of impact at a wind speed of 220 fps is given in fig. B-17.

Interpolating from the cumulative probability graph, fig. B-17, for

$V_{\text{WIND}} = 220 \text{ fps}$, yields table B-10. The resulting histogram is shown in fig. B-18.

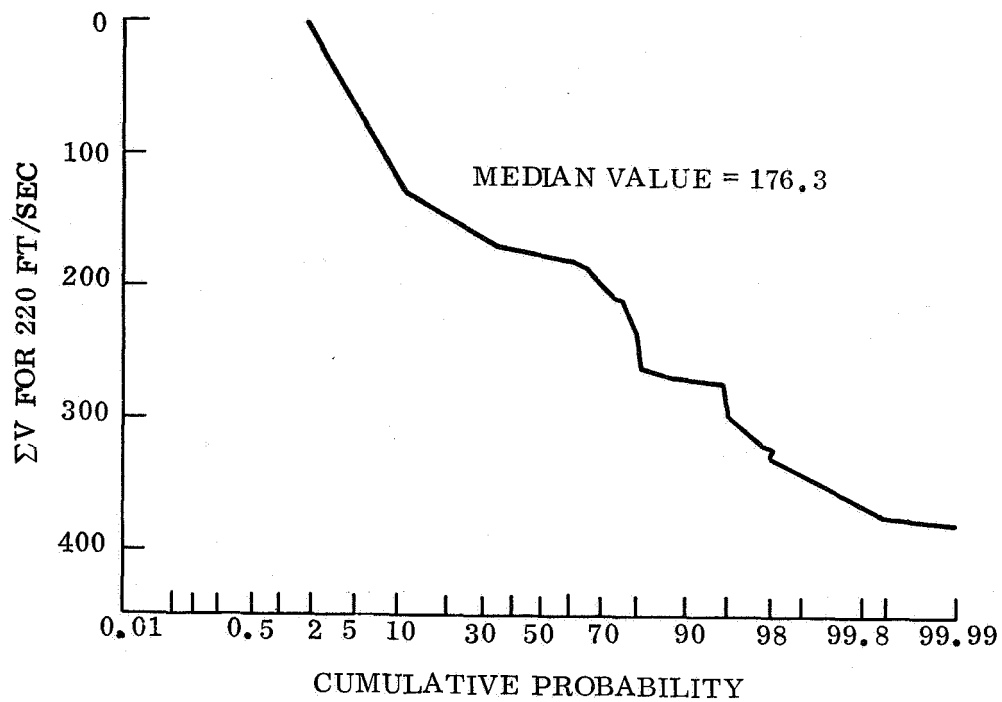


Figure B-17. Cumulative Distribution Function for Secondary Impact Velocity Based on a Wind Speed of 220 fps

TABLE B-10. SECONDARY IMPACT VELOCITY CUMULATIVE PROBABILITY FOR 220 FPS

| Σ V Value | Cumulative Probability (%) | Probability (%) Density |
|-----------|----------------------------|-------------------------|
| 0 | 1.8 | |
| 25 | 2.6 | 2.6 |
| 50 | 4 | 1.4 |
| 75 | 5.5 | 1.5 |
| 100 | 8 | 2.5 |
| 125 | 10.6 | 2.6 |
| 150 | 21 | 10.4 |
| 175 | 45 | 24 |
| 200 | 71 | 26 |
| 225 | 78 | 7 |
| 250 | 81 | 3 |
| 275 | 95 | 14 |
| 300 | 95.5 | 0.5 |
| 325 | 98.1 | 2.6 |
| 350 | 99.4 | 1.3 |
| 375 | 99.9 | 0.5 |
| 400 | 100 | 0.1 |

The previous statistical analyses were performed for the purposes of ascertaining the probability of experiencing a secondary impact velocity less than or equal to some specified value. Based upon the limited first-order approximations used, the following general trends are indicated.

B.2.3.2 Omnidirectional Lander

For this configuration the secondary impact velocity is not as important as with the multidirectional Lander. This is true since the entire Lander is designed for the same impact velocity conditions of 100 fps descent velocity and 220 fps wind velocity. For the extreme wind velocity of 220 fps which is as great as if not greater than a 3σ design figure, the cases analyzed to date show that 75 percent of the time the secondary impact velocity will be 210 fps (the resultant design velocity vector) or less. For this wind speed the Lander flips over about 92 percent of the time.

It is also noted that for a wind velocity of 110 fps, the secondary impact velocity will be 210 fps or less about 99 percent of the time, given that the Lander does in fact flip over. For the cases examined to date, only 25 percent of the time will the Lander actually flip over.

B.2.3.3 Multidirectional Lander

Similar probabilities can be determined for the multidirectional Lander. For a wind velocity of 220 fps, the Lander will flip over and impact on its back end about 92 percent of the time. The secondary impact velocity will exceed 100 fps about 92 percent of the time. Again the wind speed used is very unlikely to be attained. This is based on the probabilistic considerations in the latest NASA/LRC Mars Mission Model dated May 1968.

If the lower wind velocity of 110 fps is postulated then the Lander secondary impact velocity is less than or equal to 100 fps about 81 percent of the time. This assumes that the Lander does in fact flip over. The limited number of cases analyzed to date indicate that for the wind speed of 110 fps the Lander flips over only about 25 percent of the time. From the curves presented in figs. B-15 and B-16 other velocities may be investigated if desired.

References:

- B-1. Kornhauser, M. "Structural Effects of Impact", Spartan Books, 1964.
- B-2. Young, C. W. "The Development of Empirical Equations for Predicting Depth of an Earth-Penetrating Projectile", Sandia Laboratory SC-DR-67-60, May 1967.
- B-3. Mars Engineering Model Parameters for Mission and Design Studies, Preliminary Draft, Langley Research Center, May 1968.

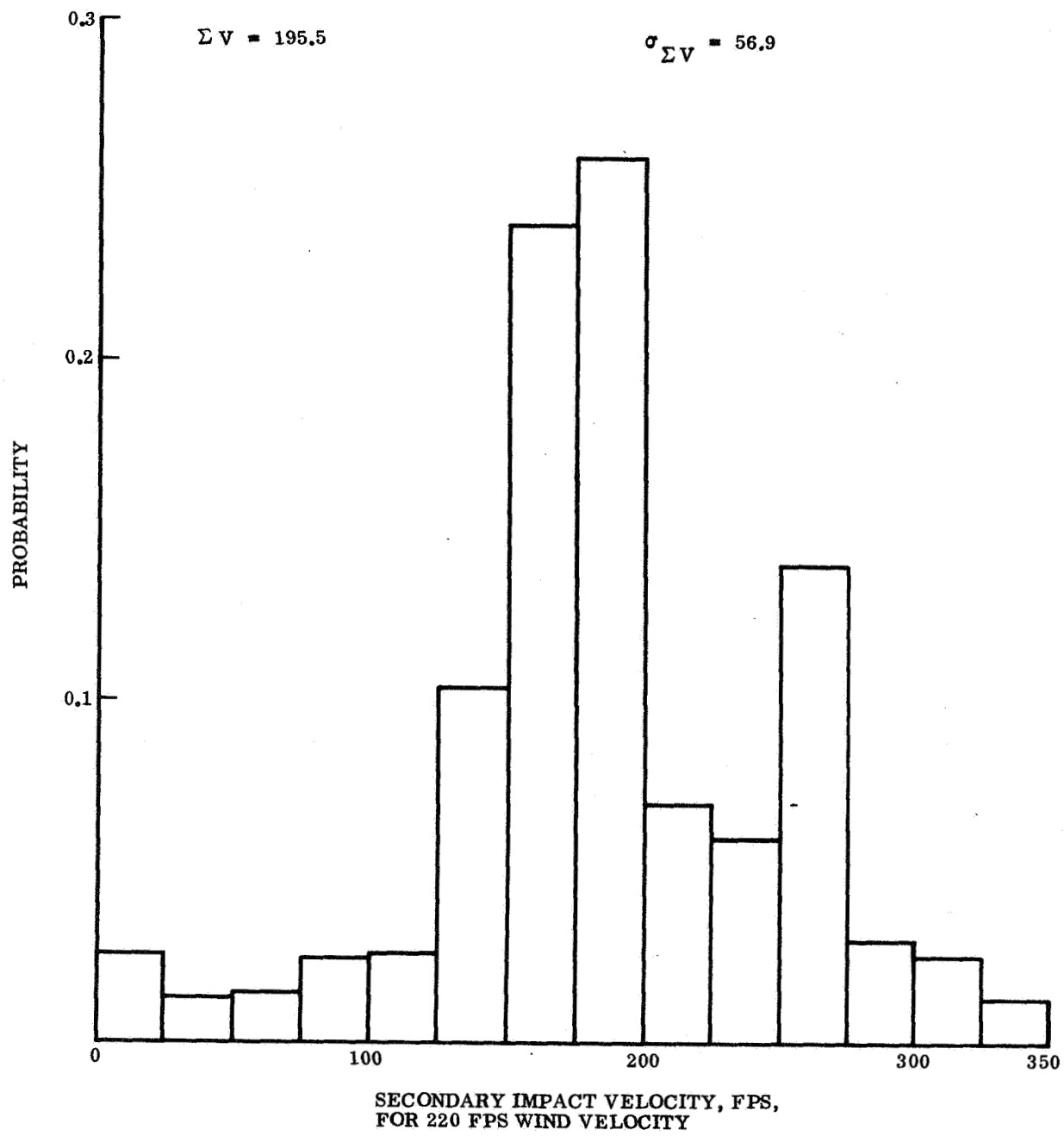


Figure B-18. Histogram for Secondary Impact Velocity for a Wind Speed of 220 fps

APPENDIX C
EFFECTS ON POINT DESIGNS DUE TO VARIATIONS
IN ASSUMED DESIGN PARAMETERS

APPENDIX C

EFFECTS ON POINT DESIGNS DUE TO VARIATIONS IN ASSUMED DESIGN PARAMETERS

The Capsule impact attenuation system design is necessarily based on nominal values for various design parameters and surface conditions. This section indicates the effects on the design due to variations in the reference conditions while identifying those sources in which perturbations are especially significant. It is important to recognize that the variations to be discussed are truly of statistical character due to uncertainties in the problem. Therefore the following discussion assumes that these variations have occurred when, in fact, their probability of occurrence is often exceedingly small.

C.1 MARTIAN SURFACE DEFINITIONS AND TOUCHDOWN CONDITIONS

This first group of variables which produce design perturbations includes:

1. ground wind velocity
2. descent velocity
3. surface slopes
4. surface bearing strength
5. rock outcrop definition
6. parachute sway
7. rigid body g-tolerance
8. payload density and system weight

In general, if the ground wind velocity and/or the descent velocity are other than the values assumed in a particular design the crush-up stroke provided will not be correct. If the actual velocities are less than the design values the stroke is on the conservative side and the deceleration load will be attenuated below the specified g-loading. If the actual velocities are in excess of those assumed in design then the resulting insufficient stroke will allow higher g-loads to be transmitted to the container structure and its contents. Since stroke required varies as the square of the component velocity normal to the surface slope, the perturbations introduced by this effect can be substantial. The velocity squared effect also influences the kinetic energy to be absorbed in the attenuator. This implies that impact velocities greater or less than those assumed will require larger or smaller volumes of crush-up material for the dish configuration. This aspect of the problem is included in the

stroke discussion since it is the stroke thickness which in conjunction with rock protection requirements determines the volume of energy-absorbent material provided.

Variations in ground surface slopes enter the capsule impact attenuation design in two ways. First, the surface slopes interact with the horizontal wind and Capsule descent velocity to produce the normal velocity component perpendicular to the surface. As just described this normal velocity vector affects the length of the stroke and the size of the attenuator. The effect of slope angle variations can not be generalized since it must be considered in conjunction with particular wind and descent velocity components. If for a particular landing situation the wind velocity is more than the descent velocity then a decrease in slope angle (flatter slope) will decrease the normal velocity and hence the stroke required for attenuation. An increase in slope angle will have the opposite effect. However, if descent velocity predominates over the wind velocity, then a steeper slope than the reference condition will decrease the normal velocity and thereby decrease the required stroke. A variation toward a flatter slope would produce the opposite effect.

The second effect of slope angle perturbations is on the configurations of the dish Landers. For the omnidirectional Lander this second effect by definition is eliminated. For multidirectional analysis this effect is important since the steeper slopes require added capability over and above some reference conditions. If a multidirectional Lander is designed for a certain surface but actually impacts on a flatter slope than anticipated, there will be a positive margin in the impact attenuator. If, however, a steeper slope is encountered, then insufficient stroke will be available to adequately stop the vehicle within acceptable g-levels. This is a direct consequence of the vehicle directionality as reflected in its geometrical shape.

Surface bearing strength influences the mission trade-offs and parametric studies as follows. All of the computations in a crushable honeycomb design are based on an infinitely rigid non-yielding surface. In this way rock tables may be impacted. Therefore one need only ask what effect a yielding (softer) surface would produce. In general the capability of the vehicle will not be compromised but actually enhanced. This is so since the stroke will be comprised of the honeycomb crush-up and the penetration of the yielding surface. If the surface variation results in a soft yielding surface then a smaller amount of honeycomb is required for crushing.

Variations in the rock size encountered by a Lander will also influence the design trade-offs. If a Lander is sized for rocks of a given characteristic dimension then it has the requisite capability for all intermediate sizes up to this dimension. Individual rocks in excess of this dimension will conceivably penetrate the attenuator and reach the container structure. However, all rocks in excess of a certain dimension do not necessarily have the angularity to be of potential danger. The long slender slivers that could be envisaged would no doubt snap before fully penetrating the impact attenuator. Moreover, larger rocks tend to be larger in all respects and hence more flat. As a result the net effect is that of an isolated hard surface which presents no difficulties. First intuition is therefore not accurate because in this situation larger variations are more beneficial than small variations.

Parachute sway variations do not influence the omnidirectional trade-offs and analyses. For the multidirectional Lander all sways up to and including a given design value can be safely tolerated. For sway variations in excess of the design value the directionality inherent with a multidirectional geometry render the vehicle inadequate from a stroke and crush-up area viewpoint. In essence, then, a variation which increases the sway angle necessitates more material for a multidirectional Lander if sufficient stroke and crush-up areas are to be furnished.

Two obvious points will now be mentioned. If the component g-tolerance is lower than that assumed in design, then larger strokes are required if damage is to be avoided. If the components can tolerate more severe g-loadings than planned on in the design then a positive margin exists with the design stroke. If the Lander system weighs more than anticipated in the design (as for example when a subsystem does not separate) then the kinetic energy of impact will increase; this necessitates an increment in crush-up material volume. A second effect is that the material density will increase because the required crushing stress (for a greater Lander weight) is increased. If the Lander system weighs less than anticipated then the reverse of the above argument is true. If the weight difference is a substantial negative variation, then a less dense material of reduced crushing stress ought to be used to insure crush-up behavior within allowable g-levels.

C.2 MATERIAL PERFORMANCE VARIATIONS

The second category of variables which, when perturbed, influence the design may be identified as material performance properties. These include:

1. crushing stress
2. density
3. specific energy
4. stroke efficiency
5. crush-up behavior
6. effective areas

The honeycomb material crushing stress is a prime design quantity. If for some reason the crushing stress is higher than anticipated, then the attenuator will function but the g-level will be exceeded since the g-level is directly related to the crushing stress. Should the crushing stress be lower than anticipated then the operating g-level will be lower than the design value; this means that the required stroke must be higher than anticipated in the design. A similar argument can be constructed in terms of

specific energy. If the material specific energy is lower than expected then for the same impact conditions more material is required. This means an increased weight. For a constant crushing stress and effective area the operating g-level decreases and consequently an increased stroke is indicated. For a more efficient energy absorber the reverse argument holds. The system will operate at a higher g-level with a decreased stroke.

A material density variation will by itself affect the system weight and this effect has been discussed previously.

In sizing a crush-up impact attenuator provision is made for stroke efficiency. In simplest terms this is the effect whereby a given thickness of honeycomb is not completely crushed when exposed to the design impact conditions. If the material is more efficient than assumed, no difficulty is encountered. If the material in a particular design is less efficient than assumed, and there are no rocks, then the design will be inadequate. However, for certain combinations of efficiency and rock dimensions the attenuator thickness determined by rock protection considerations is greater than that determined by a negative variation in stroke efficiency. As a result, variations in material stroke efficiency will not produce marked design perturbations.

If geometric variations from the nominal Lander geometry are introduced the effective cross sectional area which crushes up will be affected. If this area is decreased compared to the design value, then the operating g-level will be decreased requiring an increased stroke for adequate attenuation. If an excessive area is effective, then the operating g-level will be higher than desired and the components will be damaged. This would imply that the design strokes as supplied were excessive.

Finally, it goes without saying that crush-up behavior is essential for this mode of impact attenuation. Gross failure of the material by fracture of massive fragments or other non-crushing behavior will severely compromise the design integrity.

APPENDIX D.
CONSTRAINTS IMPOSED ON ORBITER

APPENDIX D. CONSTRAINTS IMPOSED ON ORBITER

D.1 MISSION AND SYSTEM SUMMARY

D.1.1 INTRODUCTION

This report describes the probable design of the Mariner Mars '73 (MM '73) Orbiter System. The system is presented as a logical evolution of the Mariner Mars '71 (MM '71) System and its predecessor, Mariner Mars '69 (MM '69). Mariner Mars '71 is described in summary form in Section D.3. For further details on MM '71, the reader is referred to General Electric Report 68SD4238, 1 April 1968, "Mariner Mars '71 Baseline Description" (ref. D-1).

Nomenclature used in this report conforms with the LRC standard space vehicle terminology. Accordingly, the Orbiter is that vehicle which orbits the planet after Capsule separation. The Spacecraft is the combined Orbiter and Capsule. For those accustomed to the Voyager vintage of space vehicle terminology, the following table may be of assistance:

| NASA/LRC Standard Space Vehicle Terminology | Voyager Terminology |
|---|---------------------|
| Spacecraft | Planetary Vehicle |
| Orbiter | Spacecraft |
| Capsule | Capsule |

The remainder of Appendix D summarizes the mission and system aspects of the MM '73 Orbiter. One of the major variables in the '73 mission design is the mode of entry of the separated Capsule; viz., direct vs. out-of-orbit entry.

Section D.2 describes two representative Spacecraft configurations which accommodate both the direct entry and the out-of-orbit entry capsule. In Sections D.3 through D.7, descriptions of the Orbiter Subsystems are presented, with emphasis on those MM '71 subsystems which will require changes for the '73 mission.

D.1.2 MISSION GUIDELINES

Table D-1 summarizes the MM '73 mission design for both the direct and out-of-orbit modes of Capsule delivery. The MM '69 and '71 missions are also summarized for comparison. Note that the MM '73 direct entry mission has been sized to be compatible with the ΔV capability of the MM '71 Orbiter, thus necessitating Type II trajectories for the direct entry mission. Note also the increase in communications range in MM '73 in contrast to the relatively short ranges of MM '69 and MM '71.

D.1.3 MARINER MARS '71 SUMMARY

The MM '73 Orbiter will evolve from the MM '71 Orbiter, which in turn is an evolution of the MM '69 Flyby Spacecraft. Since this report references the '73 system

to its predecessor, this section is devoted to a summary description of the MM '71 Orbiter. For further details, the reader is referred to ref. D-1.

The foundation for the evolution of Mars Orbiter is the MM '69 Flyby Spacecraft, shown in sketch form in the launch configuration (solar panels folded) in fig. D-1. The highlights of the '69 mission are given in table D-1. The basic element of the MM '69 Spacecraft is the equipment module or octagon, an equipment housing structure with eight electronic compartments or bays. A mono-propellant Propulsion Subsystem for midcourse corrections is mounted as an assembly in one of the bays (Bay II) of the octagon. The electronics of the other subsystems of the Spacecraft are contained in the remaining seven bays.

Electric power for the system is obtained from four solar panels, which are simultaneously deployed after separation of the Spacecraft from the launch vehicle. When deployed, the panels lie at right angles to one another in the plane formed by the upper surface of the octagon and present a total solar array area of 83 square feet.

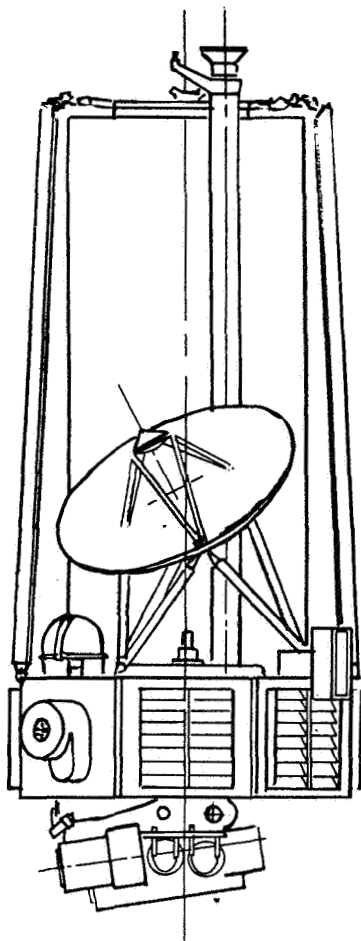


Figure D-1. Mariner Mars '69 Flyby Spacecraft

TABLE D-1. MARS MISSION COMPARISON

| Launch Vehicle | MM'69 | MM'71 | MM'73 | |
|---------------------------------------|-------------------------|--------------------------|-----------------------|-----------------------|
| | | | Direct Entry | Orbital Entry |
| Atlas (SLV3C)/Centaur | | | Titan III D/Centaur | |
| Typical Trajectories | | | | |
| Type | I | I | II | I |
| Launch Date | March 14, 1969 | May 21, 1971 | July 6, 1973 | Aug. 29, 1973 |
| Encounter Date | August 5, 1969 | Nov. 15, 1971 | April 7, 1974 | April 30, 1974 |
| Encounter Range (km) | 98 x 10 ⁶ km | 121 x 10 ⁶ km | 267 x 10 ⁶ | 294 x 10 ⁶ |
| Typical ΔV Requirements (mps) | | | | |
| Midcourse | 60 | 10 | 10 | 10 |
| Orbit Insertion | -- | 1455 | 1450 | 1480 |
| Orbit Trim | -- | 35 | 35 | 35 |
| Total | 60 | 1500 | 1495 | 1525 |
| Typical Orbital Parameters | | | | |
| Periapsis Altitude (km) | 3000 | 1000 | 1000 | 1000 |
| Apoapsis Altitude (km) | -- | 32,350 | 33,080 | 33,080 |
| Period (hours) | -- | 24 | 24.6 | 24.6 |
| Inclination | -- | 70 deg. | 84 deg. | 60 deg. |

Cruise communications to Earth at 8 1/3 and 33 1/3 bps is maintained via a low gain antenna mounted parallel to the negative roll axis atop a 95 inch long circular waveguide. High data rate communication to Earth at encounter at 16.2 Kbps is achieved via a fixed, circular, parabolic high gain antenna 40 inches in diameter.

The instruments of the four MM '69 Science Subsystems (television, ultra-violet spectrometer, infrared spectrometer, and infrared radiometer) are mounted on a scan platform below the octagon. The platform is capable of motion about two axes: clock (rotation about the Spacecraft roll axis) and cone (rotation in the plane formed by the roll axis and the platform clock angle).

The Spacecraft interface with the Centaur is accomplished via a conical frustrum shaped adapter (not shown) which tapers from 60 inches in diameter at the octagon to 54 inches at the field joint with the Centaur.

Fig. D-2 depicts the MM '71 Orbiter evolution of the MM '69 system. Fig. D-2 and the following information are indicative of our most current information about MM '71.

The most obvious and significant system change is the replacement of the '69 bay-mounted Propulsion System by a larger propulsion system mounted atop the octagon. This system is employed for all propulsive maneuvers -- midcourse corrections, orbit insertion, and subsequent orbit trims. The engine is a modification of the Rocket-dyne RS14, a bipropellant engine delivering 316 pounds of thrust at a specific impulse of 290-295 seconds. Thrust vector control is achieved by pitch and yaw gimbals, in contrast to jet vane control in MM '69. Propellant (N_2O_4 and MMH) is contained in four 6AL4V titanium tanks, each containing bladders for propellant expulsion. Helium pressurant is contained in four additional spherical tanks. Approximately 775 pounds of useable propellant result in a total ΔV capability of 1500 mps, which is adequate for the MM '71 mission.

Less obvious changes are required in other MM '69 subsystems to accommodate the orbiting nature of the MM '71 mission. Structural strengthening of the adapter (not shown) and, perhaps, the octagon is required to support the propulsion module loads. Because of the increased Sun-Mars distance (at 1971 encounter plus three months in orbit) and the greater solar array degradation with the increased 1971 mission lifetime, an increase in the total solar array area to 94 square feet is likely for MM '71. Since the panels are attached to outriggers in the MM '71 configuration, the increase in area can be accommodated by either lengthening or widening the panels, or a combination of both.

Principal changes in the Radio Subsystem involve the antennas. The 40-inch fixed dish of MM '69 is replaced by a 56-inch paraboloid of revolution which is deployed and articulated along a single degree of freedom. Likewise, the MM '69 low gain antenna structure is shortened and relocated to avoid engine plume interference. An additional secondary low gain or maneuver antenna is deployed in a direction opposite to that of the primary low gain to provide downlink coverage in the positive roll hemisphere during maneuvers. Additional switching is required to transfer among three antennas as opposed to two antennas in 1969.

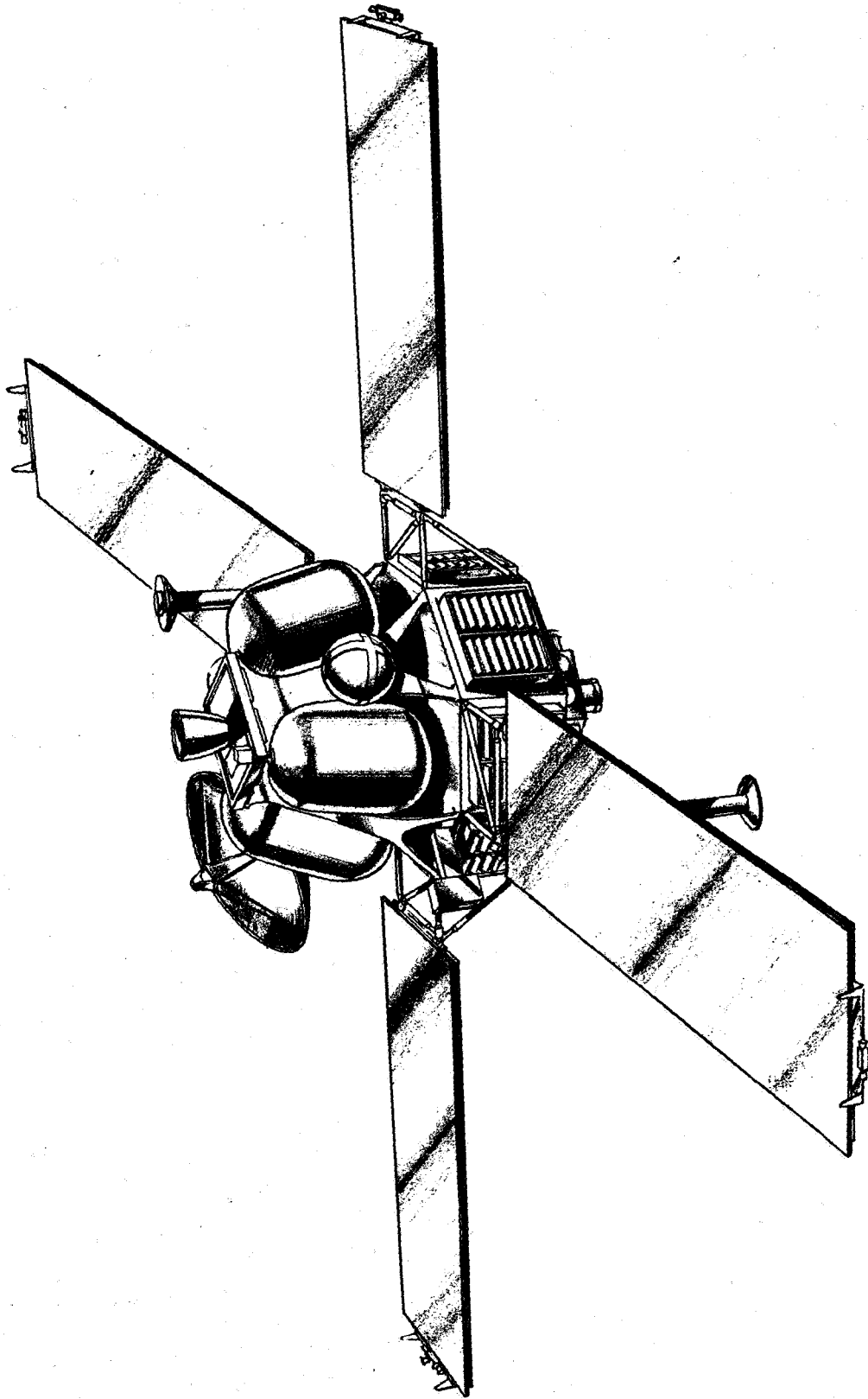


Figure D-2. Mariner Mars '71 Orbiter

As stated in Section D.5.2, the additional ground commands required for the MM '71 orbiting mission are within the capacity of the MM '69 Command Decoder, although the margin for command contingency cannot be considered comfortable. Furthermore, there is little doubt that additional Command Decoder capacity is required for the combined Orbiter-Capsule mission in 1973. It is possible that this modification will be accomplished in the MM '71 subsystem.

Additional data storage is desirable in 1971 for two reasons: (1) the increased amount of useful data that can be collected, and (2) the added protection of redundancy over the 90-day orbiting mission for which the recorders must operate. The MM '69 Data Storage Subsystem contains one analog tape recorder (ATR) and one digital tape recorder (DTR) with capacities of 1.57×10^8 and 2.3×10^7 bits, respectively. The MM '71 mission requirements are fulfilled with two ATR's and two DTR's, and the additional recorders can be located in Bay II of the octagon, which formerly housed the MM '69 Propulsion Subsystem.

In the area of mechanical devices, new mechanisms are required for the deployment of the secondary low gain antenna and for the deployment and articulation of the high gain antenna. Due to the more than doubled mass of the MM '71 orbiter, modification of the separation mechanics is also required.

Principal changes to the MM '69 Attitude Control Subsystem are in the autopilot, which must be redesigned to drive gimbals instead of jet vanes and to accommodate the different inertial characteristics of the MM '71 vehicle. The latter difference also requires a probable increase in the cold gas tankage and in the reaction jet sizing. Furthermore, it is likely that the shield of the Canopus sensor will require modification to reject Mars albedo when the orbiter is in Mars orbit.

No change is required in the MM '69 Central Computer and Sequencer for MM '71. Likewise, little or no change is required in the Scan Control Subsystem. The two narrow angle Mars gates are not required in the MM '71 flight sequence and can be omitted from the scan platform. Primary control of the MM '71 scan platform is via the reprogrammable Central Computer and Sequencer, which issues cone and clock angle change commands to the scan platform so as to cause the platform to track the local vertical in the vicinity of periapsis in an open loop fashion. For mission versatility, an increase in the range of cone and clock angle freedom over the rather restrictive range of MM '69 is desirable.

Assuming that the same four MM '69 science instruments are carried aboard the MM '71 orbiter, the Infrared Spectrometer requires significant redesign. In its MM '69 design, one of the IRS detectors is actively cooled by a two-stage cryostat for the relatively short-lived flyby encounter period. In the MM '71 version of the experiment, the detector is replaced by one with less severe cooling requirements, which can be fulfilled by sophisticated passive radiation techniques. The thermal redesign of the spectrometer also entails optical modifications. Both the Ultraviolet Spectrometer and Infrared Radiometer Subsystems appear useable as in MM '71, with possible changes in the mounting orientation of the former to reflect the difference in the Orbiter-Lander geometry. Both cameras of the MM '69 Television Subsystem are also completely useable, but is likely that optical field of view changes will be affected, again because of the Orbiter-Lander geometry.

D.1.4 MARINER MARS '73 SUMMARY

Two basic Spacecraft designs have been considered for the MM '73 mission, involving capsule delivery either prior to (direct entry) or after (out-of-orbit entry) orbit insertion. Both Orbiter designs are logical evolutions of the MM '71 Orbiter described in the previous section. The MM '73 Orbiter and its variations are described in more detail in Section D.2.3. The following is a summary of the major features of the MM '73 Orbiter design.

Since the MM '73 direct entry mission has been selected such that its propulsion requirements are compatible with the MM '71 propulsion capacity, no change to the MM '71 Propulsion Subsystem need be made for the '73 direct entry mission. From a gross configuration viewpoint, the MM '71 Orbiter as illustrated in fig. D-2, simply sits atop the direct entry capsule in the launch orientation, with the two systems mated by the Capsule adapter. The resulting Spacecraft is in turn mated to the Centaur by the Spacecraft adapter, which mates at its upper extremity with the Capsule adapter. The resulting Spacecraft configuration is depicted as fig. D-4 in Section D.2.2.

In the out-of-orbit mode of capsule entry, the amount of Orbiter propellant required to place the entire MM '73 Spacecraft into orbit is more than double the capacity of the MM '71 tanks. The most straightforward way of accomplishing the increased tankage is simply to elongate the MM '71 tanks by the addition of a cylindrical section. The pros and cons of this solution versus other alternatives are discussed in Section D.2.2. There results the Spacecraft configuration shown in orthographic projection in fig. D-12. An artist's conception of this configuration in flight is shown as fig. D-3.

Significant changes to the Structure Subsystem are required to accommodate the increased propellant tankage associated with out-of-orbit Capsule entry. Specifically the longerons, rings, and shear panels of the MM '71 octagon must be appreciably upgraded in load carrying capability to support the '73 out-of-orbit entry propulsion module.

The MM '71 Spacecraft and Centaur adapters are not applicable to the '73 Space Vehicle configuration. The former is replaced by the Capsule adapter, a structure comprised principally of two conical frustums, one on top of the other (see fig. D-12). The smaller diameter of the upper frustum connects to the bottom of the Orbiter octagon, while the Capsule canister mates to the interior of the lower frustum. The Centaur adapter of MM '69 and '71 is replaced by the MM '73 Spacecraft adapter, a two piece structure which mates at its upper extremity with the Capsule adapter and at its bottom with the Centaur. The upper member of the Spacecraft adapter is cylindrical with the same diameter as the lower end of the Capsule adapter; the lower member is an inverted conical frustum which tapers back to the smaller diameter of the interface at Centaur station 220. Since both the Centaur and the Spacecraft achieve sufficient energy for heliocentric orbit, both adapters are injected onto the Mars transfer trajectory. The Spacecraft adapter, however, remains with the Centaur, while the Capsule adapter stays with the interplanetary Spacecraft.

Four separations (and their associated electrical disconnects, as applicable) are required of the direct entry and out-of-orbit entry Spacecraft. The first separation involves

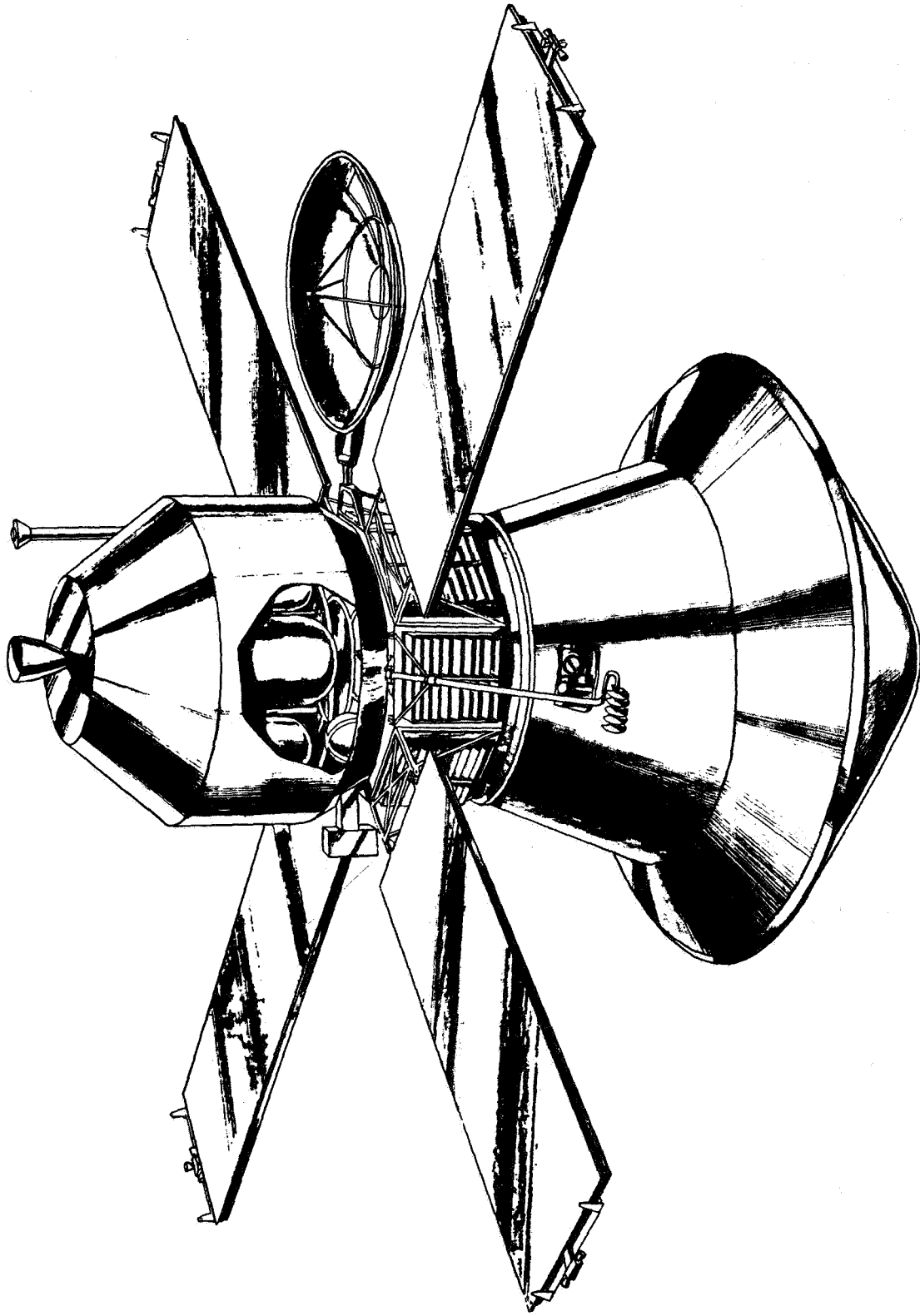


Figure D-3. Mariner Mars '73 Spacecraft (Out-of-Orbit Entry Capsule)

parting the Centaur/Spacecraft adapter and Spacecraft. The second separation is the release of the forward Capsule biobarrier, or sterilization canister forebody. Then, of course, the Capsule is released. Finally, the Capsule adapter is jettisoned to bare the basic Orbiter. Regardless of how many of the foregoing separations mechanisms are in fact assigned to the Orbiter system, the MM '71 Mechanical Devices Subsystem will undergo a significant change for MM '73.

In contrast, the Temperature Control Subsystem for the MM '73 Orbiter is similar to that of MM '71. Some change is anticipated at the flight Capsule interface to assure maximal thermal isolation of the Flight Capsule from the Orbiter.

Because of the increased Sun-Spacecraft distance at encounter and the additional power demand of the Flight Capsule, an additional solar array area increase is anticipated in MM '73. An area of 111 square feet is anticipated for the direct entry Spacecraft, and 115 square feet for its orbital entry counterpart.

Some changes are required of the Attitude Control Subsystem, but in general they are not as severe as the changes from MM '69 to MM '71. To accommodate the changes in vehicle dynamic characteristics, modifications to the autopilot electronics are again anticipated. If foresight is employed in the MM '71 change, the MM '73 change may be contained to a small electronics subassembly. Likewise, it is expected that the reaction control gas tankage and the reaction jet sizing will increase in MM '73, further changes which may be minimized in MM '73 by judicious MM '71 design. The secondary sun sensors, those sensors which cover the positive roll (anti-sun) hemisphere of the Orbiter, are blocked by the Flight Capsule in the MM '73 configuration and must be moved outboard from their MM '71 octagon location onto the reverse sides of the solar panels.

For the direct entry Orbiter, the inclusion of an approach Guidance Subsystem to minimize errors in the impact parameter is a distinct possibility. Such a system was originally planned for the MM '69 Spacecraft as an engineering experiment, but was removed prior to PTM assembly. If it is flown in MM '73 as an operational subsystem, its inclusion aboard MM '71 as an engineering experiment is a possibility.

It appears premature to extrapolate from the (already extrapolated) MM '71 Orbiter science payload prediction to a MM '73 payload, and for this reason, the MM '71 Orbiter science payload is assumed as a reference for the MM '73 mission. Accordingly, no changes are required of the MM '71 Scan Control for MM '73. Likewise, the reprogrammable MM '69 Central Computer and Sequencer appears adequate even for the diverse '73 mission. In contrast, however, the MM '69 Command Decoder, which requires expansion by MM '73, if not already accomplished in MM '71.

Again in MM '73, principal changes in the Radio Subsystem involve the antennas. As illustrated in table D-1, the more than doubled range at MM '73 encounter suggests a decrease in the prime data rate, an increased high gain antenna size, or both. It is anticipated that both will likely occur -- an increase in the high gain antenna size from the 56 inch MM '71 dish to around 63 inch (+1 dB), and a decrease in the high data rate from 16.2 Kbps to 8.1 Kbps (+3 dB). The combination is less than the 6 to 8 dB increase in range from MM '71 to MM '73, but it provides a comparable satisfactory link margin for the Orbiter.

Likewise, the MM '71 secondary low gain (or maneuver) antenna is unsuitable for the MM '73 Spacecraft, since it is deployed parallel to the roll axis into the hemisphere occupied by the Capsule (in MM '73). Even if it could be so deployed, it is doubtful whether it and its counterpart in the other hemisphere could sustain an adequate data rate at the extreme encounter ranges of MM '73. Accordingly, a new maneuver antenna with a toroidal pattern is recommended for MM '73.

An Orbiter Subsystem which has no MM '71 counterpart is the Relay Subsystem, that subsystem on the Orbiter which supports the communication link from the separated Capsule or Lander to the Orbiter. It consists of dual VHF relay antennas (attached to two solar panels) multiplexed to the relay receiver, which in turn interfaces with the Data Storage Subsystem.

In addition to the two analog recorders (ATR's) and two digital recorders (DTR's) of MM '71, two more digital tape recorders are required in the Data Storage Subsystem to accommodate the Capsule relay data. Because the inclusion of six tape recorders will probably exceed the volume of the octagon, it is probable that the DSS will be totally redesigned for MM '73. Because of the data rate differences between MM '71 and MM '73, changes are also forecast in the Flight Telemetry Subsystem.

Table D-2 presents a summary of the major MM '69 subsystem changes to accommodate the orbiting mission of MM '71, and the Capsule delivery mission of MM '73.

TABLE D-2. MAJOR SUBSYSTEM CHANGES

| MM '69 Subsystem | Change for MM '71 Orbiter | Change for MM '73 Capsule |
|--------------------|--|--|
| Power | <ul style="list-style-type: none"> • Solar Array Increase | <ul style="list-style-type: none"> • Solar Array Increase |
| Radio | <ul style="list-style-type: none"> • New Maneuver Antenna • New High Gain Antenna • Modified Low Gain Antenna | <ul style="list-style-type: none"> • New Maneuver Antenna • New High Gain Antenna • New Relay Receiver • New Relay Antennas |
| Attitude | <ul style="list-style-type: none"> • Cold Gas & Jet Size Increase • Modification of Autopilot Electronics | <ul style="list-style-type: none"> • Cold Gas & Jet Size Increase • Modification of Autopilot Electronics • Relocated Sun Sensors • Possible Approach Guidance |
| Data Storage | <ul style="list-style-type: none"> • Additional ATR • Additional DTR | <ul style="list-style-type: none"> • New Relay Recorders |
| Command | <ul style="list-style-type: none"> • Possible Decoder Expansion | <ul style="list-style-type: none"> • Probable Decoder Expansion |
| Telemetry | | <ul style="list-style-type: none"> • Data Modes for Capsule Telemetry |
| Scan Control | <ul style="list-style-type: none"> • Removal of Mars Gates | |
| Science | <ul style="list-style-type: none"> • Passive Cooling of IRS • Possible TV Field of View Changes | <ul style="list-style-type: none"> • No Estimate |
| Cabling | | <ul style="list-style-type: none"> • Three Inflight Disconnects |
| Mechanical Devices | <ul style="list-style-type: none"> • High Gain & Maneuver Antenna Deployment • High Gain Antenna Articulation • Modified Separation Mechanics | <ul style="list-style-type: none"> • Spacecraft Separation Mechanics • Modified Orbiter Separation Mechanics • New High Gain Antenna Deployment |
| Propulsion | <ul style="list-style-type: none"> • New | <ul style="list-style-type: none"> • New Tanks & Supports (for Orbital Entry Capsule) |
| Structure | <ul style="list-style-type: none"> • Strengthened Adapter • Strengthened Octagon | <ul style="list-style-type: none"> • Capsule Adapter • Spacecraft Adapter • Strengthened Octagon (for Orbital Entry Capsule) |

D.2 SYSTEM DESCRIPTION

D.2.1 ORBITER REQUIREMENTS

The primary functions of the Orbiter are: to support and carry a Flight Capsule to Mars encounter; receive and transmit to Earth data from the Capsule during pre-separation checkout, separation, descent, entry, terminal descent, and post-landed operations; support the onboard orbit science instruments; and gather, process, and transmit to Earth the orbit science data obtained on succeeding orbit passes. In order to accomplish these broad functions with a Mariner Mars '69 or '71 evolutionary type vehicle, only the definitely required design changes to the existing Orbiter are made in an attempt to maintain as much flight proven reliability as possible as well as minimize overall program costs.

During interplanetary cruise as well as succeeding mission phases, the Orbiter maintains two-way communications capability for transmitting data to Earth, for receiving commands from Earth, and for providing ranging as well as doppler tracking capability. In addition, the Orbiter provides support for the Flight Capsule in the form of providing power for thermal control (may be interrupted when assuming off-Sun attitudes), battery charging, data sampling, etc.; and it accepts already commutated status data from the Flight Capsule for transmission to Earth. The Orbiter has the capability of performing up to two interplanetary trajectory corrections; and has orbit insertion as well as a two orbit trim maneuver capability. Regardless of whether the Capsule is a direct or out-of-orbit entry type, the Orbiter is responsible for initiating the pre-separation checkout sequence and the separation sequence, and for maintaining relay communications with the Capsule from Orbiter-Capsule separation through completion of initial post-landed imaging data transmission. The Orbiter performs an orbit science data gathering mission following termination of Capsule relay transmission and jettisoning of the Capsule adapter. In addition, the Orbiter for the out-of-orbit entry concept performs limited landing site surveillance prior to Orbiter-Capsule separation. The design lifetime goal of the Orbiter is >90 days in Mars orbit.

D.2.2 CONFIGURATION SELECTION

From a configuration viewpoint, the selection of the MM '73 Orbiter can be divided into two selections according to the Mode of entry of the separated Capsule: direct or out-of-orbit.

The configuration selection for the direct entry Capsule is the more straightforward. Since the MM '73 mission with the direct entry Capsule has been tailored to be performed with the propulsion capability of the MM '71 Orbiter (see table D-1), no significant changes to the MM '71 Propulsion Subsystem are required. Changes are required to several other subsystems, and these changes are covered in more detail in Sections D.4 through D.7, which follow. For the most part, however, these changes have only a second order effect on the MM '71 Orbiter configuration.

For the direct entry Capsule, the selection of the best MM '73 Spacecraft configuration boils down to determining how best to combine the Capsule with an Orbiter similar to MM '71. The immediate choice is to mount the Orbiter (in its MM '71 launch orientation) atop the Flight Capsule, mating the two systems with a Capsule adapter. The latter also mates with the launch vehicle adapter. The preferred Spacecraft configuration for the direct entry Capsule is illustrated in fig. D-4 and covered in more detail in the next section.

The Spacecraft configuration selection process with the out-of-orbit entry Capsule is not as obvious. The added variable is the requirement that additional propellant be added to that of the MM '71 Orbiter to insert the entire Spacecraft into Mars orbit. In general, the total propellant tankage required for MM '73 is more than twice that available on the MM '71 Orbiter.

The configuration evolution to accommodate the out-of-orbit entry mission in MM '73 is depicted in a simplified manner in fig. D-5. The MM '71 Orbiter can be considered to be comprised of four major elements: the RS14 engine, the propulsion system tankage, the octagon, and the scan platform. To complete the Spacecraft configuration in MM '73, two additional elements must be added: the entry Capsule and the necessary additional propulsion tankage. The configuration selection process consists of determining the best arrangement of these six major system elements.

Assuming the constraint that the foregoing six elements must be situated adjacent to one another along the roll axis of the Spacecraft, some 720 theoretical configuration permutations can be formed. Of course, the vast majority of these are unworkable arrangements. For example, it is mandatory that the engine be located at one extremity of the arrangement so that propulsive maneuvers can be performed without jettisoning any of the other five system elements. Likewise, it is necessary for the Flight Capsule to be located at the end so that it can be separated without equipment jettisoning. Further, it is desirable that the octagon and scan platform be situated adjacent to one another as they are in the MM '69 and '71 configurations.

Applying these restrictions, the number of allowable configuration alternatives is reduced drastically from 720 to 48. Twenty four of these are tabulated in symbolic form in fig. D-6; the remaining 24 result by simply reversing each configuration (i. e., launching the configuration upside down with reference to the illustration). Referring to the figure, it would appear at first that configurations 7 - 12 and 19 - 24 violate the constraint that the Capsule must be located at one end of the Spacecraft configuration. Both the engine and the Capsule can be located at the same end of the Spacecraft, however, if conversion is made in MM '73 to multiple engines spaced around the circumference of the Capsule, as suggested by the dotted line symbology on configuration 8.

Most of the 48 configurations of fig. D-6 are also unsuitable upon closer examination. Many of them require that either the engine or all of the propulsion tanks be jettisoned to uncover the scan platform and conduct orbital science. Such a configuration limits the flexibility of the orbital mission, since orbit trims cannot be made after the jettison. This drawback eliminates configurations 3, 4, 9, 10, 13, 14, 17-24, and their reversed launch orientation counterparts, and reduces the candidates to 20 in number.

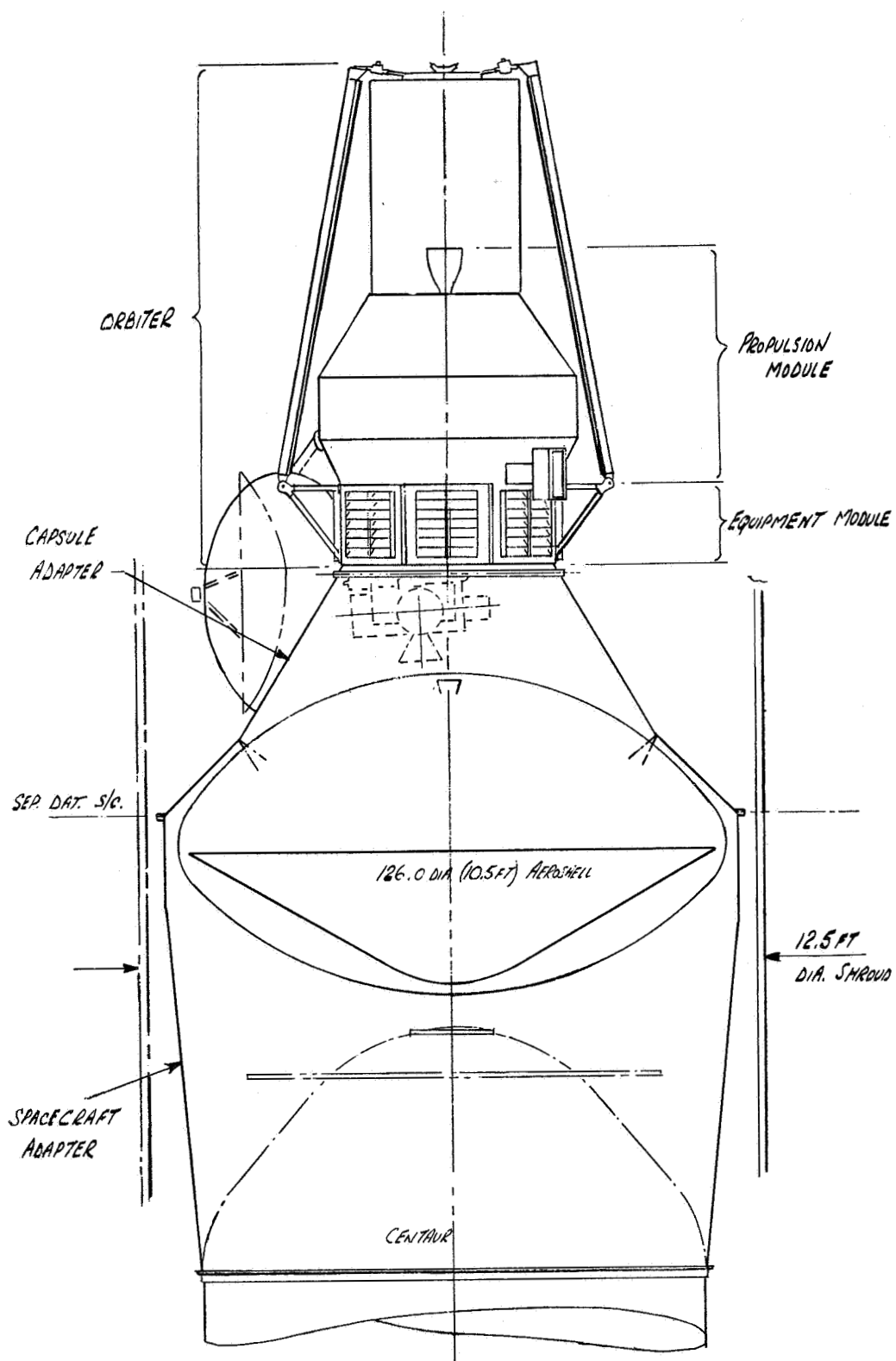


Figure D-4. Spacecraft Configuration, Direct Entry Capsule

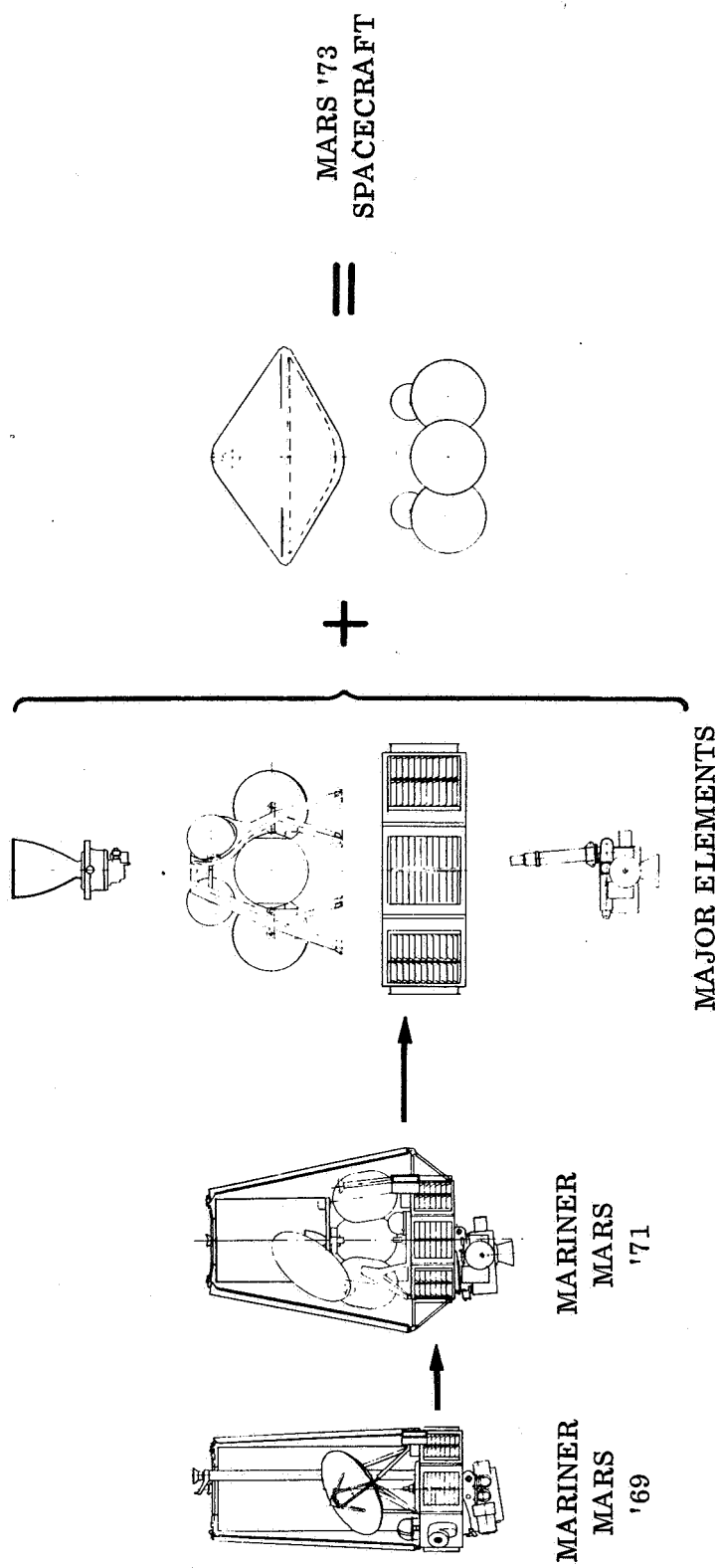
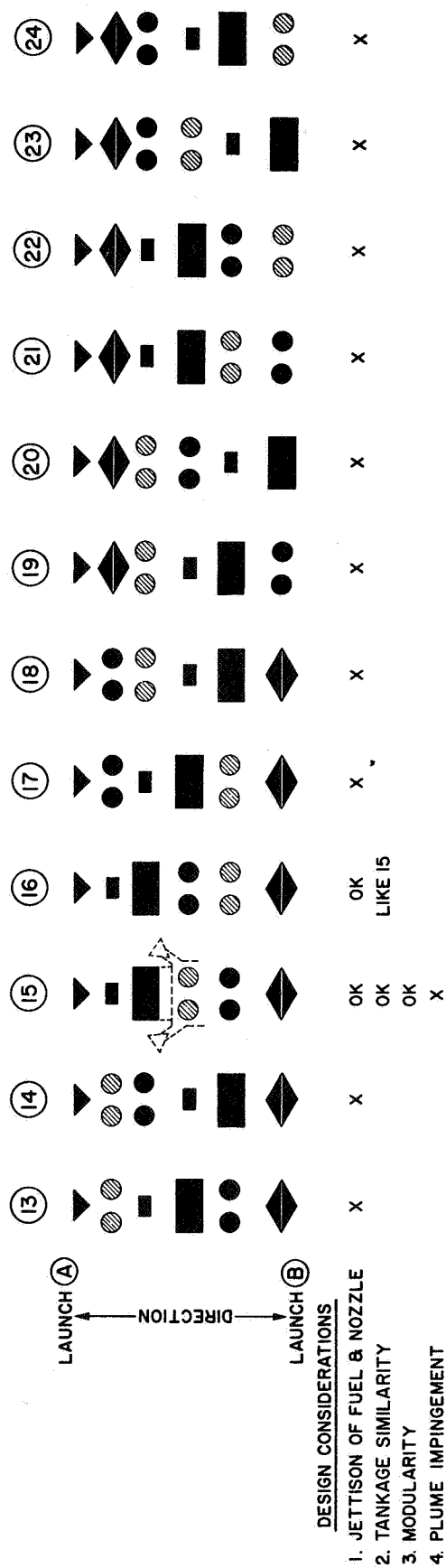


Figure D-5. Spacecraft Configuration Minimum Science Direct Entry Capsule



OK = ACCEPTABLE X = UNACCEPTABLE

Figure D-6. Screening of Candidate Out-of-Orbit Entry Configurations

This number can be halved again by noting that for each configuration there is a counterpart which differs from the former by simply interchange of the MM '71 tanks and the additional MM '73 tanks - a vague distinction at best. The remaining configurations are 1, 2, 7, 8, and 15, and their launch reversals.

Finally, configuration 7 requires that propellant lines be routed the entire length of the Spacecraft from tanks at one end to the engines at the other, thus virtually eliminating the prospect of modularity within the Orbiter system. Configuration 15 requires that the engines be clustered around the scan platform, presenting the possibility of plume contamination of orbital science instrumentation. Elimination of these two borderline arrangements reduces the alternatives to configurations 1, 2, 8 and their launch reversals.

Fig. D-7 illustrates an embodiment of the arrangement of Configuration 1. Note that some liberty has been taken with the positioning of the auxiliary tanks relative to the scan platform, in that the new tanks are mounted around, rather than below, the scan platform. In either case, the Capsule adapter and auxiliary tanks must be separated (after Capsule separation) to permit the scan platform an unobstructed view of the positive roll hemisphere. Jettisoning of some part of the structure for platform viewing is a negative feature of this and many of the following configurations.

An alternative to the configuration of fig. D-7 is shown in fig. D-8. This approach employs two additional engines connected directly to the auxiliary tanks, thereby avoiding running propellant lines (and disconnects) across the octagon-adapter interface. This approach also provides more than ample thrust to avoid any gravity loss at Mars orbit insertion. On the negative side, however, are the problems of engine plume impingement on the Spacecraft and the catastrophic failure mode associated with any single engine-out. These considerations suggest a slight preference for the former configuration.

If the reader turns the configuration of fig. D-7 upside down, he can immediately see why the reverse launch orientation is less desirable than that shown. Attaching the reverse configuration to the launch vehicle at the Capsule is undesirable because the entire length of structural shroud to that point must be taken to heliocentric injection. On the other hand, supporting the spacecraft at the MM '71 propulsion module introduces such problems as carrying the entire Spacecraft loads through the propulsion module, a significant vehicle bending moment, and solar panel stowage.

The arrangement of Configuration 2 (see fig. D-6) entails mounting the MM '71 tanks and the additional MM '73 tanks adjacent to one another. Two attractive ways of accomplishing this are shown in figs. D-9 and D-10. The former approach consists of simply stacking two MM '71 tankage modules on top of one another to provide the necessary MM '73 propellant volume. This approach requires that the MM '71 tankage volume be half that of MM '73, which in turn implies that the MM '71 tanks be somewhat oversized (about 20 percent) with respect to the amount of propellant to be carried in MM '71. (It is not likely that this additional volume would be filled with propellant in MM '71 because of the payload limitation of the Atlas (SLV3C)/Centaur.) A more

straightforward implementation of Configuration 2 is simply to increase the size of the MM '71 tanks to that required for MM '73, perhaps by the addition of a cylindrical section as shown in fig. D-10. Both approaches are attractive enough to warrant further consideration. Both alternatives are difficult to launch in the reversed orientation for reasons similar to those given for Configuration 1.

Finally, one of the most attractive implementations of Configuration 8 is displayed in fig. D-11. Note that the reverse orientation is preferred in this case; the normal launch orientation has drawbacks similar to those previously suggested for the reversal of Configuration 1. Perhaps the most obvious negative feature of Configuration 8 is that the MM '73 orientation of the MM '71 propulsion module, octagon, and scan platform is exactly upside down to that anticipated for the MM '71 configuration. If Configuration 8, however, proves to be superior to its competition, a re-examination of the MM '71 configuration arrangement may be warranted.

The four preferred configurations (figs. D-7, D-9, D-10 and D-11) were first compared with each other to determine if significant cost differences could be identified. Major cost differences are those involving development and qualification tests, and test hardware. If significant differences exist, this could be the controlling factor in the configuration selection.

Emphasis was placed on identifying significant relative differences in cost. Engineering judgement was used in making the estimates. Vendors were not contacted, nor were detailed test plans formulated for cost estimating purposes. Where components or subsystems were used without change on all four configurations, their cost was ignored, since the relative difference is zero. A more precise cost exercise could result in a change in the resulting cost figures, but should not significantly affect the relationship in the cost differences between configurations.

The following assumptions were made regarding the use of MM '71 hardware designs in MM '73:

1. Components which have been previously qualified for the 1971 mission may be used without being requalified.
2. Components which have been previously qualified for the 1971 mission but which are used in a different physical arrangement or location need not be requalified.
3. Components, such as the structure, which required a "beefing up" to carry an increased load require only a design verification test, not a complete development and qualification program.
4. New components, of course, require a full development and qualification test program.
5. Spare parts and test models from the MM '71 mission will be used to the fullest possible extent. Test models, in particular, will be modified and used in testing components modified for MM '73.

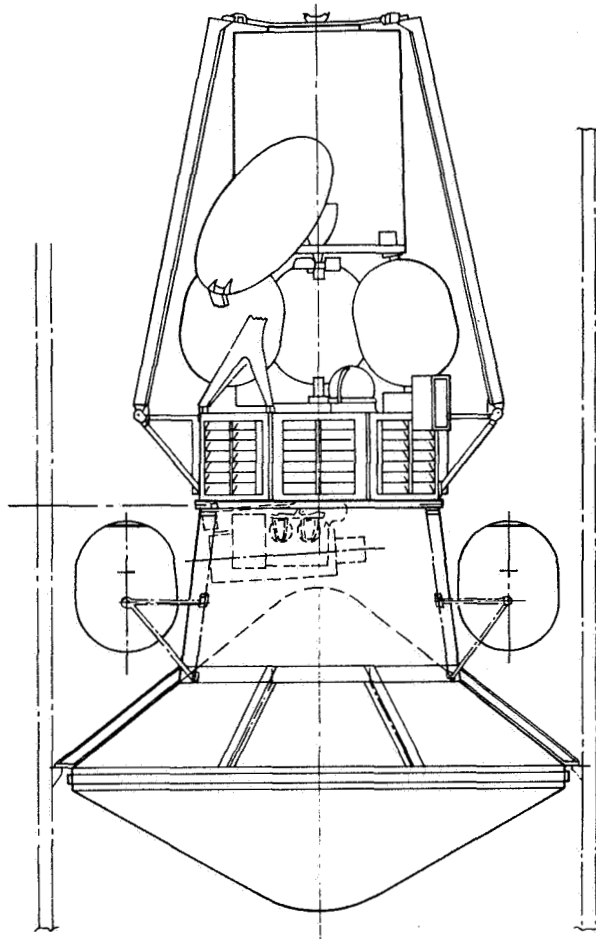
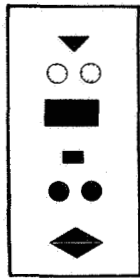


Figure D-7. Configuration 1

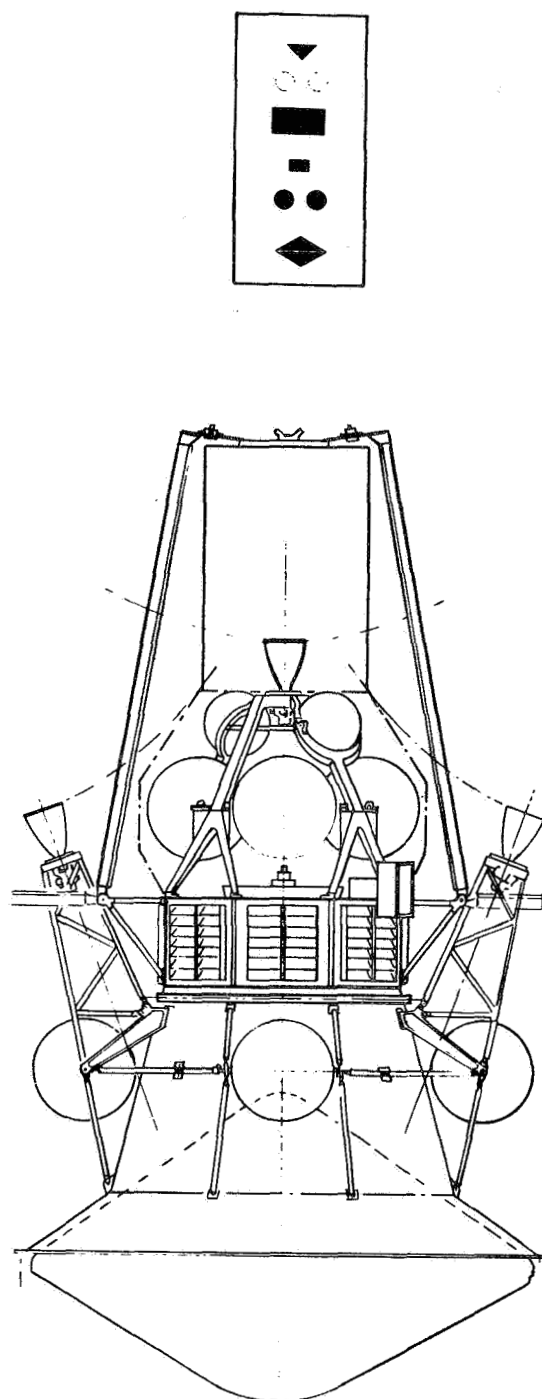


Figure D-8. Configuration 1 with Multiple Engines

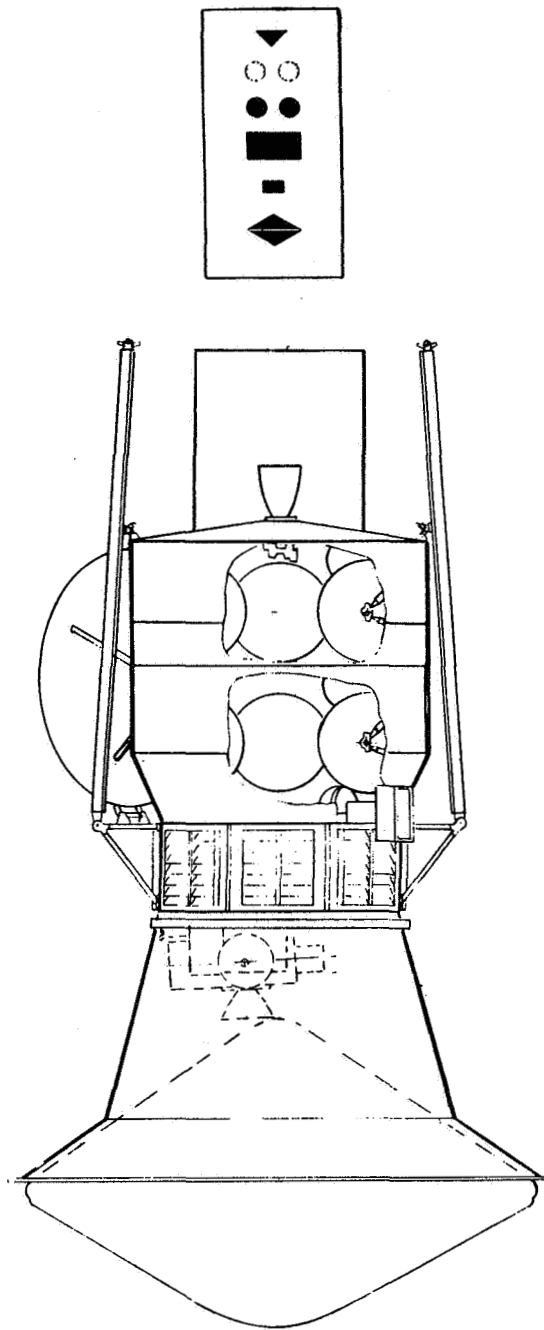


Figure D-9. Configuration 2

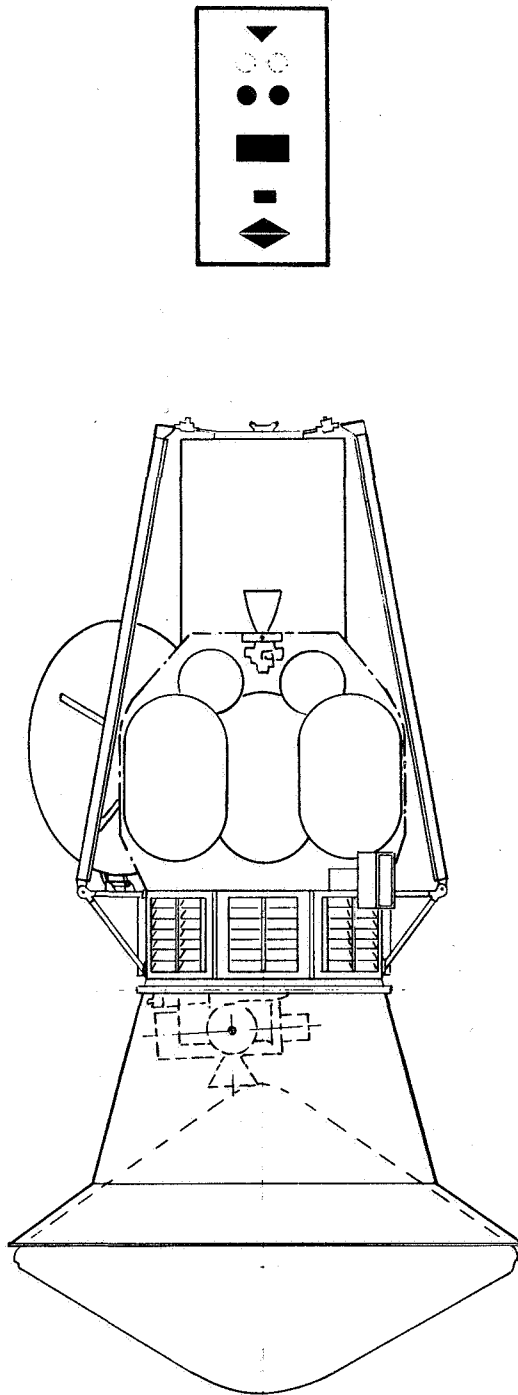


Figure D-10. Configuration 2 with Alternate Tanks

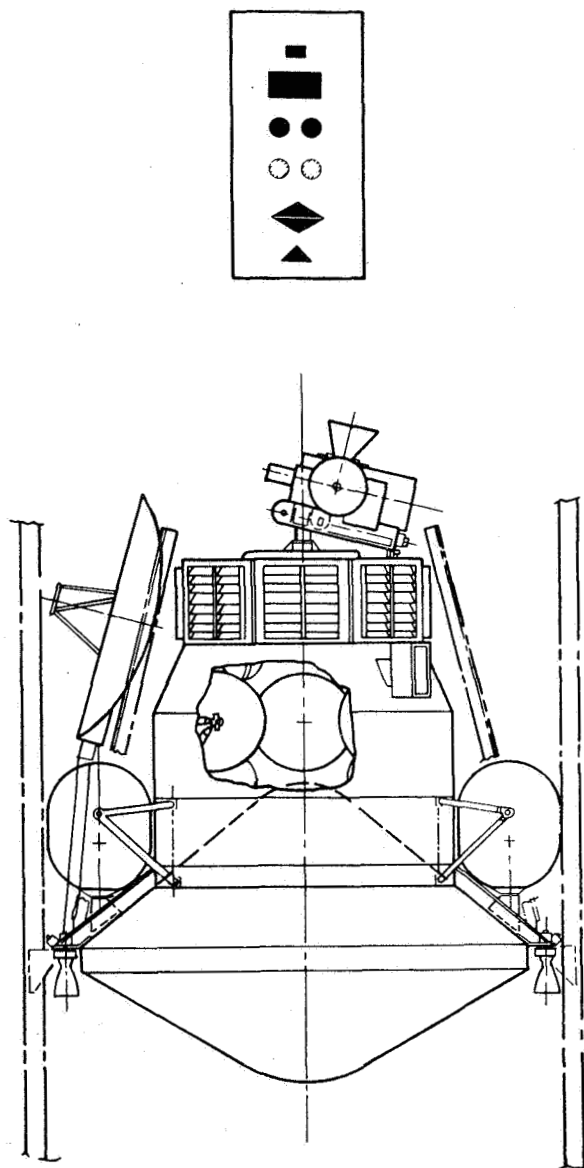


Figure D-11. Configuration 8

The subsystem most affected by the mission growth from MM '71 to '73 is the Propulsion Subsystem. It is assumed that the thrust chamber assembly (TCA) from the MM '71 Spacecraft can be used if qualified for a longer burn time. The qualification test on the thrust chamber assembly for the MM '71 mission could be extended to demonstrate the longer burn time capability (required for the first three configurations), thereby qualifying the assembly for MM '73 as well. This consideration is not applicable to Configuration 8.

Table D-3 is a summary of the design and test requirements assumed for cost comparison purposes. For convenience, the configurations of figs. D-7, D-9, D-10, and D-11 are redesignated A, B, C, and D, respectively.

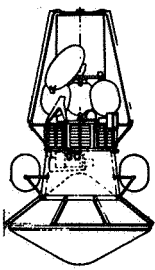
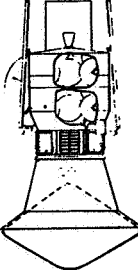
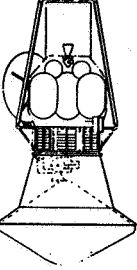
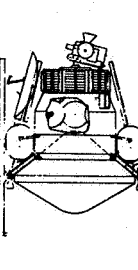
Inspection of table D-3 reveals that configuration A can utilize far more of the MM '71 system development hardware than the other three configurations. For example, the MM '71 structural test model can probably be used as is, and with the addition of structural models of the upper Capsule adapter and auxiliary propellant tanks, a structural test model for MM '73 is available. In contrast, a new STM is required for configuration C, for example, because the octagon must be redesigned to support the MM '73 propulsion tankage. Similar contrasts hold for system thermal, antenna, and separation development hardware. Hardware costs per se, however, are generally not the major portion of program costs - especially not development hardware. Accordingly, the savings accrued by re-use of MM '71 development hardware is not expected to be dramatic.

Development costs among the four competitors are expected to be comparable, with alternatives A and C probably the most attractive. On the surface, alternative A appears the simplest, but the problem of differential propellant flow rates among the eight tanks and disconnects in the propellant lines should not be underestimated. Conversely, judicious design of the MM '71 propulsion module could minimize the additional development required in MM '73 for configuration C.

Likewise, it is hard to build a convincing case for any alternative on the basis of minimum qualification and type approval test costs. For example, current JPL tankage philosophy requires that all newly purchased tanks be qualified, regardless of prior design existence. The possibility does exist that configuration A need not be qualified in vibration and thermal vacuum because of its similarity to MM '71 (above the Capsule adapter), thereby obviating the environmental requirement for a PTM; but there would still be the requirement for a vehicle for Orbiter electrical integration. Furthermore, the differences in launch vehicle environment and adapter compliance between MM '71 and MM '73 tend to cloud the case for abrogation of vibration qualification in MM '73.

Perhaps the major conclusion that can be drawn from table D-3 is that the conclusion itself is not clear. The differences among the costs of the four configurations are not significant in reference to the total cost of the Mars '73 project. Furthermore, the differences are probably comparable to any accuracy that could be claimed for the cost estimates. Although configuration A is (intuitively) the cheapest alternative, the degree of savings does not seem sufficient to warrant its selection on the basis of cost alone.

TABLE D-3. DESIGN AND TEST ASSUMPTIONS

| | A | B | C | D |
|----------------------------------|---|--|---|--|
| |  |  |  |  |
| DESIGN ASSUMPTIONS | | | | |
| Redesign | | | | |
| Electronics Module Structure | | X | X | X |
| Propulsion Subsystem Plumbing | | X | | |
| Solar Panel Latches | | X | | |
| Panel Supports | | | | X |
| New Design | | | | |
| Propulsion Module Plumbing | X | | | X |
| Engine Mounting Structure | | | | X |
| Propulsion Tank Module Structure | X | X | | X |
| Propulsion Module Separator | | X | | |
| Propulsion Tanks | | | X | |
| Plumbing Disconnects | X | | | |
| Shroud Blisters | | | | X |
| DEVELOPMENT TESTS | | | | |
| Component Development Tests | | | | |
| Solar Panel Latches | | X | | X |
| Antennas | | | | X |
| Antenna Supports | | | | X |
| Propulsion Module Development | | | | |
| Plumbing Flow Tests | X | X | X | X |
| Plume Impingement | | | | X |
| New Tanks | | | X | |
| Module Firing | | X | X | |
| Antenna Test Model | '71 ATM plus auxiliary tankage module | New | New | New |
| Structural Test Model | '71 STM plus auxiliary tankage module | New | New | New |
| Thermal Test Model | '71 TTM plus auxiliary tankage module | '71 TTM octagon and scan platform, plus auxiliary tankage module | '71 TTM octagon and scan platform, plus auxiliary tankage module | '71 TTM octagon, propulsion module and scan platform, plus panels and tankage module |
| Separation Model | '71 modified plus auxiliary tankage module | New | New | New |
| QUALIFICATION TESTS | | | | |
| Components | | | | |
| Solar Panel Latches | | X | | X |
| Propulsion Tanks | | | X | |
| Propulsion Subsystem | | | X | |
| Solar Panels | | | | X |
| Proof Test Model | Modified '71 flight spare. | New, except for some bays from '71 flight spare | New, except for some bays from '71 flight spare | New, except for some bays from '71 flight spare |

In addition to cost differences, there are several mission and project oriented differences among the four configuration alternatives; the more significant of these are summarized in table D-4.

From the viewpoint of propulsion reliability, configuration D with its separately gimballed, multiple engines probably ranks the lowest. It is true that if four engines are employed, a theoretical gain in reliability over that of a single engine system can be realized by the incorporation of pair-out logic, but in all practicality it is doubtful whether the resultant reliability of such a new system could approach that of the flight proven MM '71 engine. Of the remaining three alternatives, configuration C rates a slight edge over A and B because it involves minimum modification to the existing MM '71 propellant lines and valves.

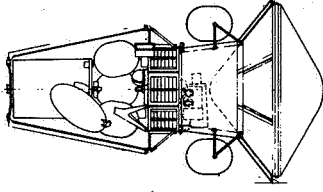
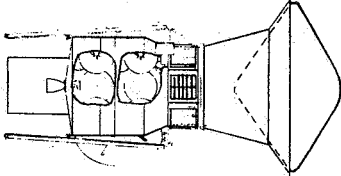
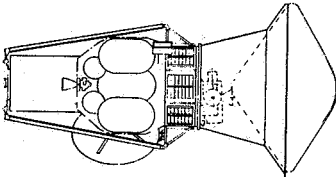
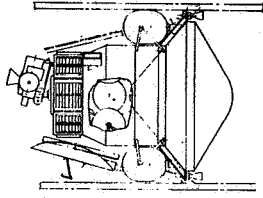
Assuming the RS14 engine is retained for MM '73, the relatively low thrust/weight ratio of configurations A, B, and C will result in a slight gravity loss at orbit insertion. The thrust/weight ratio of configuration D, even with only two RS14's, is more than adequate to avoid gravity loss. However, the multiple engines would most likely be canted to lessen plume impingement on the Capsule, thus resulting in a thrust loss of $1 - \cos \theta$, where θ is the cant angle.

The outstanding advantage of configuration D is that the scan platform field of view is totally independent of the separation of the flight Capsule and Capsule adapter. In contrast, configurations B and C require jettisoning the combined canister after-body and Capsule adapter (after Capsule separation) to uncover the scan platform. Configuration A adds propellant tanks to the combination to be jettisoned and the requirement for disconnects in the propulsion lines. Prior to Capsule separation, orbital reconnaissance of potential landing sites is at best cumbersome with the first three configurations. They require that a port be provided in the Capsule adapter to permit an external field of view for the television camera on the scan platform, and also that the entire Spacecraft be maneuvered to point the camera at Mars. This singular advantage of configuration D suggests that the assumed constraint of mounting the MM '73 scan platform on the roll axis as in MM '69 should be re-examined. If it could be shown that locating the platform adjacent to the octagon on the pitch axis, for example, could be accomplished without major perturbations, a significant negative aspect of configurations A, B, and C would be eliminated.

Flexibility for other missions -- not only to Mars, but to other planets -- should be considered. The higher thrust level of alternative D makes it more suitable from an engine viewpoint than the first three alternatives. Configuration B requires that future mission propellant requirements be approximately multiples of the MM '71 capacity. Any change in the diameter of the flight capsule perturbs the engine mounting of configuration D.

When both cost and project factors are taken into consideration, it is apparent that the selection of the optimal MM '73 Spacecraft configuration to accommodate an out-of-orbit entry Capsule is a choice among alternatives with only shadings of difference. Configuration D must be rated the least attractive of the four in view of its dissimilarity to the currently planned MM '71 configuration. Configuration A and

TABLE D-4. MISSION AND PROJECT COMPARISON

| | | A | B | C | D |
|---------------------------|-------------|---|---|---|---|
| Propulsion | Reliability |  |  |  |  |
| | Losses | Same as MM '71 with additional lines, valves, and disconnects Gravity | Same as MM '71 with additional lines and valves Gravity | Same as MM '71 Gravity | Practically a new system, but possibly with pairout feature Engine canting |
| Orbiting Science | | Requires jettison of capsule adapter and auxiliary tanks | Requires jettison of capsule adapter | Required jettison of capsule adapter | Independent of capsule mission |
| Other Mission Flexibility | | Limited by gravity loss Flexible Adapter and tank support redesign | Limited by gravity loss Requires multiples of MM '71 volume Adapter redesign only | Limited by gravity loss Flexible Adapter redesign only | None within reasonable spacecraft weights Flexible Redesign of engine and tank supports and adapter |
| Engine Capability | | | | | |
| Other Propellant Volumes | | | | | |
| Other Capsule Diameters | | | | | |

C are slightly more attractive than B because of the latter's lack of versatility for missions other than Mars '73. Configuration C is functionally the more straightforward approach of the two. With these reservations, Orbiter configuration C is selected for the out-of-orbit entry mode of Capsule delivery. The preferred Spacecraft configuration is illustrated in fig. D-12 and discussed in detail in Section D.2.3.

D.2.3 ORBITER DESCRIPTION

Contained in this section are detailed descriptions of the variations of the MM '73 Orbiter to deliver a capsule from Mars orbit and to deliver a Capsule prior to Mars orbit insertion. As suggested earlier, the Spacecraft associated with these two modes of delivery are known as, respectively, the out-of-orbit entry Spacecraft and direct entry Spacecraft.

The first part of the system description discusses in general terms the major subsystems of the MM '73 Orbiter, their functions, interrelationships, and significant modifications with respect to their predecessors in MM '69 and MM '71. Where differences exist in a given subsystem because of the mode of Capsule delivery, they will be so stressed. Detailed descriptions of the Orbiter subsystems are contained in Sections D.3 through D.7.

The succeeding two parts discuss in detail the Spacecraft and Orbiter system configurations to accommodate both modes of Capsule delivery. Emphasis is placed on the major elements of the configuration in most cases, and the configuration drawings are accordingly not overly detailed. Being the heavier of the two Spacecraft, the out-of-orbit entry Spacecraft has been selected for more detailed configuration layouts, and these are presented in Section D.2.3.3.

D.2.3.1 Orbiter Subsystems

Fig. D-13 is a functional block diagram of the Mariner Orbiter as it is envisioned for the MM '73 Mars mission. Each block represents a discrete functional subsystem of the Orbiter. Each subsystem is designated by a three or four letter code as in MM '69 (e.g., DAS - Data Automation Subsystem). Within each block are listed the major components of the subsystem. Principal electrical interfaces are indicated by arrows between subsystems. No attempt has been made to depict mechanical interfaces.

A brief description of each subsystem of the Orbiter follows. More detailed descriptions of each subsystem, including functional block diagrams and significant differences from MM '69 and '71 predecessors, are contained in Sections D.3 through D.7.

D.2.3.1.1 Propulsion Subsystem

The function of the Propulsion Subsystem is to provide sufficient impulse to the Spacecraft or Orbiter to perform one to two midcourse maneuvers (as required) to correct the heliocentric trajectory, to achieve orbit upon encounter of the planet, and to adjust the orbit once or twice (as required) to adjust the location or altitude of periapsis or the period of the orbit.

MINIMUM SCIENCE
OUT-OF-ORBIT CAPSULE

SCALE 1/20

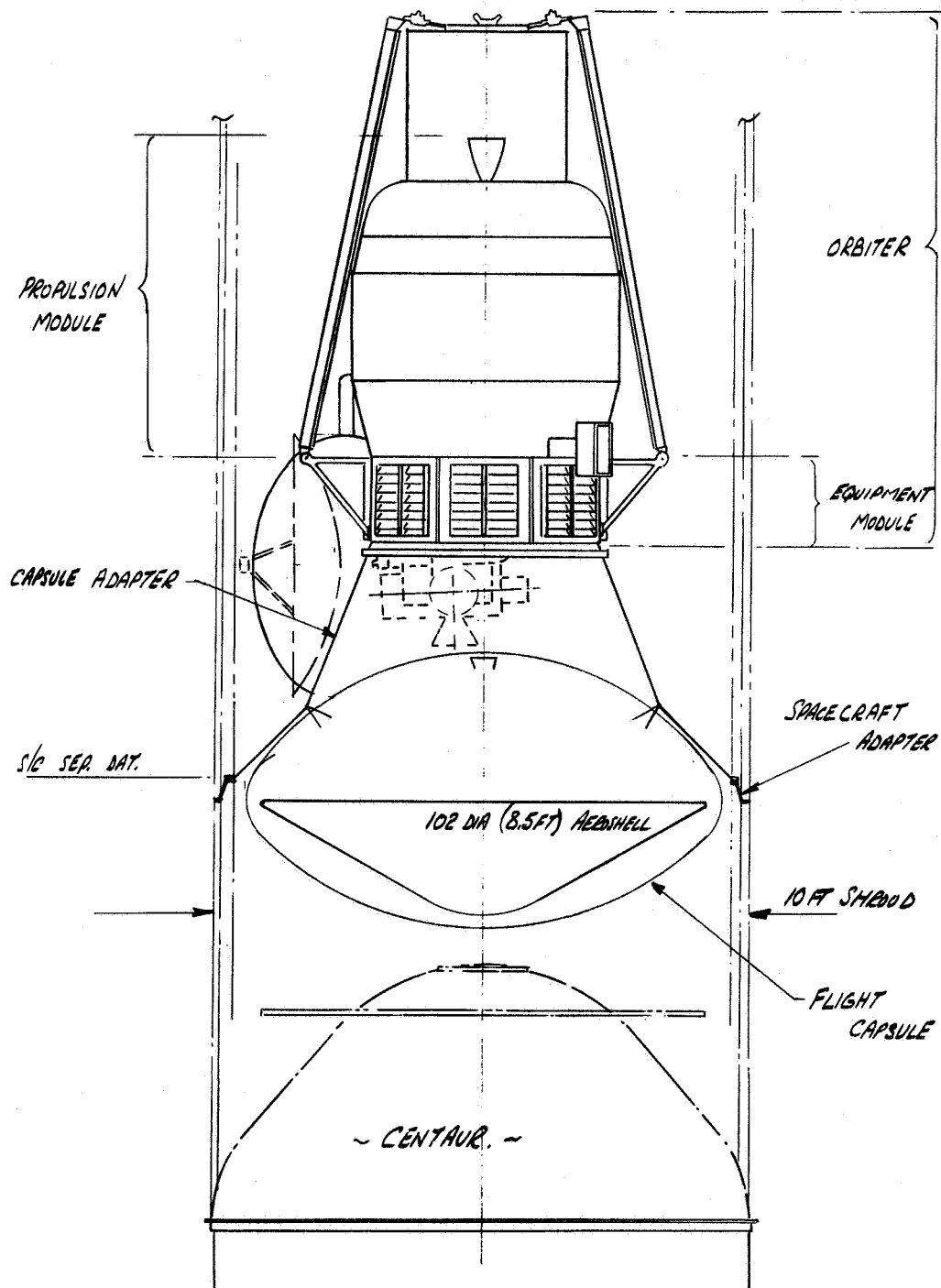


Figure D-12. Spacecraft Configuration Out-of-Orbit Capsule

FOLDOUT FRAME

FOLDOUT FRAME

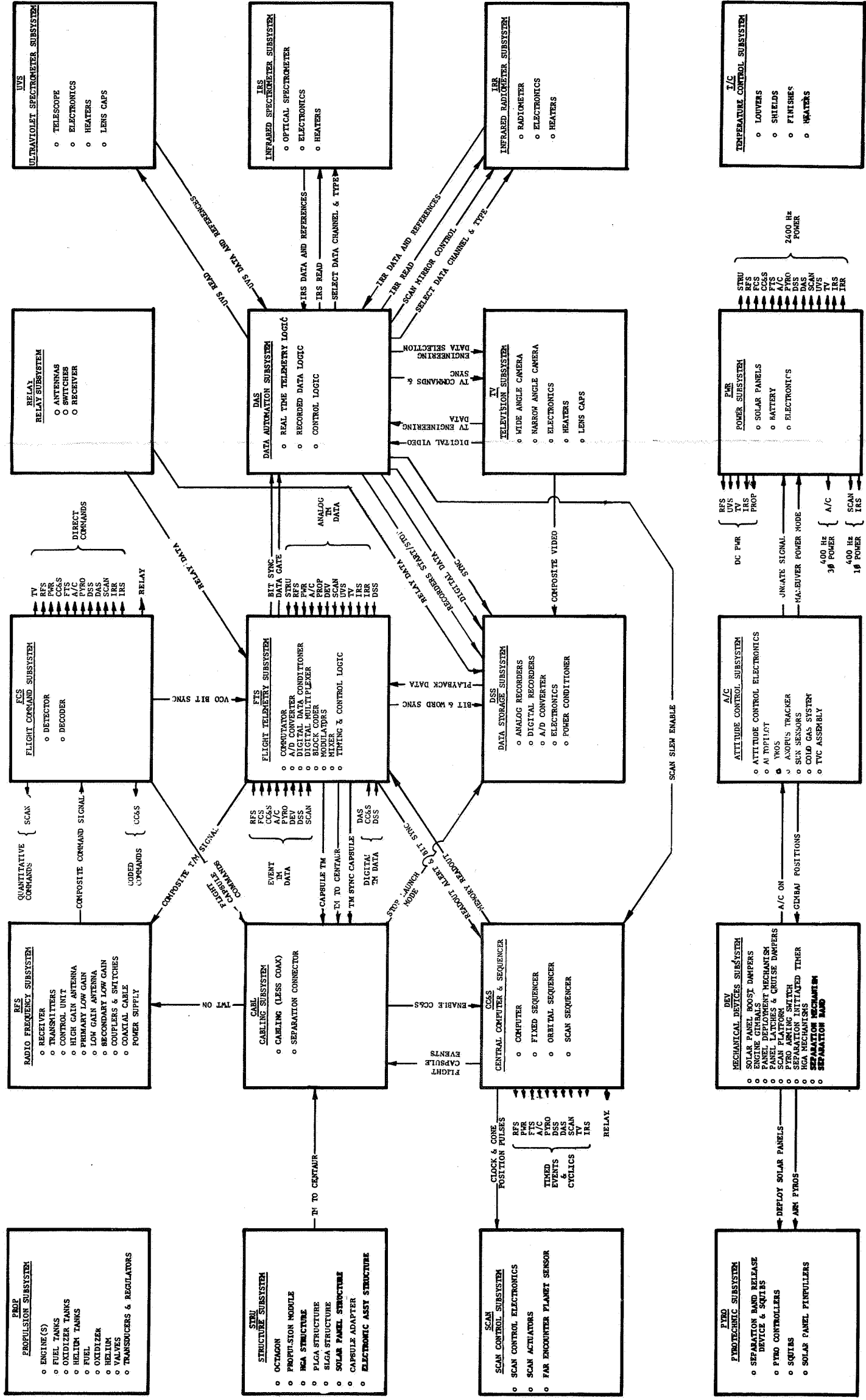


Figure D-13. Mariner Mars '73 Functional Block Diagram

The principal components of the Propulsion Subsystem are the engine, fuel and fuel tankage, oxidizer and oxidizer tankage, pressurant and pressurant tankage, and associated valves, transducers, and regulators. For both the direct and out-of-orbit entry Spacecraft, the engine is the Rocketdyne RS14, a 316 pound thruster with a specific impulse of 290 seconds, which is currently planned for use on MM '71. Fuel, oxidizer, and pressurant are monomethyl hydrazine (MMH), nitrogen tetroxide (N_2O_4), and helium, respectively.

For the direct entry Spacecraft, the mission has been designed to accommodate the impulse capability of MM '71. The subsystem weighs 980 pounds at launch and 180 pounds when all usable propellant has been expended. The propellant is contained in four spheres, each 22 inches in diameter. The increased propellant required for the orbital entry Spacecraft results in subsystem launch and burnout weights of 2,310 and 360 pounds, respectively. The volume of the four propellant tanks is increased in the out-of-orbit entry case by adding a cylindrical section to each 22 inch sphere, such that the total length of each tank is 42 inches.

For nominal system weights, the Propulsion Subsystem can depart a total impulse of 1495 meters per second to the direct entry Spacecraft, nominally apportioned among midcourse, insertion, and orbit trim to yield 10, 1450, and 35 mps, respectively. The comparable total impulse for out-of-orbit entry is 1525 mps, which results by increasing the orbit insertion ΔV to 1480 mps.

D.2.3.1.2 Engineering Mechanics

Five subsystems generally comprise the grouping known as Engineering Mechanics: Structure, Mechanical Devices, Temperature Control, Pyrotechnics, and Cabling.

The Structure Subsystem includes the octagon, propulsion module structure, superstructure, antenna structures, solar panel structure, and that portion of the Capsule adapter which may be assigned to the Orbiter. For the direct entry Spacecraft, the octagon is similar to MM '71; for the out-of-orbit entry, however, strengthening of the octagon rings, panels, and longerons is required. Likewise, in MM '73 changes are required in the length of the propulsion module structure due to the increased length of the propellant tanks for the out-of-orbit entry Spacecraft; no change is required for direct entry. New structures are required for the high gain antenna, secondary low gain antenna, and relay antennas regardless of the capsule entry mode. The MM '71 low gain antenna and solar panel structures should, however, be adequate. The MM '71 adapter is not applicable to the MM '73 mission and is replaced by the Capsule adapter, a new and larger structure which interconnects the Orbiter, flight capsule, and Spacecraft adapter (which mates the Spacecraft with the Centaur). It is problematical whether the Capsule adapter, or any part of it, will be assigned to the Orbiter system in MM '73.

The Temperature Control Subsystem is responsible for maintaining the thermal balance of the Orbiter during all phases of the mission profile: prelaunch, ascent, separation, initial stabilization, interplanetary cruise, maneuvers, and Mars orbit cruise. It consists of thermally actuated louver assemblies, thermal shields and

blankets, and selected surface finishes. The louvers are located on each of the eight electronic bays and vary the effective emittance from approximately 0.12 when closed to 0.76 if allowed to open 90° . Changes to the MM '71 subsystem are expected to be minor, involving mainly accommodating reflectance from the flight Capsule and insulation of the flight Capsule from the Orbiter.

All mechanical devices on the Orbiter are grouped into a separate functional subsystem. The Mechanical Devices Subsystem consists of the solar panel boost dampers, latches, deployment mechanisms, and cruise dampers; the high gain antenna deployment and articulation mechanisms; the pyro arming switch and separation initiated timer; the scan platform; engine gimbals; and the octagon/Capsule adapter separation mechanism and band. The separation mechanism for the canister forebody and separated Capsule are assumed to form part of the Capsule system; separation between the Spacecraft and Spacecraft adapter is also assumed not to be assigned to the Orbiter. Among those devices which are in the main unchanged from MM '71 are the scan platform, solar panel mechanics (although some minor change may be necessary to accommodate the panel-mounted antennas), pyro arming switch and separation initiated timer (although both must be relocated from the octagon to the Capsule adapter/Spacecraft adapter interface), and engine gimbals. A new deployment mechanism is required for the high gain antenna, but the MM '71 high gain articulation mechanism may suffice for MM '73 with repositioning. Likewise, the MM '71 separation V-band is applicable to MM '73, but the separation spring-loaded pistons must be redesigned to accommodate Orbiter separation from the Capsule adapter, as well as emergency separation from the entire Flight Capsule and Capsule adapter. A separate discussion of the Mechanical Devices Subsystem has not been considered necessary (in Section D.4) since the devices themselves are covered in varying depth in the other subsystem descriptions (e.g., high gain antenna articulation is discussed as part of the Radio Subsystem).

The Pyrotechnic Subsystem (sometimes considered part of the Propulsion group) includes the squib actuated devices of the Orbiter and the electronic units which fire the squibs. The subsystem is involved in the performance of solar panel deployment, high gain antenna deployment, propulsion maneuvers, Capsule adapter separation, scan platform unlatching, and Spacecraft separation (if assigned to the Orbiter). The subsystem is comprised of squib-actuated band release devices, squib-actuated pin-pullers, valve squibs, and two identical pyro control units. The latter redundantly store energy, exercise command control, and switch firing power to selected squibs. In general, the recharge time of the control unit capacitors prohibits successive firing events from being spaced any more closely than 90 seconds. In view of its simplicity and similarity to MM '71, a detailed description of the Pyrotechnics Subsystem has been omitted.

The Orbiter Cabling Subsystem electrically interconnects the various electronic assemblies, subsystems, and subassemblies of the Orbiter and adapters. The principal elements of cabling are the upper and lower ring harnesses and assembly harnesses. The former interconnect assemblies and subsystems on the top and bottom surfaces of the octagon, respectively. The latter interconnect subassemblies into functional subsystems and provide connections external to each assembly in the eight

major electronics assemblies of the octagon. Also included in the Cabling Subsystem are the separation connectors. The MM '73 Spacecraft in toto requires three such electrical disconnects at the following separation planes:

1. Spacecraft adapter/Spacecraft
2. Separated Capsule/canister afterbody
3. Orbiter/Capsule adapter

It is clear that the last disconnect is part of the Orbiter; it probably can be similar to its MM '71 predecessor if ample spare pins are provided in MM '71 for MM '73 Capsule functions. It is equally clear that the second disconnect will be assigned to the Capsule system. Since it must carry prelaunch umbilical and flight functions for both the Capsule and the Orbiter, the first disconnect is the largest of the three, and its system assignment is also problematical. Because the Cabling Subsystem is tied so closely to the detailed electrical design of the Orbiter, further description is considered premature at this time.

D.2.3.1.3 Telecommunications

Four subsystems classically comprise the planetary telecommunications group: Radio, Command, Telemetry, and Data Storage. The addition of the Capsule system in MM '73 adds a newcomer to this grouping, the Relay Subsystem. Also, because of its significant interfaces with the Flight Telemetry and Data Storage Subsystems, the Data Automation Subsystem is included in the telecommunications group in this discussion.

The keystone of the telecommunications is the Radio Frequency Subsystem, that subsystem functionally responsible for S-band reception from and transmission to the stations of the Deep Space Instrumentation Facility (DSIF), detection and demodulation of the signal received at the Spacecraft, coherent frequency translation of the uplink signal for subsequent downlink transmission, and modulation of the downlink carrier. Comprising the subsystem are three antennas (high gain, primary low gain, and secondary low gain), two redundant 20-watt TWT power amplifiers and exciters, a phase tracking receiver, and associated switching and isolation. Except for two antennas and their switches, the components are identical to MM '69 and MM '71. The high gain antenna is a prime focus paraboloid with a diameter of 63 inches and a nose gain of 29.4 dB. It is deployed and then steered along a single axis through an angular range of approximately 35° (for a 90-day orbiting mission). The primary low gain antenna is similar to that used on MM '69 and '71. It is pointed along the negative roll axis, and its pattern is symmetrical about the axis, with a peak gain of 7.5 dB and a 3 dB beamwidth of 80° . The secondary low gain antenna is mounted on the tip of one of the solar panel structures and is oriented such that its toroidal-shaped pattern lies roughly in the plane of the ecliptic. It has a gain of 4.5 dB and a beamwidth of 50° . Switching is arranged so that transmission can occur on any antenna, while reception can only occur on the two low gains. The high gain antenna is employed principally for high data rate transmission to Earth; the primary low gain

for low rate cruise attitude communications; and the secondary low gain for downlink telemetry when the spacecraft is in a maneuver attitude.

The Flight Command Subsystem operates on subcarriers from the Radio Subsystem, demodulates and decodes the command information, and issues commands to the applicable subsystems of the Orbiter and to the Capsule. The subsystem employs three types of commands:

1. Direct commands, which are single, discrete switch closures and are used by the majority of subsystems.
2. Coded commands, which are binary data streams sent to the CC&S and Capsule sequencer for updating information stored therein.
3. Quantitative commands, which are binary data streams sent to the scan control subsystem for updating of scan platform cone and clock references.

The command subsystem consists of a command detector and a command decoder. Because of the additional commands required by the flight capsule, the MM '69 decoder will require expansion by MM '73, if not before.

The Flight Telemetry Subsystem conditions, encodes, and multiplexes Spacecraft engineering data. Two modulated data channels are sent to the Radio Subsystem, a high rate channel and a low rate channel. The high rate channel is employed for Orbiter and Capsule science data from the data storage and relay subsystems and functions in two modes, depending on which DSN antenna is in view of the Orbiter. A rate of 8.1 or 4.05 kbps is employed to the 210 foot diameter antenna at Goldstone, while 500 or 250 bps is used for 85 foot dishes. The former are exactly half those planned for MM '71; the 500 and 250 bps rates are new to MM '73. The higher of each pair of rates can be sustained to a worst-case range of 330×10^6 km. Spacecraft engineering data is transmitted at either $8\frac{1}{3}$ or $33\frac{1}{3}$ bps on the low rate channel.

The Data Storage Subsystem consists of two MM '69 analog tape recorders (ATRs), two MM '69 digital tape recorders (DTRs), and two new DTRs for relay data storage. Each ATR has a storage capacity of 1.57×10^8 equivalent bits of data; each MM '69 DTR can store 2.3×10^7 bits, and each new DTR 8.4×10^7 bits. The ATRs are employed exclusively for storage of orbital television; the MM '69 DTRs are used to store other orbital science, and the new DTRs are reserved for Capsule relay data. Playback rates are consistent with the MM '73 telemetry data rates; record rates accommodate the Capsule relay data rates as well as the MM '69 orbital science data rates.

The data automation subsystem controls, encodes, and multiplexes the orbiter science and routes it to either the flight telemetry subsystem or data storage subsystem for direct or delayed transmission, respectively. The MM '69 DAS is briefly described in Section D-5. Since the DAS is so highly dependent on the actual orbital science, no forecast of the particulars of the MM '73 DAS is attempted.

The relay subsystem accepts data from the separated Capsule during Capsule cruise and entry and from the Lander during post-impact operation and routes it to the FTS or the DSS for direct or delayed transmission to Earth. Relayed data is received on a 400 MHz carrier at 1340 bps during cruise and entry and 160 kbps after landing. Reception is accomplished by selectively switching between two identical antennas mounted at the tips of orthogonal solar panels. Each antenna is a turnstile over a ground plane with a gain of +4 dB on axis and +3 dB at $\pm 55^\circ$ off axis. The antenna switch output proceeds through a receiver and FSK demodulator prior to routing to the DSS or FTS. The relay subsystem is entirely new for the MM '73 capsule mission.

D.2.3.1.4 Guidance and Control

The Power Subsystem provides a central supply of power to operate the electrical equipment on board the Spacecraft, switching and control functions for the effective management and distribution of the power, and a control timing function for the Orbiter. Power is derived from four photovoltaic solar panels with a total area of 111 to 115 square feet. Stored power is provided via a rechargeable battery. Principle power distribution is ac; viz., 50 volts rms, 2400 Hz, square wave. Also available are 400 Hz (both single and three-phase) and unregulated dc at 25 to 50 volts. In addition to the array and battery, the Power Subsystem includes two redundant boost regulators, two redundant 2400 Hz inverters and clocks, two 400 Hz inverters (one for each phase), battery charging circuitry, and boost mode sensing and control electronics to prevent undesired array/battery sharing when the Spacecraft is sun oriented.

The attitude control subsystem acquires and stabilizes the Spacecraft to the Sun and Canopus, maneuvers the Spacecraft to any spatial attitude for subsequent propulsive velocity increments, and maintains vehicle attitude and stability during engine firings. Comprising the subsystem are Sun sensors, the Canopus sensor, the gyro control unit, attitude control electronics, the cold gas system, and engine gimbal actuators. For MM '73, the view of the MM '71 secondary Sun sensors located on the positive roll side of the octagon is blocked by the flight Capsule; the sensors required relocation outboard on the solar panels. Changes to the Canopus sensor light shield are likely to minimize solar reflections from the flight Capsule. The autopilot electronics will undoubtedly be changed to accommodate the different dynamic characteristics of the MM '73 Spacecraft. Similarly, additional cold gas is required.

In the direct entry mode of Capsule delivery, the addition of an approach guidance subsystem is possible, especially if the accuracy with which the impact parameter (B) can be determined by the DSIF results in excessive landing site dispersions. Such a subsystem was originally planned for MM '69, but was removed prior to PTM assembly. Its relative state of readiness makes it a definite candidate for MM '73.

The Central Computer and Sequencer (CC&S) is a special purpose digital processor which generates and distributes on-board commands so that the spacecraft can perform its mission automatically. Functions controllable by the CC&S include panel deployment and initial stabilization, maneuvers and engine firings, orbital sequencing of instruments and the scan platform, and high gain antenna articulation. The CC&S

consists of a reprogrammable computer and a maneuver sequencer. Computer re-programming is accomplished via coded commands through the flight command subsystem. The maneuver sequencer functions as a redundant source of critical maneuver and burn timing commands. Readout of the CC&S may be accomplished via the flight telemetry subsystem for ground verification of the contents of the computer memory. Although the entire MM '73 mission profile cannot be programmed into the limited MM '69 computer memory, the 128-word memory is sufficiently large such that minimal ground reprogramming is anticipated to conduct a nominal MM '73 mission automatically. With this qualification, the MM '69 CC&S appears adequate for MM '73.

The scan control subsystem controls the pointing of the scan platform during the orbital mode of the mission. Control is nominally from the CC&S, with backup by ground (quantitative) commands via the FCS. In its MM '71 mode of operation, the scan control is commanded to track the local vertical by pulses from the CC&S which represent increments in the nadir cone and clock angles. Modifications to the MM '69 subsystem are anticipated for use aboard MM '71; provided these are accomplished, no further modification is foreseen for MM '73.

D.2.3.1.5 Science

MM '69 carries four science subsystems: television, infrared spectrometer, infrared radiometer, and ultraviolet spectrometer. It has been suggested that all four of these experiments could be carried aboard the MM '71 Orbiter, with major modification to the cooling mechanism of the IRS. However, experiment selection for MM '71 has not been announced at the time of this writing. In view of the lack of definition of the MM '71 orbital payload, no attempt has been made to extrapolate to a reasonable successor payload for the Orbiter in '73.

D.2.3.2 Spacecraft Configuration - Direct Entry Capsule

Fig. D-14 depicts the spacecraft configuration for a typical direct entry Capsule. The illustrated aeroshell diameter is 10.5 feet. Fig. D-14 is a replica of fig. D-4, which was presented in Section D.2.2 as the typical product of the direct entry Spacecraft configuration evolution. Sitting atop the Capsule adapter is the MM '73 orbiter, which, from a configuration viewpoint, is a replica of the MM '71 orbiter. This configuration requires a bulbous shroud 12.5 feet in diameter.

Shown in fig. D-15 is an alternate direct entry Spacecraft configuration with a larger 14 foot Capsule. The shroud diameter must increase to nominally 16 feet to accommodate this configuration. The diameters of both the Capsule adapter and Spacecraft adapter must increase correspondingly to accommodate the 14 foot Capsule, but the basic Orbiter configuration is unperturbed by Capsule variations.

D.2.3.3 Spacecraft Configuration - Out-of-Orbit Entry Capsule

Fig. D-16 illustrates the Spacecraft configuration to accommodate a typical (8.5 foot) out-of-orbit entry Capsule within a standard 10 foot shroud. This configuration

is a replica of that presented as fig. D-12 at the conclusion of the out-of-orbit entry configuration evolution study. Note the increased size of the propulsion module in contrast to the direct entry configurations.

Fig. D-17 is a more detailed general arrangement drawing of the sketch of fig. D-16. The reader should note the following significant features of this configuration, all of which represent significant departures from MM '71:

1. Increased propellant tank volume by the addition of cylindrical sections.
2. Stowage of the new 63 inch high gain antenna in the space between the Capsule adapter and the shroud.
3. Location of the dual VHF relay antennas at the tips of the positive X- and Y-axis solar panels.
4. Location of the secondary low gain (maneuver) antenna at the tip of the negative Y-axis solar panel.
5. Mounting of the primary low gain antenna above octagon bay VI, and lengthening of the antenna to compensate for the increased length of the propulsion module.
6. Interface of the Orbiter with the Capsule adapter.

Details of the propulsion module and the Capsule adapter are given in Section D.4.

Fig. D-18 depicts the fields of view of the following components of the out-of-orbit entry Spacecraft:

1. Primary and secondary sun sensors.
2. Canopus sensor.
3. Scan platform.
4. High gain antenna.
5. Primary low gain antenna.
6. Secondary low gain antenna.
7. Relay antennas.

D.2.4 FLIGHT CAPSULE INTERFACES

Prior to Orbiter-Capsule separation, telemetry, command, power, thermal, and mechanical interfaces exist between the flight Capsule and the Orbiter. Following separation, a telemetry interface exists. These interfaces are discussed in detail below.

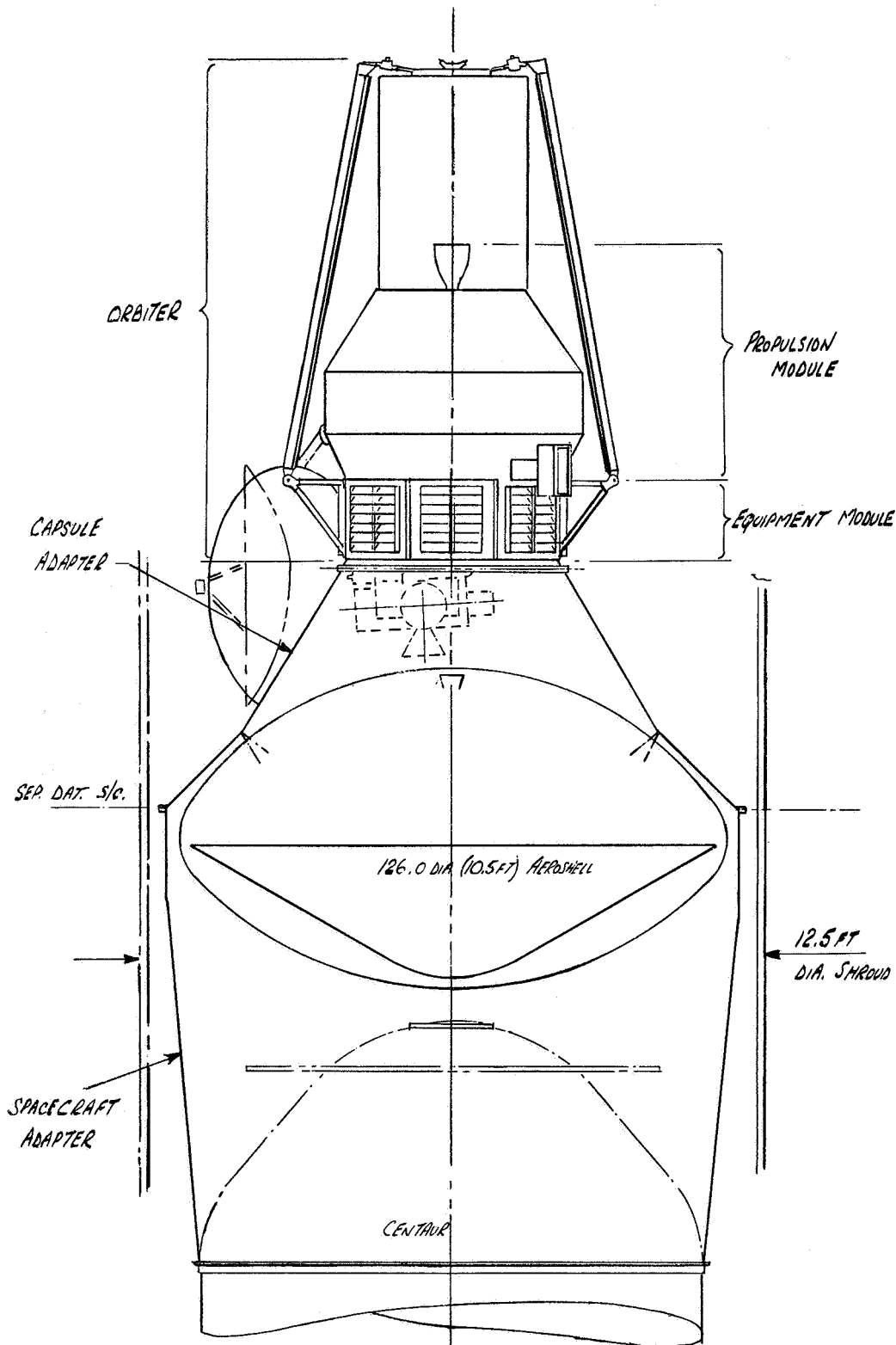


Figure D-14. Spacecraft Configuration - Minimum Science Direct Entry Capsule

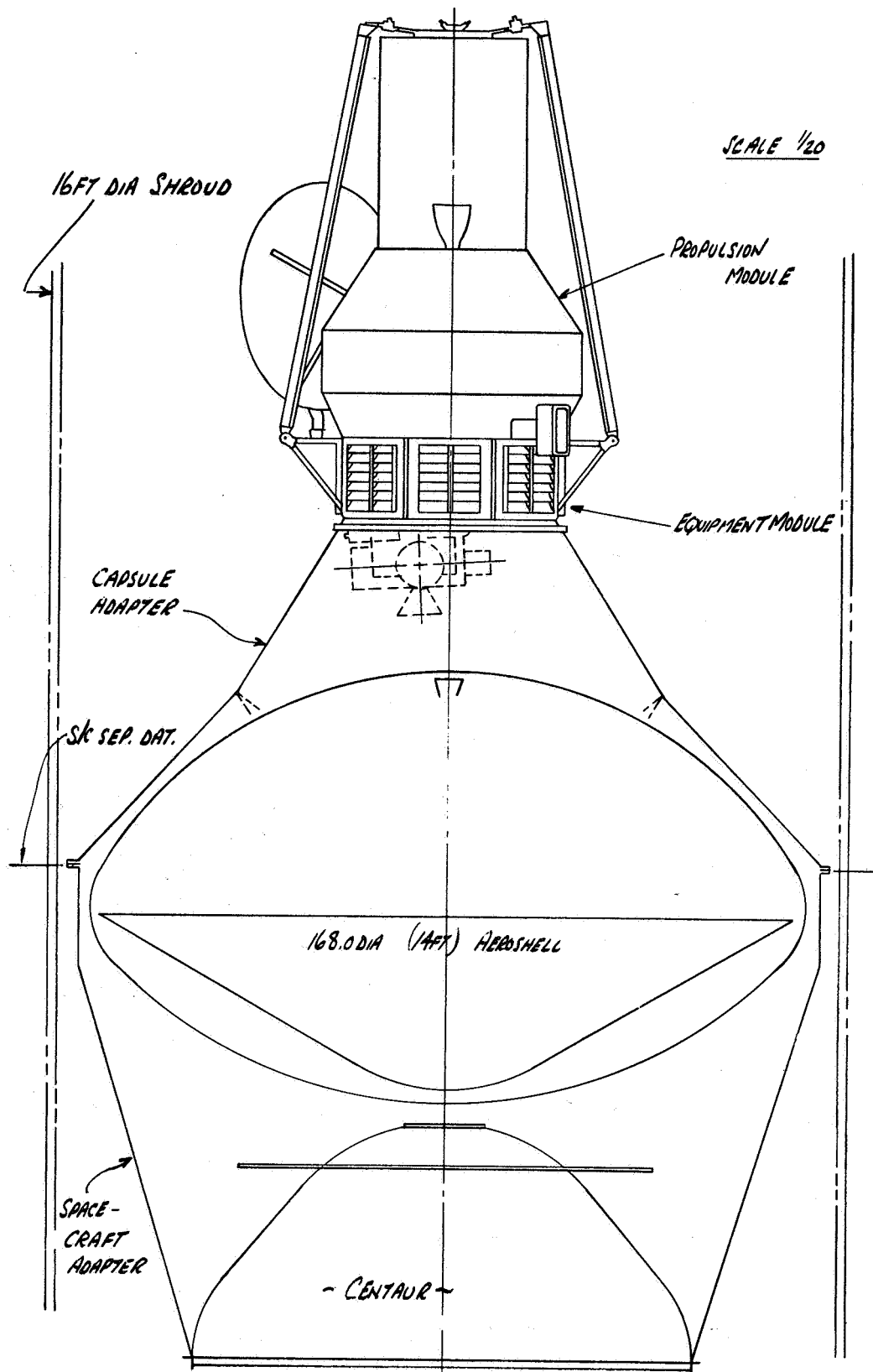


Figure D-15. Spacecraft Configuration - Maximum Science Direct Entry Capsule

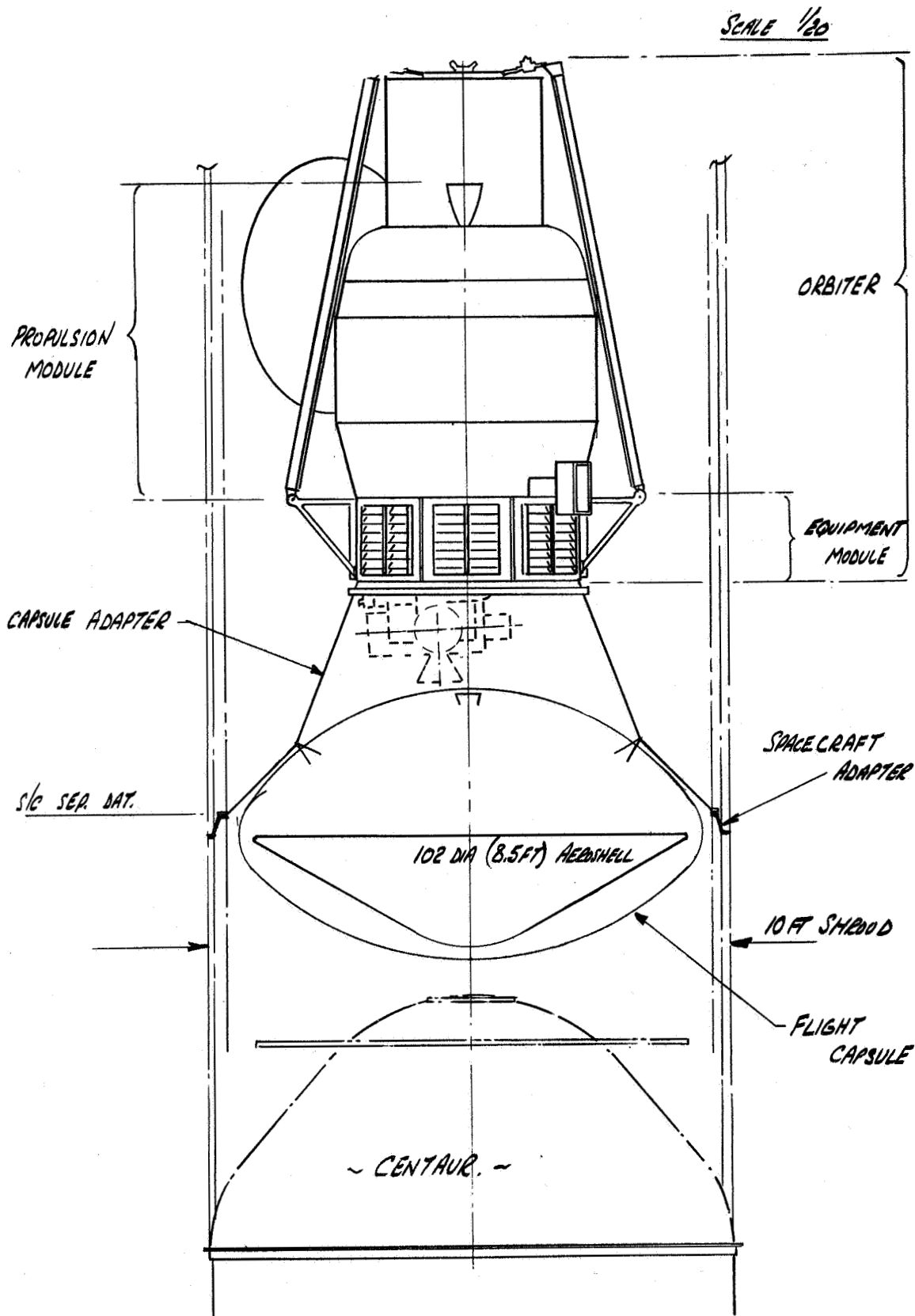
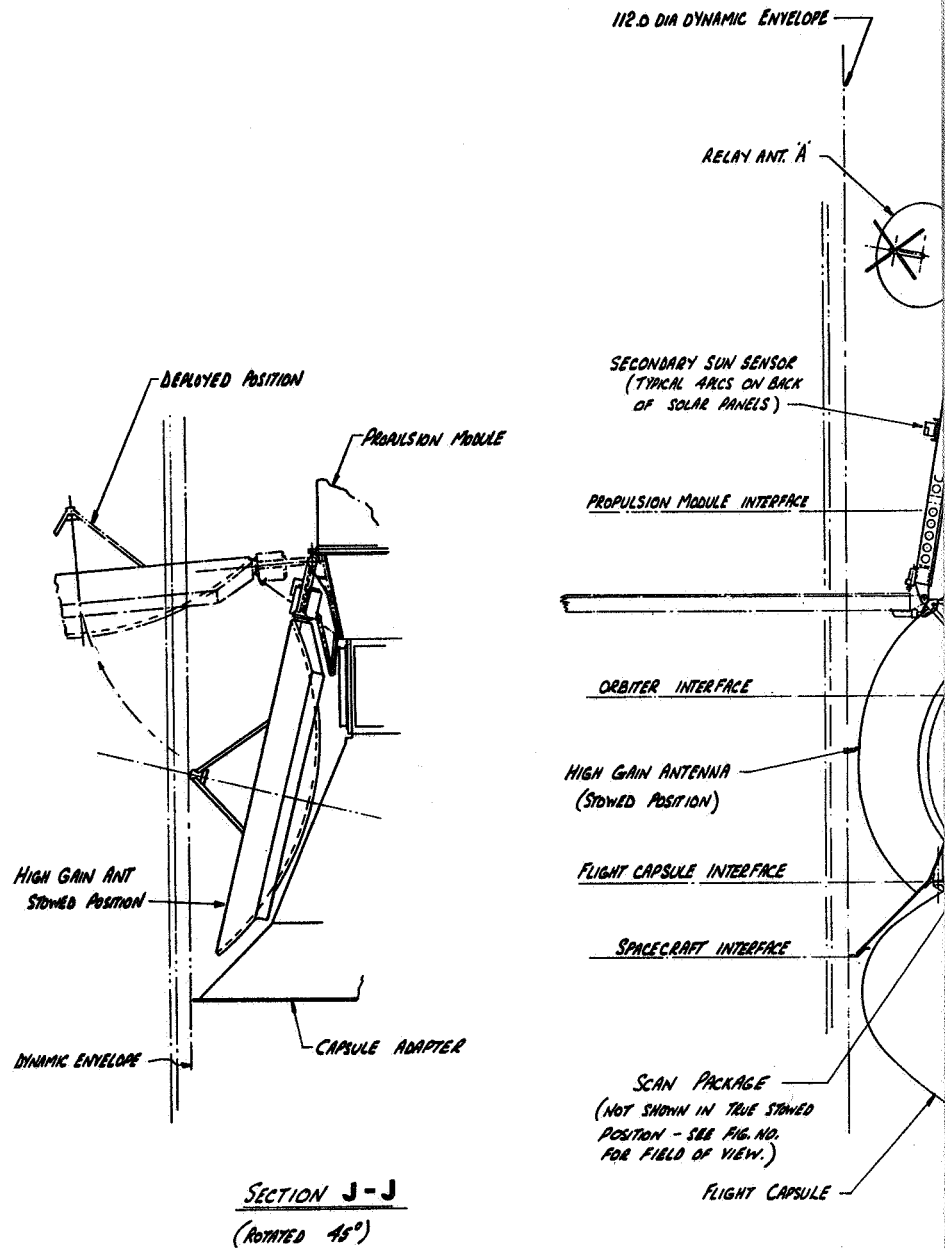


Figure D-16. Spacecraft Configuration - Minimum Science Out-of-Orbit Entry Capsule

FOLDOUT FRAME 1



FOLDOUT FRAME 3

FOLDOUT FRAME 2

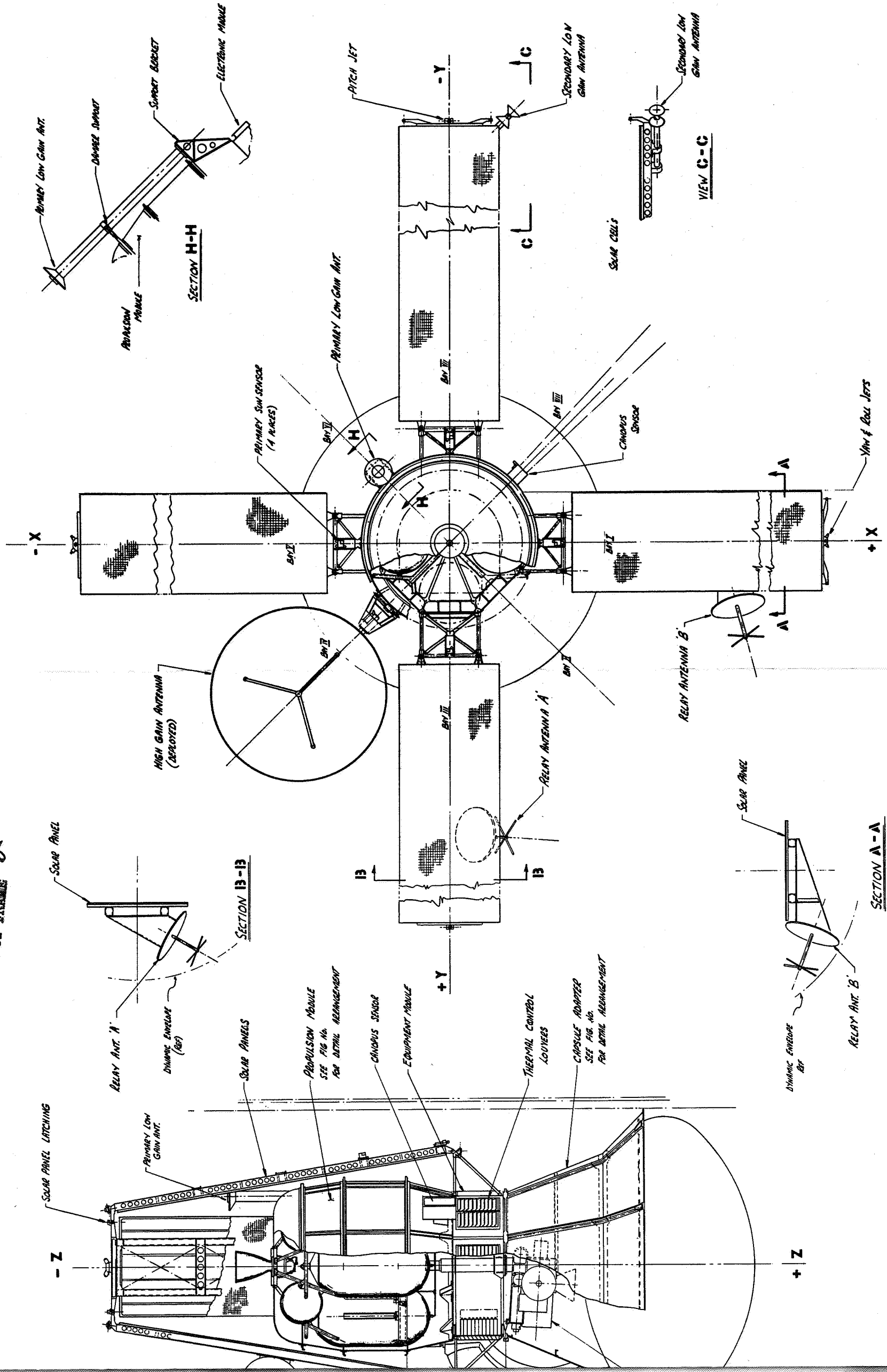


Figure D-17. Spacecraft General Arrangement

FOLDOUT FRAME 2

FOLDOUT FRAME 1

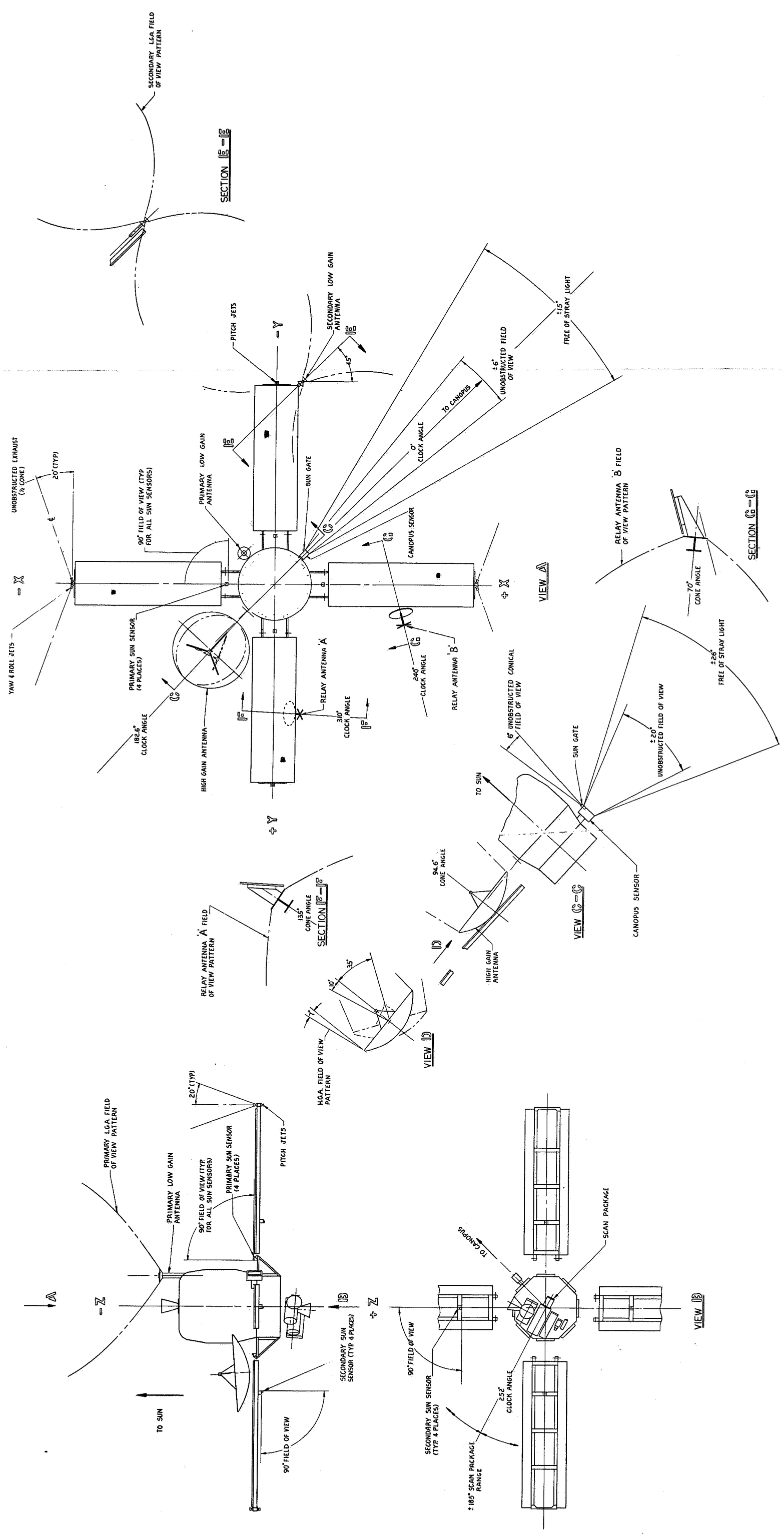


Figure D-18. Spacecraft Fields of View

D.2.4.1 Telemetry and Command

During the initial mission phases, flight Capsule engineering status is monitored by way of the Orbiter telemetry link. In order to minimize the number of wires crossing the Orbiter-flight Capsule interface as well as to keep the Lander telemetry subsystem dormant until pre-separation checkout, a commutator is included as part of the total canister design, and flight Capsule status is sampled during the cruise portion of the mission by this means. The amount of flight Capsule data transmitted during these early mission phases is less than 1 bps and has little impact on the Orbiter cruise telemetry data rates of 8 1/3 and 33 1/3 bps.

Approximately 24 hours before physical separation, Capsule pre-separation check-out is initiated. All flight Capsule subsystems which can be activated on a practical basis undergo a complete status check. If feasible, the Capsule relay link is energized and checked out through the use of dummy loads. Either the VHF relay link or direct readout of the Capsule telemetry subsystem results in a 1340 bps rate of flight Capsule status data being passed across the Orbiter-flight Capsule interface. This data is transmitted in real time by the Orbiter to verify flight Capsule status on Earth prior to Orbiter-Capsule separation.

Shortly before separation, the relay radio link between the Orbiter and the Capsule is activated once again, and a 1340 bps data rate assumed by the link. This data rate is maintained until the end of the post impact set-up time with the exception of a reduced duty cycle being utilized during the lengthy Capsule cruise period. The relay data is stored on board the Orbiter for subsequent transmission to Earth. During the total Capsule cruise, entry, terminal descent, impact, set-up, and post impact mission period of time, it is impossible to provide adequate viewing capability with one relay antenna on board the Orbiter in either a direct or an orbital entry mission, and two antennas are included in the design with switching from one to the other occurring at the appropriate mission time. (See Section D.5.6 for details). During the post impact imaging mission, the relay link data rate is increased to 160 bps as real time transmission of the imaging data is made to the Orbiter, where it is stored and read back to Earth at a rate compatible with the Orbiter capability.

Table D-5 summarizes the command requirements imposed upon the Orbiter Central Computer and Sequencer, command subsystem, and on-board devices as a result of the presence of the flight Capsule. It is assumed that canister forebody separation is initiated by the Capsule sequencer as part of the separation sequence. In addition, Capsule separation is also initiated by the Capsule sequencer while canister afterbody/adaptor (or emergency Capsule jettison) is performed by the Orbiter. This design concept minimizes the required number of separation signals and eliminates firing signals from crossing in-flight disconnects.

D.2.4.2 Power

The Orbiter provides all power requirements for the flight Capsule during interplanetary cruise with the exception of the interruption of thermal control power when performing off-Sun maneuvers. The raw array/battery thermal control power

TABLE D-5. FLIGHT CAPSULE COMMAND LIST

| Function | Command Source | | | |
|--|-----------------|-----|-----------------------------|------------------------|
| | Orbiter CC&S | GND | Misc. Orbiter Sources | Command Destination |
| Capsule Launch Mode Off | | X | X | Capsule |
| Update Capsule Sequencer (2) | | X | | Capsule |
| Capsule Power On/Off | X | X | | Orbiter |
| Start Capsule Battery Charging | X | X | | Orbiter |
| Stop Capsule Battery Charging | X | X | | Orbiter |
| Switch to Internal/External Power (Capsule Sequencer Prime Source) | | X | | Capsule |
| Start/Stop Capsule Checkout | X | X | | Capsule |
| Separation Sterilization Canister Forebody (Capsule Sequencer Prime Source) | | X | | Capsule |
| Enable/Disable Capsule Separation | | X | | Capsule |
| Start Separation Sequence (Below Initiated With One Command) | | | | |
| A. Start Capsule Seq. | X | X | | Capsule |
| B. Relay Radio On (1340 bps Rate Utilizing Primary Relay Antenna) | X | X | | Orbiter |
| Select High Relay Rate (160 Kbps) | X | X | X | Orbiter |
| Select Secondary Relay Antenna | X | X | | Orbiter |
| Select Low Relay Rate (1340 bps) | | X | | Orbiter |
| Select Primary Relay Antenna | | X | | Orbiter |
| Separate Canister Afterbody/ Adapter (Emergency Sep.) | X | X | | Orbiter |
| Relay Radio Off | X | X | | Orbiter |

required is dependent on the specific Capsule mission (i. e., flight Capsule diameter) as well as the desired temperature which is to be maintained. During interplanetary cruise to Mars, an abundance of Orbiter power is available; and thus, an ideal steady state temperature of +60°F is assumed to be maintained (although the allowable equipment range is between -40°F and +125°F. As the Spacecraft-Sun distance increases, Orbiter power must be used more conservatively; and, with the initiation of Capsule battery charging about 30 days before separation, a +20°F Capsule temperature requirement is assumed (to allow for an expected drop of about 50°F from separation to entry and still maintain the above -40°F restriction). Assuming the above temperature level requirements, the Orbiter power required for thermal reasons is as presented in table D-6. Interruption of thermal control power during the off-Sun orientation of the Spacecraft has little effect on Capsule subsystem temperatures, especially since the flight Capsule is normally located on the dark side of the spacecraft.

In addition to the thermal power, a total of approximately 5 watts of power is required for flight capsule status data collection, etc.; 15 watts for 20 day period for Capsule battery charging; and an estimated 75 watts for Capsule subsystem checkout during the pre-separation checkout period - all of which are raw array/battery dc power. An additional 0.2 watts of 2.4 KHz wave power is supplied to the relay subsystem during pre-separation checkout as well as from shortly before Orbiter-Capsule separation until after Capsule landing and termination of relay operation. Table D-6 summarizes the overall power requirements imposed on the Orbiter in support of a Capsule mission.

D. 2. 4. 3 Mechanical and Thermal

Three major interfaces accommodated by the Capsule adapter are the spacecraft interface, the Orbiter interface, and the Flight Capsule interface. The spacecraft inflight separation is accomplished at the spacecraft interface between one end of the Capsule adapter and the adapter system. This interface is described in Section D. 2. 7. The Orbiter interface located at the other end of the Capsule adapter and the flight Capsule interface at the mid-section of the Capsule adapter integrate the orbiter and Flight Capsule and are discussed in this paragraph. Although geometrically similar, different Capsule adapter sizes accommodate various Flight Capsule diameters. Capsule adapter physical descriptions are given in Section D. 4. 1.

The interface between the Orbiter and the Capsule adapter is similar to the MM '69 and '71 Spacecraft/adapter interface. An Orbiter ring and a Capsule adapter ring mate at the interface plane and are clamped together by a V-band separation mechanism. Separation springs provide a nominal separation velocity (approximately 3 ft/sec) to the Capsule adapter and canister afterbody when this mass is ejected. The separation velocity and tumbling rate of the Capsule adapter are not critical for this sequence. This separation system is so designed that it will function properly with or without the Capsule mass as a part of the separated system.

The thermal interface differs from the normal Mariner Orbiter because the Capsule adapter acts as a large radiating fin during cruise. Reasonable thermal

TABLE D-6. FLIGHT CAPSULE POWER REQUIREMENTS

| Mission Phase Power Use | Interplanetary Cruise (watts) | 30 to 10 Days Before Separation (watts) | 10 to 1 Days Before Separation (watts) | Pre-separation Checkout (watts) | Post Separation Checkout (watts) | Post Separation (watts) |
|-------------------------------|-------------------------------------|--|---|---------------------------------------|---|-------------------------------|
| | | | | | | |
| Thermal | | | | | | |
| A. Typical Out-of-Orbit Entry | 18 | 12.5 | 12.5 | 75 | 12.5 | |
| B. Typical Direct Entry | 28 | 20 | 20 | | 20 | |
| Status | 5 | 5 | 5 | | 5 | |
| Battery Charging | | | | | | |
| Relay Link | | 15 | | | | 0.2 |

isolation for the Orbiter is maintained by covering the Capsule adapter with super-insulation and by insulating the canister afterbody between the Capsule and Orbiter and insulating the dark side of the Orbiter.

The electrical interface plug, similar to Mariner, is redesigned to accommodate additional channels for power supply, monitoring, command signals, etc. to the Flight Capsule.

The mechanical interface between the Capsule adapter and the Flight Capsule comprises two mating rings with eight symmetrically located bolts at Capsule adapter longerons. This bolt connection is designed to provide access to the bolt from outside the adapter. Since there is no field joint requirements nor separation requirement for this interface the electrical interface becomes a continuous flexible cable across this juncture with a disconnect plug provided at the canister/canister adapter interface. Thermal isolation for the flight capsule is maintained by the common purpose superinsulation covering the capsule adapter.

D. 2. 5 MM'71 AND '73 COMMAND STRUCTURES

Table D-7 is a tabulation of the probable Mariner Mars '71 and '73 command requirements. The format is intended to show the correlation of ground commands, CC&S commands, and other on-board commands. Where substantial similiarity exists between MM'69 commands and proposed commands, the MM '69 command numbers are listed. New commands are so designated.

Table D-8 is a numerical tabulation of the quantities of ground, CC&S, and on-board commands required for the '71 and '73 orbiters.

D. 2. 6 FLIGHT SEQUENCE

Figure D-19 is a flow diagram which depicts the major mission flight events of the orbiter and Capsule and their relative timing.

D. 2. 7 SPACE VEHICLE

D. 2. 7. 1 Introduction

The conceptual designs selected for detailed definition include a direct entry and an out-of-orbit entry Capsule mission as the prime candidates of comparison for a 1973 Mars mission. These Capsule mission concepts may be combined with their corresponding Orbiter conceptual designs. The out-of-orbit entry Capsule is generally accommodated by the standard 10 ft. diameter shroud, while the direct entry mission generally requires a bulbous shroud between the standard 10 ft. and the maximum allowable 16 ft. diameter shroud. The launch vehicle selected for the 1973 mission (regardless of entry mode or Orbiter concept) is the Titan IIIC Centaur. Figure D-20 portrays the launch configurations of the extremes of these space vehicle conceptual designs as well as interface details of the integration of the Spacecraft and launch vehicle. The Spacecraft and launch vehicle have functional,

TABLE D-7. MM '71 AND '73 COMMAND CORRELATION

| Function | Destination | Ground Command | CC&S Command | Misc. On-Board Command |
|--|-------------|------------------|--------------|------------------------|
| <p>LAUNCH:</p> <p>CC&S output enable.</p> <p>DSS launch mode terminate: Allows DSS to turn off recorders at their next ends-of-tape. Circuit routed through both separation connectors.</p> <p>TWT on: Effective only in the event of a TWT off launch. Circuit is routed through both separation connectors.</p> <p>A/C on.</p> <p>Pyro arm: Arms pyro subsystem.</p> <p>Solar panel deploy: Unlatches solar panels for deployment.</p> <p>Deploy high-gain antenna.</p> <p>DSS power on/off. Power on Power off</p> <p>MANEUVER:</p> <p>Sequencer load: Used by fixed sequencer to enter maneuver parameters.</p> <p>Propellant enable: Opens explosive isolation valves in propellant lines; automatically selects next set of explosive valves.</p> | | | | |
| | CC&S | | | I1 |
| | DSS | | | I2 |
| | RFS | | | I4 |
| | A/C | (Refer to DC-13) | L2 | S3 |
| | | | | S1 T1 |
| | Pyro | | L1 | T2 |
| | Pyro | | New | New (SIT) |
| | Pwr | DC-47 | L3 | |
| | | | | |
| | CC&S | CC-4 | | |
| | Pyro | New | | |

TABLE D-7. MM '71 AND '73 COMMAND CORRELATION (CONT)

| Function | Destination | Ground Command | CC&S Command | Misc. On-Board Command |
|---|-------------|----------------|--------------|------------------------|
| <p>Pressurant enable: Opens explosive isolation valve in pressurant line; automatically selects next explosive valve.</p> <p>Tandem maneuver; Places CC&S logic in the tandem standby mode. Enables the tolerance detector.</p> <p>Maneuver enable:</p> <p> Enables CC&S output commands to A/C</p> <p> Turns off A/C subsystem if DC-13 was used to turn it on.</p> <p> Enables CC&S start and shutoff commands to propulsion.</p> <p>Maneuver start: Initiates tandem or fixed sequencer maneuver routine, depending on the state of CC&S maneuver logic.</p> <p>Computer maneuver initiate: Initiates a computer-only maneuver routine if the CC&S logic is in the nontandem standby mode.</p> <p>Gyros on: Turns gyros on for warmup.</p> <p>All axes inertial: Places all axes under inertial control.</p> <p>Turn polarity set: Sets polarity of roll or pitch turn.</p> <p>Roll turn: Executes roll turn.</p> <p>Pitch turn:</p> <p> Executes pitch turn.</p> <p> Turns capsule power off. ('73 only)</p> | Pyro | New | | |
| | CC&S | DC-33 | | |
| | A/C | DC-14 | | |
| | A/C | | | |
| | Prop | | | |
| | CC&S | DC-27 | | |
| | CC&S | DC-32 | | |
| | A/C | | M1 | |
| | A/C | | M2 | |
| | A/C | | M3 | |
| | A/C | | M5 | |
| | A/C | | M4 | |
| | Pwr | | | |

TABLE D-7. MM '71 AND '73 COMMAND CORRELATION (CONT)

| Function | Destination | Ground Command | CC&S Command | Misc. On-Board Command |
|--|---|---|---|------------------------|
| <p>Maneuver inhibit:</p> <p>Inhibits CC&S output commands to A/C, and initiates sun and Canopus reacquisition.</p> <p>Turns on A/C subsystem if CC&S and PAS fail to do so.</p> <p>Inhibits CC&S start and shutoff commands to propulsion.</p> <p>Resets fixed sequencer.</p> <p>Places maneuver logic in nontandem mode.</p> <p>Transmit primary/secondary low-gain antenna:</p> <p>Selects primary low-gain antenna for transmission.</p> <p>Selects secondary low-gain antenna for transmission.</p> <p>Propulsion start: Opens thrust chamber solenoid valves.</p> <p>Propulsion shutoff: Closes thrust chamber solenoid valves.</p> <p>Pressurant inhibit: Closes explosive isolation valve in pressurant line; automatically selects next explosive valve.</p> <p>Propellant inhibit: Closes explosive isolation valves in propellant lines.</p> | <p>A/C</p> <p>A/C</p> <p>Prop</p> <p>CC&S</p> <p>CC&S</p> <p>RFS</p> <p>RFS</p> <p>Prop</p> <p>Prop</p> <p>Pyro</p> <p>Pyro</p> | <p>DC-13</p> <p>New</p> <p></p> <p></p> <p></p> <p></p> <p></p> <p></p> <p></p> <p></p> | <p></p> <p>New</p> <p>New</p> <p>M6</p> <p>M7</p> <p></p> <p></p> | |

TABLE D-7. MM '71 AND '73 COMMAND CORRELATION (CONT)

| Function | Destination | Ground Command | CC&S Command | Misc. On-Board Command |
|---|-------------|----------------|--------------|------------------------|
| CRUISE: | | | | |
| Cruise mode: | | | | |
| DAS, science, and scan orbital power off. Heater power on. | Pwr | | | |
| During record mode: Turns off power to the record motor and places DSS in ready mode. During playback: Stops playback in DSS. | DSS | | | |
| Turns IRS motor off. | IRS | DC-1 | N5 | |
| Selects cruise data mode. | FTS | | | |
| Data rate switch: In any data mode, To 8-1/3 bps switches the engineering channel data rate between 8-1/3 and 33-1/3 bps. To 33-1/3 bps | FTS | DC-5 | C2 C6 | |
| FTS redundant elements switch: Selects alternate redundant elements in the FTS. | FTS | DC-6 | | |
| Power amplifier switch: Selects alternate TWT. | RFS | DC-7 | | |
| Exciter switch: Selects alternate exciter. | RFS | DC-8 | Y1 | |
| Ranging on/off. Turn off Turn on | RFS | DC-9 | | |
| Transmit high/low gain antenna: | | | | |
| Selects high-gain antenna for transmission | RFS | | C3 | |
| Selects primary or secondary low-gain antenna for transmission. | RFS | New | New | |
| Battery charging on/off. | Pwr | DC-38 | | |

TABLE D-7. MM '71 AND '73 COMMAND CORRELATION (CONT)

| Function | Destination | Ground Command | CC&S Command | Misc. On-Board Command |
|---|-------------|----------------|--------------|------------------------|
| Boost mode enable/inhibit: Enable function is subject to sun gate signal. | Pwr | DC-37 | | |
| Prevents boosting when not sun-oriented. | Pwr | | | G1 |
| Battery test load: Assesses battery by toggling battery test load off/on. | Pwr | DC-50 | | |
| Platform unlatch: Permanently releases latch on scan platform. | Pyro | DC-45 | C5 | |
| Platform heater No. 2: Toggles IRS backup heater off/on. Nominally off. | Pwr | DC-34 | | |
| Computer load: Used to program computer. First of a pair of CC's required for programming the computer. | CC&S | CC-1 | | |
| Computer load: Used to program computer. Second of a pair of CC's required for programming the computer. | CC&S | CC-2 | | |
| Tolerance detector disable: Used to disable the tolerance detector, which inhibits the CC&S when the input power drops out the tolerance. | CC&S | CC-5 | | |
| Word interrogate: Effects single-word memory readout in the CC&S. | CC&S | CC-3 | | |
| CC&S readout select: With successive transmissions, initiates CC&S memory readout, or selects engineering telemetry on the engineering channel. | FTS | DC-2 | | |
| Computer enable: Enables computer output actuators. Starts computer operation after a DC-30. Resets all flags. | CC&S | DC-31 | | |

TABLE D-7. MM '71 AND '73 COMMAND CORRELATION (CONT)

| Function | Destination | Ground Command | CC&S Command | Misc. On-Board Command |
|---|-------------|----------------|--------------|------------------------|
| Computer inhibit: Inhibits computer output actuators. Halts computer operation. Resets all flags. | CC&S | DC-30 | | |
| Canopus roll control: Resets DC-15, DC-18, DC-20, and DC-40. Initiates Canopus acquisition if roll axis not under sensor control. | A/C | DC-19 | | |
| Roll search/step: Turns on gyros. Forces sensor off light source, and begins Canopus search. Subsequent to DC-18, produces a negative roll increment. | A/C | DC-21 | | |
| Inertial roll control/step: Gyros on. Places roll axis under inertial control. Positive roll increment on subsequent transmission. | A/C | DC-18 | | |
| Canopus gate override: Removes Canopus brightness gate thresholds. Turns off gyros, if gyros were on only because of absence of Canopus acquisition signal. | A/C | DC-15 | | |
| Roll control inhibit: Inhibits roll axis control. Turns off gyros, if gyros were on only because of absence of Canopus acquisition signal. | A/C | DC-20 | | |
| Gyros off: Forces gyros to turn off in spite of any inputs to the gyro control OR gate. | A/C | DC-40 | | |
| Adaptive gate step: Successively steps lower Canopus brightness gate to lower values. When minimum setting is reached, next command resets lower gate to its maximum setting. | A/C | DC-12 | Y2 | |
| Canopus cone angle step: Advances cone angle to next position. | A/C | DC-17 | C1 | |

TABLE D-7. MM '71 AND '73 COMMAND CORRELATION (CONT)

| Function | Destination | Ground Command | CC&S Command | Misc. On-Board Command |
|---|-------------|----------------|--------------|------------------------|
| <p>FAR ENCOUNTER: (MM '71 only)</p> <p>Far-encounter position:</p> <p> Selects far-encounter references. Enables far-encounter planet sensor.</p> <p> Enables far-encounter logic; effective only if DSS is in the ready mode.</p> <p>Far-encounter-planet-sensor control: Switches platform control in far-encounter-planet-sensor loop.</p> <p>Far TV picture: Records a TV picture on analog tape machine.</p> <p>ORBIT:</p> <p>TV covers deploy.</p> <p>Science phase:</p> <p> DAS, DSS, science, and scan orbital power on. Heater power off.</p> <p> Turns off battery charger.</p> <p> Places FTS in orbit mode.</p> <p> Starts IRS motor.</p> <p> Disables far-encounter planet sensor. (MM '71 only)</p> <p> Places DSS in ready mode.</p> | | | | |
| | Scan | | | |
| | DSS | DC-28 | F1 | |
| | Scan | DC-35 | | |
| | DAS | DC-36 | F2 | |
| | | | | |
| | TV | DC-46 | N7 | |
| | Pwr | | | |
| | Pwr | | | |
| | FTS | | | |
| | IRS | | | |
| | Scan | DC-25 | N1 | |
| | DSS | | | |

TABLE D-7. MM '71 AND '73 COMMAND CORRELATION (CONT)

| Function | Destination | Ground Command | CC&S Command | Misc. On-Board Command |
|--|-------------|----------------|-------------------|------------------------|
| <p>Orbital sequence enable/inhibit:</p> <p>Places DAS in orbit mode.</p> <p>Places DAS in standby mode.</p> <p>Start/stop orbital TV:</p> <p>Start collection of orbital TV pictures.</p> <p>Stop collection of orbital TV pictures.</p> <p>Start/stop orbital nonvideo data:</p> <p>Start collection of orbital nonvideo data.</p> <p>Stop collection of orbital nonvideo data.</p> <p>Release scan control pulse trains.</p> <p>Cone angle positive step: Positively steps cone angle reference value a variable number of increments.</p> <p>Cone angle negative step: Negatively steps cone angle reference value a variable number of increments.</p> <p>Clock angle positive step: Positively steps clock angle reference value a variable number of increments.</p> <p>Clock angle negative step: Negatively steps clock angle reference value a variable number of increments.</p> | DAS | DC-26 | N6 | |
| | DAS | | New | |
| | DAS | New | New | |
| | DAS | | New | |
| | DAS | New | New | |
| | DAS | | New | |
| | CC&S | | | New (DAS) |
| | Scan | QC-1 | New (Pulse train) | |
| | Scan | QC-2 | New (Pulse train) | |
| | Scan | QC-3 | New (Pulse train) | |
| | Scan | QC-4 | New (Pulse train) | |

TABLE D-7. MM '71 AND '73 COMMAND CORRELATION (CONT)

| Function | Destination | Ground Command | CC&S Command | Misc. On-Board Command |
|--|-------------|----------------|-------------------|------------------------|
| Normal record mode. | DSS | New | | |
| Advance record mode to next state. | DSS | New | | |
| Digital tape track switch: Steps digital tape machine No. 1 to next track and steps digital end-of-tape counter No. 1 | DSS | DC-22 | | |
| Digital tape track switch: Steps digital tape machine No. 2 to next track and steps digital end-of-tape counter No. 2. | DSS | DC-22 | | |
| Analog tape track switch: Steps analog tape machine No. 1 to next track and steps analog end-of-tape counter No. 1 | DSS | DC-23 | | |
| Analog tape track switch: Steps analog tape machine No. 2 to next track and steps analog end-of-tape counter No. 2. | DSS | DC-23 | | |
| Analog erase: Effective only when DSS is in the ready mode. | DSS | DC-39 | | |
| High-gain antenna positive step: Positively steps high-gain antenna reference value a variable number of increments. | RFS | New (QC) | New (Pulse train) | |
| High-gain antenna negative step: Negatively steps high-gain antenna reference value a variable number of increments. | RFS | New (QC) | New (Pulse train) | |
| Transmit 8.1/4.05 kbps | FTS | | New | |
| Transmit 500/250 bps | FTS | | New | |
| Science off precondition: Preconditions TV and IRR for power turn-off. | TV IRR | DC-48 | | |

TABLE D-7. MM '71 AND '73 COMMAND CORRELATION (CONT)

| Function | Destination | Ground Command | CC&S Command | Misc. On-Board Command |
|--|-------------|----------------|--------------|------------------------|
| PLAYBACK: | | | | |
| Normal playback mode. | DSS | New | | |
| Advance playback mode to next state. | DSS | New | | |
| ATR playback mode: Initiates playback of analog recorders. | DSS | | New | |
| DTR playback mode: Initiates playback of digital recorders. | DSS | DC-3 | P1 | |
| ATR playback low/high data rate: Selects low/high data rate in ATR playback mode. | FTS DSS | New | | |
| DTR playback low/high data rate: Selects low/high data rate in DTR playback mode. | FTS DSS | New | | |
| CAPSULE: ('73 only) | | | | |
| Capsule launch mode off. | Cap. | New | | New (SC) |
| Update capsule sequencer: Used to program sequencer. First of a pair of CC's required to program the capsule sequencer. | Cap. | New (CC) | | |
| Update capsule sequencer: Used to program sequencer. Second of a pair of CC's required to program the capsule sequencer. | Cap. | New (CC) | | |
| Capsule power on/off: Provides/withholds power to the flight capsule system. | Pwr | New | New | |
| Power on | | | Refer to M4 | |
| Power off | | | | |

TABLE D-7. MM '71 AND '73 COMMAND CORRELATION (CONT)

| Function | | Destination | Ground Command | CC&S Command | Misc. On-Board Command |
|---|-------|-------------|----------------|--------------|------------------------|
| <p>Start/stop capsule battery charging</p> <p>Switch to internal/external power: Switches flight capsule to spacecraft or internal power. (Capsule sequencer prime source.)</p> <p>Start/stop capsule checkout.</p> <p>Separate sterilization canister forebody. (Capsule sequencer prime source.)</p> <p>Enable/disable capsule separation.</p> <p>Start separation sequence:</p> <p> Start capsule sequencer.</p> <p> Relay radio on. (500 bps rate utilizing primary rate antenna.</p> <p>High rate relay. (16.2 kbps)</p> <p>Select secondary relay antenna.</p> <p>Low rate relay (500 bps)</p> <p>Select primary relay antenna</p> <p>Separate canister afterbody/adapter. (Emergency separation)</p> <p>Relay radio off.</p> | Start | Pwr | New | New | |
| | Stop | | | New | |
| | | Cap. | New | | |
| | Start | Cap. | | New | |
| | Stop | | New | | |
| | | Pyro | New | New | |
| | | Cap. | New | | |
| | | | | | |
| | | Cap. | | New | |
| | | Relay | New | | |
| | | Relay | New | | New |
| | | Relay | New | New | |
| | | Relay | New | | |
| | | Relay | New | | |
| | | Pyro | New | New | |
| | | Relay | New | | |

physical, and electrical interfaces, and the space vehicle has interfaces with launch operations--all of which are discussed below.

D.2.7.2 Spacecraft - Launch Vehicle Integration

When the Spacecraft is mounted on the launch vehicle, it is capable of maintaining launch readiness in a fueled and mated condition for the full duration of a 30-day launch period. Thermal control (air conditioning) is provided from external space vehicle sources through an access door above the spacecraft-launch vehicle in-flight separation interface; and, at least when considering the standard Titan III shroud, such access doors can be included in the shroud design as required. On pad direct communication from the spacecraft to the launch complex equipment is provided through another transparent door provided for that purpose. During ascent through the Earth's atmosphere, aerodynamic protection and adequate thermal control is provided by the launch vehicle payload fairing, and telemetry data transmission from lift-off through separation from the Centaur is nominally planned by way of the launch vehicle only.

TABLE D-8 COMMAND SUMMARY

| | Ground Commands | | | CC&S Commands | | | Misc. On-Board Commands |
|--|-----------------|----|----|---------------|-------------|--------|-------------------------|
| | DC | QC | CC | Discrete | Pulse Train | Cyclic | |
| Number of MM'69 commands | 49 | 4 | 5 | 28 | 1 | 2 | 14 |
| Number of MM '69 commands retained in MM '71 | 39 | 4 | 5 | 22 | 0 | 2 | 8 |
| Number of new commands in MM '71 | 15 | 2 | 0 | 12 | 6 | 0 | 2 |
| Number of MM '71 commands | 54 | 6 | 5 | 34 | 6 | 2 | 10 |
| Number of MM '69 commands retained in MM '73 | 36 | 4 | 5 | 20 | 0 | 2 | 8 |
| Number of new commands in MM '73 | 29 | 2 | 2 | 20 | 6 | 0 | 4 |
| Number of MM '73 commands | 65 | 6 | 7 | 40 | 6 | 2 | 12 |

Two types of adapter systems are employed to mount the spacecraft on the launch vehicle. One design accommodates Spacecraft configurations that can be encapsulated in a standard 10 ft diameter shroud. The other adapter system provides support for those spacecraft that exceed the limitations of a 10 ft diameter shroud and require a bulbous (or hammerhead) shroud as an aerodynamic fairing. The physical interface and separation plane between the Spacecraft and the launch vehicle is provided by these two types of adapter systems.

The adapter system consists of eight bathtub fittings for those Spacecraft that fit within the 10 ft diameter shroud. These eight fittings attach to the shroud longerons at eight symmetrical locations and mate with the Capsule adapter at the separation plane as shown in detail B in Fig. D-20. The mechanical interface comprises these mating surfaces and a captive bolt and separation nut attachment at each of the eight fittings along with eight separation springs. A description of this interface structure is summarized in Section D.4.1.

Spacecraft encapsulated in bulbous shrouds are supported by the forward Centaur kick ring at Centaur Station 220. The adapter system that carries the loads between the spacecraft and the Centaur is a semi-monocoque conical frustum as shown in Fig. D-20. This figure also shows how the interface rings for the capsule adapter and the adapter system mate at the spacecraft interface plane to form the mechanical interface. Eight captive bolt and separation nut attachments join these two rings and employ eight springs to impart the proper separation velocity. A structural description of this adapter system is also discussed in Section D.4.1.

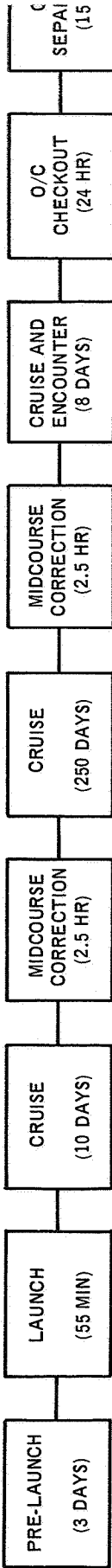
The electrical interface between the spacecraft and the launch vehicle consists of a modified 84 pin connector currently used on the Mark 12 Program. The electrical exchanges through this connector consist of ground power, launch monitor control, and orbiter and capsule telemetry while on the launch pad. All of these functions go through the structural shroud to launch complex umbilicals below the Spacecraft-launch vehicle in-flight disconnect. In addition to the above, Spacecraft telemetry data is passed through the electrical in-flight disconnect to the launch vehicle telemetry system and transmitted to Earth during launch and injection. Since squib firing circuits are not routed through the electrical separation connector, direct wiring from the launch vehicle to the Centaur side of the interface first separates the electrical in-flight disconnect and then supplies the firing pulses required to initiate Spacecraft-Centaur physical separation. The Orbiter Central Computer and Sequencer as well as Pyrotechnic Subsystem are dormant until physical separation takes place, and spacecraft-launch vehicle separation is totally dependent on launch vehicle initiation.

D.2.7.3 Space Vehicle - Launch Operations System Integration

The Launch Operations System includes both the facilities and services required for a Titan Mars 1973 Mission. The launch vehicles undergo the standard integrate-transfer-launch procedure as required by the specific Titan vehicle under consideration. Either Launch Complex 40 or 41 will be utilized; and although two launches are planned, it is assumed that only one launch complex will be utilized in order to

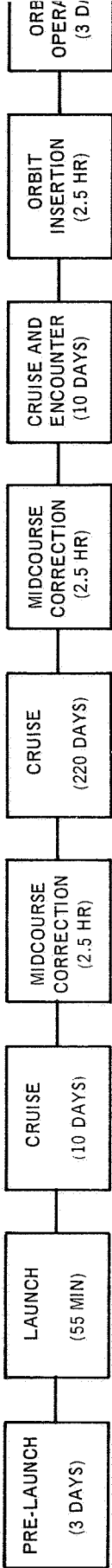
DIRECT ENTRY MISSION

TRAJECTORY CLASS: TYPE II
LAUNCH WINDOW: OPEN - JUNE 20, 1973
CLOSE - JULY 20, 1973
ARRIVAL DATE: MARCH 1/APRIL 10, 1974
INJECTION ENERGY: C₃ MAX = 39 KM²/SEC²
ORBIT INSERTION: ΔV MAX = 1.44 KM/SEC
NOM. ENTRY ANGLE: γ_E = -20.5°



ORBITAL ENTRY MISSION

TRAJECTORY CLASS: TYPE I
LAUNCH WINDOW: OPEN - AUGUST 3, 1973
CLOSE - SEPTEMBER 2, 1973
ARRIVAL DATE: APRIL 2/APRIL 27, 1974
INJECTION ENERGY: C₃ MAX = 28 KM²/SEC²
ORBIT INSERTION: ΔV MAX = 1.50 KM/SEC
NOM. ENTRY ANGLE: γ_E = -16.0°



* SEE TABLE 2.2-1 FOR DETAILS ON VARIABLE TIMES.

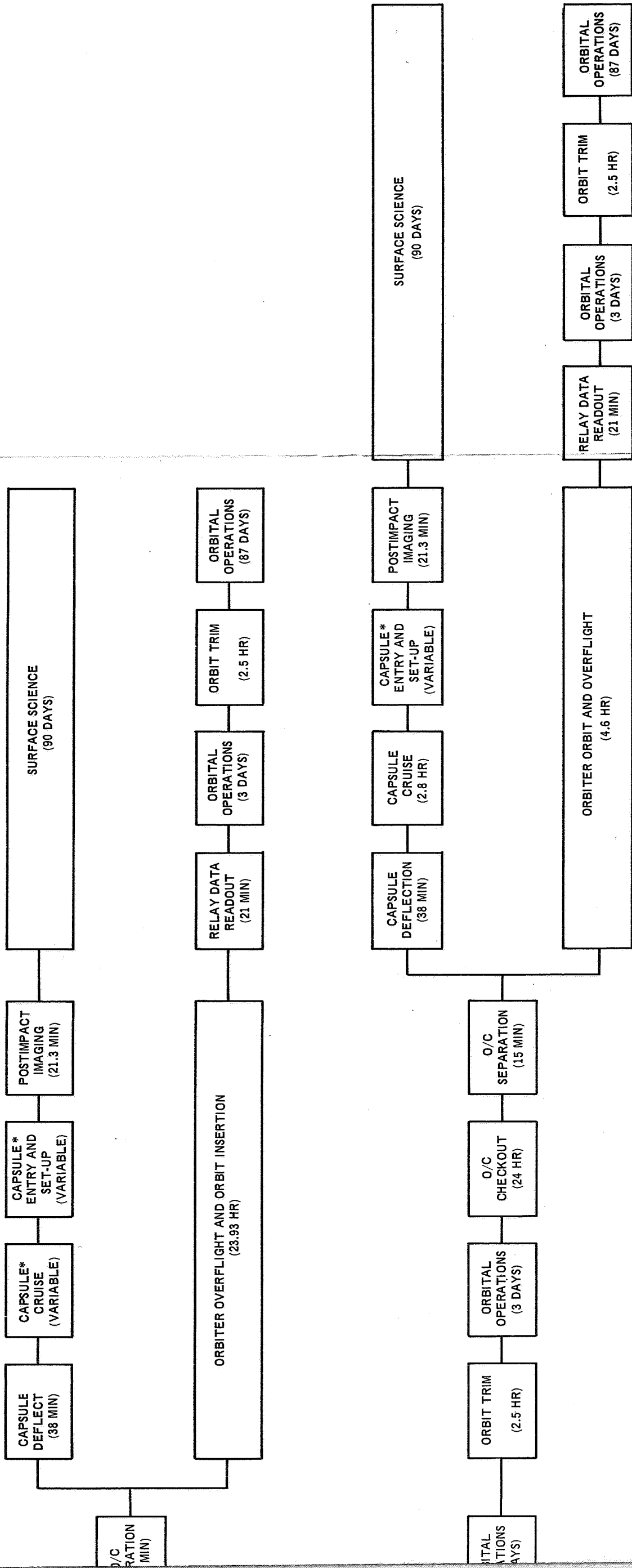
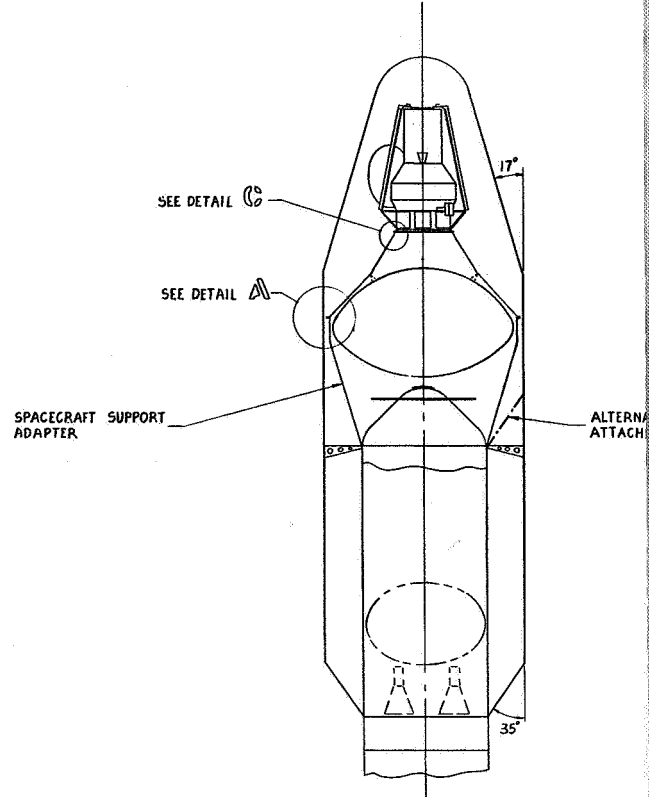
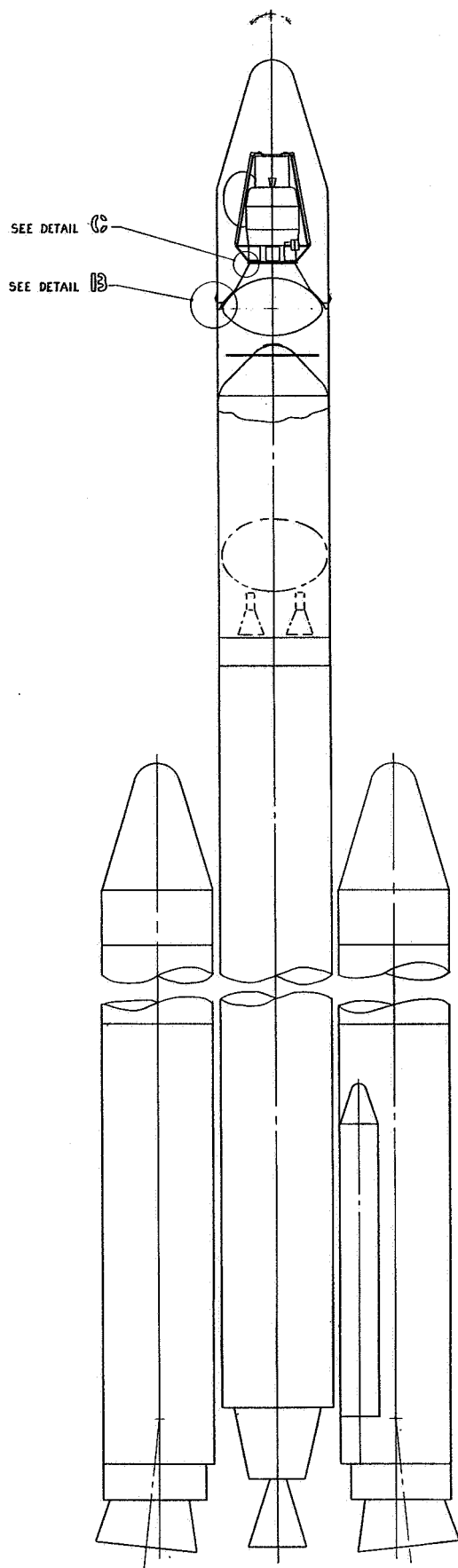


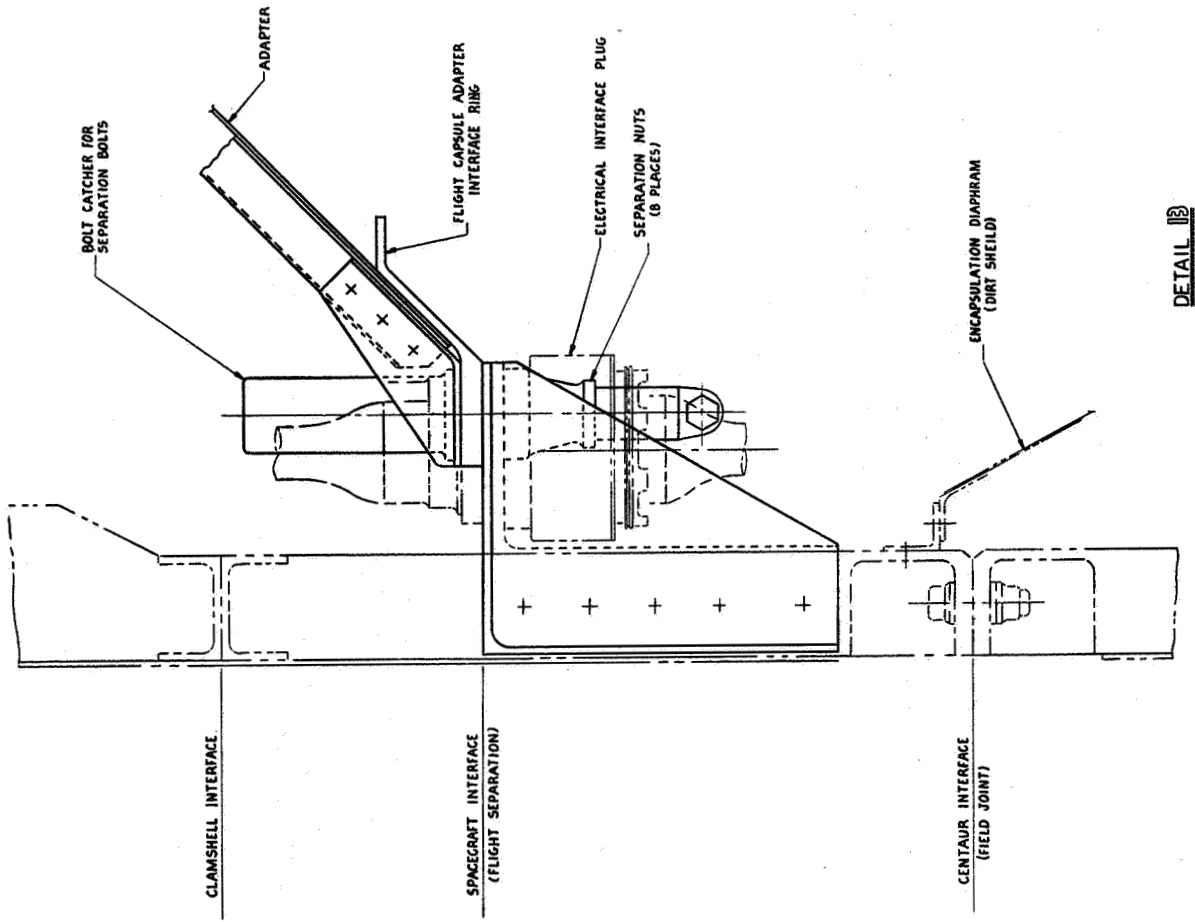
Figure D-19. '73 Mars Mission Profiles



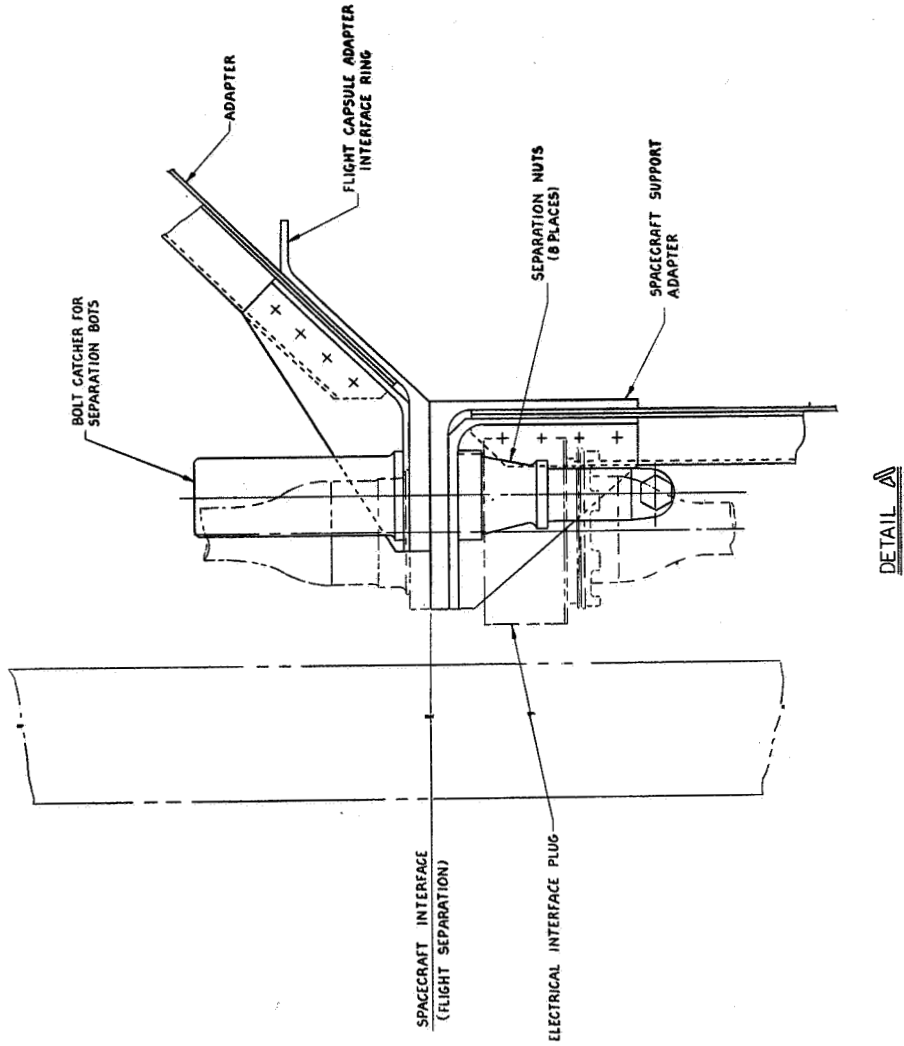
1975-77 MISSION MAXIMUM CAPSULE SCIENCE
DIRECT ENTRY LAUNCH CONFIGURATION
TITAN III F/CENTAUR LAUNCH VEHICLE

1973 MISSION MINIMUM CAPSULE SCIENCE
OUT-OF-ORBIT ENTRY LAUNCH CONFIGURATION
TITAN III C/CENTAUR LAUNCH VEHICLE

3
BOLDOUT



2



TE HAMMERHEAD
MENT

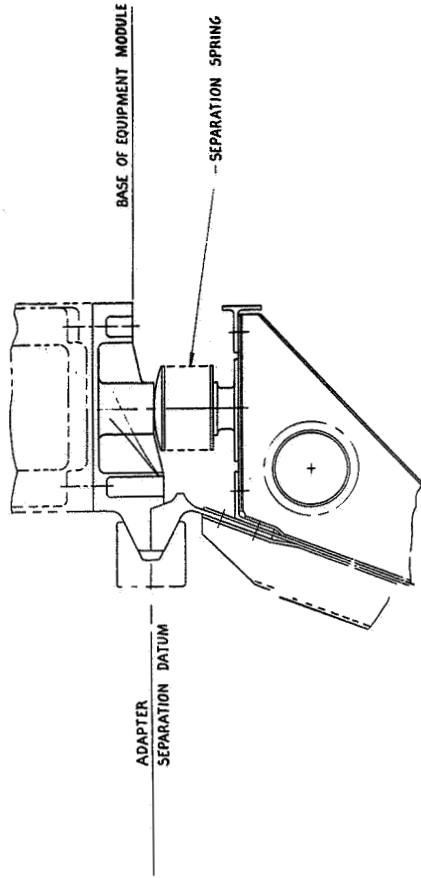


Figure D-20. Conceptual Launch Configurations and Integration Details

minimize the modifications required as well as services rendered (i.e. the first launch takes place very early in the launch window, with the second launch occurring as soon as feasible afterward).

Upon arrival at the launch facility, both the Orbiter and the Capsule undergo post-transport verification tests, assembly (if required), system tests, and DSN-71 compatibility tests as required. Pyros, attitude control and pressurant, etc. gasses, and fuels are loaded, and the Capsule undergoes a terminal sterilization as well as a post sterilization performance check. The Capsule and Orbiter are then mated, and launch vehicle and range equipment compatibility checks are made. Before mating with the launch vehicle, the Spacecraft is encapsulated within the shroud with the nose section serving as a protective cover for the upper portion of the vehicle and an encapsulation diaphragm serving as a dirt shield for the lower and (thus assuring cleanliness of the Spacecraft during pre-launch vehicle mating launch pad operations). * This assembly is then supported and transported by the appropriate assembly, handling, and shipping equipment and mated to the launch vehicle on the launch pad at the Centaur interface (field joint). J-FACT tests as well as all other standard launch pad activities are then performed, and Launch Operations System responsibilities with the space vehicle terminate with the separation of the Spacecraft from the Centaur following heliocentric injection.

D.2.7.4 Mars Characteristics

The Spacecraft-Centaur mass property interface requirements are dictated by Spacecraft/launch vehicle compatibility criteria, launch vehicle strength capability, payload frequency criteria, Centaur main engine gimbal angle capability, spacecraft CG off-sets, etc.

The criteria are summed up in the following table.

| CRITERIA | CRITICAL VALUES | REFERENCE |
|--|--|-----------|
| Launch Vehicle Strength | Combination of payload load factors, weight and CG locale do not yield loads in excess of Centaur structural capability. | 1 |
| Spacecraft Frequency | 10 Hz minimum cantilever value, for Titan II payloads mounted on their adapters. | 2 |
| Payload Spectrum System Requirements | Permissible payload tumbling rates following separation 3 deg/sec. | 3 |
| Centaur Main Engine Gimbal Angle Capability | Allowable spacecraft CG radial off-set (no more than 5.5 inches for a 1000-lb spacecraft) | 3 |

*This procedure applies to the 10 foot diameter shroud. For bulbous shroud configurations, MM '69 techniques should be applied.

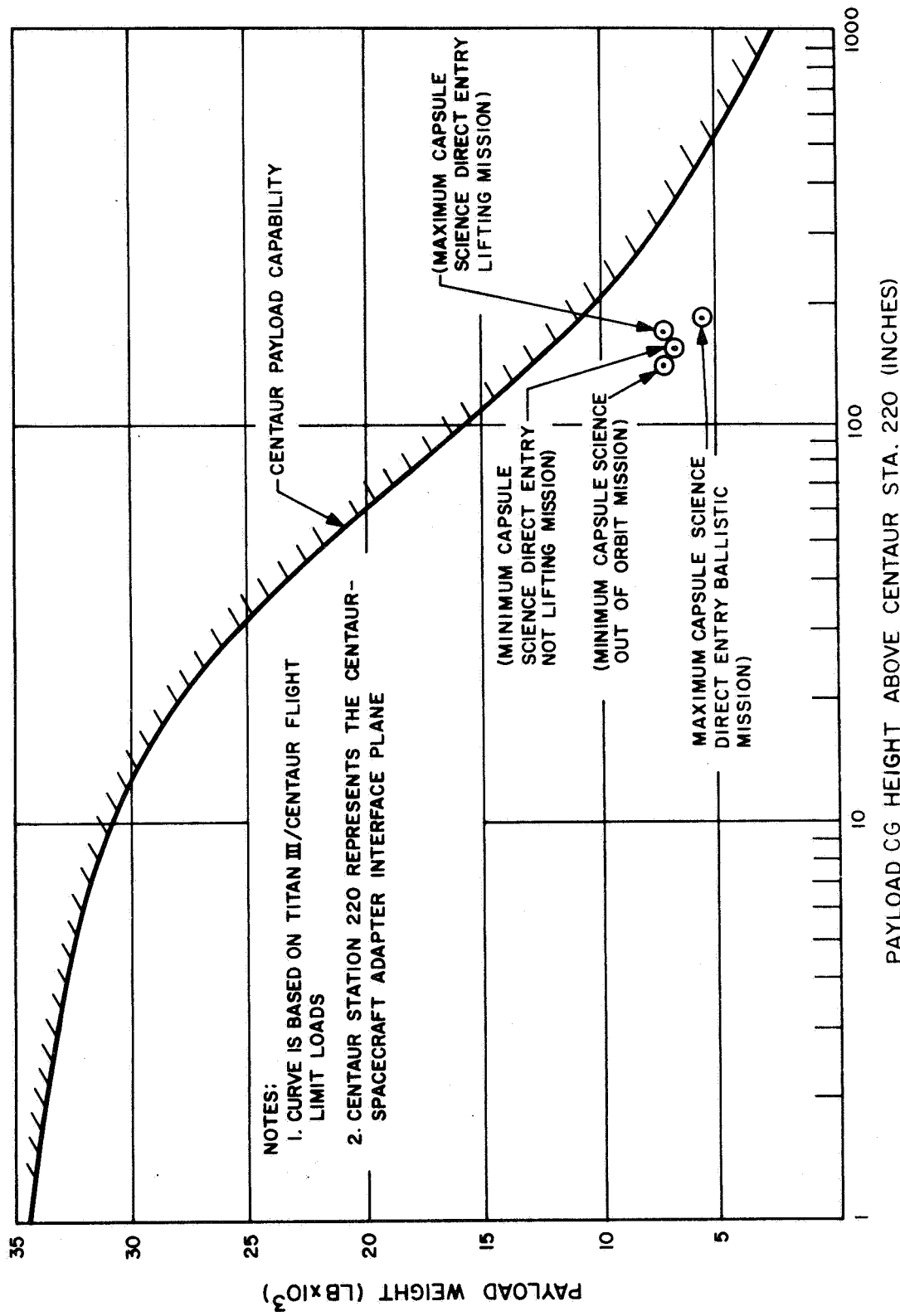


Figure D-21. Maximum Allowable Payload Weight and C.G. Height Based on Centaur Strength Capability

Centaur structural capacity is dictated by vehicle maximum strength capability, which is critical at Centaur Station 409 (ref. D-2). This maximum allowable strength capability is related to specific combinations of payload weight and c.g. height, the latter being measured forward of Centaur Station 220. (Centaur Station 220 is the Centaur-spacecraft adapter interface plane). For Titan/Centaur flight limit load factors of -6g (longitudinal) and 2g (lateral) maximum allowable values of spacecraft weight as a function of c.g. distance from separation plane have been established. This relationship is presented in Fig. D-21. Discrete points representing the spacecraft point designs under consideration all fall within the Centaur strength capability bounds, as shown in Fig. D-21.

The minimum allowable frequency value (10 Hz) for Titan III payloads is imposed to reduce payload dynamic loads and to minimize Tital control stability problems.

Spacecraft c.g. radial offset affects separation system performance (with respect to the resulting Spacecraft tumbling rate). The Centaur main engine gimbal angle and hence, the engine trim capability, likewise are affected by the c.g. offset. Based on earlier Voyager studies involving Saturn-V sized payloads (20,000 lb, 20 ft. diameter X 20 ft.), a maximum allowable radial c.g. offset of 3 inches can be maintained for a spacecraft of that size. Rigid static balancing procedures could furthermore result in a practical maximum value of 1 inch. Hence, on the much smaller spacecraft under consideration herein, c.g. radial offsets should not exceed 1 inch. This should not pose any launch vehicle interface problems.

D.3 PROPULSION SUBSYSTEM

D.3.1 FUNCTIONAL DESCRIPTION

The Propulsion Subsystem provides impulse for the payload and velocities shown in table D-9.

TABLE D-9. PROPULSION REQUIREMENTS

| | Out-of-orbit Entry | Direct Entry |
|----------------------------------|--------------------|---|
| Approximate payload weight* (lb) | 2649 to 3063** | 2644 to 3578** (Spacecraft) 963 (Orbiter) |
| Velocity Increments | | |
| Midcourse (mps) | 10 | 10 |
| Orbit Insertion (mps) | 1480 | 1450 |
| Orbit Trim (mps) | 35 | 35 |

* Vehicle less propulsion hardware and propellants

** Depending on specific point design

Although the propellant weight and propellant dependent hardware weight is significantly higher in the out-of-orbit entry case than for direct entry, both are functionally identical, and therefore, the discussion presented herein is equally applicable to both. Differences between the systems are discussed in Section D.3.3.

The subsystem is a modular assembly consisting of propellant and pressurant tanks, thrust chamber, lines, valves, and other associated components and supporting structure. A schematic of the system is shown in fig. D-22, and a description of major components is presented below.

D.3.1.1 Thrust Chamber Assembly

The Rocketdyne extended duration RS14 is a 316 ft-lb thrust bipropellant engine using the hyperbolic space storable propellants nitrogen tetroxide (N_2O_4) and monomethyl hydrazine (MMH). The thrust chamber is cooled by boundary layer control and radiation. The nozzle, beyond an expansion ratio of 3.2, is radiatively cooled and is gimballed for thrust vector control.

D.3.1.2 Propellant and Pressurant Tanks

The propulsion module contains four identical 6A14V titanium tanks, each containing a Teflon/aluminum laminate bladder for positive propellant expulsion and propellant-pressurization gas separation. Helium pressurization gas is contained in four identical spherical 6A14V titanium tanks.

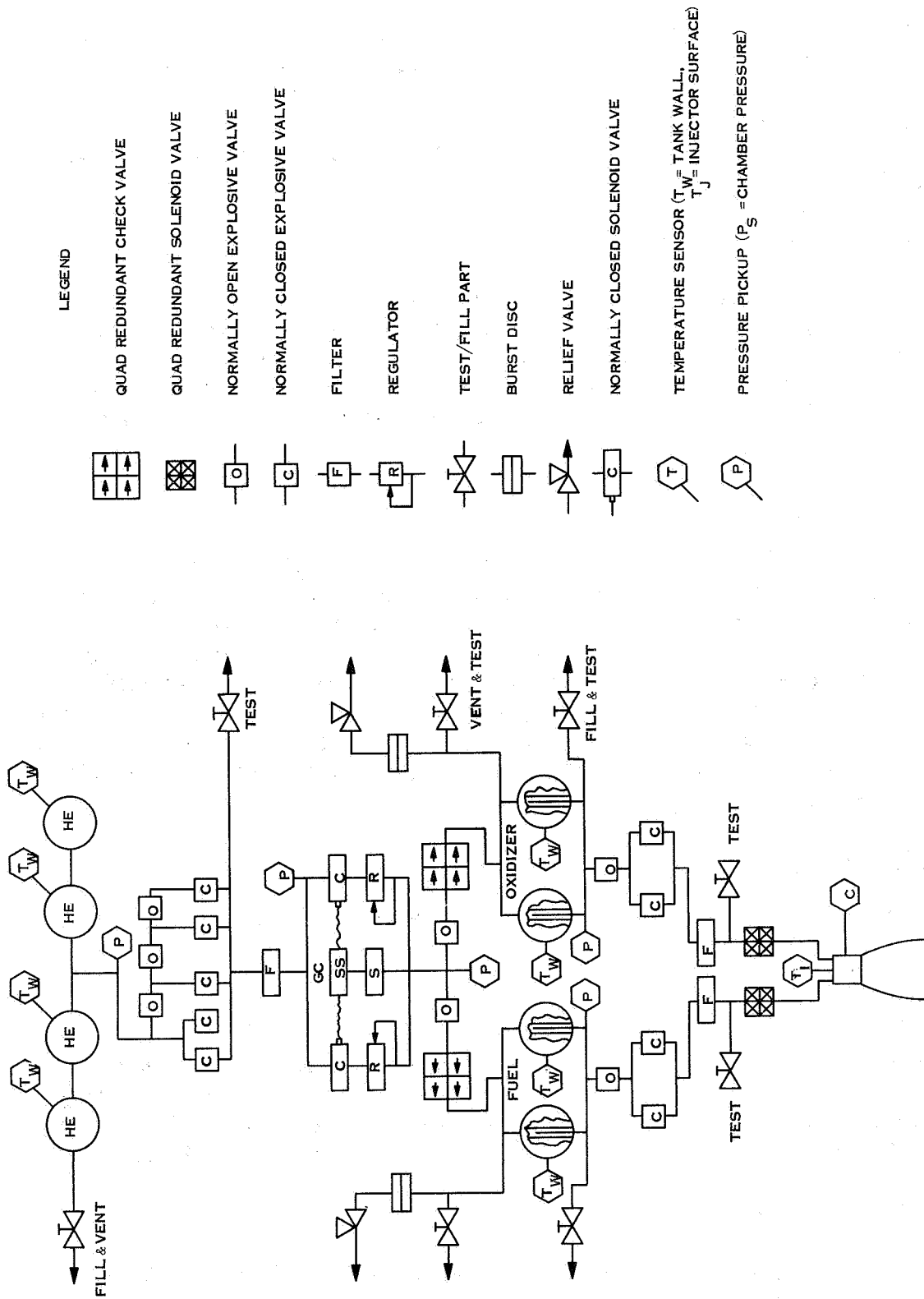


Figure D-22. Propulsion Subsystem Schematic

D.3.1.3 Controls

Propellant and pressurant gas control is provided by solenoid and explosive valves, shown in fig. D-22, for operation and isolation functions, respectively. Use of series-parallel and quad-redundant networks provides assurance of valve opening or isolation of the system as desired. Redundant regulators connected via a pressure sensing and switching network are used to provide pressurant gases to the propellant tanks at constant pressures.

D.3.2 SUBSYSTEM OPERATION

The firing of the Propulsion Subsystem is controlled by the CC&S which receives the time and direction of the maneuver through the ground-to-spacecraft communication link. Firing duration may be determined by accelerometer outputs or by a timer. Explosive valves are activated by signals from the Pyrotechnic Subsystem upon command from the CC&S. The sequence of events for the midcourse, orbit insertion and orbit trim firings follows.

D.3.2.1 Midcourse Firings

Prior to the first midcourse firing, the normally closed explosive valve (see fig. D-22) in the pressurant line, which keeps the regulator isolated from tank pressure before and during launch, is actuated. Explosive isolation valves in the propellant lines are also opened at this time. Engine firing is commenced by opening the thrust chamber solenoid valves. The propellants are hyperbolic. Firing is terminated by closing the solenoid valves. The normally open explosive valve in the pressurant line is fired to isolate the regulator until the next midcourse firing. The second midcourse follows the same procedure, except that the pressurant isolation valves may remain open after the firing.

D.3.2.2 Orbit Insertion Firing

Pressurant isolation valves may still be open from the second midcourse firing, and engine operation is as described above.

D.3.2.3 Orbit Trim Firing

Orbit trim firing proceeds as described for midcourse firings. Following the orbit trim firing, the pressurant isolation valves are fired to prevent escape of gas during orbital operation. The propellant isolation valves are also fired to preclude the possible intermixing of escaping propellant vapors, which might produce a slight thrust.

D.3.3 COMPARISON TO MARINER '71 DESIGN

Table D-10 summarizes the differences between the Mariner Mars '71 Propulsion Subsystem and the MM '73 subsystems for both direct and orbital entry mode spacecraft. From this table, it is evident that the MM '71 and direct entry systems are intentionally

TABLE D-10. COMPARISON OF MM '71 AND MM '73 PROPULSION SUBSYSTEMS

| | MM '71 | MM '73 | |
|---|---------------------|--|-------------------------------------|
| | | Direct Entry | Orbital Entry |
| Functional | | | |
| Total ΔV Capability | 1500 | 1495 | 1525 |
| Payload Weight (lbs) | 963 (all maneuvers) | 2644 to 3578* (midcourse) 963 (all others) | 2649 to 3063* (all maneuvers) |
| Physical | | | |
| Propulsion System Weight **(lbs) | 951 | 951 | 2557 to 2940* |
| Propellant Weight (lbs) | 796 | 796 | 2161 to 2492* |
| Tank Size (inches) | 21.7 diameter | 21.7 diameter | 22 diameter 45.6 to 51.5 length* |
| * Depending on specific point design ** Does not include propulsion module structure | | | |

identical, and therefore, interchangeable. Also by intention, the out-of-orbit and direct entry fixed hardware (all thrust level dependent hardware) is identical. However, because of the larger orbital weight of the out-of-orbit mode, the variable hardware (all total impulse dependent hardware) is significantly larger. Thus, new propellant and pressurant tanks and a new propulsion structure are required.

D.3.4 SUBSYSTEM CHARACTERISTICS

D.3.4.1 Physical Characteristics

For direct entry point designs (based on the weights and velocities shown in table D-11), table D-12 gives the dimensions of the principal components. For the direct entry case, the Spacecraft Propulsion Subsystem data is essentially independent of Capsule weight; for example, a 1000 lb increase in Flight Capsule weight results in only about 3 more pounds of propellant. Similar data for the out-of-orbit entry case is presented parametrically as a curve in fig. D-23, where component and subsystem weight and size are plotted as a function of useful orbital weight.

D.3.4.2 Performance Characteristics

Table D-13 presents the pertinent performance data for the Propulsion Subsystem.

TABLE D-11. PROPULSION SUBSYSTEM WEIGHT BREAKDOWN -
DIRECT ENTRY

| | |
|---|--------------|
| Hardware Weights (lbs) | |
| Pressurant Tank (Four) | 45.2 |
| Propellant Tanks (Four) | 34.8 |
| Thrust Chamber Assembly | 21.6 |
| Controls and Miscellaneous Bracketry | 27.5 |
| Structure | <u>23.6</u> |
| (1) TOTAL HARDWARE (Dry) | 152.7 |
| Pressurant and Propellant Weights (lbs) | |
| Pressurant Gas | 4.8 |
| Residual Propellant | <u>24.4</u> |
| (2) TOTAL RESIDUALS | 29.2 |
| Useable Propellant | 796.0 |
| (3) TOTAL PRESSURANT AND PROPELLANT | <u>825.2</u> |
| Subsystem Weights (lbs) | |
| Burnout [(1) + (2)] | 181.9 |
| Launch [(1) + (3)] | 977.9 |

TABLE D-12. PROPULSION SUBSYSTEM PRINCIPAL DIMENSIONS -
DIRECT ENTRY

| | |
|---|------|
| Propellant Tank Diameter (in.) | 21.6 |
| Propellant Tank Length (in.) | N/A |
| Pressurant Tank Diameter (in.) | 11.3 |
| Overall Propulsion Module Envelope | |
| Diameter (in.) | 64.0 |
| Length (in.) | 37.0 |
| Thrust Chamber Exit Diameter (in.) | 5.74 |
| Thrust Chamber Extension Below Module (in.) | 13.5 |
| All Pressurant Lines (in.) | 1/4 |
| All Propellant Lines (in.) | 3/8 |

TABLE D-13. PROPULSION SUBSYSTEM PERFORMANCE

| | |
|--|------------------------------------|
| Thrust Chamber (RS14) | |
| Thrust (ft-lb) | 316. |
| Specific Impulse (ft-lb-sec/m-lb) | 290. |
| Minimum Impulse Bit** (ft-lb-sec) | 12.6 |
| Chamber Pressure (psia) | 125. |
| Mixture Ratio (oxidizer/fuel) | 1.6:1 |
| Propellants | N ₂ O ₄ /MMH |
| Expansion Ratio | 30:1 |
| Chamber Wall Temperature (deg F) | 2150 |
| Subsystem | |
| Total Burning Time (seconds) | |
| Orbital Entry | 1983 to 2287* |
| Direct Entry | 730 |
| Propellant Tank Pressure (psi) | 300 |
| Helium Tank Pressure (psi) | |
| Initial | 3600 |
| Final | 400 |
| <p>* Depending on specific point design</p> <p>** The minimum impulse bit shown is not that of which the engine is capable but is the result of the 50 msec minimum firing time induced by the resolution of the Central Computer and Sequencer.</p> | |

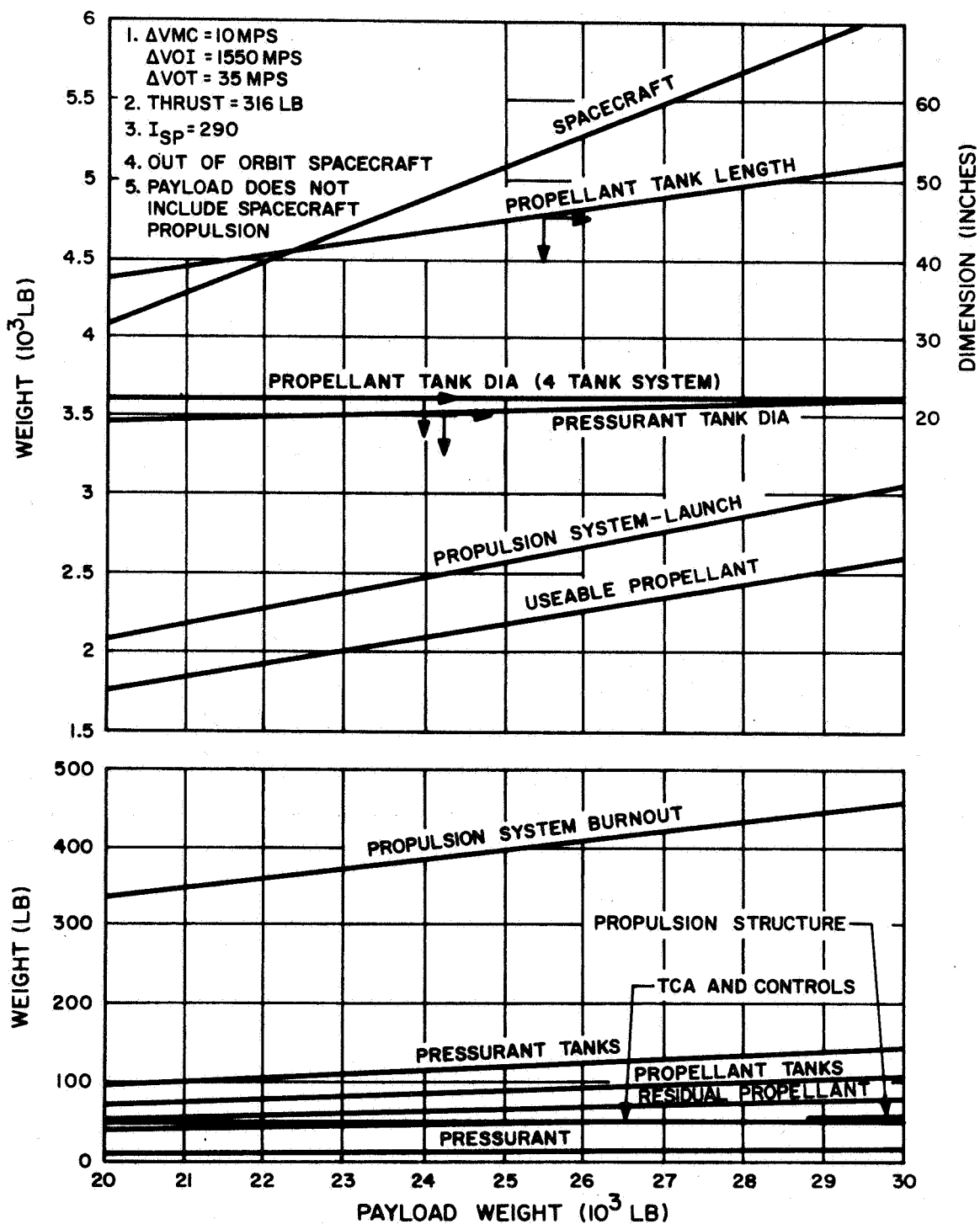


Figure D-23. Propulsion Subsystem Weights as a Function of Payload Weights

D.4 ENGINEERING MECHANICS

D.4.1 STRUCTURE

D.4.1.1 Design Approach

D.4.1.1.1 Design Requirements

The functional requirements of the Structure Subsystem are to:

1. Structurally integrate, within its allocated weight, those subsystems which comprise the Orbiter.
2. Provide mechanical support and alignment for all flight equipment.
3. Transmit structural loadings on flight equipment to the launch vehicle during critical (lift-off and powered flight) loading conditions.
4. Provide Orbiter compatibility both with the allowable space envelope and with the launch vehicle.
5. Impart sufficient rigidity to deployed appendage structures, e.g., solar panels, high-gain antenna, etc., to preclude both excessive deflection and deleterious interactions with the Orbiter Attitude Control Subsystem.

The structural design of the Orbiter must be primarily controlled by flight operations and requirements. The Structure Subsystem also provides a means for testing, shipping and handling the assembled Orbiter.

The critical loading conditions and other prime design criteria imposed on the Structure Subsystem are dictated primarily by the launch vehicle selection, shroud geometry, and Spacecraft size and weight. For Titan III C/Centaur payloads employing the (non-bulbous) standard Titan III shroud (or equivalent) and weighing approximately 4000 pounds, such flight environments are summarized in table D-14, based on GE environmental studies, Titan III flight data measurements cited in NASA CR-66204, data cited in Titan and Centaur payload planner's guides, and information received from Martin-Denver regarding Titan III flight loadings. Appropriate structural design criteria data is also included in table D-14. These flight environments are applicable to the Orbiter employed for the out-of-orbit Capsule entry mission.

The direct Capsule entry mission requires the employment of a bulbous (hammer-head) fairing. This change will basically affect only the acoustic field and random vibration environments of table D-14. Changes in environmental levels brought about by the use of a 16-foot (nominal) diameter bulbous shroud are given in table D-15.

TABLE D-14. TITAN III/CENTAUR FLIGHT LIMIT ENVIRONMENTS AND CRITERIA

| | | |
|--|---|--|
| 1. Flight (Limit) Environments and Criteria | | |
| A. Quasi-Steady Acceleration | | |
| <u>Condition</u> | <u>Longitudinal Limit Load Factor (g)</u> | <u>Lateral Limit Load Factor (g)</u> |
| Titan III Burn (max. longitudinal) | +6.0 | ± 2.0 |
| Titan III Burn (min. longitudinal) | -3.0 | ± 2.0 |
| Centaur Thrust Cutoff (Max. Long.) | +1.6 | ± 0.9 |
| Centaur Thrust Cutoff (Min. Long.) | -1.5 | ± 0.9 |
| B. Equivalent Static Loads for Secondary Structure and Equipment | | |
| 36 g | | |
| C. Minimum Allowable Payload Frequency | | |
| 10 Hz, for spacecraft and adapter cantilevered off Titan station 77.0 (or equivalently, Centaur station 220). | | |
| D. Random Vibration (Spacecraft System and Equipments) | | |
| <u>Frequency (Hz)</u> | <u>RMS Acceleration (g)</u> | <u>Power Spectral Density (g²/Hz)</u> |
| 20 - 125 | 9.9 | 0.014 |
| 125 - 250 | | * |
| 250 - 1000 | | 0.070 |
| 1000 - 2000 | | ** |
| *Linear increase at the rate of +6 db/octave | | |
| **Linear decrease at the rate of -9 db/octave | | |
| E. Acoustic Field | | |
| The acoustic fields are given in Figure D-24. These represent those sound pressure levels within the fiberglass shroud. | | |
| F. Pyrotechnic Shock | | |
| Shock spectra produced by shroud separation enveloped by that equivalent spectra produced by a half-sine pulse of 175g peak amplitude and 0.4 milliamp duration. | | |
| 2. Factors of Safety | | |
| <u>Item</u> | <u>Safety Factor</u> | |
| | <u>Limit</u> | <u>Ultimate</u> |
| Primary structure/ major mass items | 1.00 | 1.25 |
| Secondary structure and equipment | 1.00 | 1.50 |

Note: The acoustic field and random vibration levels apply for payloads encapsulated by a non-bulbous (10-foot nominal diameter) fiberglass honeycomb fairing.

TABLE D-15. ENVIRONMENTAL CHANGES DICTATED BY PROPOSED (16-FOOT DIAMETER) BULBOUS FAIRING

1. Acoustic Field

The acoustic fields are given in Figure D-25. These represent those sound pressure levels within the shroud.

2. Random Vibration - Spacecraft System and Equipments

| Frequency (Hz) | RMS Acceleration (g) | Power Spectral Density (g ² /Hz) |
|-------------------|-------------------------|--|
| 20 - 125 | 17.9 | .056 |
| 125 - 1000 | | .21 |
| 1000 - 2000 | | * |

*Linear Decrease at the rate of -9 DB/octave

Note: These flight limit environments are based on the following assumptions: (1) the bulbous fairing employs the same fiberglass honeycomb as found in the standard shroud; and (2) the acoustic field during transonic flight increases in intensity by 6 DB as a result of the wake separations induced by the fairing hammerheading.

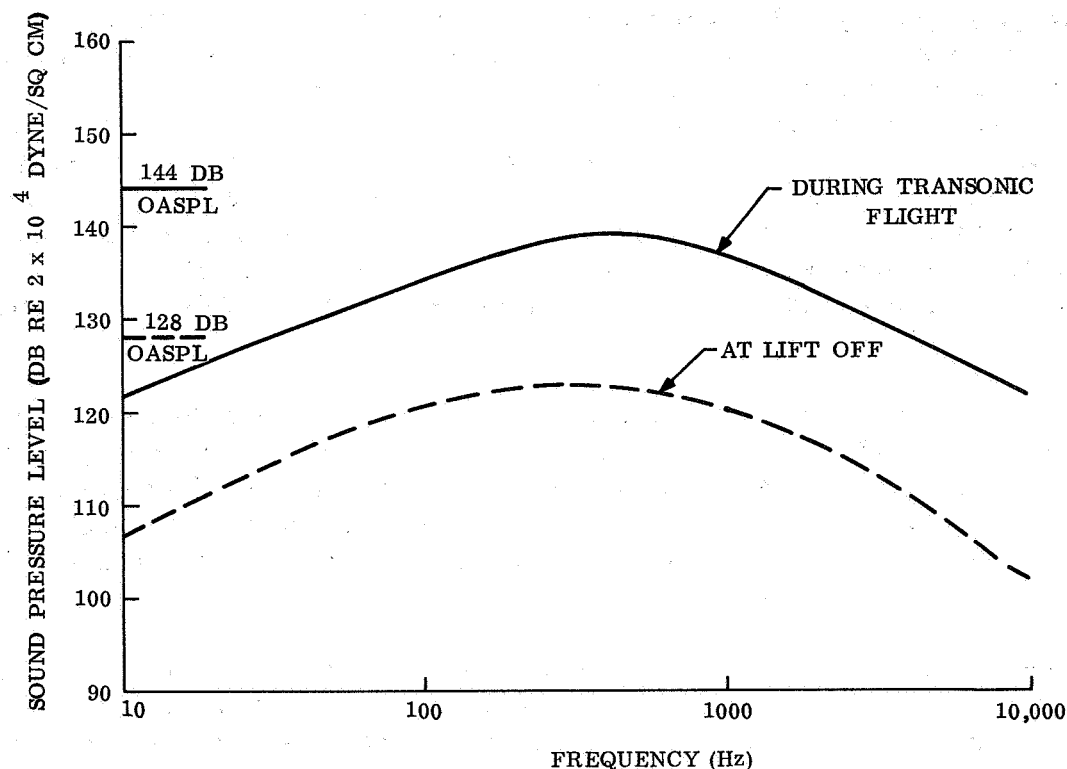


Figure D-24. Acoustic Fields Within Standard 10-Foot Diameter Titan Fairing

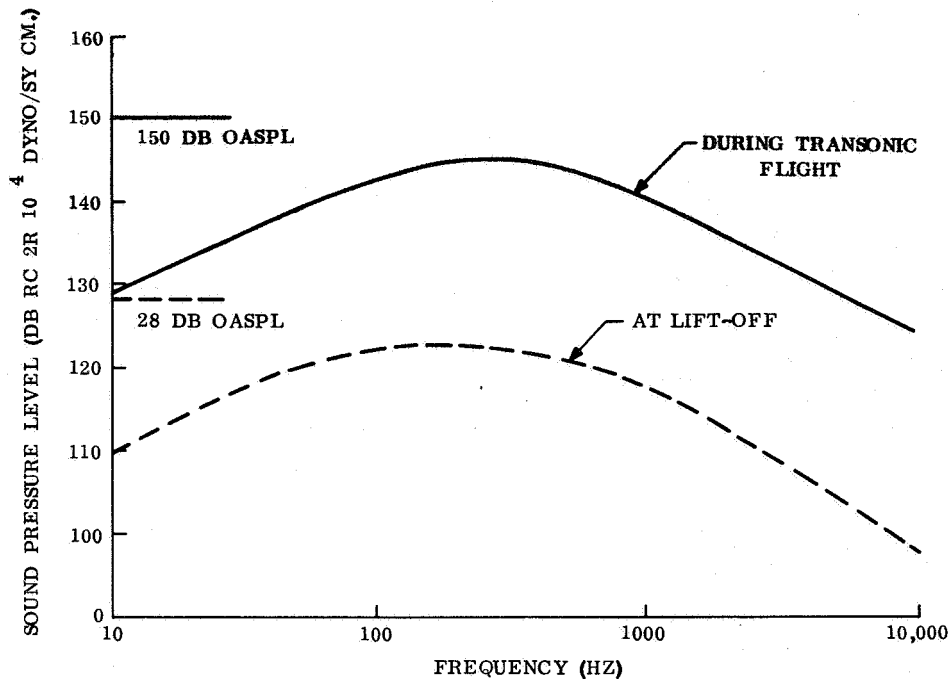


Figure D-25. Predicted Acoustic Fields Within Proposed Bulbous (16-Foot Diameter) Titan Fairing

D.4.1.1.2 Design Synthesis

A. Basic Requirements - The prime function of the Structure Subsystem is essentially structural loading transmission. By virtue of its unique role, the structure has common interfaces with all subsystems. The Structure Subsystem must fulfill its basic role at the expenditure of the smallest possible weight. This dictates the use of lightweight constructions comprised of materials compatible with both the space environment and with other Orbiter subsystems. The Structure Subsystem in addition must allow for: (a) easy access to Spacecraft equipment; (b) packaging of other subsystems in accordance with their unique functional requirements; (c) utilization of existing Mariner subsystems and structure; and (d) commonality with the structures of the other systems of the space vehicle.

Particular emphasis has been placed on housing the Propulsion Subsystem in a structural assembly that affords it complete modularization. This assembly must have rigidity sufficient to preclude excessive elastic deformations of the support structure during retrofire operations and excessive deformations of fuel lines. Based on impact penetration analyses, micrometeoroid protection must also be provided for the individual fuel and oxidizer tanks.

In synthesizing the Structure Subsystem, effort has been made to utilize existing Mariner Mars '69 and expected Mariner Mars '71 flight hardware where possible. Special attention has been focused on the MM '69 octagon, which provides the Orbiter

with a structural module amenable to housing a spectrum of diverse electronic assemblies. The gages and geometry of the MM '69 octagon appear to have been dictated primarily by electronic packaging and thermal control considerations. This structure appears to require only minimal changes to be capable of bearing the Mariner Mars '71 Propulsion Subsystem on its forward bulkhead.

B. Orbiter Structure-Spacecraft Adapter Relationship - The basic functions of the Spacecraft adapter are to: (1) provide for structural loading transmission from the Spacecraft to the launch vehicle; and (2) provide spacecraft-launch vehicle compatibility. The latter is measured by the compliance of the Spacecraft-adapter structural arrangement with the minimum frequency requirements of the launch vehicle. Since adapters are non-redundant load paths that bear no equipment (i. e., unlike other elements of Spacecraft primary structure, they do not also function as mountings for hardware) they are more compliant than other Spacecraft structural elements. Hence, the fundamental frequency of the Spacecraft-adapter arrangement is generally established by Spacecraft mass properties and adapter elasticity.

While the Spacecraft adapter is not an integral part of the Orbiter system, it is nevertheless a functional part of the Spacecraft/Orbiter Structure Subsystem. Failure to treat the Spacecraft adapter as such could result in an unwieldy design. To preclude this, the Spacecraft adapter has been structurally considered (and is discussed herein) as an integral part of the functional Orbiter Structure Subsystem.

C. Modular Arrangements - The Structural Subsystem of the Orbiter (plus Spacecraft adapter) is comprised of the four modules (propulsion, equipment, Capsule adapter, and Spacecraft adapter) shown schematically in fig. D-26, plus appendage structures (e.g., solar panels, high-gain antenna, etc.). The locations of these four modules relative to each other are identical for the various out-of-orbit and direct entry missions. The location of the Orbiter-capsule interface plane is also independent of mission mode.

The major elements of each module are tabulated in matrix form in table D-16 for both mission modes.

Perusal of table D-16 and fig. D-26 reveals the following salient results of the Orbiter Structure Subsystem design synthesis:

- In all direct entry Capsule configurations, the structure forward of the Orbiter-Capsule interface plane is identical.
- In all direct entry Capsule configurations, the propulsion module and octagon structural elements are identical to those anticipated in Mariner Mars '71.
- The high-gain antenna structures for all configurations are identical (63 inch diameter parabolic dishes).
- In the out-of-orbit entry Capsule configuration, the rings and longerons of the MM '71 octagon require increases in thickness to accommodate the heavier propulsion module.

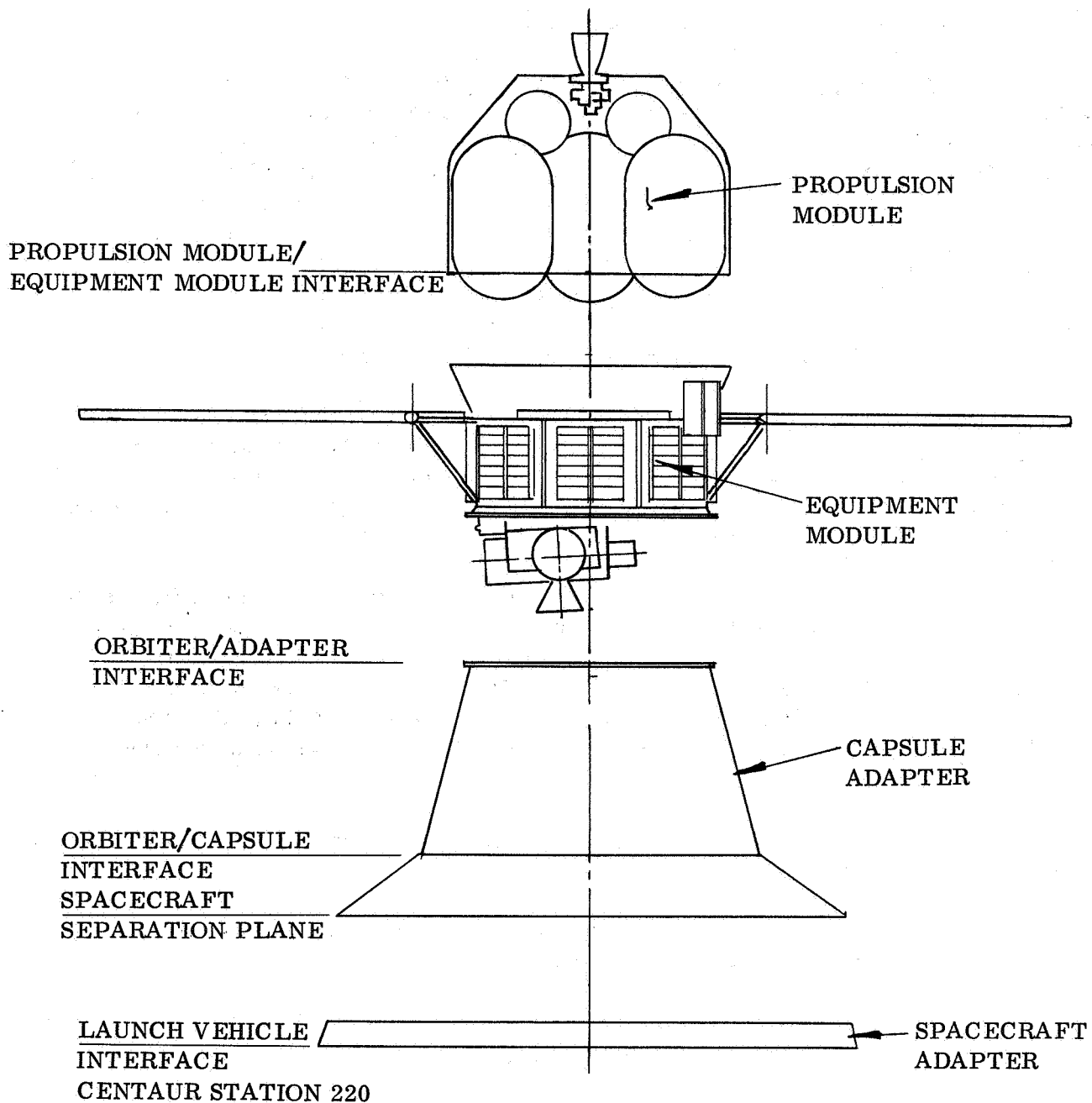


Figure D-26. Schematic of Orbiter Modular Arrangement (Applicable to All Missions / Configurations)

TABLE D-16. MAJOR ORBITER STRUCTURAL ELEMENTS

| Mission Module | Direct Entry Capsule Configuration (Figure D-4) | Out-of-Orbit Capsule Entry Configuration (Figure D-12) |
|--------------------|---|---|
| Propulsion | <ul style="list-style-type: none"> a. Outer Shell Structure¹ b. Conical Frustum Adapter Structure¹ (To Octagon) c. Fuel and Oxidizer Tank Fwd Support Structure¹ d. Tank Aft Support Beams¹ e. Pressurization Tank Support Structure¹ f. Thrust Chamber Support Structure¹ g. Octagon Interface Structure (Bulkhead)¹ | <ul style="list-style-type: none"> a. Outer Shell Structure b. Conical Frustum Adapter Structure (To Octagon) c. Fuel and Oxidizer Tank Fwd Support Structure d. Tank Aft Support Beams e. Pressurization Tank Support Structure f. Thrust Chamber Support Structure g. Octagon Interface Structure (Bulkhead) |
| Equipment | <ul style="list-style-type: none"> a. Mariner Octagon¹ b. Electronics Packaging Structure¹ c. Solar Panel Support Structure¹ d. PSP Support Structure¹ e. Sensor Support Structure¹ f. High-Gain Antenna Support Structure¹ | <ul style="list-style-type: none"> a. Mariner Octagon² b. Electronics Packaging Structure¹ c. Solar Panel Support Structure² d. PSP Support Structure¹ e. Sensor Support Structure¹ f. High-Gain Antenna Support Structure¹ |
| Capsule Adapter | <ul style="list-style-type: none"> a. Octagon Interface Structure (Bulkhead) b. Upper Adapter (Conical Frustum) c. Interface Ring d. Lower Adapter (Conical Frustum) | <ul style="list-style-type: none"> a. Octagon Interface Structure (Bulkhead) b. Upper Adapter (Conical Frustum) c. Interface Ring d. Lower Adapter (Conical Frustum) |
| Spacecraft Adapter | <ul style="list-style-type: none"> a. Conical Frustum Adapter Section b. Cylindrical Adapter Section | <ul style="list-style-type: none"> a. Adapter-Spacecraft Interface Ring b. Cylindrical Adapter Section (Structural Shroud) |
| Appendages | <ul style="list-style-type: none"> a. Solar Panel Structure b. High-Gain Antenna Structure | <ul style="list-style-type: none"> a. Solar Panel Structure b. High-Gain Antenna Structure |

1. Propulsion module and equipment module structural elements identical to those of Mariner Mars '71
2. Gages of all elements of Mariner Mars '71 octagon must be increased.

- The anticipated Mariner Mars '71 propulsion module is thus employed in all configurations except for the out-of-orbit Capsule.
- The Spacecraft adapter and those elements of the Capsule adapter aft of the Capsule-Orbiter interface plane, vary significantly with Capsule size, geometry and weight.

D.4.1.1.3 Module Design Approaches

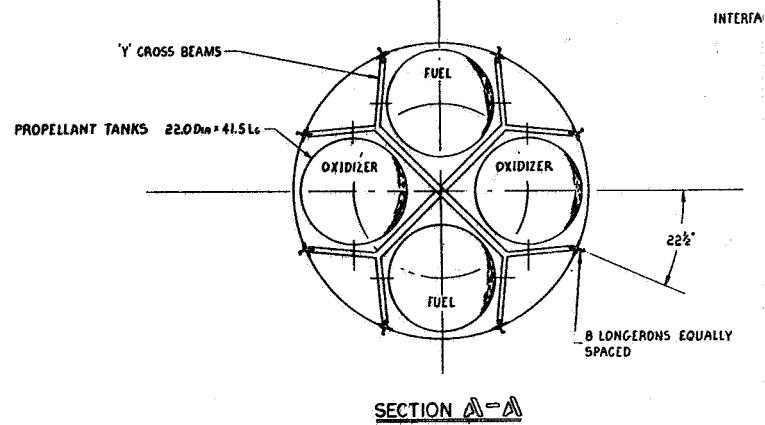
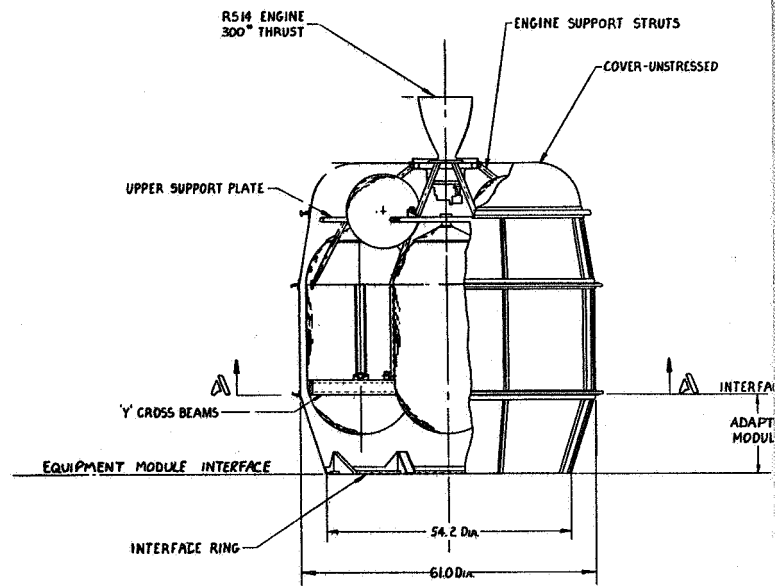
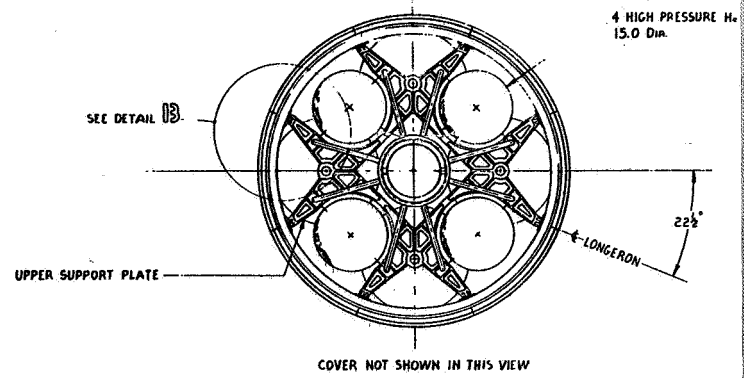
A. Propulsion Module - The propulsion module structure serves to support the elements of the Propulsion Subsystem, and transmit the boost phase structural loadings induced on its elements aft towards the Centaur. The propulsion module structure must also: (1) afford sufficient protection against possible micrometeoroid penetrations; and (2) provide the tanks with a support stiff enough to enable the achievement of Spacecraft frequency requirements.

The preferred propulsion module structural arrangement consists of beam frameworks (or spiders) supporting the four tanks, encapsulated within a semimonocoque shell (see fig. D-27). Other arrangements were considered. A minimum weight truss/strut tank support structure, while meeting strength requirements, invariably lacks the rigidity necessary to achieve spacecraft frequency requirements. The truss/strut arrangement is also prone to excessive deformations under quasi-steady loading, creating significant potential propellant line failure modes. These problems can be eliminated by replacing the strut/truss propulsion module (axial load members) by shear beam frameworks. This arrangement, however, greatly increases structural weight.

The best practical propulsion module arrangement consists of: (1) a semimonocoque shell encapsulating the propellant and oxidizer tanks; (2) an interior planar shear beam arrangement (spider) to which each tank is attached at two points near its aft extremity, and (3) an internal planar shear beam gridwork onto which the forward extremities of the tanks are attached. This allows for short, direct load paths; the longitudinal forces, bending moments and most (roughly 70 percent) of the lateral forces resulting from tank external loadings are transmitted to the outer shell by the aft spider arrangement. The forward beam gridwork transmits the remainder of the tank lateral loadings to the external shell. Shear beams with deep flanges (and lightning holes to conserve weight) produce the necessary strength and rigidity. The circumferential and longitudinal shear continuity of the external shell structures enables the transmittal of loads aft to the equipment module, in the form of differential bending. The resulting structural arrangement, employing minimum gauges, has ample strength and rigidity. The structural weight of such an arrangement is only slightly heavier than strut/truss tank supports (which meet only the strength requirements).

The encapsulating external shell structure also enables another criterion to be met - that of micrometeoroid protection. Employing a recently-developed micrometeoroid penetration criterion (ref. D-5), which was employed in conjunction with the MM '73 mission micrometeoroid flux defined in ref. D-6, it has been established

FOLDOUT FRAME



2
FOLDOUT FRAME

FOLDOUT FRAME
3

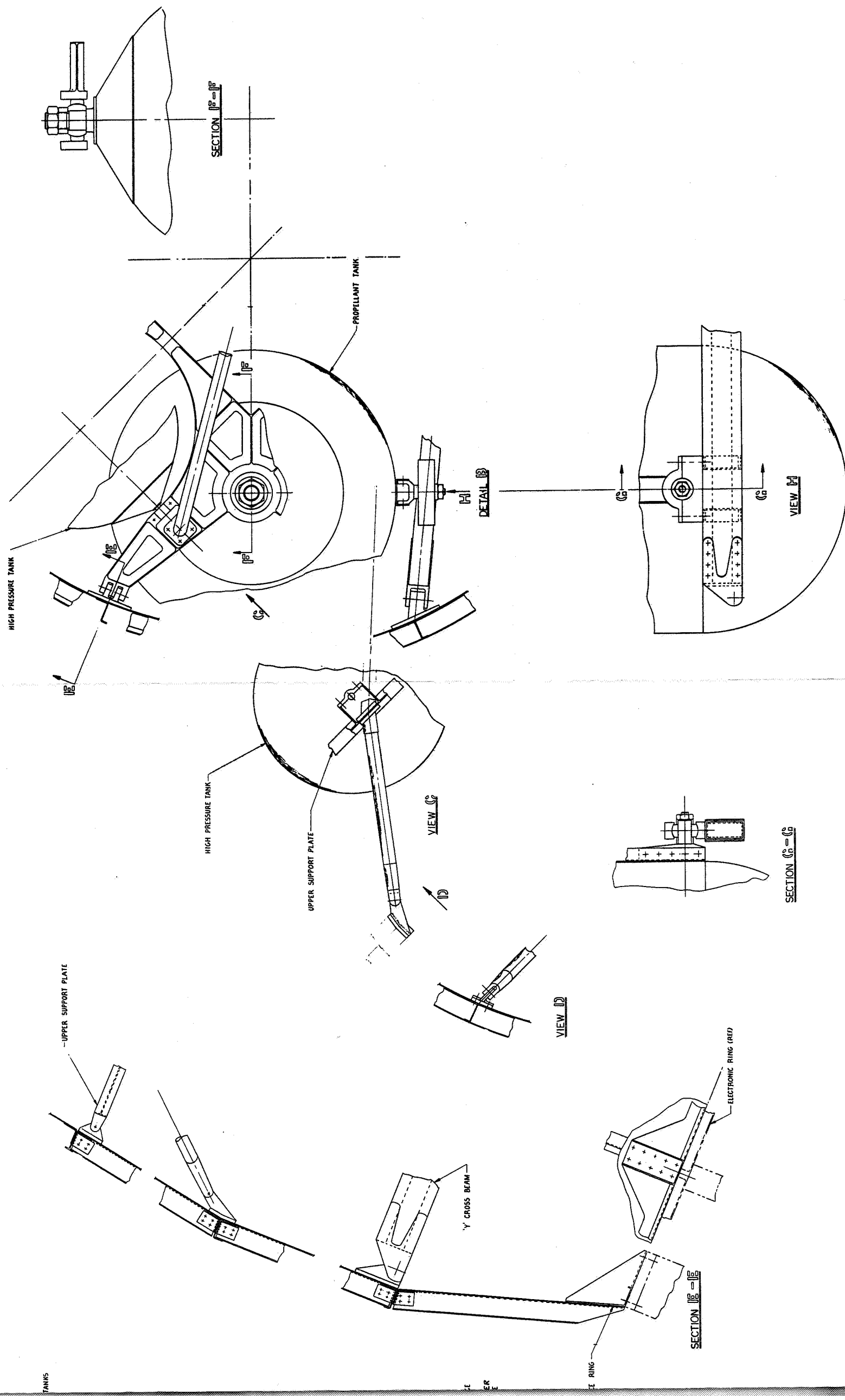


Figure D-27. Propulsion Module Structural Elements

that micrometeoroid protection bumpers are required. It has furthermore been shown that an external shell structure encapsulating these tanks will furnish adequate protection against micrometeoroid damage.

Thus, the encapsulated tank propulsion module concept illustrated in fig. D-27 is utilized in all Orbiter configurations. Except for the Spacecraft with the orbital entry capsule, this propulsion module structure is built around the MM '71 Propulsion Subsystem.

B. Equipment Module - The equipment module has as its nucleus, the MM '71 octagon. This structure is approximately 54 inches across and 18 inches high and provides for eight electronic assemblies. The electronics packaging structure includes the chassis and subchassis of the eight electronic assemblies, or bays, which form an integral part of the Orbiter structure, in that they function as thermal-shear panels for the primary vehicle structure. Also included as an integral part of the octagon is the scan platform support structure, a strut/truss framework.

For those configurations which employ the MM '71 propulsion module, it follows that the MM '71 equipment module and octagon structure can also be employed. Structural investigations as to how MM '71 octagon primary structure will differ from its '64, '67, and '69 predecessors have been initiated. Documentation of the previous octagon structures (ref. D-7 and D-8), gives information regarding panel longeron and ring geometry and cross-sections, but none regarding wall thicknesses.

Employing minimum gauges for these structural elements and material properties data from MIL-HDBK-5A, it appears that the panels and longerons of the MM '64 and MV '67 octagon structures are capable of bearing the MM '71 propulsion module. This suggests that the gages and geometry have been dictated primarily by electronics packaging and thermal control considerations. The octagon rings were also investigated. It was found that the addition of the MM '71 propulsion module at the top of this octagon requires one-gage increases in the thickness of both top and bottom rings.

These studies also indicate that the increased propulsion module size and weights required for the orbital entry Capsule mission require further gage increases, not only in the forward and aft rings of MM '71 octagon structure, but also in the longerons. The I-shaped longerons employed on this configuration require three-gage increases (to 0.070 inch).

These findings, while indicative, must be classified as preliminary, pending further review of the details of the octagon structural elements.

C. Capsule Adapter - The Capsule adapter physically interconnects the Orbiter and the Capsule and transmits boost phase loading from the Capsule and Orbiter aft towards the Centaur. The structural elements of this module (fig. D-28) are:

1. Octagon interface structure, a bulkhead that allows for stress field transitions between the equipment module octagon and the conical frustum employed for the upper adapter structure.

2. The upper adapter structure, a shell that provides the structural connection between the Orbiter and Capsule.
3. The interface ring provides a structural connection between the two shell elements of the Capsule adapter and the canister adapter.
4. The lower adapter, a conical shell frustum which furnishes a physical connection between the upper adapter and the Spacecraft separation plane. This element, following Spacecraft separation, performs no function other than that of a micrometeoroid protection bumper for the capsule.

Following Capsule separation, the entire Capsule adapter becomes unnecessary and is consequently separated from the Orbiter. The V-band clamp attaching this module to the equipment module is severed by pyrotechnic release devices during this procedure.

Both the upper and lower adapter are of semi-monocoque construction, with their eight (8) longerons aligned to those of the octagon. This construction, featuring longitudinal and circumferential shear continuity, provides high levels of strength and stiffness at small expenditures of structural weight.

As illustrated in fig. D-28, the upper and lower adapters are mated by a field joint at their common junction with the interface ring. The latter element is located on the interior of the assembly to allow the capsule to bear against it. The bolts of the canister adapter are secured to this ring. Access holes are provided in the aft end of the upper adapter to allow for this assembly procedure.

D. Spacecraft Adapter - The Spacecraft adapter, the function of which is to transmit boost phase loads from the Spacecraft proper to the Centaur, is comprised of two structural elements: (1) a cylindrical section permitting full clearance between the Spacecraft adapter and the Capsule; and (2) a conical frustum interconnecting the larger (Capsule-dictated) diameter to the smaller diameter (nominally 10 feet) Centaur at Centaur station 220. A bolted field joint mates the two elements comprising the adapter module. This module provides mounting locations for Spacecraft separation devices, connectors, etc.

D.4.1.1.4 Appendage Design Approaches

The principal deployed appendages are the four solar panels and the high gain antenna. The possibility of employing a separate appendage module was considered. Such a functional module, located between the propulsion and equipment modules, would serve to support major deployed appendages and attitude control components. The synthesis of such a module was concluded to be inconsistent, however, with the minimum change design approach employed for the Orbiter.

The four deployable solar panel structures are attached to support struts that are an integral part of the equipment module. These structurally interchangeable fiberglass honeycomb panels are supported at their hinge points in a nearly vertical

position for launch. Lateral support for each panel is furnished by a pair of boost dampers running between the tips of adjacent panels. The panels are released by pin pullers at one end of each boost damper pair and are deployed approximately 90° by redundant torsion spring dampers.

The high gain antenna, featuring a parabolic honeycomb dish, is attached to the forward ring of the equipment module octagon. This deployable antenna is supported vertically at its base by brackets and laterally by cruise dampers.

D.4.1.2 Orbiter Designs for Direct Entry Missions

D.4.1.2.1 Modules Common to All Capsules

Regardless of the Capsule size and payload composition, the propulsion and equipment modules of the Orbiter are identical. The appendages likewise remain the same. The Capsule adapter and Spacecraft adapter, however, vary with Capsule size geometry.

The propulsion module and the propellant and oxidizer tank support structural arrangements are described in para D.4.1.1.3. The forward beam gridwork and aft shear beam spider arrangements onto which the tanks are mounted are attached to the eight longerons of the external shell structure. The two pressurization tanks are supported from the forward propulsion tank beam arrangements by means of support bracket fittings. The thrust chamber is supported by an eight-strut space truss, whose members are attached to the external shell longerons at an intermediate ring.

The structural elements of this anticipated Mariner Mars '71 propulsion module structure are described in table D-17, which includes structural member identifications, material requirements, physical geometry and modes of failure. This description is based on preliminary analyses based on the loadings given in para D.4.1.1.1.

The Mariner Mars '71 equipment module will also be employed in all configurations. Estimates of the structural characteristics and elements of this module based on Mariner Mars '64 and '67 octagon descriptions, were described in para D.4.1.1.3. It has been determined that the elements of this magnesium structure appear to have been dictated primarily by electronic packaging and thermal control considerations. Hence, the MM '64 octagon 4" × 1 3/4" I-section longerons, employing an .040" (minimum) gage, are structurally adequate for the MM '71. The forward and aft octagon rings, both 4" × 3/4" I-shapes, require .050- and .060-inch gages, respectively, to accommodate the '71 propulsion system.

D.4.1.2.2 Minimum Weight Capsules

The Capsule weight in geometry largely determine the general arrangement of the Capsule adapter and Spacecraft adapter for the direct entry Capsule configurations. This paragraph discusses the lighter weight direct entry Capsules.

TABLE D-17. STRUCTURAL ELEMENTS OF MARINER MARS '71 PROPULSION MODULE

| Member | Material | Physical Geometry | Mode of Failure |
|---|--|--|------------------------------------|
| Octagon Interface Ring | 7075T6 Alum. Roll, Forging | Modified Channel, $t = .050$ " | Flange Crippling |
| Octagon Adapter Frustum (a) Longerons (8) (b) Skin Panels (8) | 7075T6 Alum. Extrusions 2024T4 Aluminum | Modified Z - Section, $t = .050$ " .032" Thick, Beaded at Min. Spacing | Flange Crippling Shear Buckling |
| Outer Shell (a) Longerons (b) Skin Panels | 7075T6 Alum. Extrusions 2024T4 Aluminum | Modified Z - Section, $t = .050$ " .032" Thick, Beaded at Min. Spacing | Flange Crippling Shear Buckling |
| Aft (Spider) Support Ring | 7075T6 Alum. Rolled Forging | Built-up Section Comprised of Modified Angle and Channel, Both .050" Thick | Flange Crippling |
| Intermediate (Thrust Chamber Strut Support) Ring | 7075T6 Alum. Rolled Forging | Modified Z Section, $t = .050$ " | Flange Crippling |
| Forward Support Ring | 7075T6 Alum. Rolled Forging | Built-up Section Comprised of Modified Angle and Channel, Both .050" Thick | Flange Crippling |

TABLE D-17. STRUCTURAL ELEMENTS OF MARINER MARS '71 PROPULSION MODULE (Continued)

| Member | Material | Physical Geometry | Mode of Failure |
|--|----------------------------|--------------------------------|---|
| Aft Propellant Tank Support (Spider) Structure | 7075T6 Aluminum | Built-up 1.5" x 3.0" Box Beam | (a) Flange Compression Yielding (b) Web Shear Yielding |
| Thrust Chamber Support Struts | 6061T6 Aluminum | 1" O.D. x 1/32" W.T. Tubing | Buckling |
| Forward Propellant Tank Support (Beam) Structure | 7075T6 Aluminum Extrusions | Modified Channel, $t = .050$ " | Flange Crippling |

Typical semi-monocoque shell elements within the Capsule adapter are: (1) a 42-inch high upper adapter conical frustum having a 31° cone angle and maximum diameter of 100 inches; and (2) an 18-inch high lower adapter conical frustum with a 45° cone angle and a maximum diameter of 138 inches. The structural elements of the Capsule adapter are described in table D-18.

The semi-monocoque shell elements of the Spacecraft adapter include: (1) a cylindrical section 22 inches high and 138 inches in diameter; and (2) a conical frustum 88 inches high with maximum and minimum diameters of 138 inches and 120 inches, respectively. The structural elements of the spacecraft adapter are described in table D-19.

D.4.1.2.3 Maximum Weight Capsules

For the larger capsules, typical semi-monocoque shell elements within the Capsule adapter are: (1) a 42-inch high upper adapter conical frustum having a 31° cone angle and maximum diameter of 104 inches; and (2) a 42 inch high lower adapter conical frustum with a 42° cone angle and a maximum diameter of 180 inches. The structural elements of this adapter are described in table D-20.

The semi-monocoque shell elements of the Spacecraft adapter include: (1) a cylindrical section 22 inches high and 180 inches in diameter; and (2) a conical frustum 96 inches high having maximum and minimum diameters of 180 inches and 120 inches, respectively. The structural elements of this spacecraft adapter are described in table D-21.

D.4.1.3 Orbiter Design for Out-of-Orbit Entry Missions

D.4.1.3.1 Propulsion Module

The out-of-orbit entry Capsule mission configuration requires the usage of larger propellant and oxidizer tanks than for MM '71. The structural arrangement and details of the propulsion module are described in para D.4.1.1.3. The structural elements of the propulsion module are described in table D-22. This description encompasses material requirements, physical geometries, modes of failure and margins of safety. The latter data was established from structural member sizing based on the design environments of para D.4.1.1.1.

D.4.1.3.2 Equipment Module

The Mariner equipment module, suitably reinforced to sustain loads induced by a larger and heavier propulsion module, will be employed. Estimates of the structural characteristics and elements of this module based on Mariner Mars '64 and '67 octagon descriptions are described in para D.4.1.1.3. The MM '64 octagon 4 inches \times 1 3/4 inches I-section longerons require a .070 inch gage to be structurally adequate for this configuration. This reflects a three-gage increase over that found in the existing octagon longerons.

TABLE D-18. STRUCTURAL ELEMENTS OF CAPSULE ADAPTER
(TYPICAL LIGHTWEIGHT DIRECT ENTRY CAPSULE)

| Member | Material | Physical Geometry | Mode of Failure |
|--|------------------------------|-------------------------------------|--------------------|
| Octagon Interface Ring | 7075T6 Alum. Roll Forging | Modified I-Section $t = .050"$ | Flange Crippling |
| Upper Adapter Frustum Section | | | |
| (a) Longerons (8) | 2024T4 Aluminum | 1.5" x 1.5" x .050" Hat Sections | Flange Crippling |
| (b) Skin Panels (8) | 2024T4 Aluminum | .032" Thick Beaded at Min. Spacing | Shear Buckling |
| (c) Intermediate Ring (Panel Breaker) | 2024T4 Aluminum | 1" x 1" x .040" Hat Section | Shear Web Yielding |
| Capsule Interface Ring | 7075T6 Aluminum Roll Forging | Modified Channel, $t = 0.125"$ | Flange Crippling |
| Lower Adapter Section (Capsule Shroud) | | | |
| (a) Longerons (8) | 2024T4 Aluminum | 1.5" x 1.5" x .050" Hat Sections | Flange Crippling |
| (b) Skin Panels (8) | 2024T4 Aluminum | .032" Thick, Beaded at Min. Spacing | Shear Buckling |
| Spacecraft Adapter Ring | 7075T6 Rolled Alum. Forging | Modified Z Section, $t = 0.19$ | Flange Crippling |

TABLE D-19. STRUCTURAL ELEMENTS OF SPACECRAFT ADAPTER
(TYPICAL LIGHTWEIGHT DIRECT ENTRY CAPSULE)

| Member | Material | Physical Geometry | Mode of Failure |
|-----------------|--------------------------------|---|-------------------------|
| Forward Ring | 7075T6 Alum. Rolled Forging | 4" x 4" Angle Section, Leg Thickness of 0.19" and 0.10" | Compression Yielding |
| Skin Panels (8) | 2024T4 Aluminum | .032" Thick, Beaded at Min. Spacing | Shear Buckling |
| Longerons (8) | 2024T4 Aluminum | 1.5" x 1.5" x .050" Hat Section | Flange Crippling |

TABLE D-20. STRUCTURAL ELEMENTS OF CAPSULE ADAPTER
(TYPICAL HEAVYWEIGHT DIRECT ENTRY CAPSULE)

| Member | Material | Physical Geometry | Mode of Failure |
|--|--|---|---|
| Octagon Interface Ring | 7075T6 Alum. Rolled Forging | Modified Channel, $t = .050"$ | Flange Crippling |
| Upper Adapter Frustum Section (a) Longerons (8) (b) Skin Panels (8) (c) Intermediate Ring (Panel Breakers) | 2024T4 Alum. 2024T4 Alum. 2024T4 Alum. | 1.5" x 1.5" x .050" Hat Sections .032" Thick, Beaded at Min. Spacing 1" x 1" x .040 Hat Section | Flange Crippling Shear Buckling Shear Web Yielding |
| Capsule Interface Ring | 7075T6 Alum. Rolled Forging | Modified Channel, $t = .125"$ | Flange Crippling |
| Lower Adapter Frustum Section (Capsule Shroud) (a) Longerons (8) (b) Skin Panels (8) | 2024T4 Alum. 2024T4 Alum. | 1.5" x 1.5" x .050" Hat Sections .032" Thick, Beaded at Min. Spacing | Flange Crippling Shear Buckling |
| Spacecraft Adapter Ring | 7075T6 Alum. Rolled Forging | Modified Z Section, $t = 0.19"$ | Flange Crippling |

TABLE D-21. STRUCTURAL ELEMENTS OF SPACECRAFT ADAPTER
(TYPICAL HEAVYWEIGHT DIRECT ENTRY CAPSULE)

| Member | Material | Physical Geometry | Mode of Failure |
|-----------------|--------------------------------|---|-------------------------|
| Forward Ring | 7075T6 Alum. Rolled Forging | 4" x 4" Angle Section, Leg Thicknesses of 0.19" and 0.10" | Compression Yielding |
| Skin Panels (8) | 2024T4 Alum. | .032" Thick, Beaded at Min. Spacing | Shear Buckling |
| Longerons (8) | 2024T4 Alum. | 1.5" x 1.5" x .050" Hat Sections | Flange Crippling |

TABLE D-22. STRUCTURAL ELEMENTS OF PROPULSION
MODULE (OUT-OF-ORBIT CAPSULE)

| Member | Material | Physical Geometry | Mode of Failure | Margin of Safety |
|---|--|--|------------------------------------|------------------|
| Octagon Interface Ring | 7075T6 Alum. Rolled Forging | Modified Channel, $t = .050$ " | Flange Crippling | High |
| Octagon Adapter Frustum (a) Longerons (8) (b) Skin Panels (8) | 7075T6 Alum. Extrus 2024T4 Alum. | Modified Z-Section, $t = .050$ " .032" Thick, Beaded at Min. Spacing | Flange Crippling Shear Buckling | High High |
| Aft (Spider) Support Ring | 7075T6 Alum. Rolled Forging | Built-up Section Comprised of Modified Angle and Channel, Both .050" Thick | Flange Crippling | +0.50 |
| Intermediate (Thrust Chamber Strut Support) Ring | 7075T6 Alum. Rolled Forging | Modified Z-Section, $t = .050$ " | Flange Crippling | High |
| Forward Support Ring | 7075T6 Alum. Rolled Forging | Built-up Section Comprised of Modified Angle and Channel, Both .050" Thick | Flange Crippling | High |

TABLE D-22. STRUCTURAL ELEMENTS OF PROPULSION
MODULE (OUT-OF-ORBIT CAPSULE) (Continued)

| Member | Material | Physical Geometry | Mode of Failure | Margin of Safety |
|--|-------------------------|-------------------------------|-----------------------------|------------------|
| Aft Propellant Tank Support (Spider) Structure | 7075T6 Alum. | Built-up 1.5" x 3.0" Box Beam | Flange Compression Yielding | +0.32 |
| Thrust Chamber Support Struts | 6061T6 Alum. | 1" O.D. x 1/32" W.T. Tubing | Web Shear Yielding | +0.42 |
| Forward Propellant Tank Support (Beam) Structure | 7075T6 Alum. Extrusions | Modified Channel, t = .050" | Buckling | High |
| | | | Flange Crippling | High |

The forward and aft rings, both 4 inches \times 3/4 inches I-shapes, both require .060 inch gages to accommodate the larger and heavier propulsion system required for this mission. While the aft ring gage is identical to that required for the MM '71 octagon, the forward ring thickness must be increased by one gage.

The shear panels within this revised octagon structure are of .032 inch thick 2024T4 aluminum, and are of beaded construction (.040-inch beads at minimum spacing), or the equivalent.

D.4.1.3.3 Capsule Adapter

Typical semi-monocoque shell elements within the Capsule adapter are: (1) a 36 inch high upper adapter conical frustum having a 22° cone angle and a maximum diameter of 80 inches; and (2) an 18 inch high lower adapter conical frustum with a 45° cone angle and a maximum diameter of 113 inches. The eight longerons of the shells within this adapter are aligned with those of the octagon.

In the out-of-orbit entry mission, it is necessary to furnish the scan platform with planet viewing capability prior to capsule separation. This requirement has resulted in a large (8" \times 8") circular cutout in the forward extremity of the upper adapter structure. This cutout, affecting roughly 20% of the length of this shell, provides a sufficient loss of shear continuity so as to affect the torsional rigidity of the orbiter. To compensate for this, the cross-sections of the eight longerons must be increased (to 3" \times 3" \times .050 boxes) in this region. An intermediate ring is placed in the center of, or halfway up the length of, this conical frustum structural element. This ring serves to: (1) reduce the length over which this increased longeron cross-section is required; (2) act as a panel breaker, and (3) provide doubler-type restraints. Aft of this intermediate rings, the longeron cross-sections, 1 1/2" \times 1 1/2" \times .050 hat sections, are sized by strength requirements, not stiffness criteria. Compensation for this cut-out results in a structural weight increase of 7 pounds. The effectiveness of this modification can be demonstrated by the resulting Spacecraft torsional frequency of 10.8 Hz, a value sufficiently above the minimum allowable requirement (10 Hz) for Titan III/Centaur payloads.

Descriptions of the structural elements of the Capsule adapter are furnished in table D-23.

D.4.1.3.4 Spacecraft Adapter

The elements of the Spacecraft adapter consist of: (1) a Spacecraft adapter Z-section ring section, and (2) a structural fairing, consisting of a semi-monocoque cylindrical shell 10 feet in diameter and 8 feet long. The latter element, exposed to aerodynamic flows, will be required to transmit to the Centaur those loadings sustained by the spacecraft fairing during boost.

The structural elements of this Spacecraft adapter are described in table D-24.

TABLE D-23. STRUCTURAL ELEMENTS OF CAPSULE
ADAPTER (OUT-OF-ORBIT ENTRY CAPSULE)

| Member | Material | Physical Geometry | Mode of Failure |
|--|-----------------------------|---|--------------------|
| Octagon Interface Ring | 7075T6 Alum. Rolled Forging | Modified Channel, $t = .050$ " | Flange Crippling |
| Upper Adapter Frustum Section | | | |
| (a) Skin Panels (8) | 2024T4 Alum. | .032" Thick, Beaded at Min. Spacing | Shear Buckling |
| (b) Intermediate Ring | 2024T4 Alum. | 1" x 1" x .040" Hat Section | Shear Web Yielding |
| (c) Longerons (8) Forward of Intermediate Ring | 2024T4 Alum. | 3" x 3" x .050" Hat Section with .050" Butt Strap | Flange Crippling |
| (d) Longerons (8) Aft of Intermediate Ring | 2024T4 Alum. | 1.5" x 1.5" x .050" Hat Section | Flange Crippling |
| Capsule Interface Ring | 7075T6 Alum. Rolled Forging | Modified Channel, $t = .125$ " | Flange Crippling |
| Lower Adapter Frustum Section (Capsule Shroud) | | | |
| (a) Longerons (8) | 2024T4 Alum. | 1.5" x 1.5" x .050" Hat Section | Flange Crippling |
| (b) Skin Panels (8) | 2024T4 Alum. | .032" Thick, Beaded at Min. Spacing | Shear Buckling |
| Spacecraft Adapter Ring | 7075T6 Alum. Rolled Forging | Modified Z Section, $t = 0.19$ " | Flange Crippling |

TABLE D-24. STRUCTURAL ELEMENTS OF SPACECRAFT ADAPTER
(OUT-OF-ORBIT ENTRY CAPSULE)

| Member | Material | Physical Geometry | Mode of Failure |
|--------------|--------------------------------|---------------------------------------|------------------|
| Forward Ring | 7075T6 Alum. Rolled Forging | Modified Z-Section, $t = 0.19$ in. | Flange Crippling |

D. 4.2 TEMPERATURE CONTROL SUBSYSTEM

The Temperature Control Subsystem must maintain all components of the Orbiter within specified bounds to assure requisite functioning of the Spacecraft system during its mission life, viz.:

1. Pre-launch and launch conditions
2. Near-Earth steady state
3. Midcourse correction transients
4. Near-Mars steady state
5. Mars orbit insertion and orbit trim transients
6. Eclipse of the Sun by Mars

Passive control, incorporating coatings, multiple layer radiation barrier thermal insulation blankets (superinsulation), and equipment thermal inertia is used where it can meet thermal requirements. It is augmented by thermostatically activated louvers and heaters as required.

Thermal design of the Spacecraft is based on the concept of temperature control by regulating the quantity of rejected heat from an insulated enclosure. The insulated vehicle surface serves as the enclosure while the active control louver system provides the regulated heat rejection. Various subsystems are in operation throughout the flight, and a portion of the power dissipated from these is used to maintain internal equipment at its desired operating temperatures. Excess heat is rejected from the Spacecraft primarily through the louver system.

The thermal control design is similar to that of Mariner Mars '69. The Orbiter is isolated, insofar as possible, from the effects of the large variation in solar heating between Earth and Mars. Maximum conduction and radiative coupling is provided between the equipment and propulsion tank compartments. Local hot spots are avoided by providing good thermal conduction joints and by enhancing internal radiation exchange by painting internal surfaces with a highly emissive black paint. In this manner, propellant tanks are essentially slaved to the electronic equipment bay compartment and are maintained at temperatures fairly close to that of the electronics. To allow for

contingencies, strip heaters are applied to propellant tanks and lines to prevent freezing. The use of louvers on the electronic bays minimizes temperature excursions due to changes in the solar intensity, variations in internal power, and heat leak through the insulation blanket, and also allows for inherent uncertainties in the predicted environment. In addition, it provides the versatility for accommodating design changes as the Orbiter system design evolves.

External appendages are controlled independently by employing suitable coatings and, in the case of the scan platform, by utilizing insulation blankets, sunshades and heaters.

The overall temperature control approach is basically conservative, providing appropriate margins and allowing for uncertainties in analytic and test techniques and uncertainties in thermal properties. The thermal paints selected have demonstrated the highest degree of stability among those used on Spacecraft and are capable of reasonable handling, cleaning, and repairing. As a general rule, only flight proven hardware and techniques are utilized in the Temperature Control Subsystem.

D. 4. 2. 1 Functional Description

Thermal control of the Mariner Mars '73 Orbiter is accomplished in a manner similar to Mariner Mars '69 through the use of:

1. Thermally actuated louver assemblies
2. Thermal blankets
3. Selected surface coatings and finishes
4. Electrical heaters

D. 4. 2. 1. 1 Louver Assemblies

The radiating plate of each equipment bay has an approximate area of 1.4 square feet and is coated with a white paint (Z-93 ZnO/Potassium Silicate) having an emissivity of ~ 0.92 and a solar absorptivity of ~ 0.17 . Consideration should be given to other stable white paints presently in development. All bays are equipped with a louver assembly that attaches to a supporting structure at the periphery of the radiator plates.

The louver assembly consists of blades driven in pairs by spirally wound bimetallic assemblies. Each louver blade is a thin-walled aluminum tube with cover sheets, approximately 0.005 inch, formed into a box section. The blades have highly polished specular surfaces (either highly polished aluminum or gold coated aluminum) to yield maximum heat dissipation when fully opened and maximum insulating characteristics when fully closed. Design of the assembly should assure at least 5:1 effective emissivity range for the heat dissipation (from 0.15 when fully closed to 0.75 when fully opened). If solar panel heat dissipation seriously interferes with the heat dissipating capability of a particular bay which has a good view of the solar array, the louver blades may have to be pegged to ensure requisite performance.

D.4.2.1.2 Thermal Blankets

Multilayered blankets (1/4 mil aluminized crinkled mylar sheets) are used on MM '69 where relatively large areas of the Spacecraft are to be insulated. The criteria for selection of the thermal blankets are:

1. Weight
2. Thermal performance
3. Adhesive characteristics of the aluminum
4. Ability of the outer cover to withstand a wide range in temperature.

Gold-coated mylar appears attractive for the insulation blankets for MM '73 based on results of the PVTIS program (JPL Contract 951537). The PVTIS tests indicated that aluminized mylar has a pronounced tendency to discolor or have the vapor-deposited aluminum coating completely removed from the substrata when exposed to ETO cycles with high relative humidity. Vapor-deposited gold on mylar has successfully survived ETO and heat sterilization tests, exhibits good adhesion, and is at least equivalent to aluminized mylar in thermal performance. Gold-coated Mylar with Kapton outer sheets provide an effective insulation system if ETO decontamination or high humidity are anticipated.

D.4.2.1.3 Surface Coatings

A basic thermal control device to be used in the design of the Mariner Mars '73 Orbiter is the application of specific surface coatings to the various surfaces. The basic criteria for selecting the proper thermal control coatings involve the following considerations:

1. The appropriate combination of thermo-optical properties for achieving requisite temperatures.
2. Adhesion characteristics
3. Satisfactory performance in the terrestrial environment
 - a. Durability
 - b. Ability to be cleaned, repaired and handled
4. Satisfactory performance in the space environment

Table D-25 lists coatings which have been used on Mariner Mars and other Spacecraft and which have potential application to the Mariner Mars '73 Orbiter.

TABLE D-25. THERMAL COATINGS

| Coatings | Solar Absorptivity | Emissivity | α/ϵ | Mariner Mars '71 Applicability |
|---|--------------------|------------|-------------------|---|
| Metals | | | | |
| Aluminum (Polished) | < 0.2 | < 0.05 | | Attitude control nozzles |
| Gold | 0.24 | < 0.05 | ~5.0 | Internal surfaces where high reflectivity is desired. |
| Rhodium | | < 0.05 | | |
| Conversion Coatings | | | | |
| Dow 7 | | 0.7 | | Utilized on magnesium for high emittance applications, e.g., electronic chassis |
| Alzak | 0.18 | 0.73 | 0.25 | Equipment bay radiator plates |
| Black Paints | | | | |
| Cat-a-lac (Epoxy) | | > 0.9 | | Internal surfaces of Spacecraft, back of solar array |
| 3M Optical Velvet | | | | |
| Parsons Black (Lacquer) | | | | |
| White Paints | | | | |
| Vitavar PV 100 (TiO ₂ pigment in silicone alkyd binder) | 0.21 | 0.83 | 0.24 | Equipment bay radiator panels |
| Z-93 (ZnO in Potassium) | 0.17 | 0.92 | 0.19 | Equipment bay radiator panels |
| S-13 HT (Zn in methyl silicone) | 0.2 | 0.9 | 0.22 | Equipment bay radiator panels |
| Rutile (TiO ₂ in methyl silicone) | 0.23 | 0.85 | 0.27 | Equipment bay radiator panels |
| Metal Filled Paints | | | | |
| Chrome Oxide Pigmented Polyurethane | ~0.7 | ~0.7 | ~1.0 | High gain antenna |
| D4D-Aluminum leak pigment in silicone-alkyd | 0.26 | 0.27 | 0.96 | External equipment (to minimize mars orbit transients) |

In general, the radiating areas for the louver radiating plates and the backs of the solar panels are coated with high emissivity coatings. The high emissivity coatings on the back of the solar arrays provide low solar cell temperatures to enhance electrical efficiency, and on the radiating plates assure maximum panel heat dissipation to space with the louvers open.

The internal surfaces of the Orbiter are generally coated with highly emitting paints to maximize the radiative heat transfer between large interior areas of the vehicle in order to create as uniform an environment as possible.

D. 4. 2. 1. 4 Electrical Heaters

Thermostatically controlled heaters can be used to hold components within narrow temperature bands. Either thermostats, proportional controllers, or on-off heaters may be used to control the heating rate. Electrical heaters should be provided in areas where analysis and tests indicate that the insulation, coatings, or thermal inertia of the subsystem is not sufficient to maintain the temperature levels within acceptable tolerance ranges.

In certain areas such as the propellant tanks, strip heaters (approximately 5 watts) may need to be added to provide redundancy in the Temperature Control Subsystem. External gas lines (as dictated by analysis and space chamber testing) might also be provided with heaters to protect against freezing of the fuel.

D. 4. 2. 2 Modifications to MM '69 and '71

In general, the Temperature Control Subsystem of the Orbiter follows closely that of Mariner Mars '69. However, the following specific areas may be modified from the Mariner Mars '69 design:

1. Thermal control of the infrared spectrometer
2. Delineation of propulsion system and addition of louvers in Bay II
3. Additional heaters
4. Thermal blankets change to gold coated mylar
5. TCFM deletion.

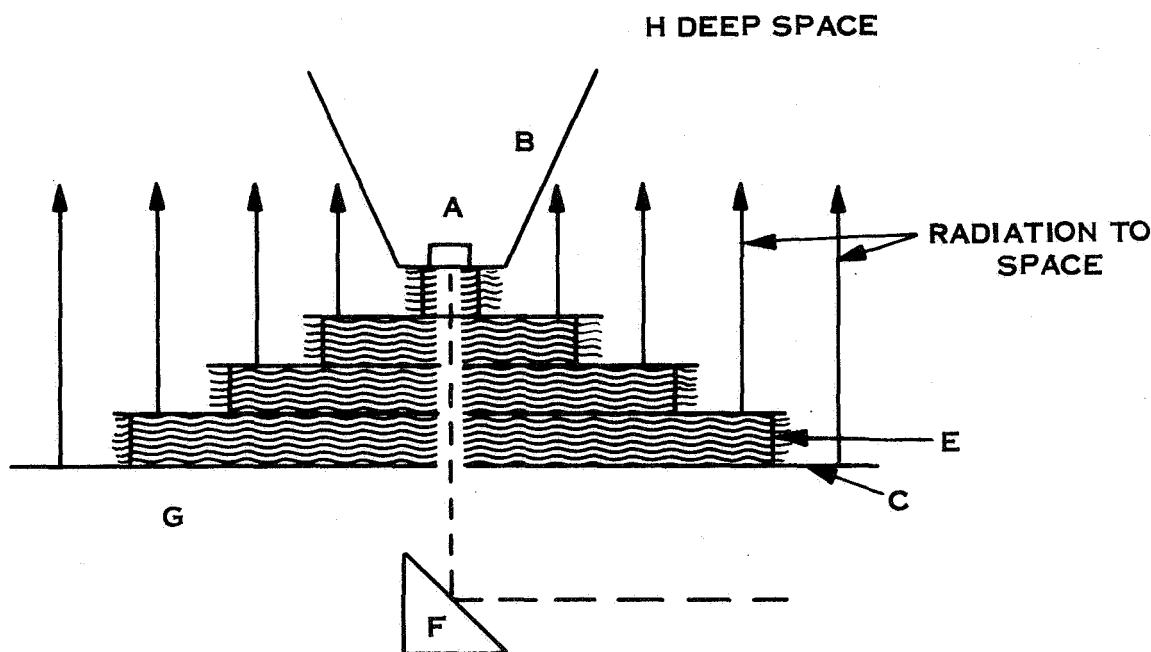
D. 4. 2. 2. 1 Infrared Spectrometer Thermal Control

Thermal control of the Infrared Spectrometer (IRS) is significantly different from that used in the MM '69 Spacecraft. The MM '69 requirements call for an operating time of approximately 1/2 hour, which implies that an active cooling control system may be used to bring the IRS detector down to the proper temperature operating range.

Present design estimates for the Orbiter suggest an operating time of nominally 3 to 6 months at IRS (4-14 μ) detector temperature of 80° K. With such a long operational

time, the use of actively controlled cooling appears infeasible, since this requires an excessive amount of coolant to be stored in the Spacecraft. It therefore appears that a major design effort is necessary to redesign the IRS detector so that passive techniques can be employed to hold the temperature of this device to 80°K .

Possible design changes include (a) the placement of the detector on thermal radiation barriers to insulate the detector from the Spacecraft environment, (b) maximizing the radiating area of the detector to deep space conditions and (c) the employment of thermal shields around the detector section which will not allow stray radiation to impinge on the detector face. A simplified schematic diagram of one proposed redesign is shown in fig. D-29.



- A - IRS DETECTOR
- B - HIGHLY REFLECTING THERMAL SHIELD
- C - HIGHLY CONDUCTING ALUMINUM PLATES
- D - SUPERINSULATION BLANKETS
- E - LOW CONDUCTIVITY FASTENERS
- F - PRISM
- G - SPACECRAFT THERMAL ENVIRONMENT
- H - DEEP SPACE

Figure D-29. Brief Schematic Diagram of Proposed Redesign for IRS Detector Positioning

D.4.2.2.2 Removal of Propulsion System From Bay II

The Mariner Mars '69 spacecraft has its monopropellant propulsion system in Bay II. It is now proposed that this bay carry data storage equipment. Maximum power dissipation for this bay is approximately 15 watts. To allow more precise control over possible temperature excursions, a louver assembly should be attached to this bay.

D.4.2.2.3 Additional Heaters

Dependent upon results of a detailed thermal analysis of the entire Orbiter coupled with vacuum chamber testing, it may be necessary to add heaters to external and internal components which fall below the minimum allowable temperatures during certain phases of the mission. From previous studies conducted, a total heater power capability of approximately 10 watts is required to maintain operating temperatures on all equipments. Provision should be made for approximately another 10 watts as contingency heating for the propellant tankage, cold gas tankage, and various valves and pipe lines internal and external to the vehicle.

D.4.2.2.4 Thermal Blankets

Mariner Mars '69 thermal insulation blankets are aluminized mylar. It is proposed that the Orbiter thermal blankets be gold coated mylar. The main advantages of using the gold coated mylar are that it does not degrade in the ETO decontamination process and that it can take a high humidity environment for a prolonged period of time with little change to its thermal characteristics. The effective emissivities of the two types of insulation blankets are comparable.

D.4.2.2.5 Temperature Control Flux Monitor

At the present time it does not appear likely that the temperature control flux monitor will be flown on the Orbiter.

D.5 TELECOMMUNICATIONS

D.5.1 RADIO FREQUENCY SUBSYSTEM

D.5.1.1 Functional Description

The Mariner Mars 1973 Radio Subsystem performs the following functions:

1. Receives the r-f signal transmitted to the Spacecraft from the DSIF.
2. Coherently translates the frequency of the received r-f signal by a fixed ratio of 240/221.
3. Demodulates the received r-f signal and sends a composite command signal to the Spacecraft Command Subsystem.
4. Detects the ranging signal transmitted to the Spacecraft by the DSIF.
5. Modulates the transmitted signal with a composite telemetry signal.
6. Modulates the transmitted signal with a ranging signal.
7. Transmits to the DSIF a modulated r-f signal that is phase coherent with either the received signal or with an internally generated r-f source.

In performing these functions, the subsystem is further constrained by the availability of only one 210 foot DSIF antenna with an acceptable viewing time of approximately ten hours. For the remaining time, communications are to the 85 foot antennas. Command capability must be maintained through a low gain antenna throughout the mission.

D.5.1.1.1 Subsystem Description

A block diagram of the Radio Subsystem is shown in fig. D-30. The configuration combines two exciters and two Travelling Wave Tube (TWT) power amplifiers in a redundant manner with selection based on either onboard failure sensing circuits or command from the ground. One receiver is used throughout the mission and is connected to either the primary low gain antenna (PLGA) or the secondary low gain antenna (SLGA). The three antennas (PLGA, SLGA, and HGA) are connected to the bay components by circulator switches, a coaxial switch, and a diplexer. The subsystem can transmit on any antenna and can receive on either the PLGA or the SLGA.

The power output level is 20 watts at 2295 MHz, and the receiver threshold for an unmodulated carrier applied at the preselector input is -151 dBm.

All components with the exception of the antennas are identical to the Mariner Mars '71 Radio Subsystem.

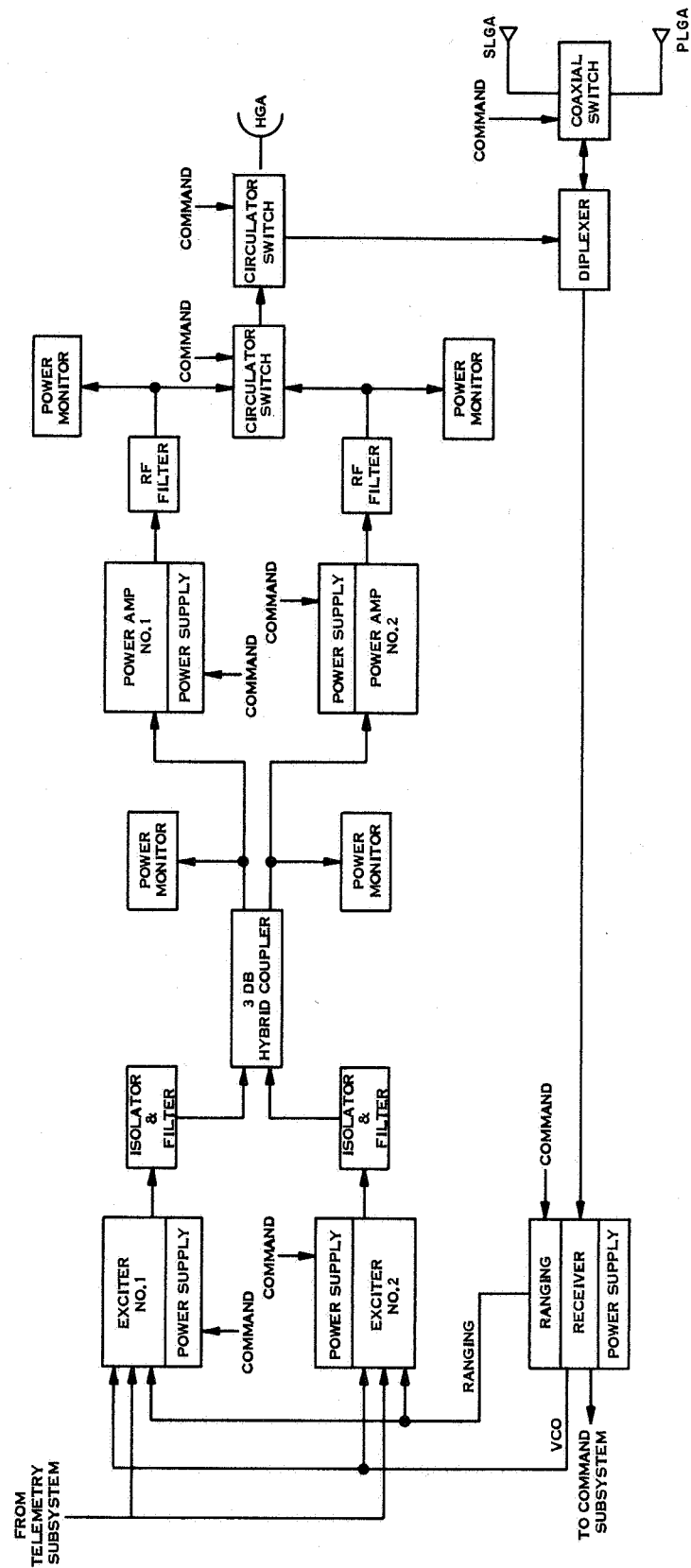


Figure D-30. Mariner Mars '73 Radio Subsystem Block Diagram

D.5.1.1.2 Receiver

The receiver is a double superheterodyne, narrowband, automatic phase tracking type and operates at a nominal frequency of 2113 MHz. The receiver recovers command and ranging information from the uplink signal. Command data is sent to the Command Subsystem.

Ranging data from the uplink signal is sent to the exciters to modulate the orbiter transmitter in order to support the turn around ranging function. The ranging function can be commanded on or off. The VCO output is sent to the exciters whenever the uplink signal is present, thus providing a downlink carrier frequency which is 240/221 times the uplink frequency and is phase coherent with it.

D.5.1.1.3 Transmitter

The two exciters are identical and can be turned on either by command or by on-board failure sensing circuits. The exciters contain their own crystal oscillator source, which is used when the uplink signal is not present. The purpose of the exciter is to provide a means of phase modulating the composite telemetry or ranging signals onto the carrier and to multiply this signal up to the desired S-band frequency. The exciters and power amplifiers are coupled together by a 3-dB hybrid coupler such that either exciter can drive either power amplifier.

A 20-watt power level is obtained by the use of traveling wave tube amplifiers (TWTA) in two identical power amplifier packages, which are activated by command or onboard failure sensing circuits.

D.5.1.1.4 Antennas

The antennas are: high gain antenna (HGA), primary low gain antenna (PLGA), and secondary low gain antenna (SLGA). The antennas have following functions:

1. Provide adequate downlink support to permit attainment of data rates which are compatible with the storage capability and the scientific mission requirements.
2. Support a data link for purposes of maneuver attitude verification.
3. Support the command link throughout the mission.
4. Support a downlink during cruise.
5. Support an r-f link during prelaunch operations.

The HGA is a prime focus paraboloid whose nominal diameter and gain are 63 inches and 29.4 dB, respectively. The antenna is single-axis steered through a clock-cone range of approximately 35° for the 90-day orbiting phase. This antenna is available for downlink communication from approximately 20 days before early encounter through about 140 days after early encounter.

The PLGA with a gain of 7.5 dB minimum and 3 dB beamwidth of 80° is the same antenna that is used for MM '69. The pattern is pointed along the -Z axis and is symmetrical about this line. As shown in fig. D-31 this antenna can support the 33 1/3 bps engineering link to the 210 ft dish to approximately 250×10^6 km, and the 8.3 bps link to beyond maximum range with proper pointing. Communications to the 85 ft DSN can be maintained only to 115×10^6 km and then only at the 8.33 bps rate.

For cruise communications to the 85 ft dish beyond this range several options are possible. First the link has nominal performance to 165×10^6 km; a lower rate of 4.167 bps could be added to the spacecraft providing communication to nominally 230×10^6 km, where the Earth enters the HGA pattern. Second, the articulation range of the HGA could be increased (by perhaps double axis steering) to make the HGA usable during cruise phase beyond 115×10^6 km. Since the spacecraft can communicate with the Earth via the 210 foot dish throughout the mission, it is felt that either of these options may be provided as a redundancy consideration, but not as part of the primary design.

The secondary low gain antenna (SLGA) has a toroidal-shaped pattern which is aligned so that its major radiation is in the ecliptic. The gain is 4.5 dB, with a beamwidth of 50° . The primary purpose of this antenna is to support the downlink during maneuver attitudes. This is accomplished by rolling the spacecraft about the Z axis for any thrust orientation, until the Earth is in the pattern. Again from fig. D-31 maneuver attitude verification can be accomplished through the 210 foot DSN to a range of approximately 300×10^6 km. Maintenance of the link through the 85 ft DSN, however, is only good to a distance of about 80×10^6 km. It is assumed that all maneuvers, including orbit insertion, will be in view of the 210 ft antenna at Goldstone.

The Radio Subsystem is connected to the antennas so that it can transmit through any one of the antennas and so that it can receive through either the PLGA or the SLGA.

D.5.1.1.5 R-F Switches and Diplexer

The two circulator switches provide the same function as in the MM '69 vehicle. An additional switch (single-pole, double-throw coaxial) enables selection of the PLGA or the SLGA.

The diplexer is a two-band bandpass filter which provides attenuation of the power amplifier noise spectrum in the vicinity of 2115 MHz to prevent significant degradation of the receiver noise figure, and to attenuate any power amplifier spurious outputs.

D.5.1.1.6 Radio Modes

The modes of operation from launch to encounter are given in table D-26.

D.5.1.2 Modifications of Mariner Mars '71

The only differences between the Radio Subsystems of the MM '73 and the MM '71 vehicles are in the antennas.

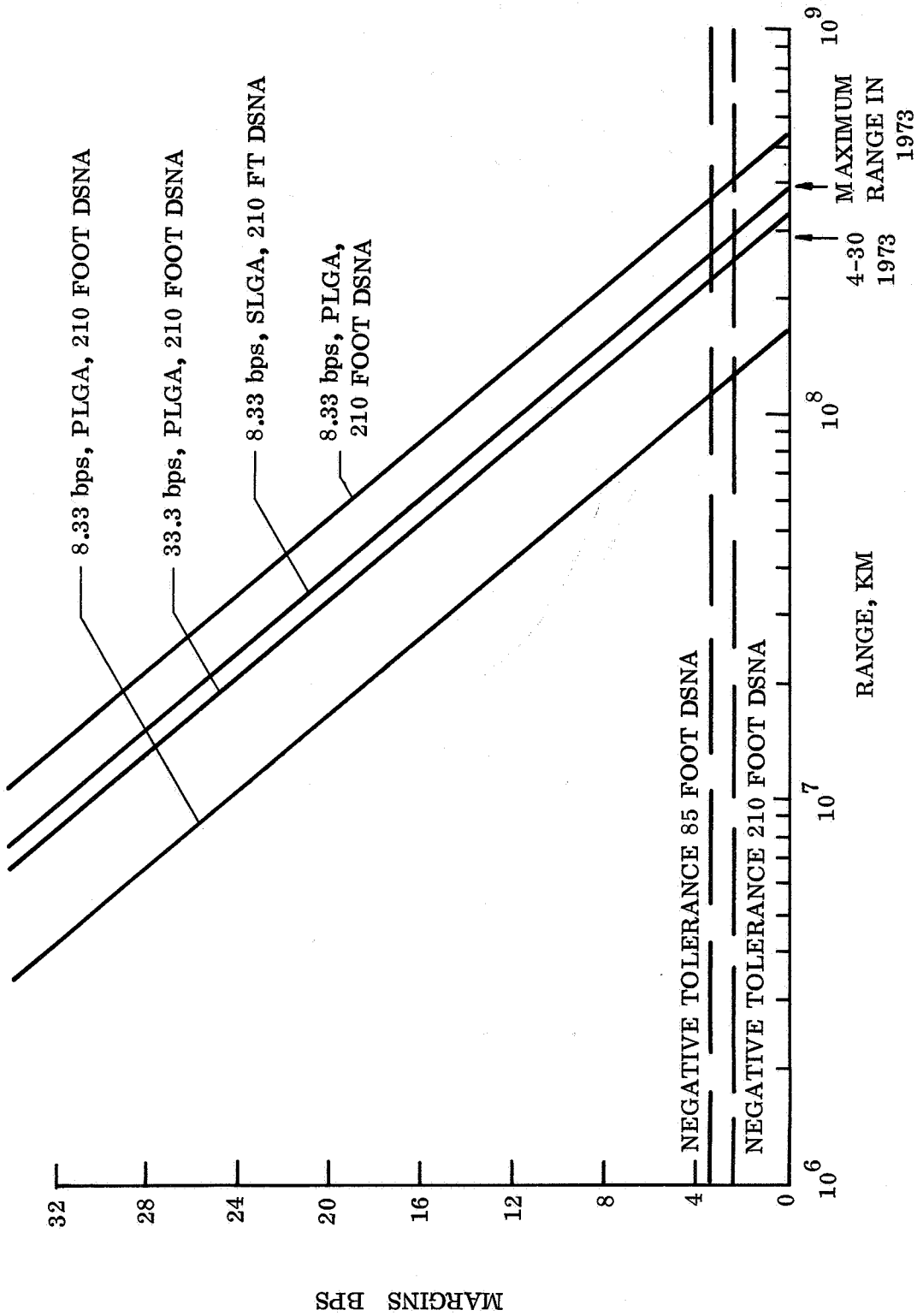


Figure D-31. Margin vs Range for Low Gain Antennas

TABLE D-26. RADIO MODES

| Mode | Power (watts) | Antenna | Data Rate (bps) |
|------------------|------------------|-------------|--------------------|
| Cruise | 20 | PLGA HGA | 33.3/8.33 |
| Maneuver | 20 | SLGA | 8.33 |
| Orbit (to 85 ft) | 20 | HGA | 500 and 8.33 |
| (to 210 ft) | 20 | HGA | 8,100 and 66.67 |
| Capsule Checkout | 20 | HGA | 500 |

D.5.1.2.1 High Gain Antenna

The orbiting phase of the MM '73 Orbiter has been taken as 90 days. During this time photographs of the Martian surface are taken on each orbit and stored in the tape recorders for later transmission to Goldstone. The period of time that data can be sent to that station is estimated to be ten hours. The size of the antenna must be increased over that of MM '71 to compensate for the increased range, and its articulation angle must be increased because of the new geometry.

The above considerations in conjunction with the physical constraints of the spacecraft configuration lead to a HGA with the following characteristics:

1. Diameter = 63 in.
2. Gain = 29.4 dB
3. HPBW = 5.7°
4. Deployed with its articulation axis aligned to 182.6° clock and 94.6° cone.
5. Stepped about a single axis in 0.1° steps to required positions during the orbit phase.

Fig. D-32 shows the out-of-plane pointing error and loss which results from single axis steering. One notes that as much as a 140 day mission can be supported by this method without serious link degradation. This approach reduces both the mechanical and electrical complexity of the steering sequence.

D.5.1.2.2 Secondary Low Gain Antenna

The SLGA antenna has a toroidal shaped pattern oriented in a plane parallel to the XZ plane and has the following parameters:

1. Type: slot fed, biconical
2. Mounted on a solar panel to put major radiation in ecliptic plane.
3. Gain = 4.5 dB
4. HPBW = 50° normal to toroidal plane.

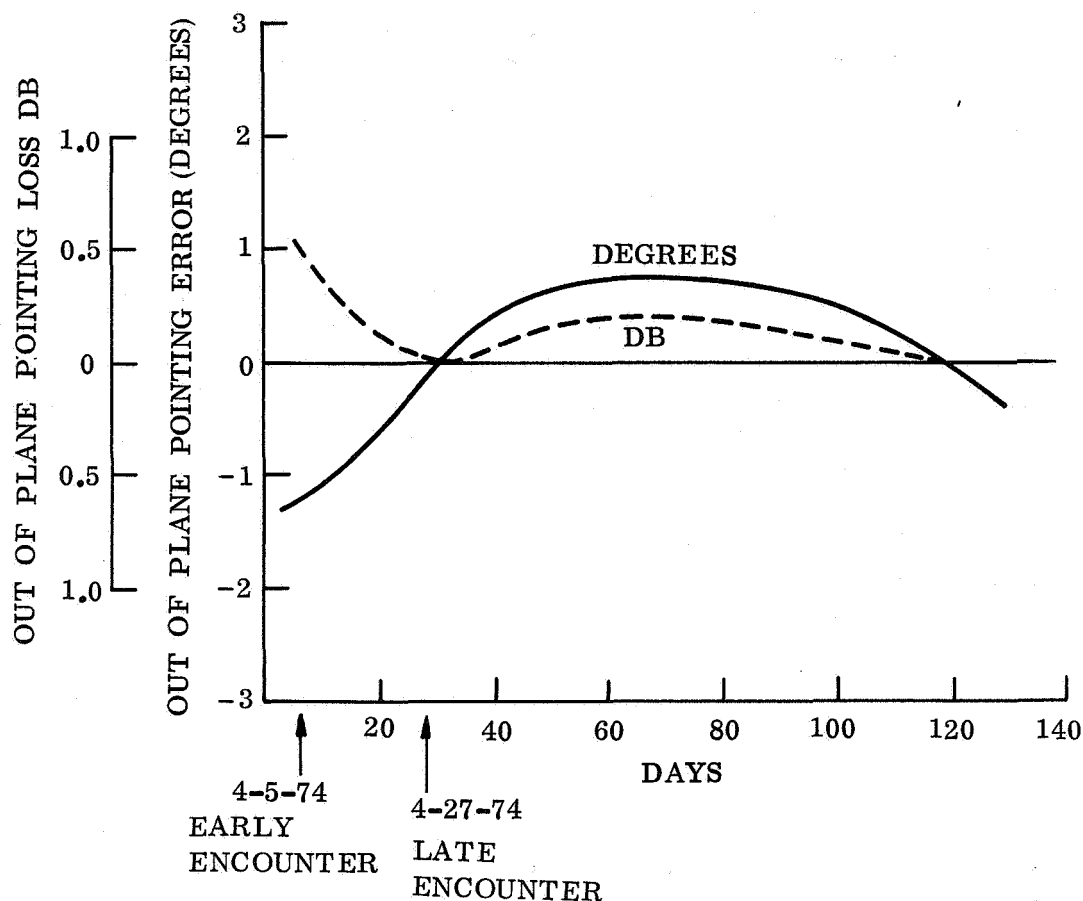


Figure D-32. Out-of-Plane Loss Due to Single Axis Steering of 63 Inch High Gain Antenna

D.5.1.3 Performance Characteristics

Table D-27 shows the various radio links for telemetry and command. For the command links, the 85 ft, 100 kw range corresponds to approximately 70 percent spherical coverage at the encounter 290×10^6 km. Utilizing the 210 ft DSN for command increases that coverage to approximately 76 percent. Both of these estimates are based on the Mariner C low gain antenna, (which has a similar pattern to the MM '69 antenna) and the proposed SLGA. They are included to indicate the relative extent of command coverage when using the two different DSN antennas.

TABLE D-27. SUMMARY OF R-F LINK PERFORMANCE

| Transmission Mode | Data Rates | Reception Mode | Greyout Range (10 ⁶ km) |
|-------------------|-------------|----------------|------------------------------------|
| 20 watt, HGA | 8,100/66.67 | 210 | 340 |
| 20 watt, HGA | 500/8.33 | 85 | 340 |
| 20 watt, PLGA | 33.3 | 210 | 255 |
| 20 watt, PLGA | 8.33 | 85 | 115 |
| 20 watt, SLGA | 8.33 | 210 | 300 |
| 20 watt, SLGA | 8.33 | 85 | 81 |
| 100 kw, 85 ft | 0.5 | PLGA | 770 |
| 100 kw, 85 ft | 0.5 | SLGA | 485 |

This design of the telemetry link for the 1973 mission assumes that no commands will be sent via the 210 ft dish. This permits realization of a lower received noise temperature by not requiring that the antenna be in the diplexed configuration.

Figs. D-31, D-33, and D-34 show the predicted r-f link margin versus range for the various telemetry and command modes and antennas. The curves for the 85 ft DSNA are based on EPD-283 with the antenna in its normal configuration. The curves for the 210 ft DSNA, however, assume a nondiplexed configuration for that antenna. The value used for antenna temperature is 29°K worst case. Additionally the negative tolerance on the gain of the 210 is taken to be 0 dB. The justification for this is taken from SPS 27-48, Vol. II and is based on the fact that the 210 ft dish elevation angles are above 20° for the science link to earth.

Using the Mark I planetary ranging system, with the PLGA on the uplink, HGA on the downlink, and the 210 ft DSNA, the ranging capability will greyout at 205×10^6 km, with nominal performance to 320×10^6 km. This requires diplexing the 210 ft dish and this fact is included in the above figures. Ranging performance can be extended, if necessary, by modifying the antenna switching portion of the Radio Subsystem or by using a new ranging scheme under development. The turnaround ranging capability of the spacecraft is represented in fig. D-35.

D.5.2 COMMAND SUBSYSTEM

D.5.2.1 Functional Description

The Command Subsystem, fig. D-36, accepts the composite command sync and command data subcarriers from the Radio Frequency Subsystem, demodulates the subcarriers, and with a matched filter, detects the command data. The data signal is decoded, and direct (DC), coded (CC), and quantitative (QC) commands are distributed to the subsystems addressed by the received commands.

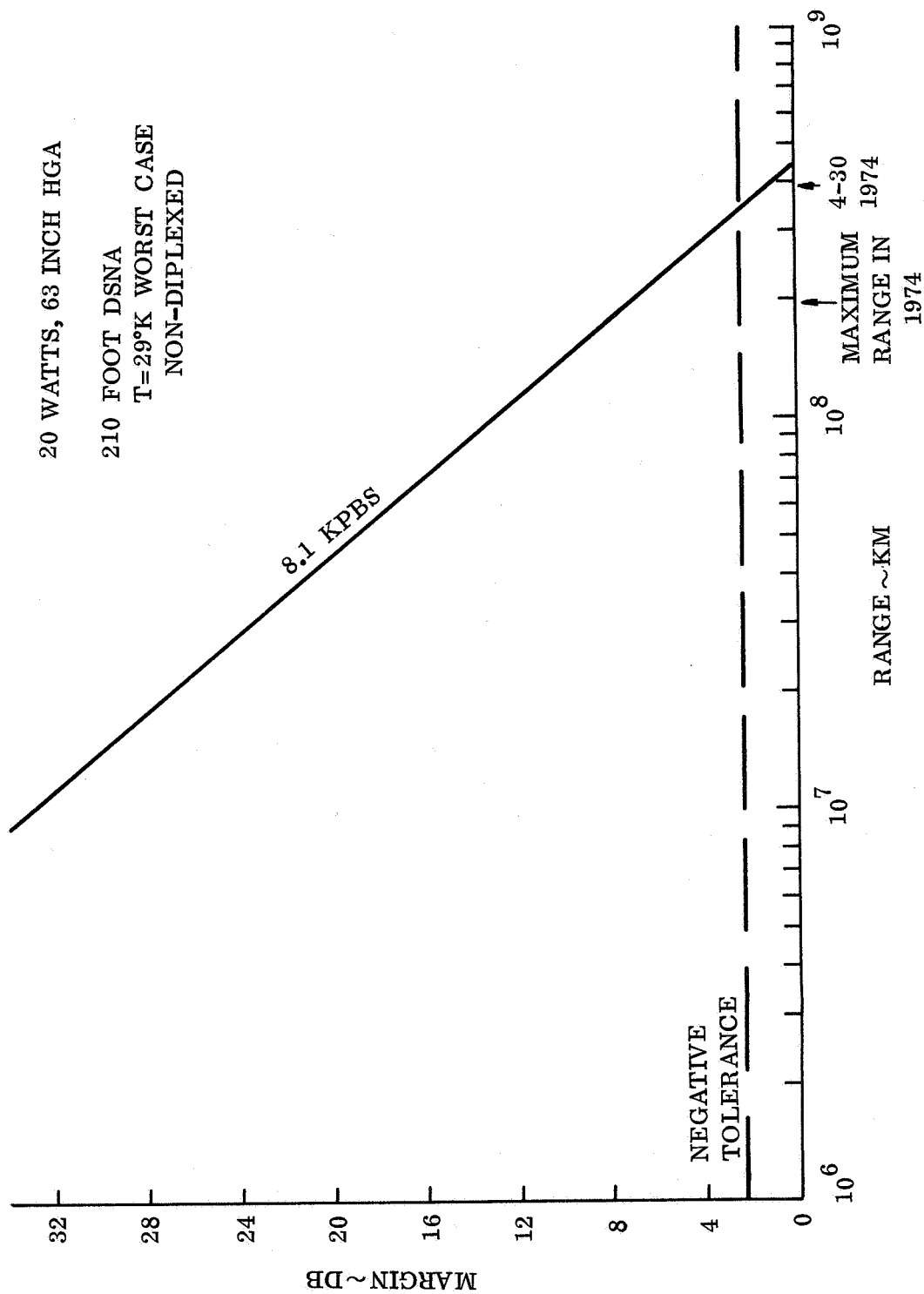


Figure D-33. Margin vs Range for High Gain Antenna

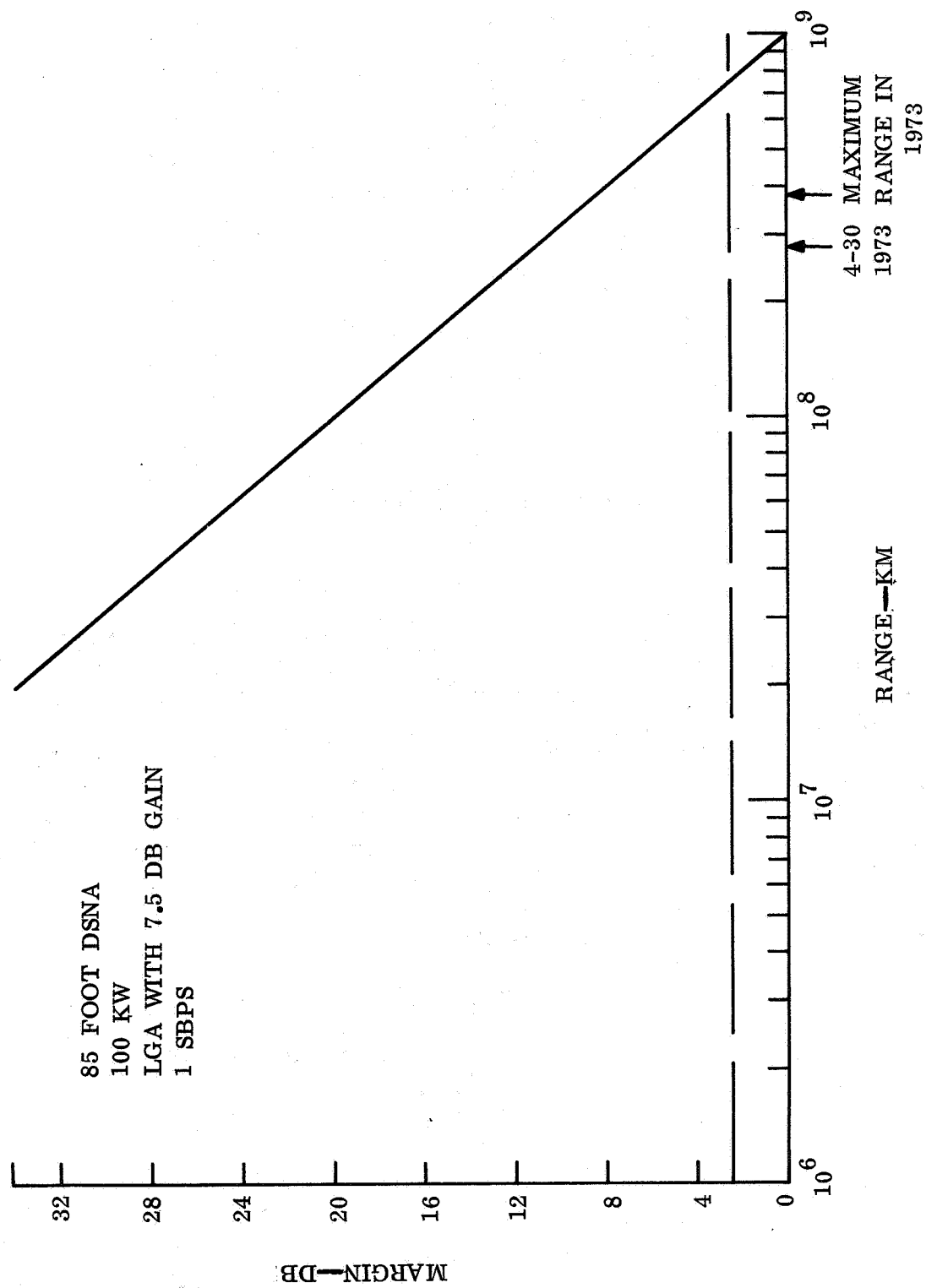


Figure D-34. Command Margin vs Range

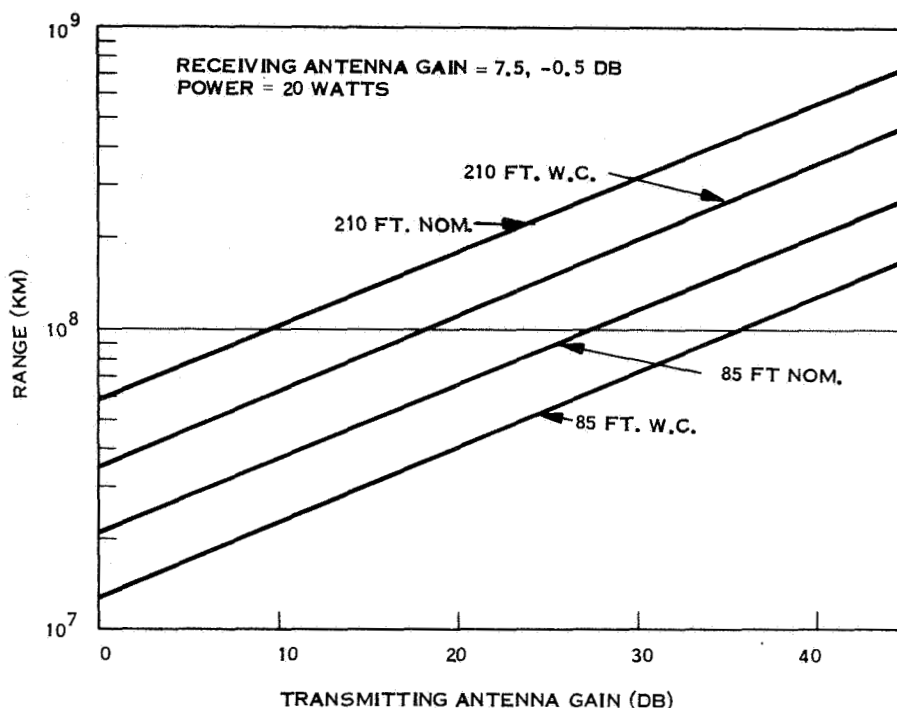


Figure D-35. Ranging Channel Range vs Antenna Gain

The command detector is shown in fig. D-36. The data subcarrier at f_s is bi-phase modulated by the data (D) at 1 bps, and by a 1/2 cps square wave which enables the detection ambiguity to be resolved. The data subcarrier is separated from the PN sync subcarrier by filtering and is processed to provide the reference for the subcarrier phase lock loop. The VCO is used as the reference for detecting the data and for driving the PN generator. The phase of the PN generator is stepped until the output reaches synchronism with the received PN sequence, and then sync search is stopped and decoding is enabled. The PN generator state is decoded to provide bit sync signals for the data channel matched filter and for the decoding operations.

The basic direct command word format is shown below:

| | | | | | | | | | | | | | | | | | | | | | | | | | | |
|----------|------------|---|---|----------------|---|---|---|---|---|-----------|----|----|----|----|----|----|----|----|------------|----------|----|----|----|----|----|----|
| Bit No. | 1 | 2 | 3 | 4 | 5 | 6 | 7 | 8 | 9 | 10 | 11 | 12 | 13 | 14 | 15 | 16 | 17 | 18 | 19 | 20 | 21 | 22 | 23 | 24 | 25 | 26 |
| Function | Word Start | | | DC Sub-Address | | | | | | | | | | | | | | | DC Address | | | | | | | |
| Value | 1 | 1 | 0 | 0 | 0 | 0 | 0 | 1 | 1 | All Zeros | | | | | | | | | | Variable | | | | | | |

Before the Decoder Program Control Unit will recognize a command, 26 consecutive zeros must be received. Decoding of the command begins upon receipt of the word

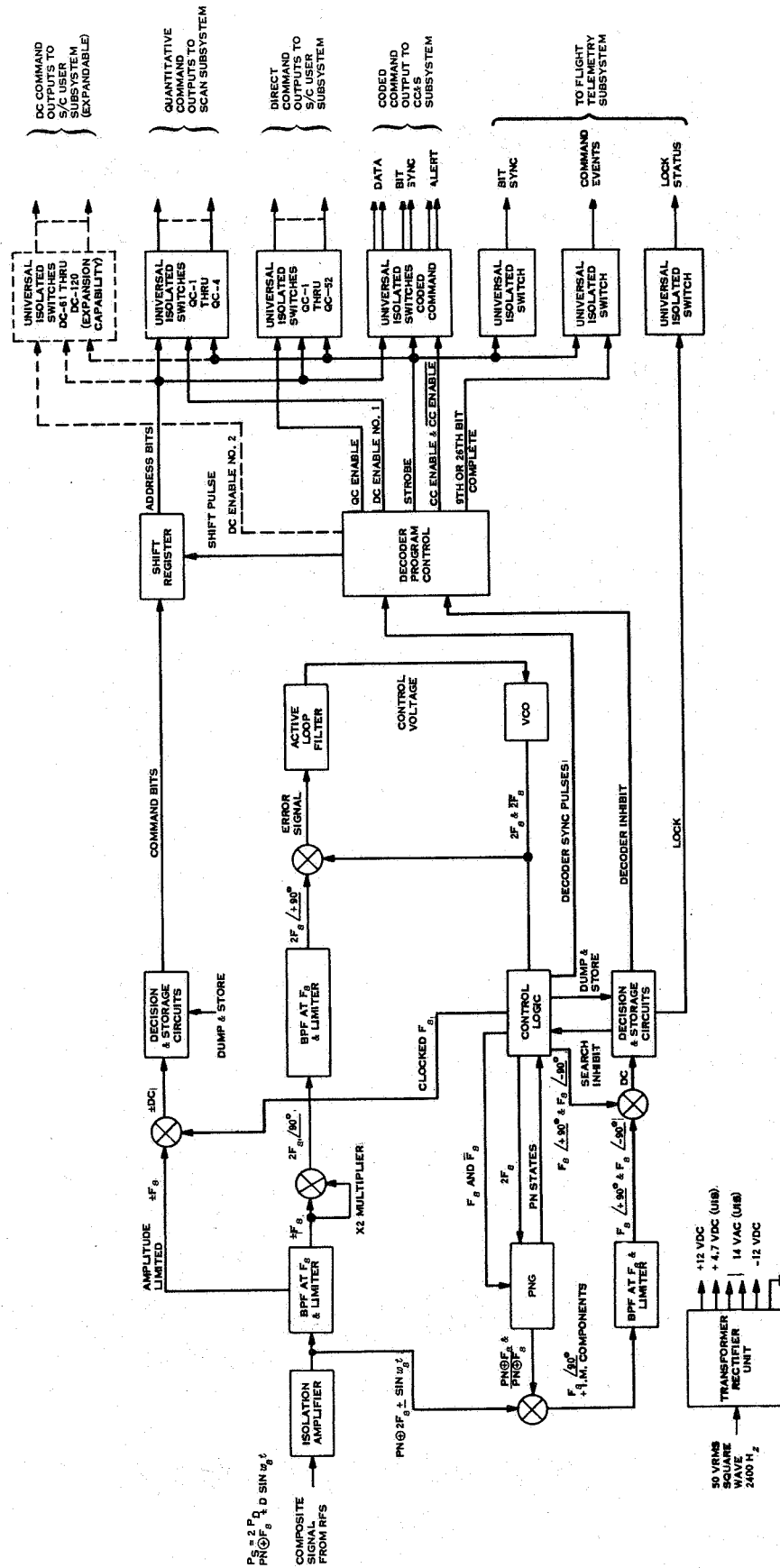


Figure D-36. Command Subsystem

start sequence, 110. Bits 4 through 9 denote whether the succeeding command is a DC, CC or QC. The allowed combination of bits 4 through 9 are restricted in order to prevent single errors in detection from leading to a false command either from a false word start signal or from errors in the command bits themselves. The particular sequence of bits 4 through 9 shown above denotes that a DC is being sent. For this case, bits 10 through 19 are zeros and 20 through 26 define the specific DC. Other selected sequences of bits 4 through 9 denote CC's and QC's. After the Program Control Unit recognizes a DC subaddress, the bits which follow are shifted out to the decoding matrix. After all 26 bits have been received, the matrix is interrogated and a specific isolated switch is closed, completing the decoding operation. If a CC or QC is received, the bits following the subaddress are routed to the CC&S or Scan Control Subsystems respectively.

Mariner Mars '69 is required to provide 49 DC's, 4 QC's and 5 CC's. In MM '73 the number of DC's increases to 65, a number greater than the MM '69 capability of 63 commands. This capability, however, may be expanded to accept a greater number of commands without modifying the basic scheme. For example, additional DC subaddresses are available, for each of which 63 additional separate commands can be generated. (Alternately, up to 8 of these subaddresses could be used for added QC words, or up to 8 for added CC words.)

Such an increase does, however, require additional logic capability in the Command Decoder. It is probable that such Command Decoder modification will be required in MM '73.

D.5.2.2 Performance Characteristics

1. The threshold input composite subcarrier power to noise density ratio is 16.5 ± 1 dB for a bit error probability of 10^{-5} .
2. The threshold command word error probability is less than 10^{-6} .
3. The probability of no response at threshold is less than 10^{-2} .
4. The command bit rate is 1 bps.

D.5.3 FLIGHT TELEMETRY SUBSYSTEM

D.5.3.1 Functional Description

The Flight Telemetry Subsystem provides signal conditioning, encoding, and time multiplexing of the spacecraft engineering data, coding of the digital science data, and relaying of capsule data. Two modulated data channels are provided, one high rate and one low rate, which are frequency multiplexed and outputted to the r-f exciters. In addition, the FTS provides for mode and data rate switching depending on the requirements of the mission phase.

A block diagram of the FTS is shown in fig. D-37. The engineering measurements are commutated in ten decks sampled at four rates, as in MM '69. Analog data is

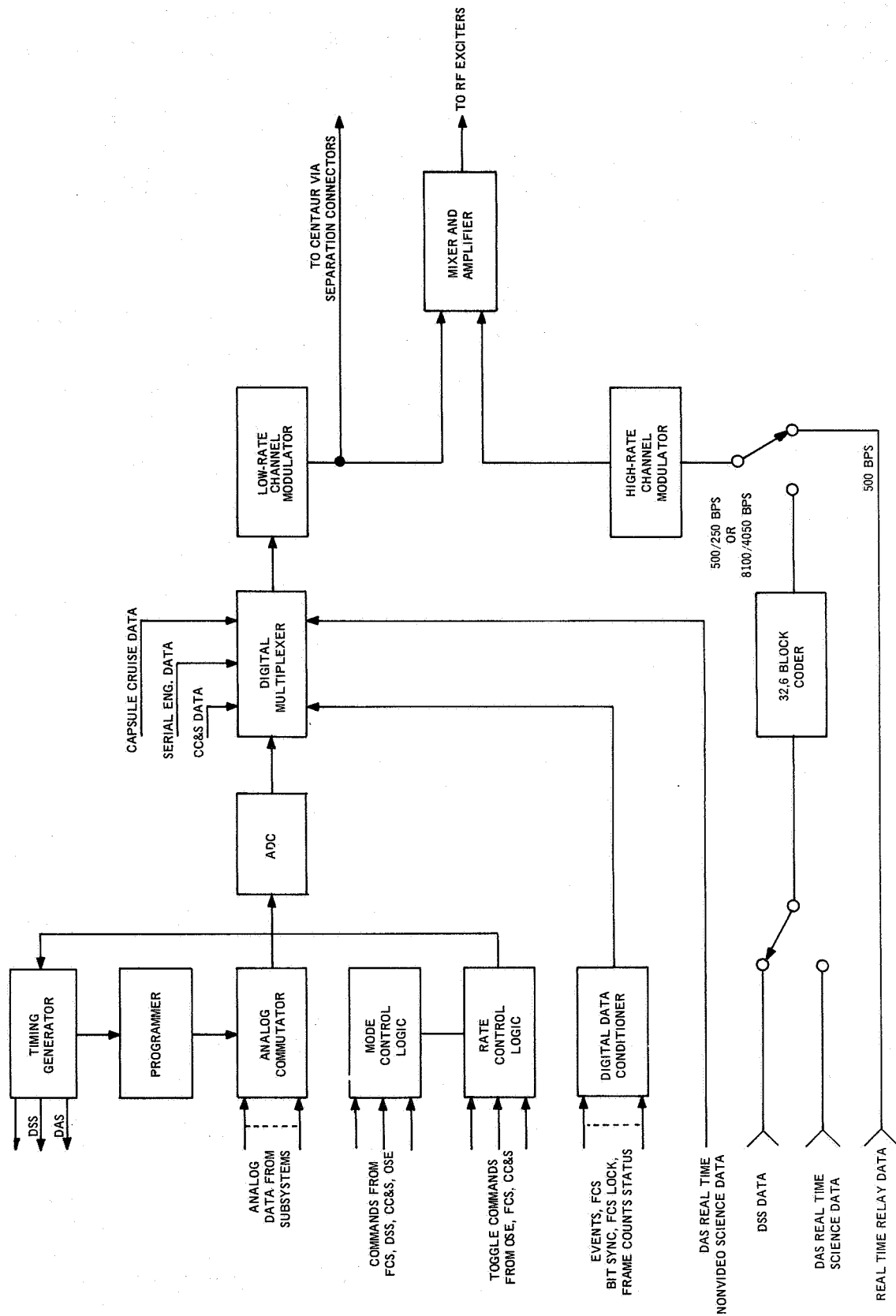


Figure D-37. Flight Telemetry Subsystem

conditioned to a 3v standard range, converted to a digital number by the analog-to-digital converter and multiplexed with serial digital engineering data and event data. When commanded, the CC&S memory can be read out through the digital multiplexer. During the science collection period, when in view of the 210 ft receiving antenna, real time non-video science data is multiplexed with the engineering data on the low rate subcarrier.

The 32.6 block coder encodes the stored serial bit stream from the Data Storage Subsystem containing video, non-video, and capsule relay data. As a backup, high rate real time non-video science can be read out from the DAS on this channel.

Table D-28 shows data rates versus mission phase. The low rate channel is placed on a high frequency subcarrier compatible with the DSN Multi-Mission Telemetry Demodulator (MMTD). The high rate channel coded data is modulated on a subcarrier using three cycles of subcarrier per coded bit, which allows the use of the ground decoding hardware built for MM '69 by the "High Data Rate Project". The uncoded data on the high rate channel (500 and 250 bps) is split-phase modulated.

TABLE D-28. DATA RATES VERSUS MISSION PHASE

| Mission Phase | R _H (bps) | R _L (bps) |
|------------------------|----------------------|----------------------|
| Cruise and Maneuvers | -- | 33 1/3/8 1/3 |
| Orbit | | |
| Trans. to 85' Antenna | 500/250 | 8 1/3 |
| Trans. to 210' Antenna | 8100/4050 | 66 2/3 |

D.5.3.2 Operation

D.5.3.2.1 Cruise and Maneuvers

Orbiter engineering data and capsule engineering data are collected and transmitted at 33 1/3 or 8 1/3 bps depending on the communication range. The capsule engineering data is multiplexed within the capsule data handling subsystem and is read out to the orbiter Telemetry Subsystem.

D.5.3.2.2 Capsule Checkout

During capsule checkout, orbiter engineering data at 8 1/3 bps is transmitted over the low rate channel, while the high rate channel handles the capsule checkout data at 500 bps.

D.5.3.2.3 Capsule Cruise

Capsule data which occurs once per hour in 60 second bursts, is stored for later transmission. The data is routed directly to the modulator without coding. The low rate channel continues to transmit engineering data.

D.5.3.2.4 Capsule Entry

Capsule relay data is handled the same as during capsule cruise.

D.5.3.2.5 Capsule Post Impact

Capsule relay data is stored on the digital tape recorders for later transmission over the high rate channel with coding.

D.5.3.2.6 Orbital Operation

Until the communication link thresholds, stored data is coded and transmitted at 8.1 kbps when in view of the 210 ft antenna at Goldstone and at 500 bps when in view of the 85 ft antennas. When the link thresholds, the data rates are reduced by a factor of two which permits operation until the end of the mission.

During periapsis passage, the low rate channel is used for multiplexed engineering and non-video science data. For the remainder of the orbit, only engineering data is transmitted over this channel.

D.5.3.3 Performance Characteristics

D.5.3.3.1 Data Rates and Modes

Data rates and data modes are presented in table D-29. Worst case data rate capability is presented in figs. D-38 and D-39.

D.5.3.3.2 Accuracy

The accuracy of the analog-to-digital conversion is ± 1 percent of full scale for the 0-3v, and ± 1.5 v signals, and ± 3 percent for the 0 - 100 mv signals.

D.5.3.3.3 Sampling Rates

The sampling times are given in table D-30.

TABLE D-29. RELAY DATA COLLECTION

| Mission Phase | Duration (seconds) | Data Rate (bps) | Total Bits |
|------------------------------------|---------------------|-----------------|--|
| Pre-separation | 900 | 1,348 | 1.2×10^6 |
| Separation to Engine Burn | 1836 | 1,348 | 2.46×10^6 |
| Capsule Cruise | 60 seconds/ hour | 1,348 | 1.6×10^5 (out of orbit) 1.9×10^6 (direct entry) |
| Entry | 1251 | 1,348 | 1.68×10^6 |
| Set up | 150 | 1,348 | 2.01×10^5 |
| Post Impact | 480* | 160,000 | 7.68×10^7 |
| Total | | | 8.43×10^7 |
| *Only 480 seconds of data recorded | | | |

TABLE D-30. TIME BETWEEN SAMPLES (SEC)

| Rate | Deck | | | |
|---|------|--------|--------|---------|
| | High | Medium | Low | Low-low |
| 8 1/3 | 16.8 | 168.0 | 1680.0 | 3360. |
| 33 1/3 | 4.2 | 42.0 | 420.0 | 840. |
| 66 2/3* | 6.3 | 63.0 | 630.0 | 1260 |
| *non-video science data occupies 2/3 of the format. | | | | |

D.5.4 DATA STORAGE SUBSYSTEM

D.5.4.1 Functional Description

The Data Storage Subsystem (DSS) provides buffering between the high rate video, non-video science, and Capsule relay data and the lower Spacecraft transmission rates. In order to minimize costs, the proposed subsystem attempts to make maximum usage of the existing MM '69 hardware.

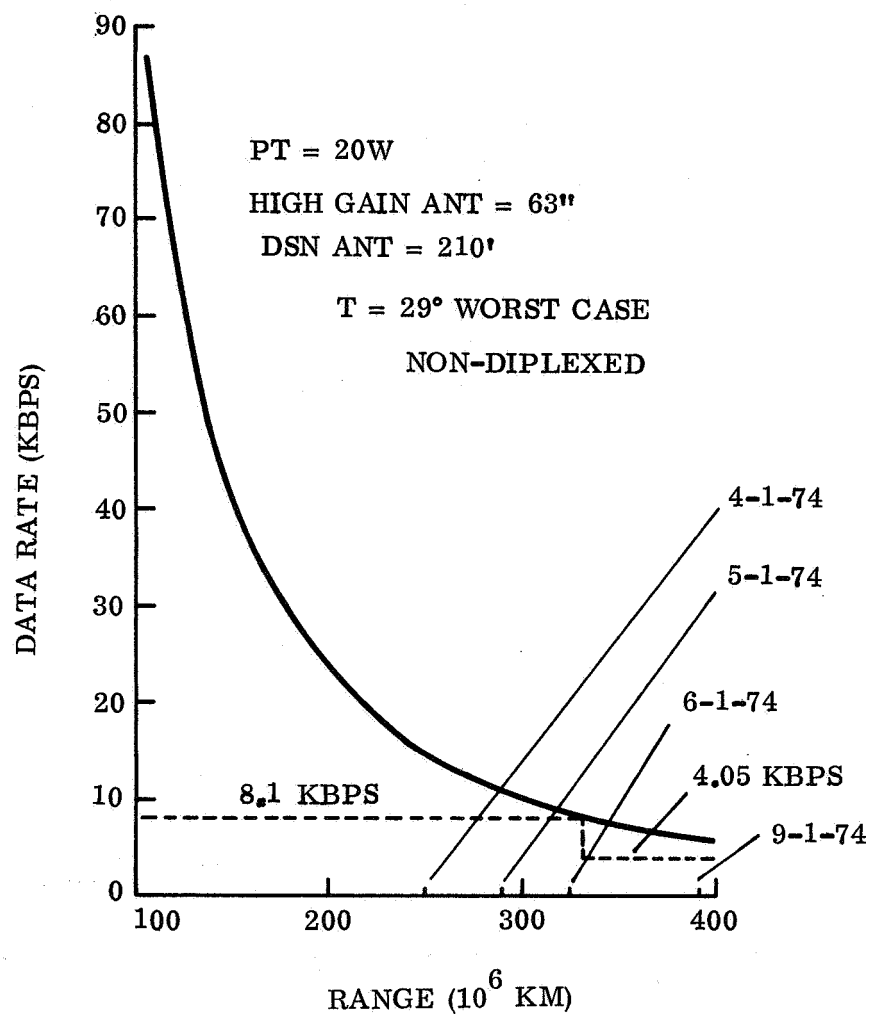


Figure D-38. Worst Case Data Rate Capability (210 ft DSNA)

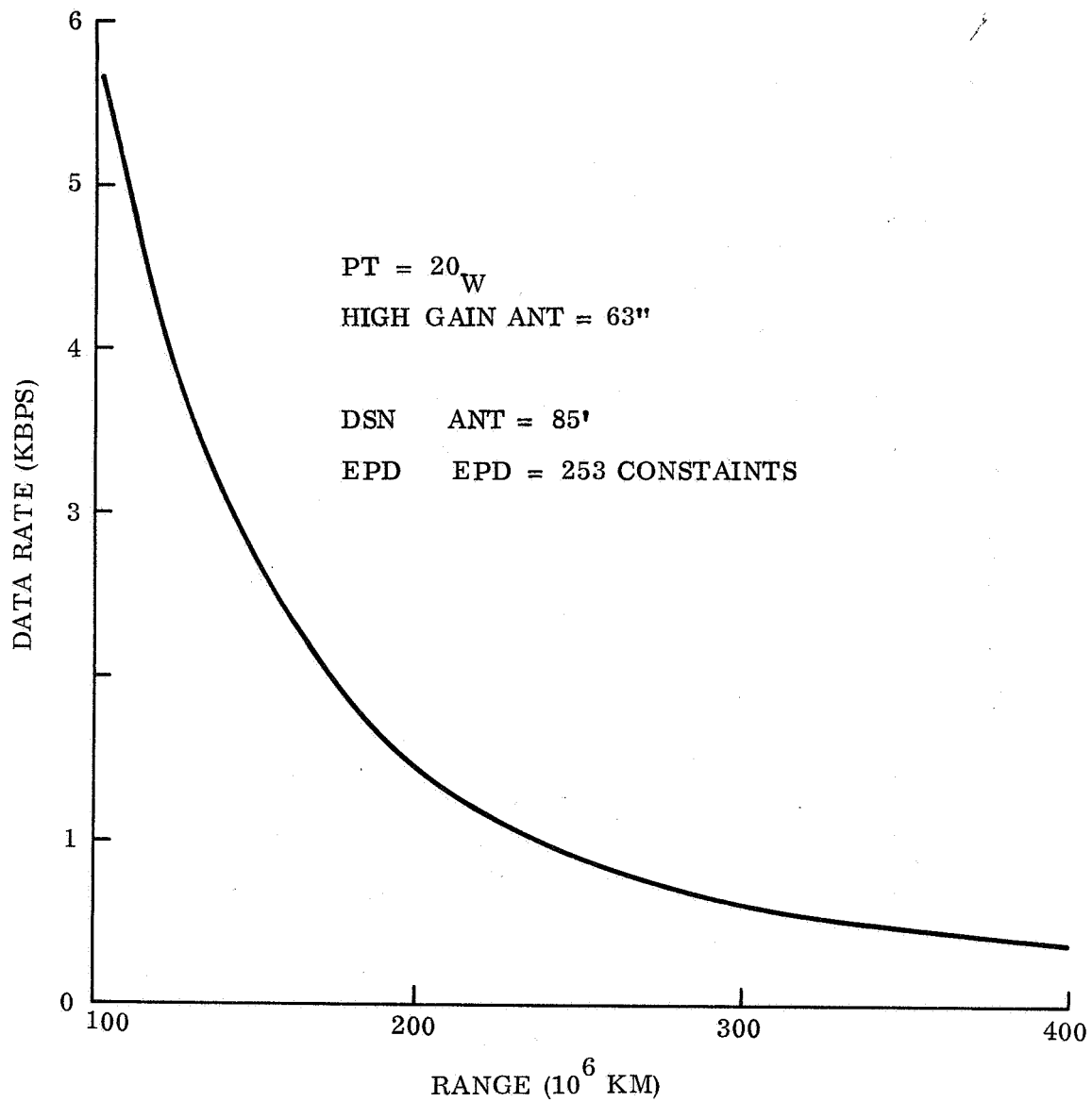


Figure D-39. Worst Case Data Rate Capability (85 ft DSNA)

A block diagram of the DSS and its major interfaces is shown in fig. D-40. Two sets of recorders are provided to yield a greater capacity as well as degraded mode redundancy for storage of the orbiter science data. These recorders are nearly identical to the MM '69 designs. Two additional digital recorders are provided for storage of the Capsule relay data. Each of these recorders can satisfy the relay data requirements, shown in table D-29. If size, and weight limitation prohibit six recorders, one set of the orbital science recorders may be eliminated, or the relay data digital recorders designed to accommodate the orbiter data requirements as well.

Only analog TV data and sync information are stored on the two analog tape recorders (ATR). For normal orbiter operations, a continuous data stream is presented to the ATR's from the TV subsystem by alternating between high and low resolution pictures. Multiplexed digital TV data and non-video science data are stored on the two digital tape recorders (DTR 1). During capsule entry and post impact operation, relayed data is stored on the two relay digital tape recorders (DTR 2).

The analog recorders record data only during the TV collection period at periapsis, each providing 24 minutes of recording capability. The orbital science digital recorders operate in two data collection modes: spacecraft TV data multiplexed with non-video science data and spacecraft non-video science data. The number of record speeds could be reduced to one by providing a buffer for the non-video science data, and reading to the DTR at 16.2 kbps.

The orbital collection profile is shown in fig. D-41 for early mission operation. Although each ATR has a 24-minute recording capability, only 40 minutes of recording can nominally be used because of Goldstone view (playback time) limitation.

The ATR data samples are converted to six bit words and are read out only while in view of the 210 ft antenna at Goldstone in order to read out at a high S/N. The word rate clock from the FTS controls the read out of the ATR to the analog-to-digital converter, so that the ATR data samples are in word synchronization with the FTS code structure. The phase-lock loop controlled servo is used as in MM '69. The digital tape recorders are read out both to the 210 ft and 85 ft receiving antennas.

The readout profile of the tape recorders is shown in fig. D-42 for early mission operation. Due to data rate limitation both sets of orbital science recorders cannot be read out completely on a daily basis. The controller provides control during the record and playback cycles to exchange or delete recorders. The relay data recorders are inserted in the playback sequence when filled or when the data collection period is finished.

D. 5. 4. 2 Modification to MM '71

The proposed subsystem design required changes in the read and playback rates of the proposed MM '71 recorders to accommodate the MM '73 transmission rates. In addition, new recorders must be developed to satisfy the relay data requirements.

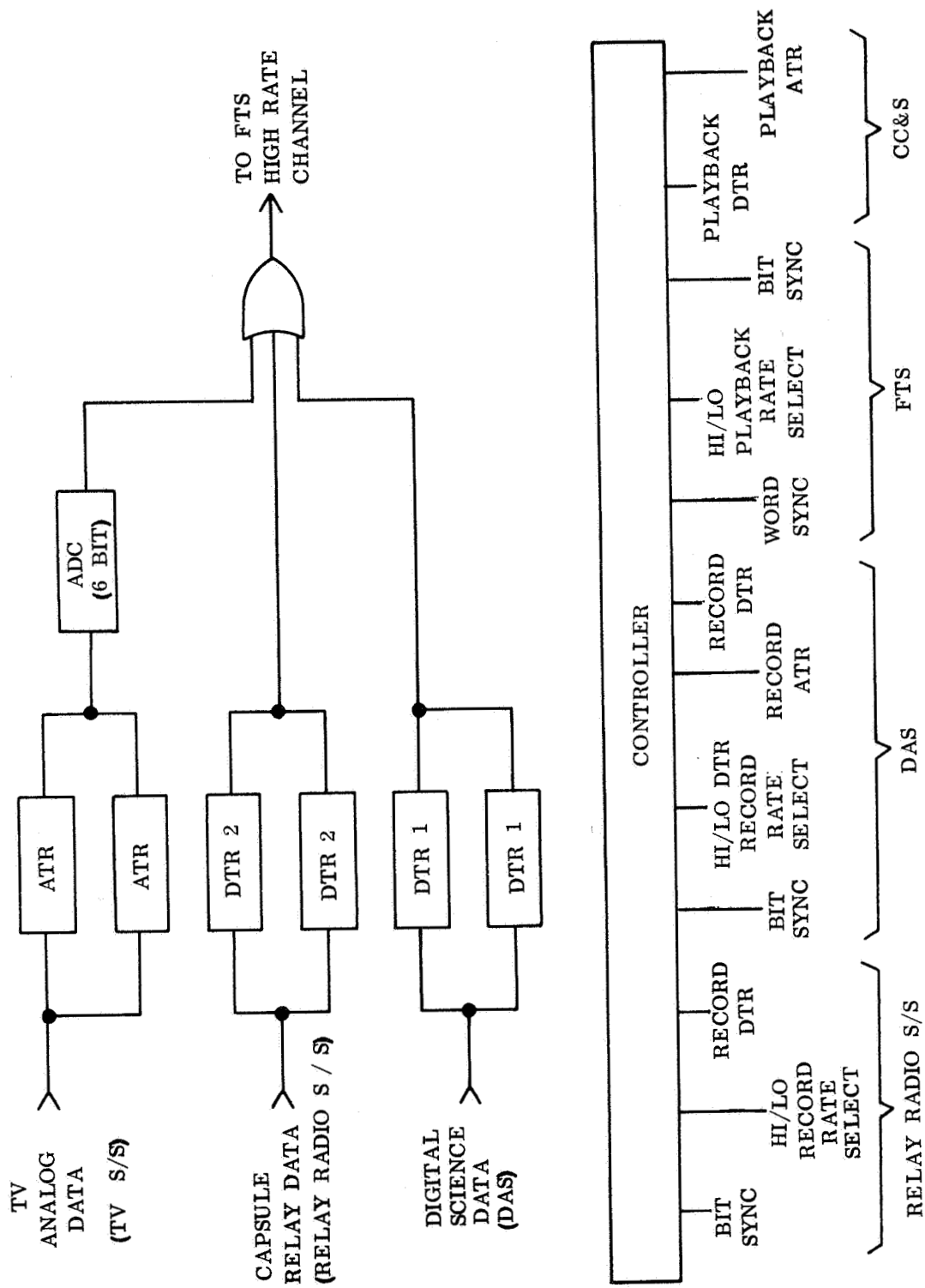


Figure D-40. Mariner Mars '73 Orbiter Data Storage Subsystem

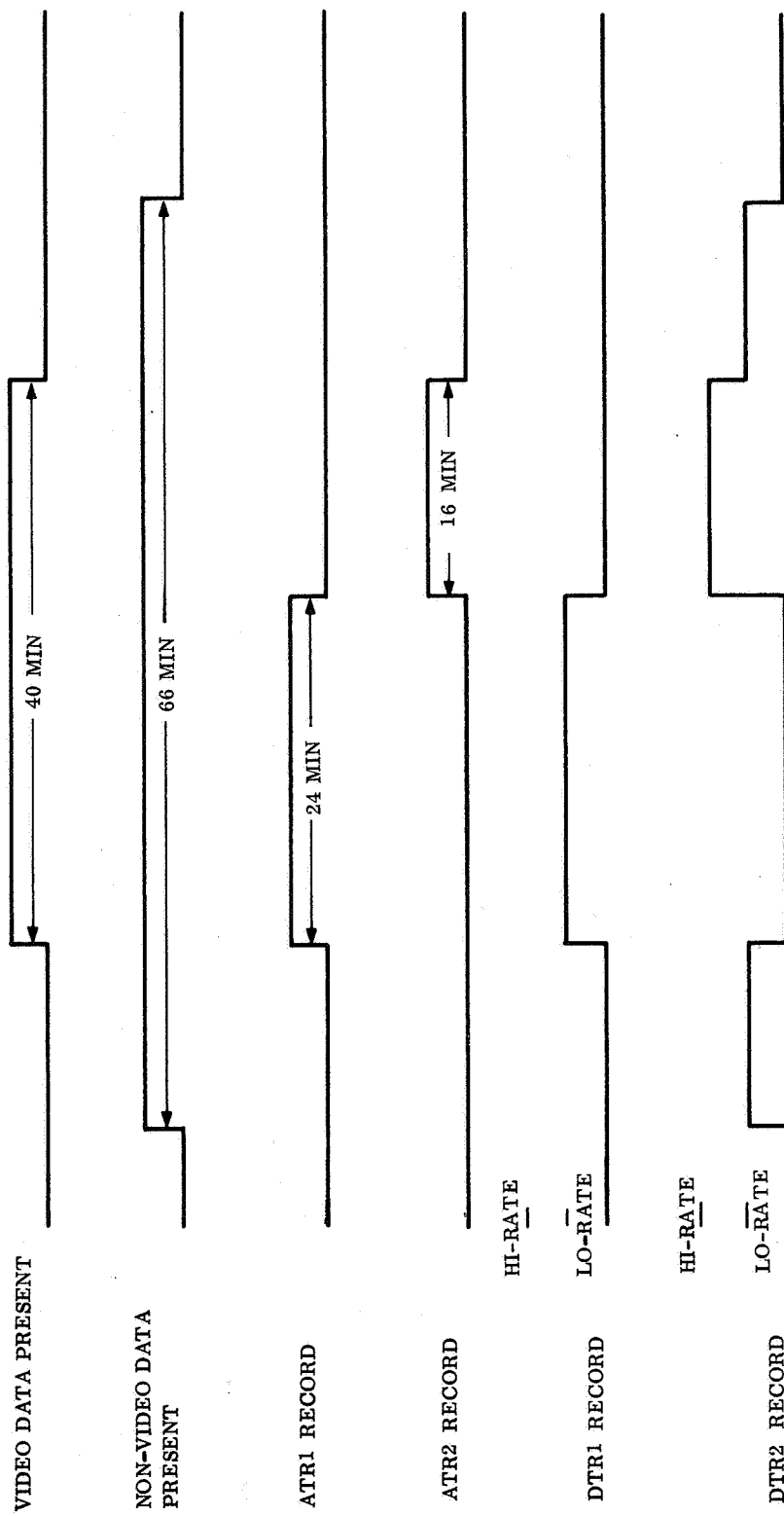


Figure D-41. Tape Recorder Collection Profile During Periapical Passage

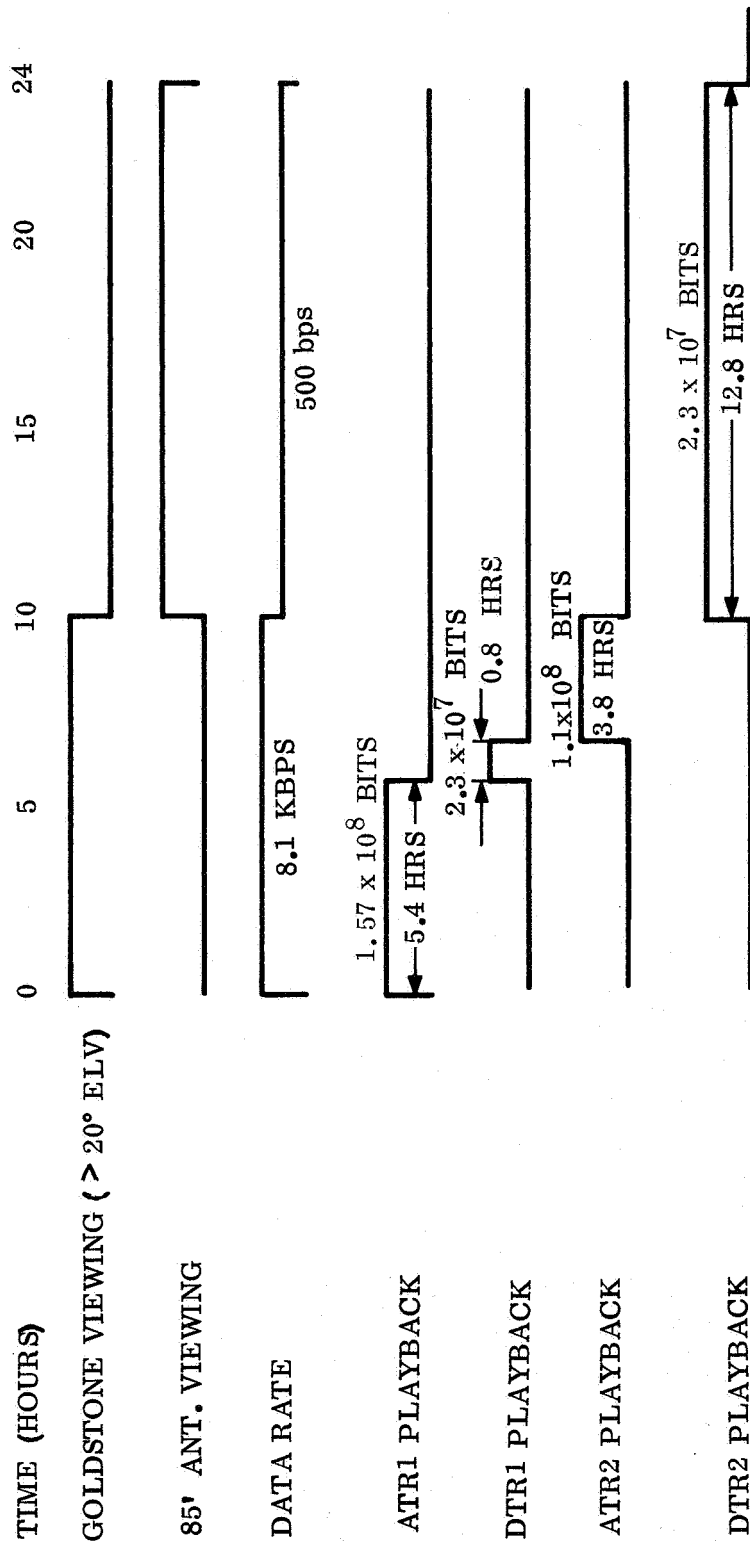


Figure D-42. Tape Recorder Readout Profile

D.5.4.3 Performance Characteristics

Table D-31 lists the performance parameters for the ATR and DTR's.

TABLE D-31. RECORDER CHARACTERISTICS

| | ATR | DTR 1 | DTR 2 (estimates) |
|--|-------------------------------------|---|--|
| Record Format | Direct | PCM Bi-phase Mark | PCM Bi-phase Mark |
| Capacity (bits) | 1.57×10^8 (equivalent) | 2.3×10^7 | 8.4×10^7 |
| Packing Density | 1580 cycles/in. | 1350 bits/in. | 5000 bits/in. |
| Number of Tracks | 4 | 4 | 2 |
| Tape Length (ft) | 360 | 360 | 700 |
| Tape Width (in.) | 1/4 | 1/4 | 1/4 |
| Record Speeds (ips) | 12.0 | 12.0 3.55 | 32.0 0.268 |
| Playback Speeds (ips) | 0.85 (8.1 kbps) 0.43 (4.05 kbps) | 6.0 (8.1 kbps) 3.0 (4.05 kbps) 0.37 (500 bps) 0.18 (250 bps) | 1.62 (8.1 kbps) 0.81 (4.05 kbps) .1 (500 bps) .05 (250 bps) |
| S/N | 32 db | N.A. | N.A. |
| Size | 6.5 in. x 7.5 in. x 8.5 in. | 6.5 in. x 7.5 in. x 8.5 in. | 450 in. ³ |
| Weight (includes control electronics) | 17 lbs | 17 lbs | 15 lbs |

D.5.5 DATA AUTOMATION SUBSYSTEM

Since the design of the Data Automation Subsystem (DAS) is a direct function of the science payload, it is premature to configure the subsystem in detail at this time. Presented is a conceptual design which assumes the same science payload as is expected for the MM '71 mission.

D.5.5.1 Functional Description

The Data Automation Subsystem (DAS) controls and sequences the science instruments, accepts and converts the resulting measurement data, codes and formats the data into frames, provides temporary storage, and routes the data to either the Flight Telemetry Subsystem (FTS) or the Data Storage Subsystem (DSS) for direct or delayed transmission to the earth.

A functional block diagram is presented in fig. D-43 and shows the major interface lines. The real-time non-video science and engineering data, which is multiplexed with orbiter engineering data, is processed by the science engineering data processor and the analog to pulse width converters (A/PW) before being readout to the FTS. The real time format is assumed basically the same as MM '69.

The master oscillator and sequencer provides the timing for the sampling and formatting of the TV and high rate non-video science data.

A/PW counters convert the Infrared Spectrometer (IRS) and Ultraviolet Spectrometer (UVS) data to digital signals. The IRS, UVS data are buffered and inserted into the DSS digital recorded data format, under the control of the digital multiplexer.

Coding is generated for insertion into the TV analog data format during the TV line retrace time by the TV analog PN and ID generator. The analog and digital formats are assumed basically the same as MM '69.

D.5.5.2 Modification to Mariner Mars '71

No attempt has been made to configure the Data Automation Subsystem in detail, since the DAS design is a direct function of the science payload, and payload final selection is premature at this time.

Functionally the proposed DAS is similar to the DAS for MM '69. However, it is expected that as the MM '73 program progresses, significant implementation changes will be required when the orbital science payload is defined in detail.

D.5.6 RELAY SUBSYSTEM

D.5.6.1 Functional Description

The Relay Subsystem performs the following:

1. Receives the r-f signal transmitted to the Orbiter from the Capsule, from separation to impact.
2. Receives the r-f signal transmitted to the Orbiter by the Capsule during the first periapsis passage.
3. Demodulates the received r-f signal and sends it to the Telemetry and Data Storage Subsystem of the Orbiter.

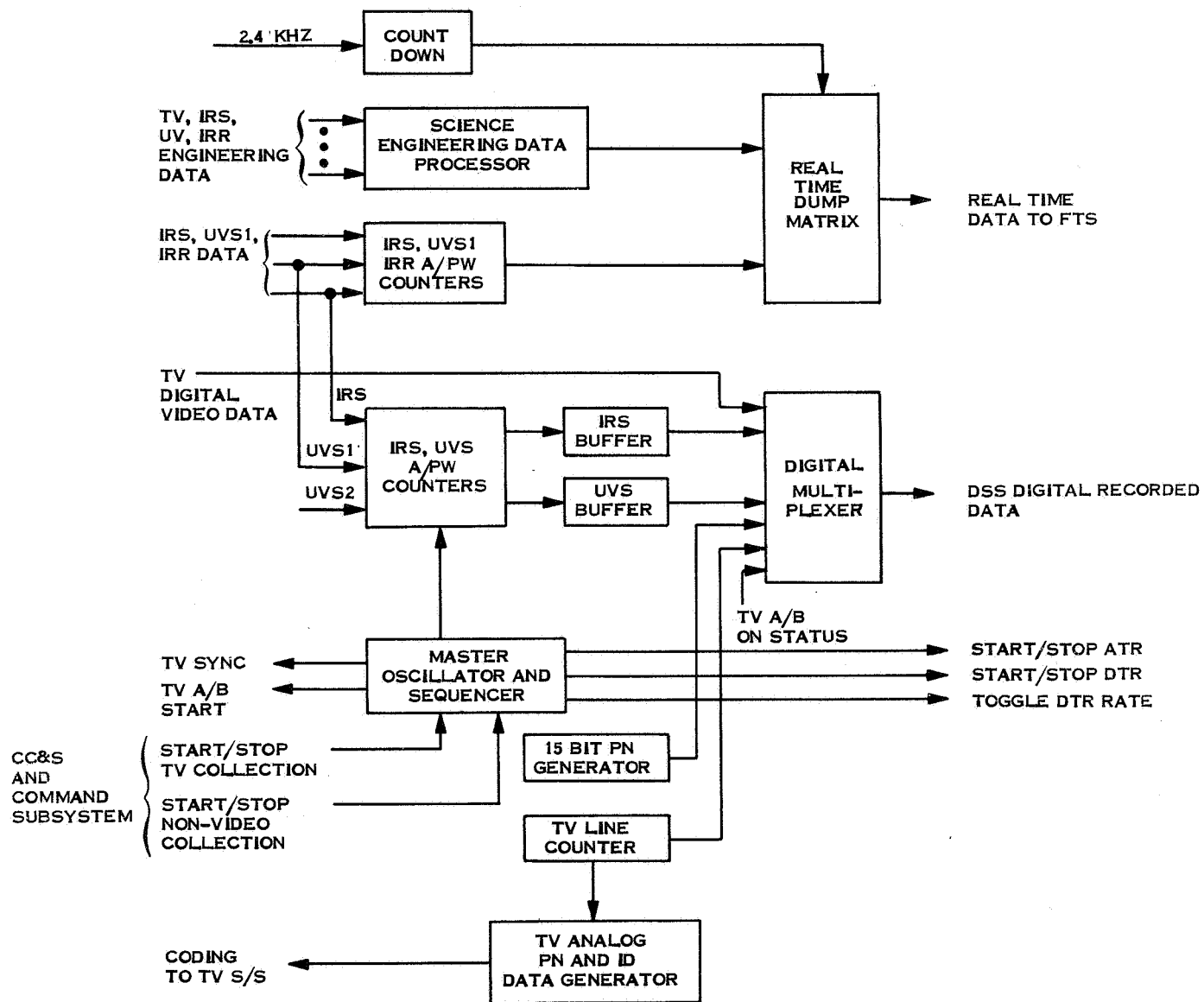


Figure D-43. Data Automation Subsystem

4. Transmits an r-f signal to the Lander to enable initiation of the uplink for a periapsis pass.

D.5.6.2 Subsystem Description

The Relay Subsystem on the Orbiter consists of the necessary antennas to support the r-f link, the receiver required to receive and demodulate the signal, and the beacon transmitter to turn on the Capsule relay transmitter. Figure D-44 is a block diagram of the subsystem. It is utilized during descent to receive a rate of 1340 bps from the Capsule for about one minute out of each hour for both the direct entry case and the out-of-orbit entry case. For the post-impact science transmission, the receiver accepts data at a rate of 160,000 for a period of 8 minutes enabling the accumulation of 7.67×10^7 bits.

D.5.6.3 Receiver

The receiver is a superheterodyned, wideband, FSK device with a 4 dB noise figure. The signal, after r-f amplification, is translated to a wideband (1.86 MHz) i-f amplifier. From this, it is separated into two channels centered 1.2 MHz apart each having a bandwidth of 660 kHz.

The outputs of the two envelope detectors are differenced and the result is combined with $2 f_s$, converting the split-phase signal to NRZ. Bit sync is then used to match filter detect the data.

Two synchronization loops, one for each bit rate, are mechanized as shown in fig. D-45. The input is squared and filtered to generate a frequency component at the data rate frequency, $2 f_s$. A phase lock loop driven by the proper frequency acquires and tracks the phase of the $2 f_s$ signal. Signal presence is determined by a quadrature detector for each loop.

D.5.6.4 Antennas

The antenna gain required for the relay link is 2 dB. This gain can be achieved over an angle of 120° by using a turnstile over a ground plane with a dipole-to-reflector electrical spacing of 130° . Fig. D-46 shows the antenna, and fig. D-47 shows the pattern. The two crossed dipoles are fed by a coaxial split balun transformer. One dipole is slightly longer than a half wavelength, the other slightly shorter to obtain circular polarization on axis. The antenna provides +4 dB gain on its axis and +3 dB at $\pm 60^\circ$, including the polarization loss. The antenna is fed by type RG-142 coaxial transmission line with type N terminals. Prelaunch checkout is enabled by r-f test probes which are connected to the orbiter umbilical by RG-188 coaxial line.

D.5.6.4.1 Location of Relay Antennas

1. Direct Entry. During the capsule descent, the Orbiter is Sun-Canopus stabilized for the first 23 of the 24 hours before impact. At about one hour

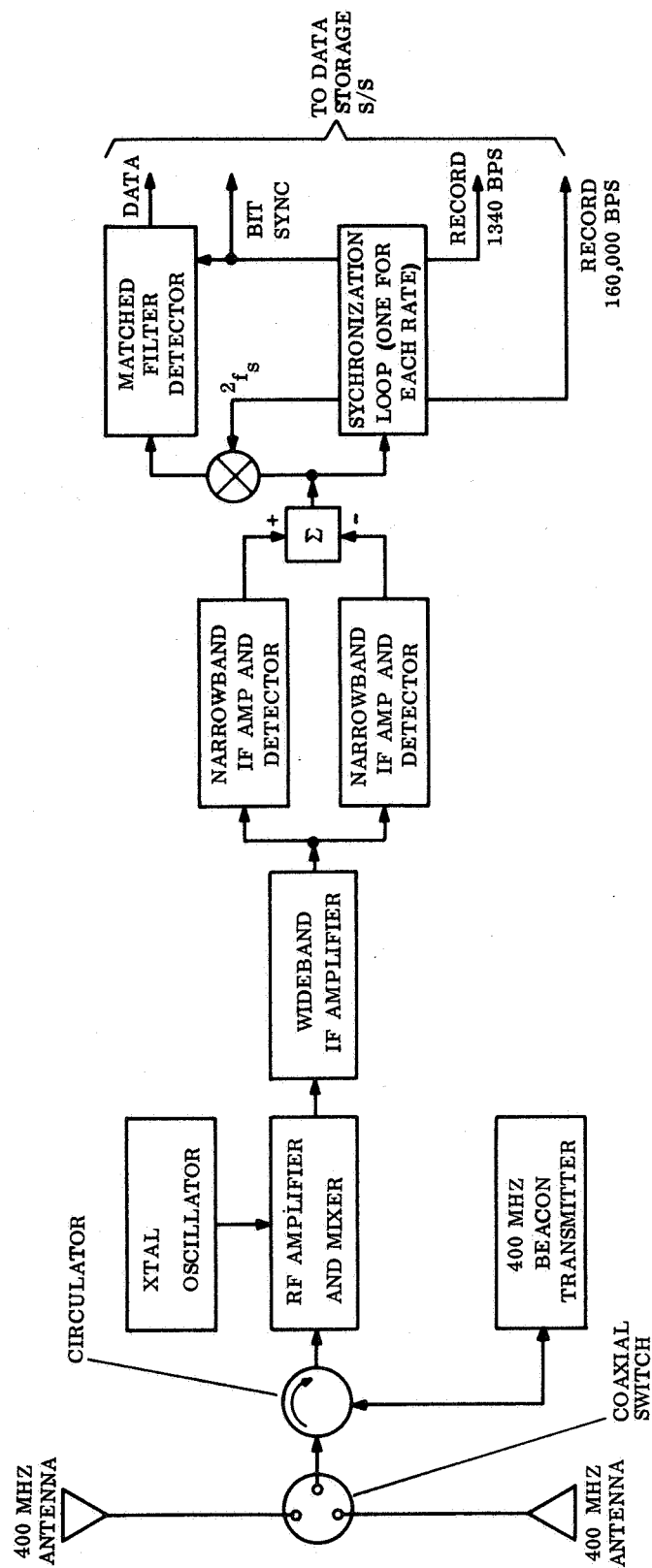


Figure D-44. Relay Subsystem

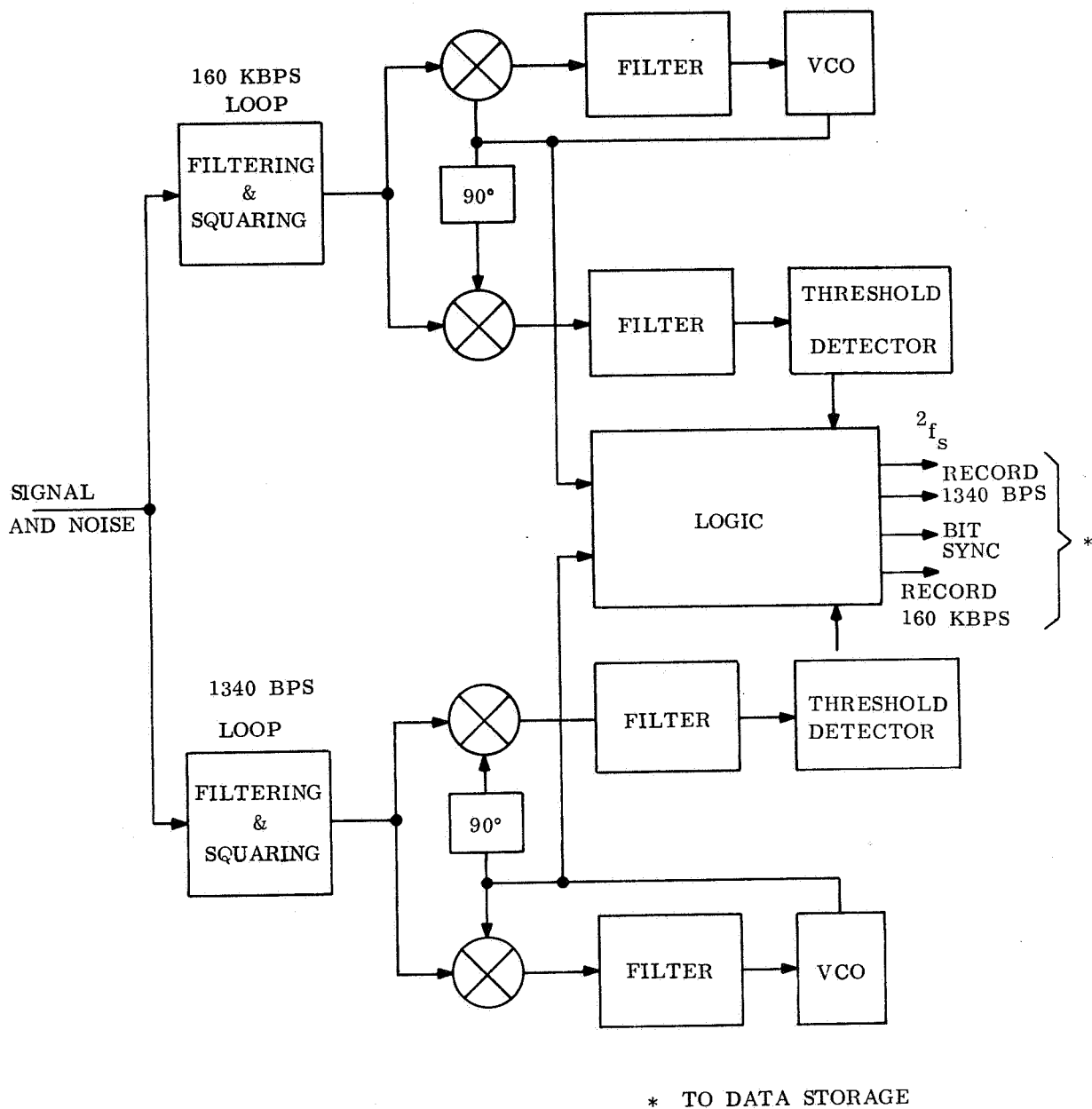


Figure D-45. 160 kbps and 1340 bps Synchronization Loops

before impact, the orbiter assumes insertion attitude, which points the engine nozzle roughly at the Capsule. This attitude is maintained until after the data transmission has been completed.

The required angular coverage for the high rate period of communications is from the $-Z$ axis downward in the YZ plane for a total of 150° . Two antennas are used to provide this coverage. The primary antenna, used throughout the descent and the first part of the periapsis passage, is pointed at a vehicle clock angle of 0° and a vehicle cone angle of 50° . The secondary antenna, utilized during the latter part of the periapsis pass, is pointed at a clock angle of 0° and a cone angle of 135° . Both antennas are mounted so that orbiter appendage reflections are minimized.

2. Orbital Entry. This case provides a more favorable communications geometry. The orbiter stays on the celestial references throughout the communication period. The angular coverage required from entry to 31.5° setting is 141° for the VM-8 atmosphere, the worst case. As for the direct entry system, two turnstiles are used. The primary one is pointed at a vehicle clock angle of 310° and a vehicle cone angle of 135° , the secondary antenna is pointed at a clock angle of 240° and a cone angle of 70° . Again, both antennas are located so that back reflections from orbiter surfaces do not seriously affect the pattern.

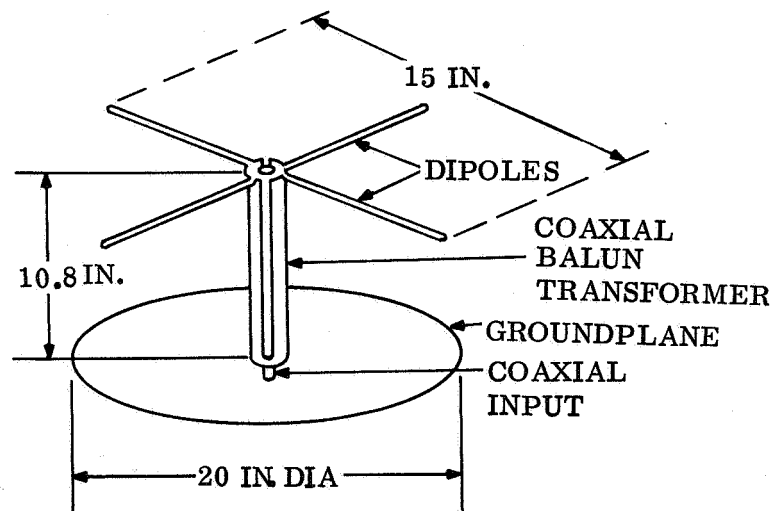


Figure D-46. Relay Antenna (Turnstile Over Ground)

D.5.6.4.2 Alternate Antenna Approach

An alternate approach to obtain the required angular coverage is to use one antenna and alter its position by a gimbaling mechanism.

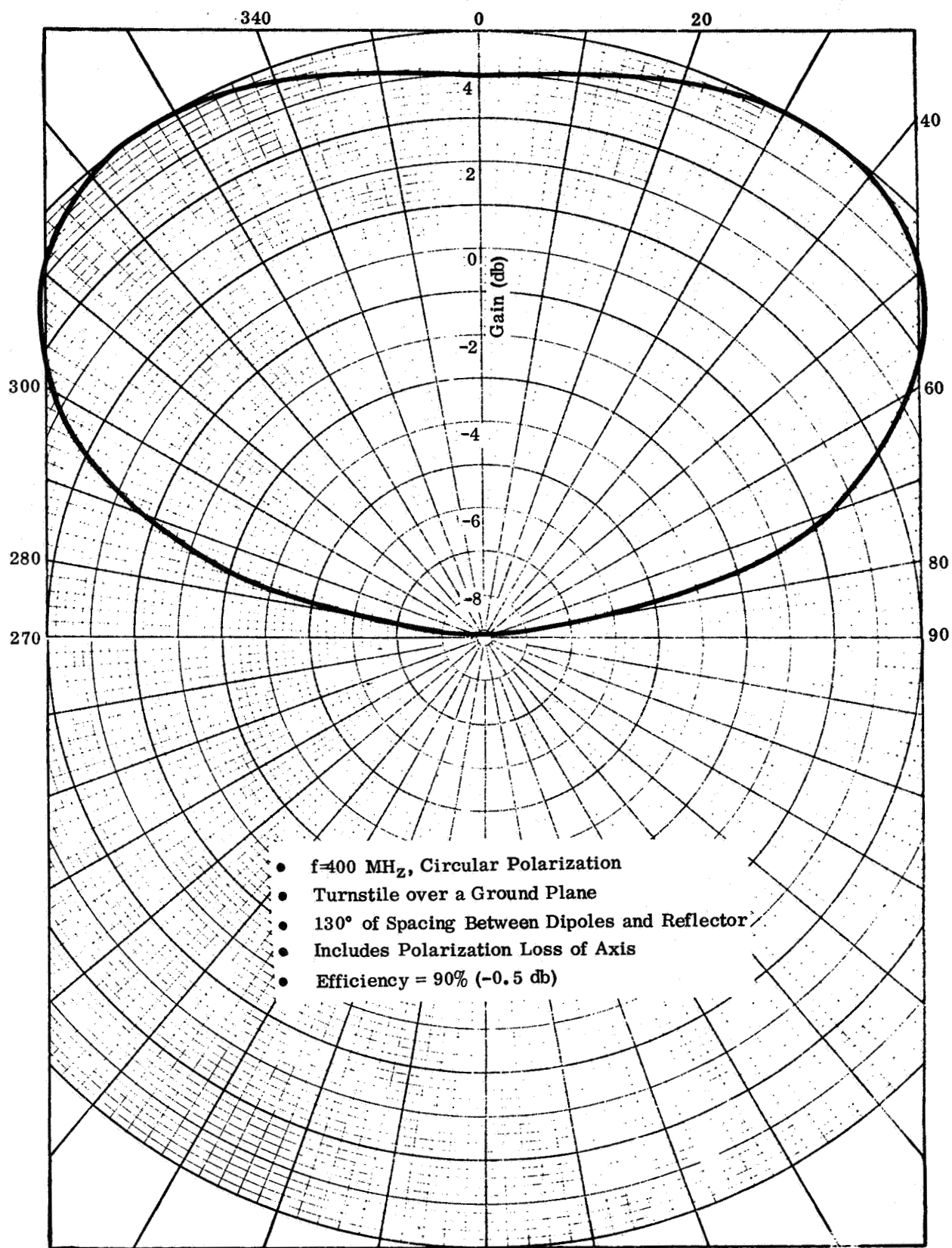


Figure D-47. Relay Antenna Pattern

This method has three basic disadvantages. First, the position change, which must be made after the cruise phase of the mission, has a greater probability of failure, due to exposure to the space environment for such a long time, than does the actuation of a coaxial switch which has been located within a thermally controlled electronics bay. Second, repositioning the antenna occurs during reception of the high rate post-periapsis data. Switching required only milliseconds, whereas moving the antenna with its settling transients requires much more time than this with an attendant effect on the data reception. Third, the gimballed antenna must be placed so that, in each of its two positions, no back reflections from the Orbiter surfaces distort the pattern. This requires a long boom, which adds deployment complexity and tends to offset the apparent weight disadvantage of using two antennas.

D.5.6.5 Coaxial Switch

A single-pole, double-throw switch is used to connect to the desired antenna. The switch is a latching type, weighs six ounces, and has less than 0.2 dB insertion loss, more than 40 dB of isolation, and a VSWR of less than 1.2:1.

D.6 GUIDANCE, CONTROL, AND POWER

D.6.1 POWER SUBSYSTEM

D.6.1.1 Functional Description

The Power Subsystem provides electrical power to operate the Spacecraft electrical equipment. It also provides switching and control functions to manage and distribute that power, and provides timing and synchronizing signals.

The simplified functional block diagram of the Mariner Mars '73 Power Subsystem is shown in fig. D-48. Primary power is generated by the solar array and is used to power the Spacecraft and recharge the battery. Power from the array or battery is supplied to some users directly, and the remainder is conditioned to ac and distributed to the Spacecraft Subsystems.

Raw power from the Orbiter is also used to supply the following functions on the Capsule:

1. Thermal control power.
2. Charging the battery prior to separation.
3. Checkout of experiments prior to separation.

Power is distributed to the loads in the following forms:

1. Unregulated dc, 25 to 50 volts, to the Radio Subsystem, battery chargers, heaters, and to the Propulsion Subsystem and autopilot servos.
2. 2.4 kHz, single-phase, square-wave ac at 50 vrms, +2 to -3 percent to the majority of the Spacecraft loads.
3. 400 Hz, single-phase, square-wave ac at 28 vrms, +5 percent to the scan platform and infrared spectrometer motors.
4. 400 Hz, three-phase, stepped square-wave ac at 27.2 vrms, ±5 percent, to the gyro motors.

The main booster regulates the unregulated dc to 56 dc, ±1 percent for use by the inverters. This regulated dc is not distributed.

Redundancy is provided in both the main boost regulator and the 2.4 kHz inverter. If the boost regulator, the inverter, or the clock (one is incorporated in each 2.4 kHz inverter) should fail, a new boost regulator and inverter are substituted, switched as a pair. On-board failure detection is provided for this function.

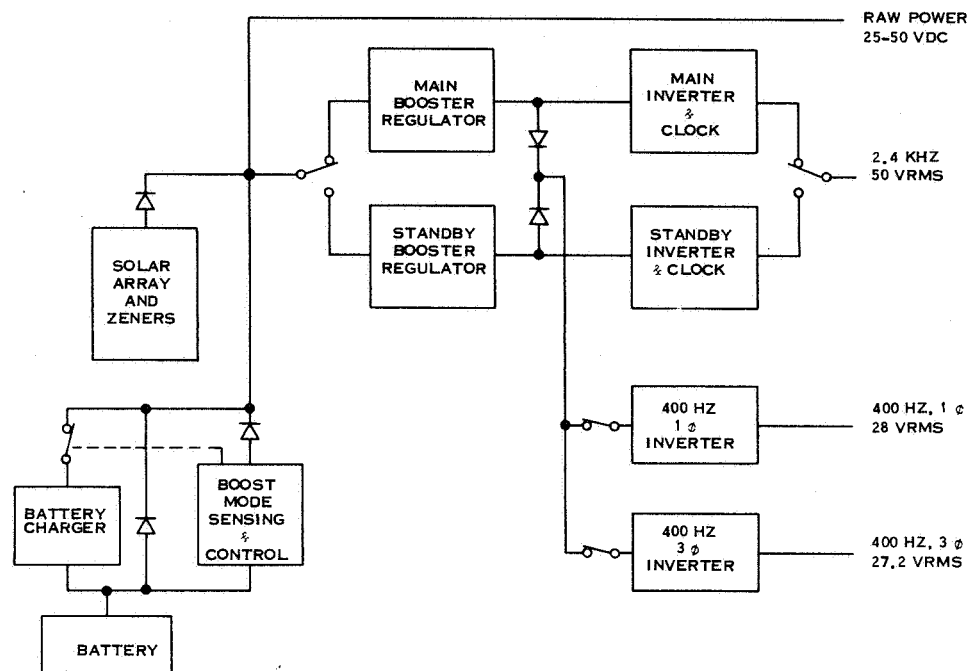


Figure D-48. Power Subsystem Functional Block Diagram

The boost mode sensing and control unit is provided to eliminate undesired array/battery load-sharing. When the Spacecraft is oriented to the sun, as indicated by a sun-gate signal from the Attitude Control Subsystem an unregulated bus voltage of less than 31.5 volts will result in a pulse output from the booster converter sufficient to drive the array/battery voltage higher than the array maximum power output voltage, and force the array out of the load-sharing mode with the battery.

D.6.1.2 Modifications to MM '71

The solar array area must be increased from 93.4 ft² to 115.5 ft² for the out-of-orbit entry case and to 111.0 ft² for the direct entry case. This is necessary to account for higher loads due to the Capsule demands and greater sun-Spacecraft distance at the end of the mission.

Based on the solar cell data of Section D.6.1.3, the MM '73 array will have a unit power output of 4.15 watts/ft² at 1.666 AU. The required array areas have been calculated based on the loads specified in tables D-32 and D-33, for the out-of-orbit and direct entry cases, respectively. In calculating the array area required a 10 percent margin for load growth has been allowed.

TABLE D-32. SPACECRAFT SUBSYSTEM POWER ALLOCATION (OUT-OF-ORBIT ENTRY)

| Electrical Loads | Launch | Sun Acquisition | Cruise I | Cruise II | Maneuver | Orbit Insertion | Orbit Trim | Orbit Cruise | Lander separation Checkout | TV Sequence | Playback |
|--------------------------|--------|-----------------|----------|-----------|----------|-----------------|------------|--------------|----------------------------|-------------|----------|
| 2.4 kHz | | | | | | | | | | | |
| DAS | | | | | | | | | | 20. | |
| TVS | | | | | | | | | | 32. | |
| IRR | | | | | | | | | | 3. | |
| IRS | | | | | | | | | | 4. | |
| UVS | | | | | | | | | | 12. | |
| FTS | 15 | 15 | 15 | 15 | 15 | 15. | 15. | 15. | 15. | 15. | 15. |
| FCS | 3.2 | 3.2 | 3.2 | 3.2 | 3.2 | 3.2 | 3.2 | 3.2 | 3.2 | 3.2 | 3.2 |
| CC&S | 24 | 24 | 24 | 24 | 24 | 24 | 24 | 24 | 24 | 24 | 24 |
| DSS | 54 | | | | | | | 20 | 20 | 27 | 20 |
| A/C1 | 13 | 25 | 4 | 4 | 23 | 23 | 23 | 4 | 4 | 4 | 4 |
| A/C2 | | | | | 10.5 | 10.5 | 10.5 | | | | |
| SCNE | 5.3 | 5.3 | 5.3 | 5.3 | 5.3 | 5.3 | 5.3 | 5.3 | 5.3 | 16.5 | 5.3 |
| RFS | 31.4 | 31.4 | 31.4 | 31.4 | 31.4 | 31.4 | 31.4 | 31.4 | 31.4 | 31.4 | 31.4 |
| GYRE | 8. | 8. | | | 8.0 | 8. | 8. | | | | |
| T/C1 | 54 | 54 | 54 | 54 | 54 | 54 | 54 | 54 | 54 | | 54 |
| PYRO | | 1. | 1. | 1. | 1. | 1. | 1. | 1. | 1. | 1. | 1. |
| PWRD | 2.25 | 2.25 | 2.25 | 2.25 | 2.25 | 2.25 | 2.25 | 2.25 | 2.25 | 2.25 | 2.25 |
| TOTAL | 210.15 | 169.15 | 140.15 | 140.15 | 177.65 | 177.65 | 177.65 | 160.15 | 160.15 | 195.35 | 160.15 |
| 2.4 kHz | | | | | | | | | | | |
| 400 Hz, 10 | | | | | | | | | | 3.5 | |
| IRSM | | | | | | | | | | 12. | |
| SCNM | | | | | | | | | | | |
| 400 Hz, 30 | 9. | 9. | | | 9. | 9. | 9. | | | | |
| GYRO | | | | | | | | | | | |
| 28 VDC | | | | | | | | | | | |
| VALV | | | | | 60. | 60. | 60. | | | | |
| GIMB | | | | | 35. | 35. | 35. | | | | |
| Raw Power | | | | | | | | | | | |
| T/C2 | 9.8 | 26. | 26. | 26. | 26. | 26. | 26. | 26. | 26. | 26. | 26. |
| T/C3 | 3.6 | 10. | 10. | 10. | 10. | 10. | 10. | 10. | 10. | 10. | 10. |
| TWT | 60. | 60. | 60. | 60. | 99. | 99. | 99. | 99. | 99. | 99. | 99. |
| BTCG | 0.5 | 0.5 | | 0.5 | 0.5 | 0.5 | 0.5 | | 0.5 | 0.5 | 0.5 |
| BRFS | 1.5 | 1.5 | 1.5 | 1.5 | 1.5 | 1.5 | 1.5 | 1.5 | 1.5 | 1.5 | 1.5 |
| Additional Raw Power | | | | | | | | | | | |
| Capsule Heater Power | | | | | | | | | | | |
| Capsule Status | | | 18. | 18. | | | | | 12.5 | 12.5 | 12.5 |
| Capsule Battery Charging | | | 5. | 5. | | | | 5. | 75. | 5. | 5. |
| RAW TOTAL | 75.4 | 98.0 | 120.5 | 121. | 137.0 | 137. | 137. | 154. | 224.5 | 154.5 | 154.5 |

TABLE D-33. SPACECRAFT SUBSYSTEM POWER ALLOCATION (DIRECT ENTRY)

| Electrical Loads | Launch | Sun Acquisition | Cruise I | Cruise II | Maneuver | Lander Pre-separation Checkout | Orbit Insertion | Orbit Trim | CC&S Update Orbit Cruise | TV Sequence | Playback |
|--------------------------|--------|-----------------|----------|-----------|----------|--------------------------------|-----------------|------------|--------------------------|-------------|----------|
| 2.4 kHz | | | | | | | | | | | |
| DAS | 15. | 15. | 15. | 15. | 15. | 15. | 15. | 15. | 15. | 20. | 20. |
| TVS | 3.2 | 3.2 | 3.2 | 3.2 | 3.2 | 3.2 | 3.2 | 3.2 | 3.2 | 32. | 32. |
| IRR | 24. | 24. | 24. | 24. | 24. | 24. | 24. | 24. | 24. | 3. | 3. |
| IRS | 54 | 25. | 4. | 4. | 23. | 4. | 23. | 23. | 4. | 4. | 4. |
| UVS | 13 | 25. | 4. | 4. | 23. | 4. | 23. | 23. | 4. | 12. | 12. |
| FTS | 5.3 | 5.3 | 5.3 | 5.3 | 5.3 | 5.3 | 5.3 | 5.3 | 5.3 | 15. | 15. |
| FCS | 31.4 | 31.4 | 31.4 | 31.4 | 31.4 | 31.4 | 31.4 | 31.4 | 31.4 | 3.2 | 3.2 |
| CC&S | 8. | 8. | 31.4 | 31.4 | 8. | 31.4 | 8. | 8. | 31.4 | 24. | 24. |
| DSS | 54 | 54 | 54 | 54 | 54 | 54 | 54 | 54 | 54 | 27. | 27. |
| A/C1 | 2.25 | 1. | 1. | 1. | 1. | 1. | 1. | 1. | 1. | 4. | 4. |
| A/C2 | 2.25 | 2.25 | 2.25 | 2.25 | 2.25 | 2.25 | 2.25 | 2.25 | 2.25 | 4. | 4. |
| SCNE | 5.3 | 5.3 | 5.3 | 5.3 | 5.3 | 5.3 | 5.3 | 5.3 | 5.3 | 16.5 | 16.5 |
| RFS | 31.4 | 31.4 | 31.4 | 31.4 | 31.4 | 31.4 | 31.4 | 31.4 | 31.4 | 31.4 | 31.4 |
| GYRE | 8. | 8. | 8. | 8. | 8. | 8. | 8. | 8. | 8. | 54 | 54 |
| T/C1 | 54 | 54 | 54 | 54 | 54 | 54 | 54 | 54 | 54 | 1. | 1. |
| PYRO | 2.25 | 2.25 | 2.25 | 2.25 | 2.25 | 2.25 | 2.25 | 2.25 | 2.25 | 2.25 | 2.25 |
| PWRD | 2.25 | 2.25 | 2.25 | 2.25 | 2.25 | 2.25 | 2.25 | 2.25 | 2.25 | 2.25 | 2.25 |
| 2.4 kHz TOTAL | 210.15 | 169.15 | 140.15 | 140.15 | 177.65 | 160.15 | 177.65 | 177.65 | 160.15 | 195.35 | 160.15 |
| 400 Hz, 10 | | | | | | | | | | | |
| IRSM | | | | | | | | | | | |
| SCNM | | | | | | | | | | | |
| 400 Hz, 30 | 9. | 9. | | | 9. | | | 9. | | | |
| 28 VDC | | | | | | | | | | | |
| VALV | | | | | 60. | | 60. | 60. | | | |
| GIMB | | | | | 35. | | 35. | 35. | | | |
| Raw Power | 9.8 | 26. | 26. | 26. | 26. | 26. | 26. | 26. | 26. | 26. | 26. |
| T/C2 | 3.6 | 10. | 10. | 10. | 10. | 10. | 10. | 10. | 10. | 10. | 10. |
| T/C3 | 60. | 60. | 60. | 60. | 99. | 99. | 99. | 99. | 99. | 99. | 99. |
| TWT | 0.5 | 0.5 | 0.5 | 0.5 | 0.5 | 0.5 | 0.5 | 0.5 | 0.5 | 0.5 | 0.5 |
| BIOC | 1.5 | 1.5 | 1.5 | 1.5 | 1.5 | 1.5 | 1.5 | 1.5 | 1.5 | 1.5 | 1.5 |
| BRFS | | | | | | | | | | | |
| Additional Raw Power | | | | | | | | | | | |
| Capsule Heater Power | | | 28. | 28. | | 20. | | | | | |
| Capsule Status | | | 5. | 5. | | 75. | | | | | |
| Capsule Battery Charging | | | | 10. | | | | | | | |
| RAW TOTAL | 75.4 | 98.0 | 130.5 | 141.0 | 137.0 | 232. | 137.0 | 137.0 | 136.5 | 137.0 | 137.0 |

D.6.1.3 Subsystem Characteristics

D.6.1.3.1 Solar Cell Performance

Type: Heliotek 8-mil, 2 ohm-cm, N/P cells

Nominal Efficiency: 11 percent at 28°C, A. M. O.

Current Loss Factors:

Radiation: 0.946 (10 mil glass, 9 months)

Uncertainties: 0.900

Voltage Loss Factors:

Radiation: 0.968

JPL Fit Factor: 0.977

Uncertainties include manufacturing losses, measurement uncertainties, UV losses, micrometeoroid erosion, and random cell failures. The fit factor enables the curves obtained by our computer program to fit JPL data derived from measurements made on the MM '69 solar panel at Table Mt., California. No other factors are needed, apparently, to account for filter transmission on other pre-flight losses.

D.6.1.3.2 Performance Characteristics

| Unit | Voltage Output | Rated Power Output (watts) | Rated Energy Capacity (w-hr) |
|--|----------------------|------------------------------------|------------------------------|
| Solar Array - Out-of Orbit - Direct | 50 (max) | 480 at 1.666 AU 461 at 1.666 AU | |
| Ag-Zn Battery | 25-36 | | 1200 New 900 Encounter |
| Boost Regulator | 56, $\pm 1\%$ | 250 | |
| 2.4 kHz Inverter | 50 rms, +2 to -3% | 210 | |
| 400 Hz, Single-Phase Inverter | 28 rms, +5% | 21 | |
| 400 Hz, Three-Phase Inverter | 27.2 rms, $\pm 5\%$ | 21 | |
| Battery Charger | 34.6, ± 0.2 | 1.25 amp (max) | |
| Load Share Booster Converter | 0.5 sec pulse | | |

D.6.1.4 Power Profiles and Allocations

Table D-32 lists the Power Subsystem demands for each mission phase of the out-of-orbit entry case. A similar tabulation for the direct entry case is shown in table D-33. At the bottom of each of these tables the raw power demands for the Capsule are listed. These demands include the heater power required for thermal control, the power required to monitor the status of the Capsule, and the power necessary to charge the Lander battery prior to separation.

Table D-34 lists the abbreviations used for the user subsystem and power conversion equipment.

TABLE D-34. ABBREVIATIONS

| | |
|------------|----------------------------------|
| DAS | Data Automation Subsystem |
| TVS | Television |
| IRR | Infrared Radiometer |
| IRS | Infrared Spectrometer |
| UVS | Ultraviolet Spectrometer |
| FTS | Flight Telemetry Subsystem |
| FCS | Flight Command Subsystem |
| CC&S | Central Computer & Sequencer |
| DSS | Data Storage Subsystem |
| A/C1 | Attitude Control |
| A/C2 | Autopilot |
| SCNE | Scan Control Electronics |
| RFS | Radio Frequency Subsystem |
| GYRE | Gyro electronics |
| T/C1 | Cruise ac heater |
| PYRO | Pyrotechnics |
| PWRD | Power distribution unit |
| IRSM | Infrared Spectrometer motor |
| SCNM | Scan Control motor |
| GYRO | Gyro motor |
| T/C2, T/C3 | DC heaters |
| TWT | TWT amplifier |
| VALV | Solenoid valves |
| GIMB | Thrust vector control gimbals |
| BTCG | Battery charger |
| BRFS | Boost regulator failure detector |

The gross power requirements for the out-of-orbit and direct entry mission are shown in tables D-35 and D-36, respectively. These gross requirements have been reflected to the power source using power conditioning unit efficiencies based on Mariner '69 data. In each of these missions the TV sequence phase has been used to size the solar array. Note that higher power demands do occur earlier in the mission (viz., during Lander preseparation checkout), but these are of short duration and can be accommodated by solar array/battery load sharing, if necessary.

D.6.2 CENTRAL COMPUTER AND SEQUENCER

D.6.2.1 Functional Description

The MM '73 Spacecraft will be capable of a high degree of automatic control. Supplemental control by ground command is included as necessary for some functions, and in others it is provided as a backup alternative to automatic control. The Central Computer and Sequencer (CC&S) described in this section provides the automatic control.

The CC&S is a cycled, special purpose, digital data processor, which generates and distributes the on-board commands necessary for the Spacecraft to perform its mission automatically. Except for certain optional functions described herein, the CC&S obviates the need for ground commands provided that (1) the flight is nominal (all systems are functioning as expected), and (2) trajectory corrections, instrument calibration, and alteration of time dependent or trajectory dependent sequences are not required.

The following mission phases are accommodated by the CC&S as basic requirements:

Attitude Stabilization

Pre-Maneuver

Maneuvers (Maximum of 2 midcourse planned)

Cruise

Orbit Insertion

Orbital Operations (Minimum 90 days planned)

High Gain Antenna Stepping (1 axis)

Orbit Trim

Capsule Checkout

Capsule Separation

The command list which is the basis for this functional description is based upon the Spacecraft Command Structure and Flight Sequence given in Sections D.2.6 and D.2.7. All commands from the CC&S to using subsystems are timed discrete digital states, with the exception of commands to the high gain antenna and scan platform steppers. The latter accept bursts of digital pulses whose count represents a magnitude of change.

**TABLE D-35. NOMINAL FLIGHT PHASES AND GROSS POWER REQUIREMENTS
FOR OUT-OF-ORBIT ENTRY CASE**

| Phase | Duration | Power Requirements | |
|------------------------------------|-----------------------------------|--------------------|-----------------------|
| | | Array (Watts) | Battery (Watt-hrs) |
| 1. Launch | 20.3 min | | 126 |
| 2. Sun Acquisition | 30 min (max) | | 173 |
| 3. Cruise I (Battery Charger On) | | 363 | |
| 4. Cruise II (Battery Charger Off) | | 316 | |
| 5. Maneuver | 64.8 min (1.1 min engine burn) | | 429 |
| 6. Orbit Insertion | 76.7 min (13 min engine burn) | | 529 |
| 7. Orbit Trim | 64.8 min (1.1 min engine burn) | | 429 |
| 8. Orbit Cruise CC&S Update | | 420 | |
| 9. Lander Preseparation Checkout | 30 min | 447 | |
| 10. TV Sequence | | 436 | |
| 11. Playback | | 421 | |

**TABLE D-36. NOMINAL FLIGHT PHASES AND GROSS POWER REQUIREMENTS
FOR DIRECT ENTRY CASE**

| Phase | Duration | Power Requirements | |
|------------------------------------|-----------------------------------|--------------------|-----------------------|
| | | Array (Watts) | Battery (Watt-hrs) |
| 1. Launch | 20.3 min | | 126 |
| 2. Sun Acquisition | 30 min (max) | | 173 |
| 3. Cruise I (Battery Charger On) | | 374 | |
| 4. Cruise II (Battery Charger Off) | | 336 | |
| 5. Maneuver | 64.8 min (1.1 min engine burn) | | 429 |
| 6. Lander Preseparation Checkout | 30 min | 454 | |
| 7. Orbit Insertion | 76.7 min (13 min engine burn) | | 529 |
| 8. Orbit Trim | 64.8 min (1.1 min engine burn) | | 429 |
| 9. TV Sequence | | 419 | |
| 10. Orbit Cruise CC&S Update | | 402 | |
| 11. Playback | | 402 | |

Any normal loading of the CC&S is accomplished using the coded command (CC) formats CC-1 through CC-5 shown in fig. D-49. Ground commands to the CC&S during the mission are accommodated via the Command Subsystem described in Section D.5.2. Sufficient command capacity is included both for normal CC commands to the CC&S, as well as backup of CC&S functions by quantitative (QC) or direct (DC) commands.

All of the MM '73 mission requirements can be fulfilled by the basic MM '71 CC&S hardware. A functional block diagram of the MM '73 CC&S is shown in fig. D-50 within the dashed outline. It is shown to interface with a large number of subsystems. The CC&S is a memory-oriented device consisting of two main portions. The upper portion is called the computer and contains a 128 word magnetic core storage device. The lower portion is called the fixed sequencer portion and is directed to the most critical commands related to maneuvers. Memory is applied in the form of separate pseudonoise (PN) type, shift register counters.

Each of the two portions of the CC&S have output actuators which provide the distribution to using subsystems. The computer has an output matrix to decode user addresses. Each portion can be loaded via OSE or by the Flight Command Subsystem. Each portion also gives indications of state to the Flight Telemetry Subsystem. Clock and power signals of 2.4 kHz are supplied to each portion from the Power Subsystem.

With its processor and memory, the computer portion of the CC&S is the most flexible. A single memory word contains data to enable a discrete command to a coded user on the occasion of the elapse of a pre-established increment of time (Δt). There are 128 such memory locations organized in sequential order of occurrence. Memory addresses normally step one at a time. It is possible for the memory to command itself forward or backward in large jumps to other addresses and return to normal step sequence operation. In this manner, sequences used before can be reused and the actual number of commands possible can exceed 128. Mariner Mars '73 uses this feature extensively for repeated maneuvers and orbital sequences. The MM '73 flight sequence and command list impose the memory capacity usage shown in table D-37.

Repetitious commands are required at 1-hour and 24-hour intervals throughout the mission. These cyclic commands are derived directly by countdown of the clock frequency supplied to the CC&S.

The MM '73 mission requires stepping of one axis of the HGA. Approximately 20 positions are required, each separated by 1.5 degrees. The CC&S will supply a burst of 15 pulses at 1 pps over either of two lines representing (+) increasing or (-) decreasing angle. These are supplied late in the mission with long intervals between need. The processor will gate "start" at a selected time and "stop" 15 seconds later. Two memory locations are required to preload each step. Polarity is by address selection of output line. Note that this method of deriving the train of pulses does not limit the length to 15; in fact, a complete slew is possible if desired as backup.

| | | WORD FORMAT | | | | | | | | | | | | | | | | | | | | | | | | | | | |
|--------------------|------------------------------------|-------------|---|---|---|---|---|---|---|---|----|---------|----------------|----|---------------|----|----|----|----|----|-----------|----|----|----|----|----------------------------|----|----|--|
| COMMAND BIT NUMBER | | 1 | 2 | 3 | 4 | 5 | 6 | 7 | 8 | 9 | 10 | 11 | 12 | 13 | 14 | 15 | 16 | 17 | 18 | 19 | 20 | 21 | 22 | 23 | 24 | 25 | 26 | | |
| CC&S BIT NUMBER | | | | | | | | | | | 1 | 2 | 3 | 4 | 5 | 6 | 7 | 8 | 9 | 10 | 11 | 12 | 13 | 14 | 15 | 16 | 17 | 18 | |
| BIT VALUE | CC-1 COMPUTER LOAD | 1 | 1 | 0 | 0 | 1 | 1 | 1 | 1 | 0 | 1 | 0 | PROGRAM | | | | | | | | | | | | | P A R I T Y | | | |
| | CC-2 COMPUTER LOAD | 1 | 1 | 0 | 0 | 1 | 1 | 1 | 1 | 0 | 1 | PROGRAM | | | | | | | | | | | | | | | | | |
| | CC-3 WORD INTERROGATE | 1 | 1 | 0 | 0 | 1 | 1 | 1 | 1 | 0 | 0 | 1 | MEMORY ADDRESS | | | | | | | | ALL ZEROS | | | | | | | | |
| | CC-4 SEQUENCER LOAD | 1 | 1 | 0 | 0 | 1 | 1 | 1 | 1 | 0 | 0 | 0 | REG. ADDR. | P | TIME DURATION | | | | | | | | | | P | | | | |
| | CC-5 TOLERANCE DETECTOR DISABLE | 1 | 1 | 0 | 0 | 1 | 1 | 1 | 1 | 0 | 1 | 1 | ALL ZEROS | | | | | | | | | | | | | P | 1 | | |

NOTES:

- 1) COMMAND BIT 9 IS SHIFTED TO CC USERS WITH BALANCE OF VARIABLE DATA.
- 2) WHEN PROGRAMMING THE COMPUTER PORTION OF THE CC&S BY GROUND COMMAND:
 - A) CC-1 AND CC-2 MUST BE SENT IN ORDER TO INSERT ONE COMPUTER WORD OF PROGRAM INTO THE CC&S. THE TIME BETWEEN THE START OF CC&S BIT NO.1 OF CC-1 AND THE END OF CC&S BIT NO. 18 OF CC-2 MUST BE LESS THAN FOUR MINUTES, OR THE PROGRAM INFORMATION CONTAINED IN THEM WILL BE REJECTED.
- 3) WHEN PROGRAMMING THE CC&S FIXED SEQUENCER (CC-4):
 - A) CC&S BITS NO.4 AND 5 DESIGNATE THE REGISTER INTO WHICH THE TIME DURATION PORTION (CC&S BITS NO. 7 TO 17) IS TO BE PLACED "01" FOR THE ROLL REGISTER, AND "11" FOR THE MOTOR BURN REGISTER.
 - B) CC&S BIT NO. 18 SPECIFIES POLARITY FOR BURNS; "1" = POSITIVE, "0" =NEGATIVE. FOR MOTOR BURN, CC&S BIT NO. 18 IS "1".
- 4) CC-3 CONTAINS THE ADDRESS OF THE MEMORY WORD TO BE READ OUT IN THE SINGLE WORD READOUT MODE. CC&S BIT 10 CONTAINS THE MOST SIGNIFICANT BIT.
- 5) PARITY BITS ADJUST CC&S BITS 1 THROUGH 18 TO HAVE ODD PARITY.

Figure D-49. Coded Command Work Formats

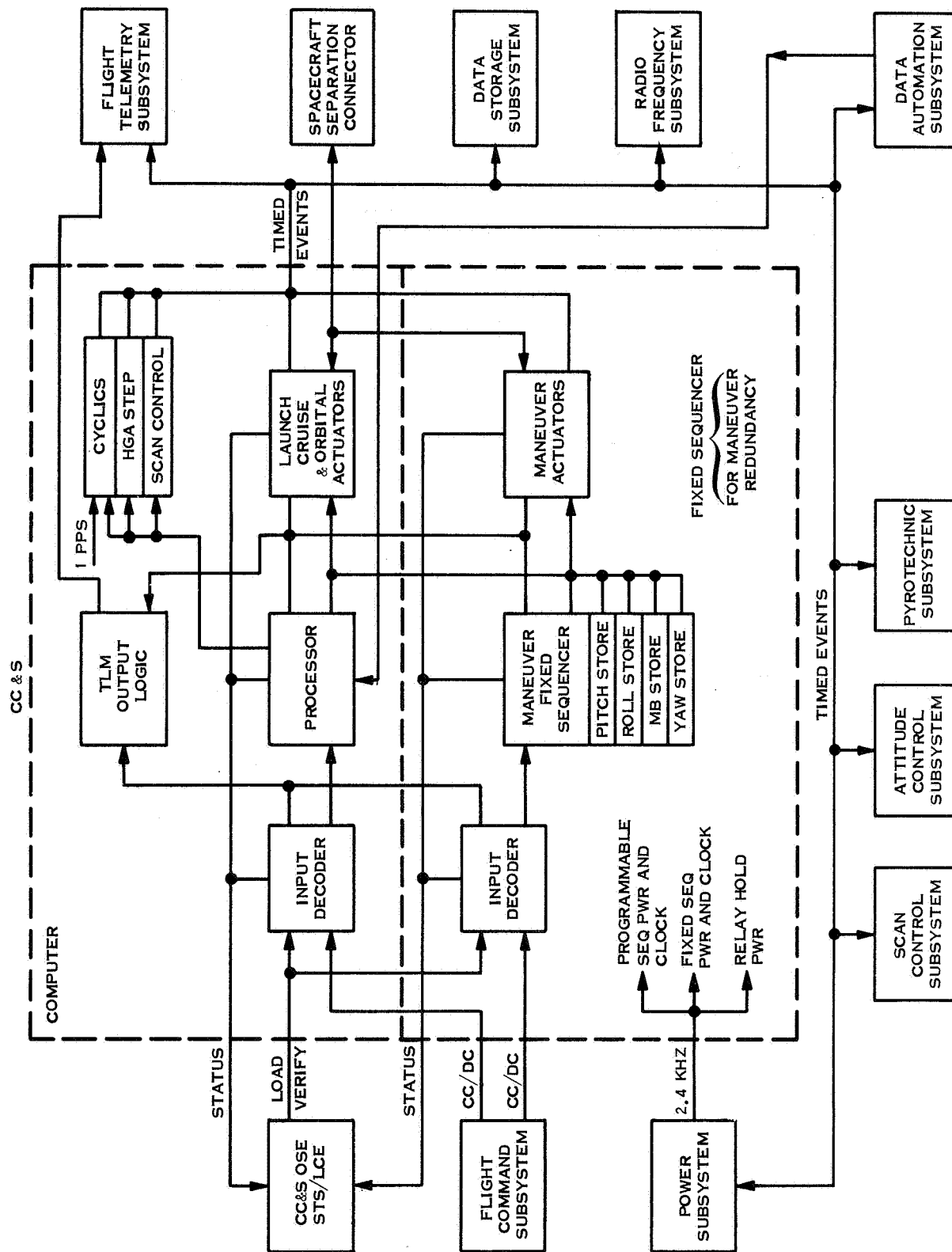


Figure D-50. CC&S Functional Block Diagram - MM '73

TABLE D-37. COMMAND LIST MEMORY CAPACITY USAGE

| Function | Destination | CC&S Command | Mission Usage | Memory Locations Required |
|--|-------------|--------------|----------------|---------------------------|
| A/C on. | A/C | L2 | 1 | 1 |
| Solar panel deploy: unlatches solar panels for deployment | Pyro | L1 | 1 | 1 |
| Deploy high-gain antenna | Pyro | New | 1 | 1 |
| Deploy secondary low-gain antenna | Pyro | New | 1 | 1 |
| DSS power off | Pwr | L3 | 1 | 1 |
| Gyros on: turns gyros on for warm up | A/C | M1 | 10 | 2 |
| All axes inertial places all axes under inertial control | A/C | M2 | 10 | 2 |
| Turn polarity set: sets polarity of roll or pitch turn | A/C | M3 | 30 | 6 |
| Roll turn: executes roll turn | A/C | M5 | 20 | 4 |
| Pitch turn: | | M4 | 10 | 2 |
| Executes pitch turn | A/C | | | |
| Turns capsule power off | Pwr | | | |
| Transmit secondary low-gain antenna: selects secondary low-gain antenna for transmission | RFS | New | 5 | 1 |
| Transmit primary low-gain antenna: selects primary low-gain antenna for transmission | RFS | New | 5 | 1 |
| Propulsion start: opens thrust chamber solenoid valves | Prop | M6 | 4 | 1 |
| Propulsion shutoff: closes thrust chamber solenoid valves | Prop | M7 | 4 | 1 |
| Cruise mode: | | N5 | Once per orbit | 1 |
| DAS, science, and scan orbital power off. Heater power on. | Pwr | | | |

TABLE D-37. COMMAND LIST MEMORY CAPACITY USAGE (Cont)

| Function | Destination | CC&S Command | Mission Usage | Memory Locations Required |
|--|-------------|--------------|---------------|---------------------------|
| During read mode: turns off power to the record motor and places DSS in ready mode. During playback: stops playback in DSS | DSS | | | |
| Turns IRS motor off | IRS | | | |
| Selects cruise data mode | FTS | | | |
| 8 1/3 bps data rate switches the engineering channel data rate to 8 1/3 bps | FTS | C2 | 1 | 1 |
| 33 1/3 bps data rate: switches the engineering channel data rate to 33 1/3 bps | FTS | C5 | 1 | 1 |
| Transmit high-gain antenna: selects high-gain antenna for transmission | RFS | C3 | Indefinite | 1 |
| Platform unlatch: permanently releases latch on scan platform | Pyro | C5 | 1 | 1 |
| Canopus cone angle step: advances cone angle to next position | A/C | C1 | 4 | 4 |
| Capsule power on: provides power to the flight capsule system | Pwr | New | 4 est. | 2 |
| Start capsule checkout | Cap | New | 1 | 1 |
| Separate canister forebody | Pyro | New | 1 | 1 |
| Start separation sequence: | | New | 1 | 1 |
| Start capsule sequencer | Cap | | | |
| Relay radio on | RFS | | | |
| Separate canister afterbody/adapter | Pyro | New | 1 | 1 |
| TV covers deploy | TV | N7 | 1 | 1 |

TABLE D-37. COMMAND LIST MEMORY CAPACITY USAGE (Cont)

| Function | Destination | CC&S Command | Mission Usage | Memory Locations Required |
|---|-------------|--------------|----------------|---------------------------|
| Science phase: | | N1 | Once per orbit | 1 |
| DAS, DSS, science, and scan orbital power on. Heater power off. | Pwr | | | |
| Turns off battery charger | Pwr | | | |
| Places FTS in orbit mode | FTS | | | |
| Starts IRS motor | IRS | | | |
| Places DSS in ready mode | DSS | | | |
| Orbital sequence enable: places DAS in orbit mode | DAS | N6 | Once per orbit | 1 |
| Orbital sequence inhibit: places DAS in standby mode | DAS | New | Once per orbit | 1 |
| Start orbital TV: start collection of orbital TV pictures | DAS | New | Once per orbit | 1 |
| Stop orbital TV: stop collection of orbital TV pictures | DAS | New | Once per orbit | 1 |
| Start orbital non-video data: start collection of orbital non-video data | DAS | New | Once per orbit | 1 |
| Stop orbital non-video data: stop collection of orbital non-video data | DAS | New | Once per orbit | 1 |
| Memory word used by CC&S to generate cone angle positive/negative step commands | --- | --- | 8 per orbit | 8 |

TABLE D-37. COMMAND LIST MEMORY CAPACITY USAGE (Cont)

| Function | Destination | CC&S Command | Mission Usage | Memory Locations Required |
|---|-------------|--------------|-----------------------|---------------------------|
| Memory word used by CC&S to generate clock angle positive/negative step commands | --- | --- | 8 per orbit | 8 |
| Memory word used by CC&S to generate high-gain antenna positive/negative step commands. (Suggestion: load only 30 days worth of steps) | --- | --- | 24 | 24 |
| ATR playback mode: initiates playback of analog recorders | DSS | New | Once per orbit | 1 |
| DTR playback mode initiates playback of digital recorders | DSS | P1 | Once per orbit | 1 |
| Jump commands used by CC&S | --- | --- | 5 plus once per orbit | 2 |
| Spares (20% of memory locations already assigned) | --- | --- | --- | 19 |

The MM '73 scan control is outlined in Section D.6.4. A scan system is employed which requires establishing slopes of straight lines for both clock and cone axes. Outputs to scan control are pulse bursts on either of two polarity lines for each of the two scan axes. These are emitted under TV picture control so that they shift immediately after a picture is taken. The pulses are derived by counting 1 pps pulses for time intervals representing a 1° angular change. There are as many as 42 TV pictures during an orbital pass. Between pictures there may be less than 1° to a maximum of 3° change. Two identical channels are required: one for clock angle, and one for cone angle. Polarity is carried separately by address selection.

The time interval representing a 1° angular change must be altered three times during an orbit for each axis. The pattern is repeatable from orbit to orbit over long periods of time. The time intervals are derived from specific start-stop time commands stored in the processor for each segment representation for each axis. This requires 12 memory addresses for the scan stepping program for an established orbital pattern: six for cone and six for clock angle. A counter register is employed for each set of six commands. The first two represent the first segment, and 1 pps counts are accumulated during the start-stop gate. The count is stored and used as a reference reset for the rest of that segment. The cycle is repeated using the next start-stop command gate, and the next, for a total of 3 segments. The next orbit is a repetition.

To return the scan platform to its initial position for the next orbit, it is required to slew both cone and clock angles by as much as 160° at a 1 deg/sec rate. The output is a 1 pps train of + and - polarity over the same lines as the scan incrementer. These are derived by programmer start-stop timed gates with polarity selection by address. The gates are part of every orbital sequence. The time selection of the gate, hence slew length, is readily reprogrammable.

D.6.2.2. Modifications to MM '71

Evaluation of MM '69 information and our estimates of MM '71 and '73 requirements indicate that the MM '73 functional requirements can be met by the MM '71 scan control without modification.

D.6.2.3 Performance Characteristics

Some of the principle performance parameters are as follows:

| | |
|-------------------|---|
| Memory Capacity: | 128 words of 22 bits each |
| Basic Clock Rate: | 1 pulse per second |
| Input Form: | MM '69 Coded Commands; 26 bit block including 9 bit address |

Output Command Timing Resolution:

| | |
|-----------------------------------|----------|
| Programmer: | 1 sec |
| Attitude Control Fixed Sequencer: | 1 sec |
| Motor Burn Fixed Sequencer: | 1/20 sec |
| HGA Stepping: | 0.1 deg |
| Scan Control: | 1.0 deg |

CC&S Timing Reference Accuracy: from Power Subsystem ± 0.01 percent.

D.6.3 ALTITUDE CONTROL SUBSYSTEM

D.6.3.1 Functional Description

The Attitude Control Subsystem (A/C) acquires and stabilizes the Spacecraft to the Sun and the Star Canopus. It then maintains the Spacecraft attitude relative to these references during the heliocentric cruise and Mars orbital phases. Upon receipt of commands from the Central Computer and Sequencer (CC&S), the A/C maneuvers the Spacecraft by sequential rotations about its axes to any arbitrary spatial attitude to perform velocity change for trajectory correction, orbit insertion, or orbit trim. During engine firing, the A/C changes the thrust vector direction by orienting a gimballed engine to maintain vehicle attitude and stability. At a signal from the CC&S at the end of the maneuver sequence, the A/C reacquires the Sun and Canopus.

During launch ascent, all parts of the A/C are unpowered except the gyros. Following separation from the launch vehicle, power is applied to the rest of the A/C. Sun sensors are used in pitch and yaw and rate signals are provided by the gyros; the Canopus sensor output is not used. The initial rates are reduced to a low value and the A/C operates to acquire the Sun. Then, a Sun gate operates to enable the Canopus sensor and to roll the vehicle about the sunline until the sensor acquires and locks on to the Star Canopus. The system discriminates against stars other than Canopus by brightness gate settings in the Canopus sensor acquisition logic. At the completion of Sun and Canopus acquisition, the gyros are turned off. The system switches to the cruise mode, in which the Sun sensors control pitch and yaw attitude and the Canopus sensor controls roll during the heliocentric cruise period. The gyros are off and control loop damping is obtained by derived rate. The A/C is capable of automatic reacquisition of Sun and Canopus references if either is lost.

When a velocity correction maneuver is commanded, the optical sensor outputs are not used. The gyros, operating in their position mode, establish an inertial reference. The gyros are torqued in sequence to produce a constant Spacecraft turning rate about the desired axis. The time the gyros are torqued is controlled to yield the desired rotation. The attitude is then controlled by the position signals from the three single-axis gyros. At the completion of the command turn sequence, the Propulsion Subsystem is initiated to supply the velocity correction. The autopilot maintains the inertial attitude of the Spacecraft by orienting a gimballed engine to control the thrust vector direction. The gyros generate position error signals, which are processed by the autopilot electronics, to drive the two engine gimbal actuators. Upon completion of the velocity correction, the CC&S commands the A/C to reacquire the Sun and Canopus and return to cruise mode.

During Capsule separation and deorbit, no action is required of the orbiter A/C system, other than maintenance of its normal Sun/Canopus orientation.

During the orbital phase of the mission, the Sun and Canopus sensors with the derived rate networks maintain attitude control. At times, the Sun or Canopus may be occulted by Mars. Since this event is accurately predictable in time, the A/C can be commanded to an inertial hold mode which used the gyro inertial reference to provide position error signals to the A/C until the occultation period is over.

D.6.3.2 Modifications for MM '73

The MM '73 orbiter is essentially a modification of the proposed Mariner '71 which in turn was a modification of the Mariner '69. For each mission, changes have been kept to a minimum, consistent with mission requirements.

The MM '69 A/C system consists of six independent assemblies:

1. Sun Sensor System
 - 4 assemblies making up the secondary Sun sensor
 - 2 assemblies making up the primary Sun sensor
 - Sun gate
2. Canopus Sensor
3. Gyro Control Subassembly
 - 3 rate integrating gyros
 - electronics
 - integrating capacitors
4. A/C Electronics
 - attitude control electronics
 - autopilot electronics
 - power supply
 - control system logic
5. Jet Vane Assembly
6. Gas Jet Assembly (Reaction Control System)

To minimize costs, changes to the MM '69 A/C equipment for both the MM '71 and the '73 missions should be made only where absolutely necessary. The functions and methods of execution are nearly identical for the three missions, and negligible changes are expected to be required. The Sun sensors and the gyro control assembly can be used without change, except for possible relocation of the Sun sensors in MM '73. The Canopus sensor is unchanged except for a possible design of the stray light baffle. Some changes are required in the attitude control electronics, especially in the autopilot section, due to changes in Spacecraft dynamics for all three missions and the use

of a gimballed engine instead of the jet vanes used on MM '69. Sizing changes of the reaction control assembly to accommodate the increased gas required are significant for the MM '73 mission. Subsystem configuration changes are expected to be minor.

D.6.3.2.1 Sun Sensors

The same Sun sensors can be used in all three missions. For the MM '73 mission, the four assemblies of the secondary Sun sensor will have to be relocated since the Capsule will be in their fields of view. Relocation to the solar panels paddles to provide necessary field of view is expected to be a minor change.

D.6.3.2.2 Canopus Sensor

The JPL Canopus sensor, which performed the 1964 Mars mission adequately, has undergone significant redesign for the 1969 mission to improve its performance. Most of the effort has been to reduce the effect of stray light and false objects. Automatic operation has been increased, and roll angle control range has been doubled to permit higher search rates.

The stray light baffle, which is attached to the sensor in front of the lens, provides unwanted light rejection due to reflections from surfaces of the Spacecraft and from the surface of Mars. The '71 and '73 Spacecrafts, which are each of a different configuration and size, will probably require redesigns of the light shield to reject Spacecraft reflected light. The design of a common baffle to be used on the MM '71 and MM '73 missions may be possible, but redesign for each mission is more likely due to the addition of the Capsule in MM '73. Reflection from Mars is less critical in that it occurs only for small periods of time. By judicious selection of the orbit, it is possible to minimize the problem. Moreover, the Canopus sensor can be locked out during this period and control maintained by gyro reference.

D.6.3.2.3 Attitude Control Electronics

Changes to the attitude control electronics will occur only in the autopilot section. The power supply and control logic are expected to be unchanged, or at most to undergo minor changes. Most of the changes will have been incorporated in the MM '71, but some electronics changes will be required for MM '73. The function of the autopilot is the same for the three missions, i. e., stabilization of the Spacecraft during engine thrusting. However, the electronic gains, compensation, and output stage design of this subsystem are dependent upon the geometric and dynamic characteristics of the Spacecraft, as well as the engine employed. These are all significantly different in the MM '71 and MM '73 missions and will require redesign of the '69 autopilot. Mathematically, or electrically these changes may be significant. Physically, the change is not expected to be significant, so that volume and weight should remain essentially unchanged. In particular, for the two later missions, the dynamic characteristics are more severe to the design of the autopilot in that a large liquid fuel mass is present which will slosh and may couple into the control system. For the MM '73 mission, the addition of a large capsule further complicates the dynamic characteristics of the Spacecraft. From early cruise mode operation to orbit operation without the capsule, the

Spacecraft moments of inertia for each axis change by factors as high as 8 to 1. There are Spacecraft center of mass (CM) shifts as fuel is expended and the Capsule is separated. The ranges of inertia changes and CM shifts are comparable whether direct or out-of-orbit entry is used. Design of the MM '71 autopilot with the probable MM '73 requirements in mind can minimize the changes if module packaging is such that gain and compensation selecting components are segregated to a minimum number of modules, or even made external to the modules.

The use of a gimballed engine rather than jet vanes of the MM '69 spacecraft produces further changes. MM '69 employs a monopropellant rocket motor for velocity changes. Thrust vectoring is achieved by inserting four jet vanes in the exhaust. Positioning the vanes either in pairs, or differentially, applies torques to the vehicle to yield pitch, yaw and roll control. Each vane is positioned by a torque motor which in turn is controlled by its respective amplifier. The MM '69 engine is not aligned with vehicle axes, and since three-axis vehicle control is obtained from a single engine, the sensor signals are resolved by means of electrical networks to yield the correct signal for each vane.

Mariner Mars '71 and '73 will employ a bipropellant rocket engine which, by virtue of high exhaust gas temperature, precludes the use of jet vanes. The entire engine is gimballed in two axes. Roll control is achieved with the cruise attitude control system using cold gas jets. If additional roll torque is required (considered unlikely), the thrusters may be increased in size, but this will not require electronic changes other than perhaps addition to the logic. A two-axis gimballed engine requires only two drive amplifiers, instead of four drive amplifiers required for the vanes.

D.6.3.2.4 Jet Vane Assembly

As stated in the previous section, jet vanes in the exhaust stream are no longer possible because of the high exhaust temperature of the bipropellant engine. Instead, the entire engine is gimballed for both MM '71 and MM '73. There should be little or no change required from the MM '71 to the MM '73 Spacecraft.

D.6.3.2.5 Gas Jet Assembly (Reaction Control System)

Nitrogen gas is stored at high pressure in tanks. The pressure is reduced through a pressure regulator and distributed to four locations on the Spacecraft. At these four locations, the gas is manifolded further and expanded through a nozzle to generate a thrust, and hence, a torque in the appropriate direction. Gas flow is controlled by solenoid valves which are operated by the respective attitude control channel.

Functionally, the gas jet systems for the three missions are identical. Physically, they are very similar. The larger size and longer time duration of the later missions requires more stored gas, and hence, larger tanks. The new Spacecraft configuration requires new tubing runs and new nozzle designs, but these changes are relatively minor. Active components, such as regulators and solenoid valves, as well as fill valves and filters, will remain unchanged.

D.6.3.3 Subsystem Alternatives

D.6.3.3.1 Velocity Control

The subsystem described involves minimum changes to the MM '69 A/C. An alternate mechanization in the area of velocity increment control has been considered and is summarized here.

Guidance maneuvers (i.e., changing Spacecraft velocity), are executed by thrusting the propulsion system until the desired velocity change has been achieved. The intelligence to terminate thrusting can be derived from two sources:

1. Knowing the mass properties of the Spacecraft and the rocket engine characteristics, it is possible to calculate the necessary thrusting time. A timer, in the CC&S, can then be used to control the engine on-time. This method is employed in MM '69.
2. An integrating accelerometer may be employed to measure the Spacecraft acceleration and calculate the actual velocity change. When the desired amount has been achieved, the engine is shut off. This method was proposed in our Voyager studies.

The timed system is the simpler of the two, both from the standpoint that the equipment used is somewhat simpler, and that it is carried for other purposes anyway. Timing is less accurate than the accelerometer system because it requires the knowledge of vehicle mass, fuel flow rate, and rocket thrust level which are not known very precisely. An error in ΔV of 1 percent would be the best expected, and 1-1/2 percent to 2 percent is more realistic. The MM '69 requires that the error in ΔV not exceed 3 percent with a design goal of 0.45 percent. Previous Mariner missions, which are flybys and generally require only one trajectory correction, operate successfully with such accuracies. In contrast, the accelerometer system is expected to control the velocity to less than 0.1 percent.

Whether the added accuracy of an integrating accelerometer is required for the MM '71 and MM '73 missions must be answered by a study of the several trajectory maneuvers with respect to mission requirements. With an accelerometer, the ΔV magnitude errors are negligible in relation to the pointing errors. If the timing system is used, this is no longer the case, since ΔV error can be about 2 percent, although an acceptable mission probably can be performed.

The penalty of incorporating an integrating accelerometer is not very great. It weighs a few ounces, its maximum dimension is two or three inches, and the power consumption is probably less than a watt. Available units were surveyed previously for Voyager studies, and several satisfactory accelerometers were found (e.g., Bell VIIB, Honeywell GG177, etc.). More significant is the method of incorporating it into the system, which will affect connectors and harness, as well as interfaces with the CC&S and Propulsion Subsystems. The cost of resolving these are not easily defined but are suspected to be significant.

D.6.3.3.2 Approach Guidance

For the direct entry Spacecraft, approach guidance may be included in the MM '73 Orbiter. The need for such an on-board system depends upon the DSIF orbit determination capability and entry corridor accuracy requirements. If approach guidance is needed, the MM '69 subsystem is satisfactory and is described below.

The MM '69 Approach Guidance Subsystem (A/G) optically tracks and takes angular measurements from the center of Mars to the Spacecraft during the time period from 10 days to 11 hours before encounter. These measurements are transmitted to Earth to provide information for an orbit determination program which computes the near Mars Spacecraft trajectory. The MM '69 subsystem can be used with little or no changes.

A block diagram of the subsystem is shown in fig. D-51. The subsystem consists of four major subassemblies.

1. Planet Center Finder

The planet center finder electronically scans the image of Mars which is focused upon the image dissector face and processes the resulting signal output to obtain the cone angle error signal, the cross-cone angle error signal and the scan radius error signal.

2. Cone and Cross-Cone Servo Assemblies

The cone and cross-cone servos use the cone and cross-cone angle error signals to control the drive motors associated with the cone and cross-cone gimbals so as to position the image of Mars at the null of the planet center finder. The cone and cross-cone gimbals optically deflect the light arriving from Mars and thereby cause the image of Mars to be positioned in response to the cone and cross-cone servos. The cone and cross-cone encoders generate digital outputs which indicate the angular positions of the cone and cross-cone gimbals.

3. Data Converter

The data converter stores the parallel digital outputs of the cone and cross-cone encoders and converts them into a serial format that is compatible with the telemetry data encoder.

4. Auxiliary Sun Sensors

The auxiliary Sun sensors produce outputs indicating the position of the Spacecraft in the limit cycle without being subject to thermal and other drifts of the Spacecraft bus structure that degrade this information as received from the attitude control Sun sensors.

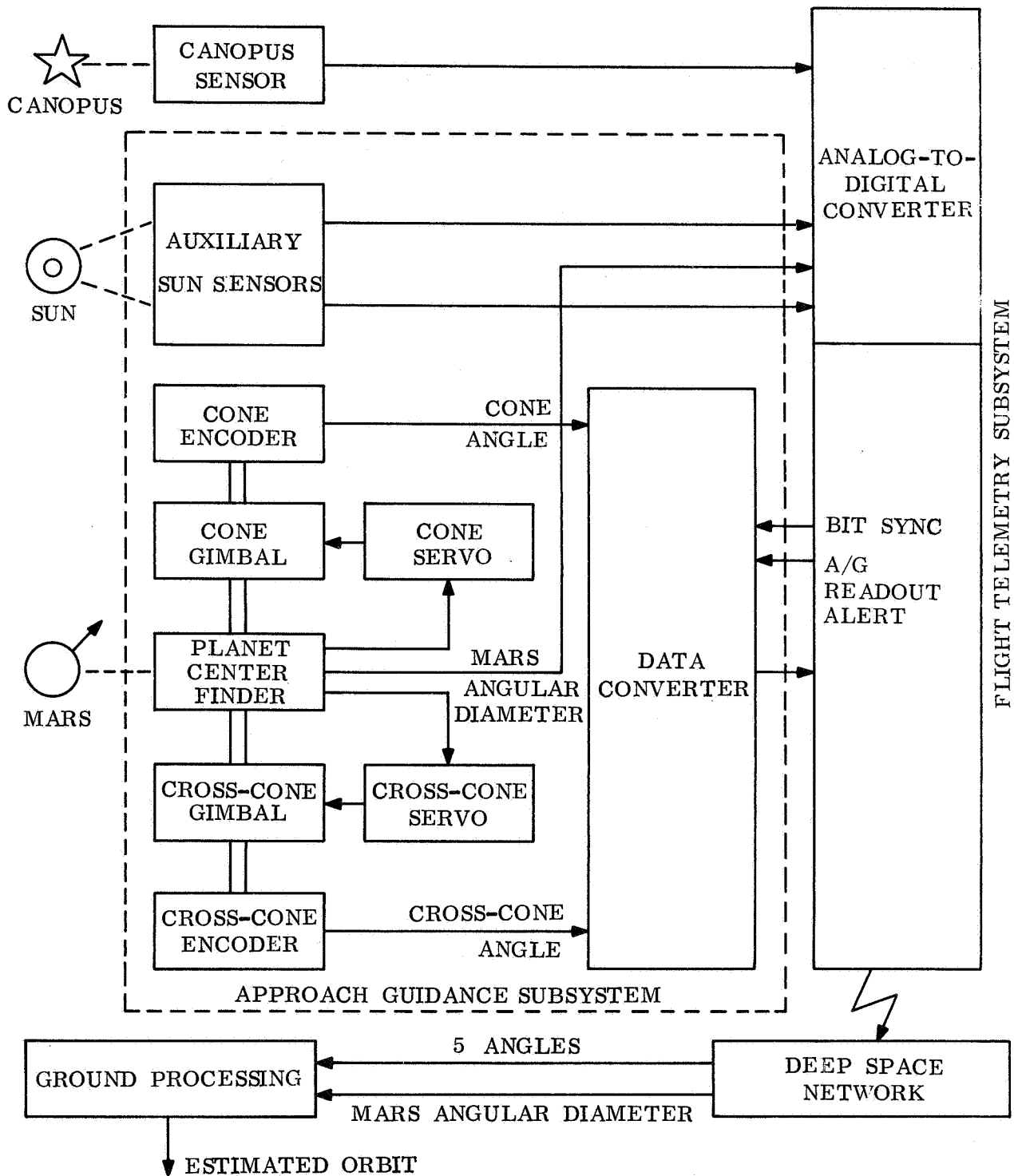


Figure D-51. Approach Guidance Subsystem Block Diagram

The Approach Guidance Subsystem operates nominally during the time period from 10 days before encounter until 11 hours before encounter. During this period, the angular diameter of Mars varies from about 0.1° to 2.0° . The Approach Guidance Subsystem operates over a range of $\pm 5^\circ$ from the alignment axis in cone angle and $\pm 5^\circ$ from the alignment axis in cross-cone angle, which for the nominal pointing direction, approximates $\pm 10^\circ$ in clock angle. The subsystem can measure navigation angles to within 0.2 milliradians (3σ).

D.6.3.4 Subsystem Performance Characteristics

The A/C can orient the Spacecraft to the Sun and Canopus from any initial orientation, and with initial rates as high as $3^\circ/\text{sec}$ about each axis. Orientation to the Sun will take place in less than 30 minutes, followed by a Canopus search and lock on in less than 70 minutes additional time. During acquisition, the initial rates are quickly reduced, and they are limited to about $0.25^\circ/\text{sec}$ as the position error is reduced. Roll rate during Canopus search is about $0.1^\circ/\text{sec}$.

During cruise and orbit modes of operation, the limit cycle rate is about 0.2×10^{-3} deg/sec. The deadband is about $\pm 0.25^\circ$ for each axis. The combined effects of all errors such as those due to deadband, alignment, null shifts and drifts, noise, and other random errors will be less than 0.5° per axis (3σ).

During commanded turns, the turning rate is about $0.18^\circ/\text{sec}$. The turn magnitude is controlled by allowing this rate to continue for a predetermined interval of time. The error between the resulting orientation and the commanded orientation depends on the magnitude of the specific turns involved, and on the total time interval. Specifically, the cruise orientation error, gyro drift errors over the turning interval, gyro rate calibration, and capacitor leakage errors are the most significant. The resulting error for a 90° turn is 0.85° (3σ).

An error analysis of the autopilot has not been made, nor have requirements been established. As noted in Section D.6.3.2.2, the autopilot requires redesign due to changes in Spacecraft dynamics and the use of a gimballed engine. Errors in attitude hold during autopilot operation (i.e., while engine is firing) are affected by Spacecraft center of mass offset and thrust misalignment. The allowable error is a function of the velocity increment to be given the Spacecraft. With a thrust misalignment angle of 0.3° , a CM angular offset uncertainty of 0.4° and an autopilot gain of 5, the steady state autopilot error is about 0.55° (3σ). Transient errors have not been evaluated.

D.6.4 SCAN CONTROL SUBSYSTEM

D.6.4.1 Functional Description

The Scan Control Subsystem controls the pointing of the scan-platform-mounted instruments in the orbital mode of the MM '73 mission. During the orbital phase, the platform is pointed to within $\pm 0.2^\circ$ of the commanded cone and clock angles. Fig. D-52 is a block diagram of the Scan Control Subsystem.

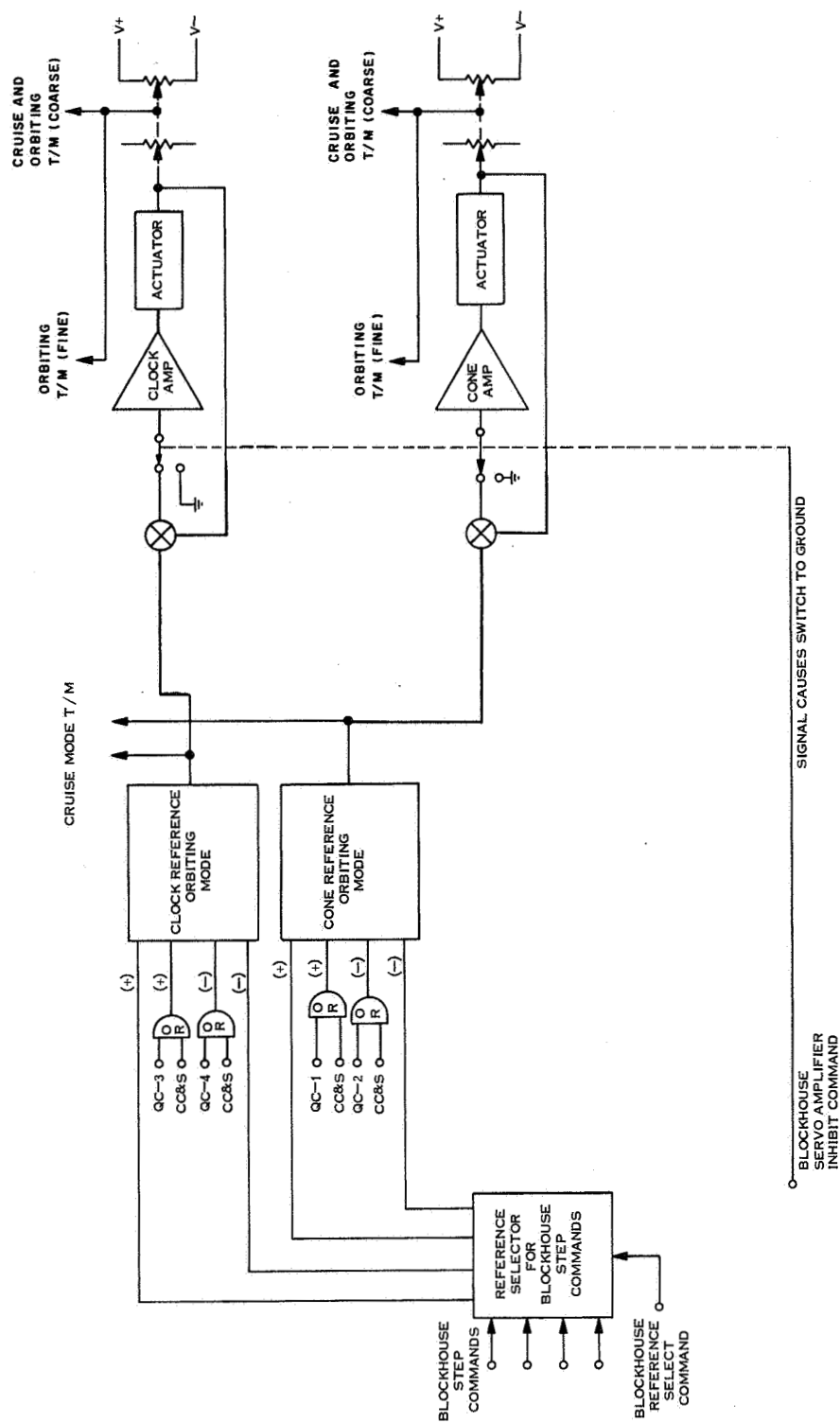


Figure D-52. Scan Control Subsystem

Following separation of the capsule adapter and orbit insertion, power to the Scan Control Subsystem is turned on and the platform slewed to the initial orbital cone and clock references by a command from the CC&S. Following ground verification of scan control and platform operation and prior to the first data-taking sequence, the orbital cone and clock references are updated, if necessary, by pulse train inputs from the CC&S. Polarities of the updates are indicated by the lines on which the inputs appear. Each update pulse corresponds to a one-degree increment in cone or clock angle. During the data-taking sequence, the references are subsequently updated by pulse train inputs from the CC&S immediately after the taking of each TV picture. Upon completion of the sequence, the platform is commanded to the initial position for the second data-taking sequence. The process of updating described above is repeated during the second and all subsequent data-taking sequences. For a 24-hour orbit, 25 to 40 positions will be commanded during a periapsis passage.

D.6.4.2 Modifications for Mariner Mars '73

Scan Control will probably not function in the MM '69 and MM '71 far encounter mode in MM '73 because of operational and physical conflict with the capsule mission. This has the following implications:

1. The far encounter cone and clock references and the FEPS will not be employed.
2. The scan platform will remain in its stowed position until after orbit insertion.
3. Science data will not be recorded during far encounter.

Our conclusion, based on the Mariner Mars '69 information at our disposal and our estimates of Mariner Mars '71 and '73 functional requirements, is that the MM '73 requirements can be met by the MM '71 scan control without modification. Extensive equipment deletions appear to be possible should deletion prove economical. These include the far encounter cone and clock references, control switches, far encounter planet sensor (FEPS) and FEPS power supply.

D.6.4.3 Performance Characteristics

In the orbiting mode, a reference line on the platform is maintained to within 1.2° of the commanded angles in cone and clock. The slewing rate in cone or clock is $1^\circ/\text{sec}$, -0 or +50 percent. Recommended ranges of gimbal freedom are as follows:

| | |
|-------------|---------------|
| Cone angle: | 75 to 180 deg |
|-------------|---------------|

| | |
|--------------|---------------|
| Clock angle: | -5 to 365 deg |
|--------------|---------------|

D.7 SCIENCE

MM '69 carries four science subsystems: television, infrared spectrometer, infrared radiometer, and ultraviolet spectrometer. It has been suggested that all four of these experiments could be carried aboard the MM '71 Orbiter, with major modification to the cooling mechanism of the IRS. However, experiment selection for MM '71 has not been announced at the time of this writing. In view of the lack of definition of the MM '71 orbital payload, no attempt has been made to extrapolate to a reasonable successor payload for the Orbiter in MM '73.

Table D-38 is a summary of the Mariner Mars '69 science payload.

TABLE D-38. MARINER MARS '69 SCIENCE PAYLOAD

| Experiment | Weight (lb) | | Data Rate: Sensor to Recorder (kbps) |
|--|------------------|---------|---|
| | Scan Platform | Octagon | |
| Medium Resolution Television Camera (MRTV) | 7 | 11.8 | 186 |
| High Resolution Television Camera (HRTV) | 28 | | 186 |
| Infrared Spectrometer (IRS) | 30 | | 1.11 |
| Ultraviolet Spectrometer (UVS) | 34.6 | | 2.67 |
| Infrared Radiometer (IRR) | 7.5 | | 9.5×10^{-3} |
| Radio Occultation | - | - | - |
| Celestial Mechanics | - | - | - |

D.8 REFERENCES

- D-1. Mariner Mars '71 Baseline Description, GE/RS Document No. 68SD4238.
- D-2. Verbal information received via telephone from General Dynamics/Convair.
- D-3. USAF/SSD Report SSD-CR-65-18 (Rev. 2), "Titan IIIA and IIIC Standard Space Launch System (SSLS) Definition for Payload Contractors", June 1966.
- D-4. NASA CR-72109, "Centaur Payload User's Manual", 1967.
- D-5. J. P. D. Wilkinson, "A Penetration Criterion for Double-Walled Structures Subject to Meteoroid Impact", GE TIS 68SD275, June 1968.
- D-6. "Natural Environment Design Criteria Guidelines for MSFC Voyager Spacecraft for Mars 1973 Mission", NASA TM X-53616, 1967, editors: D. K. Weider and C. L. Hasseltine.
- D-7. Schmueker, J. D., and Spehalski, R. J., "Mariner Mars 1964 Basic Structure Design and Development", JPL Technical Report 32-953, 1 May 1967.
- D-8. "Mariner Mars 1964 Project Report: Mission and Spacecraft Development; Vol. 1 from Project Inception Through Midcourse Maneuver", JPL Technical Report No. 32-740, 1 March 1965.